Quaternary Sea-Level and Climate Signatures in Phreatic Coastal Caves

by

Peter J. van Hengstum

Submitted in partial fulfillment of the requirements
for the degree of Doctor of Philosophy

at

Dalhousie University
Halifax, Nova Scotia
November 2010

DALHOUSIE UNIVERSITY

DEPARMENT OF EARTH SCIENCES

The undersigned hereby certify that they have read and recommend to the Faculty of Graduate Studies for acceptance a thesis entitled "Quaternary Sea-Level and Climate Signatures in Phreatic Coastal Caves" by Peter J. van Hengstum in partial fulfillment of the requirements for the degree of Doctor of Philosophy.

Dated: November 17, 2010

External Examiner: _____

Research Supervisor: _____

Examining Committee: _____

_____

Departmental Representative: _____

DALHOUSIE UNIVERSITY

DATE: November 17, 2010

AUTHOR: Peter J. van Hengstum

TITLE: Quaternary Sea-Level and Climate Signatures in Phreatic Coastal Caves

DEPARTMENT OR SCHOOL: Department of Earth Sciences

DEGREE: PhD CONVOCATION: May YEAR: 2011

_____

Signature of Author

TABLE OF CONTENTS

LIST OF TABLES

LIST OF FIGURES

ABSTRACT

Underwater (phreatic) caves are a ubiquitous landform on coastal karst terrain, but the marine geological processes operating in these systems are largely unknown. This dissertation redresses the problem by asking if Bermudian phreatic cave sediments archive sea-level and climate information? An important premise is that coastal cave environments are not identical. They can be categorized based on whether they are terrestrially-influenced (anchialine), completely flooded by saline groundwater (submarine), positioned at sea level (littoral) or in the vadose zone (vadose).

For the first time the boundary between modern anchialine and submarine cave environments has been distinguished in Green Bay Cave using a multi-proxy approach (benthic foraminifera, sedimentary organic matter content and carbon isotopic composition - $\delta^{13}C_{org}$, and grain-size analysis). Twelve push cores were extracted from Green Bay Cave and dated with twenty ^{14}C dates, recovering the first underwater cave succession spanning the Holocene (13 ka to present). Green Bay Cave transitioned through all major cave environments during Holocene sea-level rise (vadose, littoral, anchialine, and submarine), providing a sedimentary model for global cave successions.

These relationships provide a novel means to solve Quaternary sea-level and climate problems. For sea level, two examples indicate that the littoral cave can be used as a sea-level indicator, distinguished stratigraphically by microfossil or sedimentary proxies. First, the elevation and timing of when Green Bay Cave was a littoral environment indicates Bermuda experienced an abrupt ~6.4 m sea-level rise at 7.7 ka, coinciding with final collapse of the Labrador sector of the Laurentide Ice Sheet. Second, microfossils preserved in elevated caves at +21 m above modern sea level and dated to marine isotope stage 11 (U-series, amino acid racemization) are consistent with modern Bermudian caves and co-stratigraphic sea level. For climate problems, annual temperature monitoring in Walsingham Cave indicates that cave water is thermally comparable to regional oceanographic conditions in the Sargasso Sea. Three sediment cores dated with sixteen ^{14}C ages indicate that Bermuda's coldest and stormiest conditions of the last 3.2 ka occurred during the Little Ice Age (proxies: $\delta^{18}O_c$, grain size, bulk organic matter).

LIST OF ABBREVIATIONS AND SYMBOLS

AC	anchialine cave
CSC	circulated submarine cave
ISC	isolated submarine cave
E	entrance
GBC	Green Bay Cave
GH	Ghyben-Herzberg
ka	thousand years
LIA	Little Ice Age
MIS	Marine Isotope Stage
ML	meteoric lens
MWP	Medieval Warm Period
NAO	North Atlantic Oscillation
ppt	parts per thousand (salinity)
SCUBA	self-contained underwater breathing apparatus
SEM	scanning electron microscopy (or micrograph)
SGT	saline groundwater temperature
SST	sea surface temperature
Sv	Sverdrups
WH	Walsingham Cave
‰	parts per mil (stable isotopes)

GLOSSARY

anchialine cave: A phreatic cave (A) with restricted subaerial access through sinkholes, cenotes or pseudokarst openings; subsurface hydrogeologic connectivity to the ocean; flooded by a meteoric lens and/or saline groundwater, but where *terrestrial* influences (either geochemical, sedimentologic, or hydrogeologic) *dominate* the cave environment.

calcite raft: A common calcite precipitate in caves characterized by a bilateral morphology of planar versus euhedral crystal surfaces, which forms on still air-water interfaces from the pCO_2 off-gassing of carbonate-saturated groundwater and precipitation of $CaCO_3$.

eogenetic karst: Karstified carbonate sediments that are diagenetically immature, only partially-lithified, which have not experienced burial diagenesis.

freshwater lens: A distinct body of coastal groundwater that comprised of fresh water principally derived from infiltrating meteoric water. This dissertation does not use 'freshwater lens' synonymously with 'meteoric lens' because salinity is a critical variable to organisms and habitats.

Ghyben-Herzberg lens: Any coastal aquifer conforming to the Ghyben-Herzberg principle.

Ghyben-Herzberg principle: At static equilibrium in coastal aquifers, the elevation of the water table of pure fresh water above sea level is proportional to the depth of the interface with saline groundwater (halocline) below sea level, in a ratio of 1:40.

meteoric lens: A distinct body of coastal groundwater, of fresh to brackish salinity, buoyed on saline groundwater and derived from variable combinations of infiltrating meteoric water and saline groundwater.

littoral cave: A phreatic cave not completely flooded by groundwater where the presence of a water table intersecting the cave passage creates a range of phreatic (A) and vadose caves (A); sea level is within the cave passage if cave entrance opens into the open ocean. The position of cave entrances, with respect to the coastline, introduces significant environmental variability, most notably if entrance opens onto a lagoon or coastal shelf.

Little Ice Age (LIA): A period of 1-2ºC global cooling from ~1400 to 1850 AD expressed dominantly in the northern hemisphere; correlated to global glacier advances, rapid atmospheric re-organization, and decreased solar radiation.

phreatic cave: (A) Environmental context: Any cave in the phreatic zone, in telogenetic or eogenetic karst, and often accessed by sinking/rising streams or surface collapse. (sinkholes). (B) Speleogenetic context: Any cave that formed in the phreatic zone.

phreatic zone: The zone saturated by groundwater below the water table.

saline groundwater: Groundwater with salinity of at least 35 ppt located below the meteoric lens. Coastal saline groundwater is typically derived from the ocean, and may be circulating directly with the ocean through the karst platform.

submarine cave: A phreatic cave that is hydrogeologically connected to the ocean with any physical cave entrances (exits) completely flooded by sea level, wherein *marine* influences *dominate* the cave environment.

telogenetic karst: Karstified carbonate sediments that are diagenetically-mature that are completely lithified, and may have experienced burial diagenesis before re-emergence into the surface weathering environment.

vadose cave: (A) Environmental context: Any cave that is presently air-filled in the unsaturated zone, and often accessed by sinking/rising streams or surface collapse. (B) Speleogenetic context: Any cave that formed in the vadose zone.

vadose zone: The zone not saturated by groundwater above the water table.

water table: The subsurface interface between the saturated and unsaturated zone where the atmospheric pressure is equal to the groundwater pressure.

speleogenetic karst basins: void spaces in karst terrain in either the vadose or phreatic zone that are derived from speleogenetic processes (e.g., dissolution, collapse), which provide sea-level independent accommodation space for sediments, and provide habitat for subterranean ecosystems.

ACKNOWLEDGEMENTS

It is the easiest to sum up my esteem for Dave in an anecdote. When I first arrived at Dalhousie, and Dave and I were only recently acquainted, I began describing a cave abroad to Dave with evidence of foraminifera that I thought would be really swell to sample. As a young scientist, I did my utmost to scientifically justify the motivation and expense for the 'outlandish' subject of foraminifera in caves. After quietly listening to my argument, and then momentarily pausing when I finished, Dave's first response to me was: "*So, when do you want to go?*" This level of support from Dave was steadfast throughout my PhD, affording me unprecedented academic freedom – a privilege I know not all graduate students share. I am also thankful for how much I learned about foraminiferal taxonomy from Dave, and his *immediate* editing of the many chapters I presented him.

This project would never have even started without the support of many people in Bermuda. At the outset, Drs. Jack Ward, Anne Glasspool, and Wolfgang Sterrer supported my initial research proposal, and helped arrange my permits to sample in the protected underwater caves. Drs. Robbie Smith and Ian Walker continued with the administrative and governmental support as the project progressed into the final field seasons. My kindest thanks are reserved for Bruce Williams and Gil Nolan. Bruce letting me stay with his family on my first field season immediately introduced me to Bermudian hospitality, he regularly worked out all the logistics for my scientific diving, did the videography/photography, and had intimate knowledge of the cave systems. His dedication to this project is one of the primary reasons it was completed in such a timely fashion, and he happily shared his own scientific observations on Bermudian hydrogeology. Like Bruce during the first season, Gil gave up an entire week to dive with me on my last field season, and connected me with the Bermuda Zoological Society. Other members of the Bermuda Caver's Group, Leon Kemp and Paul Larrett, happily supported many swims into the main tunnels of Walsingham and Green Bay Cave Systems: carrying additional supplies in their pockets! Lastly, the Tucker family is thanked for their continual support of Bermudian cave science and property access.

Other faculty members at Dalhousie and abroad also contributed to my scientific development during the course of my PhD, and I am thankful for their help and insight. Dr. John Gosse eagerly provided academic advice throughout this project, often through impromptu meetings that helped guide my research design. Dr. Eduard Reinhardt (McMaster) provided lab facilities and discussion whenever needed, which always afforded reliable advice. Dr. Franco Medioli kindly revised an earlier draft of the thesis, and provided early suggestions to the research design. The insights provided by Drs. Martin Gibling and Neil Davies are also greatly appreciated, which helped me fully appreciate the significance of the Green Bay Cave succession, and Neil never refused to help edit a draft. Dr. Patricia Beddows (Northwestern) happily edited drafts of the QSR paper, and continually imparts me with important mentorship on hydrogeology. Dr. M. Buzas (Smithsonian) is thanked for providing good insight into an earlier draft of this work and acting as an external, and Dr. Storrs Olson (Smithsonian) kindly provided sediment from the Calonectris Pockets for analysis, as sediment no longer remains in outcrop, for which Dr. Q. Siddiqui confirmed the ostracod taxonomy. Lastly, Dr. T. Iliffe (Texas A&M) gave me access to instruments in Bermuda, which was critical for establishing the modern environmental processes in the cave. No scientist is ever isolated,

and I am thankful to all my professional mentors for being lighthouses along the way.

The most important graduate student to this work was certainly Andrew Kingston (Saskatchewan), whose interests were fundamental to the isotopic aspects of the climate project. It remains a pleasure to collectively continue our academic pursuits, already 7 years in the making. To the other students in Earth Science Department: I owe very large favors. It takes a certain type to endlessly converse with me about caves and foraminifera, so it is a good thing geologists' are usually keen naturalists! I am very thankful to Clarke Campbell, Mike Giles, and Cody McDonald for making Halifax a second home, and to the micropaleo lab – Olivia, Jen, Julie, Fred – for providing great initial critique to my fledgling ideas. Jen tirelessly read and corrected entire copies of this dissertation, which is certainly appreciated. To Shauna Little: Gratitude. Working with you every day in the summers sure made the time fly, and I am happy you became a foram enthusiast after all that picking.

My family has always been there throughout my years of studentship. My siblings, Mark and Maria, are always happy to hear about my scientific adventures, and along with my dad, have given me good doses of worry and support for being in the caves along the way. I think I have successfully rubbed-off on little Marlee and Lila, so do not be surprised if there is another butterfly-chaser in the family. To Kelly and Kelly, thank you for continually supporting my academic ambitions. Dropping by our favorite restaurant, *Steaks at Kelly's*, certainly made the minutes of analyzing hundreds of samples in one-week pass by—with the help of savory treats!

Lastly, to Taryn. My scientific contribution was only possible with your unwavering love and support. From weighing to editing, day or night, you were with me every step along the way, sharing patience when I was stressed, encouragement when I was scientifically awry, and beers during every one of my celebrations. My best friend, *I love you.*

Several agencies and organizations have provided considerable seed money to this new avenue of cave research through competitive research grants, which are all greatly appreciated. A Johanna M. Resig Fellowship from the Cushman Foundation for Foraminiferal Research generously provided capital financial support for this project. This was supplemented with student research grants from the Cave Research Foundation, Geological Society of America, the Bermuda Zoological Society, and the Sigma Xi Scientific Research Society. Lastly, I am grateful for support from a National Scientific and Research Council of Canada Alexander Graham Bell Canada Graduate Scholarship and a Killam Post-graduate Scholarship.

Chapter 1: Introduction

1.1 Problems And Hypotheses

Underwater (phreatic) coastal caves are globally distributed environments, with recognized scientific and socio-economic value to both developing and developed countries. For example, entrance fees to caves on private property can form a significant contribution to a family's gross annual income in developing countries (e.g., Mexico), yet they can also be significant commercial enterprises in developed countries (e.g., >300k tourists annually visit the Crystal Caves, Bermuda: Iliffe, 1979). Hydrogeologically, they are often saturated by lucrative freshwater resources in the coastal zone, which may be supporting up to 25% of coastal populations. However, there are no long-term hydrographic records describing their variability (Alley, 2001), and the entire environment is very sensitive to groundwater contamination (Iliffe, 1979; Einsiedl et al., 2010). Phreatic caves are also the source of significant fossil records, both human and animal. For example, some of the oldest skeletons from the America's are being recovered from Mexican underwater caves near the town of Tulum (Yucatan Peninsula), and bones of late Pleistocene megafauna (e.g., mammoths) are routinely present in Floridian phreatic caves (United States). Underwater caves also are colonized by unique ecosystems, containing species defined as critically endangered by the International Union for the Conservation of Nature because they may only be known from one specific underwater cave (e.g., Bermuda). Many ecological issues revolve around how little scientists actually know, on a global scale, about underwater cave environments and ecosystems, especially on geologic time scales. Despite these and other unique characteristics, however, underwater coastal caves have largely been marginalized in

Quaternary geoscience research in comparison to classical coastal systems (i.e., deltas, lagoons, marshes).

From a geological perspective this is curious because sediment is often described in underwater caves. This immediately poses many questions to the geologist. What types of sediments are in these caves? How do these sediments become deposited? Are the sediments stratified or homogenized? Are modern microfossils living in underwater caves, and are they preserved in the sedimentary record? And most scientifically important, what *useful* information is preserved in underwater cave sediment that is not readily available elsewhere? These unanswered questions reinforce our limited understanding of underwater coastal caves and their environmental histories. Therefore, the entirety of this dissertation begins to redress some of these problems, and challenge well-establish assumptions, by building upon our limited understanding of marine geological processes operating in underwater coastal caves. Expectations are that environmental development in phreatic coastal caves is intimately linked to sea-level and climate change.

As a result of these problems, two simple hypotheses are repeatedly tested throughout this dissertation in an effort to answer a variety of research questions:

1. Benthic foraminifera colonize and are preserved in phreatic coastal cave sediments, and
2. Sediment and microfossils preserved in phreatic coastal caves can provide proxy records of Quaternary sea-level and climate change.

1.2 Basic Concepts And Themes

A critical theme throughout this dissertation is that not all coastal cave environments are alike. They are more than simple underground voids and conduits positioned near a coast, but are in fact coastal systems with unique, predictable physical processes that are in dynamic equilibrium with external forcing mechanisms such as sea level and climate. By extension, if we can constrain the modern processes affecting these environments, then we should be able to reconstruct the paleoenvironmental response of the cave to changing forcing mechanisms. Coastal caves can even be more broadly considered a category of *speleogenetic karst basin* within the continuum of sinkholes to caves. The distinction that this research focuses on 'coastal' versus 'continental or inland' caves is relevant, as geologic conditions that influence coastal caves in eogenetic karst (diagenetically immature) cannot be assumed to be directly transferable to inland cave systems in telogenetic karst (e.g., Quaternary sea-level oscillations, hydrogeologic conditions).

The simplest way to differentiate coastal caves is by their position relative to the water table. Caves above the water table in the vadose zone are dry, and are easily explored and sampled by scientists. Therefore, sedimentary research in vadose caves is ongoing, and the results routinely provide valuable data on regional paleoenvironmental change (e.g., Hearty et al., 2004; Baldini, 2010; Medina-Elizalde et al., 2010). In contrast, caves below the water table in the phreatic zone are underwater. Underwater (phreatic) coastal caves have arguably received so little research attention because they require specialized SCUBA training for safe penetration and exploration. Phreatic coastal cave environments can be further categorized into anchialine, submarine, or littoral caves based on: (a) their elevation relative to the water table, (b) their position along coastlines

with respect to sea level at a specific point in geologic time, and (c) the relative magnitude of terrestrial versus marine influence on the cave (Stock et al., 1986). As these principles are central to this research, they are reviewed in more detail with necessary caveats throughout the dissertation. Therefore, this research focuses on underwater caves on eogenetic karst terrain, seeking to develop some unifying principles that can link environmental change between the well-studied vadose caves, and poorly-understood phreatic coastal caves (anchialine, submarine, and littoral).

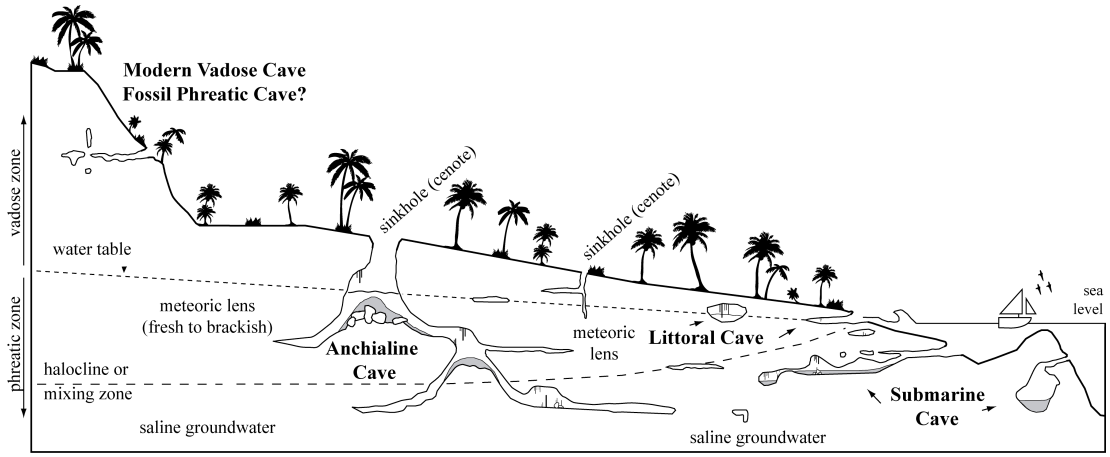

Figure 1.1: Classification of environments in coastal caves and sinkholes (cenotes), which can be collectively categorized as speleogenetic karst basins.

The last major conceptual framework required for this dissertation is the basic principles of hydrogeology. Hydrogeologic boundary conditions are imposed on coastal cave environments because (a) the caves can be flooded or drained during Quaternary sea-level cycles, and (b) physical groundwater parameters are not contiguous through the subsurface. Coastal aquifers on karst terrain are density-stratified into two gross water masses, the meteoric lens and the saline groundwater. These water masses differ in many ways, including salinity, temperature, thickness, and general circulation patterns. In

general, freshwater from precipitation creates the meteoric lens, which can be mixed to some degree with saline groundwater to become brackish. The meteoric lens flows coastward for eventual discharge into the ocean (e.g., Beddows et al., 2005, 2007). In contrast, the saline groundwater comprises seawater circulating in the karst platform due to density and thermal gradients, tidal forcing, or both (Whitaker and Smart, 1990; Moore et al, 1992; Beddows et al., 2005). These principles are expanded upon as required in subsequent chapters.

1.3 Study Site And Proxies

The archipelago of Bermuda is an excellent natural laboratory to study the research problem because coastal caves are locally abundant. All types of coastal cave environments can be found on Bermuda (vadose, littoral, anchialine, submarine), which have captivated islanders, researchers, and kings since the *Sea Venture* shipwrecked on Bermuda in 1609. Most of the research on Bermuda's underwater caves, however, has focused on the aquatic cave fauna under the pioneering efforts of Dr. T. Iliffe, which has included some hydrogeologic study as an ecological framework for the endemic cave fauna (e.g., Maddocks and Iliffe, 1986). Some superficial descriptions of Bermudian cave sediment have been published (Iliffe, 1987), providing evidence that Bermuda is a suitable location to test the hypotheses.

In general, the research is concentrated on two caves: (a) Green Bay Cave System, located on the peninsula between Harrington Sound and North Shore Lagoon, and (b) Walsingham Cavern, located on the isthmus between Harrington Sound and Castle Harbor. Both caves experience tidal forcing and have a thin, brackish meteoric lens (< 0.5 cm) buoyed on saline groundwater, and extensive underground passages. Green Bay Cave

System is of particular interest because it has two entrances. One entrance is located below sea level and opens into Harrington Sound, and the adjacent passages can be considered submarine cave environments. The other entrance into Green Bay Cave System is through a sinkhole, and adjacent passages can be considered anchialine cave environments. These two entrances are connected by almost 300 m of flooded cave passage, providing a unique opportunity to examine the boundary between anchialine and submarine cave environments both spatially in the modern environment by sampling surface sediment, and chronologically through sediment coring. In contrast to Green Bay Cave System, Walsingham Cavern only has one dominant sinkhole entrance, with ancillary openings around the periphery, and no direct passage linking it with the ocean.

The paleoenvironmental proxies used in this dissertation are: benthic foraminifera (micropaleontology), sedimentary character (particle size analysis, bulk organic matter), stable isotopes ($\delta^{18}O_{calcite}$, $\delta^{13}C_{org}$), organic matter elemental ratios (C:N), and radiocarbon (^{14}C) dating. Foraminifera are sensitive to environmental change across global coastal environments (Scott et al., 2001; Murray, 2006), so they were hypothesized to also be effective indicators in underwater caves. Sediment analysis provides an important cost-effective indicator for environmental conditions (e.g., hydraulic energy, currents, cave processes), which were hypothesized to be intrinsically linked to the type of coastal cave environment (littoral, anchialine versus submarine). Considering that primary productivity is limited in underwater caves due to the lack of light, organic matter is a critical resource and a known control on the cave benthos. Therefore, the quantity, quality, and source of bulk organic matter can be evaluated with organic geochemistry (e.g., Lamb et al., 2006). The oxygen isotopic composition of biogenic carbonate (e.g., foraminifera) is controlled by both the isotopic composition of water and temperature

(e.g., Katz et al., 2010), and was used as a thermal proxy for reconstructing climate variations. Lastly, chronologies for sediment cores from Green Bay and Walsingham Caves were developed using radiocarbon dating, all of which were calibrated with the most recent calibration curves and reservoir corrections (Reimer et al., 2009). Additional details on the methods are provided where necessary in subsequent chapters.

1.4 Central Research Questions And Dissertation Structure

The overall scientific contributions from this dissertation can be organized into three parts that generally follow the theoretical and scientific development on the subject. In short, Part I seeks to characterize the modern micropaleontological and sedimentological conditions in Green Bay Cave, which is a prerequisite for any paleoenvironmental reconstructions. Part II focuses on how and why sediments develop in phreatic coastal caves in relation to Quaternary sea-level change, and how cave environments evolve through time. Finally, Part III demonstrates that phreatic caves can preserve proxy-records of climate change, if the modern cave habitat is circulated with the ocean. Each chapter in this dissertation represents an individual scientific contribution, and is presented as a stand-alone scientific manuscript.

1.4.1 Part I: Calibrating The Modern Environment

Characterizing the modern conditions is a critical first step when working in a new environment, which will calibrate the required proxies (microfossil, sedimentologic, and organic geochemical proxies). The following research question guided research for Chapter 2: *What are the general sedimentary characteristics and ecology of foraminifera in modern underwater coastal caves?*

From previous research, foraminifera are colonizing cave entrances (Javaux, 1999; van Hengstum et al., 2008), foraminifera have been collected from recent underwater cave sediment (Sket and Iliffe, 1980), and cave sediment can contain fossil foraminifera (vadose: Proctor and Smart, 1991; phreatic: van Hengstum et al., 2009a). Therefore, based on preliminary evidence, it was hypothesized that benthic foraminifera are common throughout phreatic coastal caves, distributed along natural environmental gradients like in other coastal environments (salinity, organic matter resources, etc.). An understanding of modern marine geological processes (microfossils, sediments, geochemical, etc.) in underwater caves is a prerequisite to any research on sedimentary cores. Therefore, Chapter 2 aims to develop baseline conditions in Green Bay Cave in anticipation for reconstructing proxy-records of environmental change using sediment cores. For this chapter, P. van Hengstum completed all the field collections, laboratory analysis, foraminiferal analysis, and wrote the manuscript, while D. Scott contributed to insight into foraminiferal taxonomy and the interpretations.

1.4.2 Part II: Sea-Level Signatures In Phreatic Coastal Caves

Chapter 3 begins to question the sedimentological development and environmental change that occurs throughout coastal cave systems, and throughout all coastal speleogenetic karst basins, in response to glacioeustacy. Therefore, the following research question guided Chapter 3: *Do successions in underwater cave systems track sea-level rise?*

To investigate the problem, twelve cores were extracted from Green Bay Cave, Bermuda, affording the first complete succession from an underwater cave spanning the Holocene (13 ka ago to present). The successions provide strong evidence that coastal

caves, and all speleogenetic karst basins, transitioning through vadose, littoral, anchialine, and submarine environments in response to glacioeustacy. Therefore, I propose conceptual models describing how coastal caves environments evolve in response to sea-level forcing, during a transgressive system tract. Peter van Hengstum generated the research design and conceptual framework, completed the fieldwork, laboratory and data analysis, finalized the interpretations, wrote the manuscript, and drafted the figures. D. Scott contributed to the interpretations, M. Charette contributed to the origin of the Fe-oxide staining in the base of recovered successions, and D. Gröcke completed the mass spectrometry of the organic matter ($\delta^{13}C_{org}$).

Chapter 4 begins to examine how and why fossil foraminifera other phreatic microfossils are preserved in modern vadose caves. In an important initial study on the subject of aquatic microfossils in caves, Proctor and Smart (1991) found benthic foraminifera in Corbridge Cave (England) dated to previous Quaternary sea-level highstands using U-series aging of interspaced speleothems. Recently, benthic foraminifera were recovered in elevated vadose caves in Bermuda at +21 m above sea level, and have been debated as from either (a) +21 m sea level during Marine Isotope Stage 11, or (b) an Atlantic mega-tsunami (McMurtry et al., 2007). However, the foraminifera in the elevated Bermudian and English caves had not been compared to foraminifera living in modern coastal cave environments. Therefore, the following question guided the research contribution presented in Chapter 4: *Are microfossils in elevated Bermudian caves congruent with taxa found in modern coastal cave environments?*

To address the problem, foraminiferal assemblages preserved in Calonectris Pockets (Bermuda) were compared to the largest database of foraminifera from

Bermudian coastal environments, including caves (Javaux, 1999). It was discovered that the fossil foraminifera are indeed consistent with expected cave assemblages emplaced during a +21 m highstand scenario. For this chapter, P. van Hengstum designed the research project, obtained samples from the Smithsonian, completed the microscopy of the modern and fossil littoral cave sediments, generated the interpretations and wrote the manuscript; whereas D. Scott contributed to the interpretations and E. Javaux compiled the original database on Bermudian coastal foraminifera.

Chapter 5 re-examines the successions preserved in Green Bay Cave, compiling a foraminiferal proxy-record of environmental change in the cave throughout the Holocene flooding history. The results of Chapter 3 indicate that previously unavailable sea-level information is actually available regarding Holocene sea-level rise on Bermuda. The following research question guided Chapter 5: *Can foraminiferal paleoecology combined with sedimentology from phreatic coastal caves provide insight into Holocene sea-level rise in Bermuda?*

Bermuda is ideal for sea-level research because it has remained glacio-isostatically stable throughout the Quaternary, island subsidence rates are minor over Quaternary time scales (0.6-1.2 cm kyr^{-1}: Liu and Chase, 1989, Vogt and Jung, 2007), and the lack of an extensive coastal shelf limits hydroisostatic sea-level effects. From the analysis, evidence is provided for an abrupt sea-level rise of ~6 m in the Atlantic at 7.6 ka, using unequivocal sedimentological and microfossil proxies. Peter van Hengstum completed the fieldwork and generated the research design for this chapter, data analysis, and wrote the manuscript, while D. Scott contributed to the final interpretations.

1.4.3 Part III: Climate Signatures In Phreatic Caves

The last scientific contribution in Chapter 6 examines possible climatic signatures that may be preserved in Bermudian phreatic caves. Yamamoto et al. (2010) recovered the first paleoclimate record from a submarine cave in Japan (Daidokutsu Cave), which was a ~7 ka paleoclimate record of the East China Sea. This result suggests that North Atlantic climate records may be preserved in Bermudian phreatic caves that are in a submarine environmental state. Currently, the longest and best-resolved Bermudian climate records are from corals (e.g., ~750 years: Draschba et al., 2000). A pollen record preserved in Devonshire Marsh of terrestrial vegetation changes may indicate older climate changes in Bermuda, but the age constraint is currently insufficient for a detailed correlation to North Atlantic paleoclimate events (Rueger and von Wallmenich, 1996). The following question guided the final scientific contribution: *Does cave foraminiferal $\delta^{18}O_c$ and sedimentology document late-Holocene climate change on Bermuda?*

Three sediment cores were extracted from Walsingham Cave and dated with sixteen radiocarbon ages. Thermal cooling and maximum storminess occurred on Bermuda during the Little Ice Age (LIA), coincident with atmospheric reorganization and reduced solar radiation beginning with the Oort minimum. Decreased heat supply to Bermuda from reduced Gulf Stream transport, however, is perhaps contributing to a cooling trend initiated at 0.9 ka (Lund et al., 2006), which is observed in the cave and elsewhere in the North Atlantic basin (Mann et al., 2008; Cronin et al., 2010). Peter van Hengstum generated the research design for this project, collected the cores and initiated the temperature monitoring program, and prepared the foraminifera for stable isotope analysis and radiocarbon dating. Andrew Kingston completed the mass spectrometry and worked through data analysis and interpretations with P. van Hengstum. David Scott and

William Patterson contributed to the interpretations, Bruce Williams completed fieldwork and intellectually contributed modern thermal observations in Walsingham Cave, and P. van Hengstum wrote the manuscript and drafted the figures.

1.5 Final Prologue

The theoretical and scientific order of chapters strives for a smooth flow of logic, and the development of scientific ideas on the subject. However, each chapter is structured as a stand-alone and publishable scientific contribution, consistent with a 'sandwich style' dissertation structure. Some chapter introductions are repetitious as a result, especially with the basic concepts of coastal cave environments. At this stage of marine geological research in underwater coastal caves, however, it is challenging to avoid such repetition because many basic principles have not been previously illustrated, and are not conceptually appreciated. The primary author coined the scientific philosophical advances on coastal cave environments, generated the research design, completed all the field work requiring SCUBA, and wrote 100% of the manuscripts presented in this dissertation.

PART I: Calibrating The Modern Environment

Chapter 2: Ecology Of Foraminifera And Habitat Variability In An Underwater Cave: Distinguishing Anchialine Versus Submarine Cave Environments

Peter J. van Hengstum and David B. Scott

Dalhousie University, Centre for Environmental and Marine Geology

Halifax, Nova Scotia, B3H 4J1, Canada

Note: An edited version of this manuscript is to appear in 2011 in the *Journal of Foraminiferal Research.*

2.1 Abstract

Fossil and living foraminifera have been recovered from coastal caves but their ecology in underwater caves is unknown. Seventy-five surface sediment samples (<4 cm) were collected throughout Green Bay Cave System, Bermuda, and analyzed for foraminifera, $\delta^{13}C_{org}$, C:N, organic matter content, $CaCO_3$, and granulometry. Hydrogeologic variables (pH, salinity, dissolved oxygen, temperature) identified the two separate groundwater masses in the coastal aquifer (meteoric lens, halocline, saline groundwater). This cave is perfect for studying heterogeneous cave habitats because an anchialine cave (terrestrially-dominated) is connected to a submarine cave (marine-dominated). The anchialine cave environment consists of two groups of foraminifera: (a) the Meteoric Lens assemblage living in the brackish meteoric lens within 60 cm of sea level, and (b) the Anchialine Cave assemblage living in the saline ground water below the halocline. *Helenina anderseni*, *Discorinopsis aguayoi* and other diagnostic brackish fauna dominated habitats in the brackish meteoric lens, which transitioned into a higher diversity assemblage dominated by *Bolivina striatula* and *Rosalina globularis* below the halocline. Cave foraminifera and sediments identified the boundary between the anchialine versus submarine cave environments because the limit of terrestrial influence on the cave benthos can be quantified (e.g., $\delta^{13}C_{org}$: from -24‰ to -18‰, C:N ratio: from 11.2 to 8.3), and also corresponds to a foraminiferal change. The submarine cave environment consists of three groups of foraminifera: (a) The Entrance (or cavern) assemblage in the first ~60 m of the submarine cave dominated by *Quinqueloculina*, (b) the Circulated Submarine Cave assemblage dominated by *Spirillina vivipara* and *Triloculina oblonga* slightly further into the cave, and (c) an Isolated Submarine Cave

assemblage dominated by *Spirophthalmidium emaciatum* in the cave passages furthest away from a cave exit. Lastly, planktic tintinnids suggest that tidally forced saline groundwater circulation with the ocean plays an important role in fertilizing the cave areas with the Circulated Submarine Cave assemblage. These results indicate that coastal caves are partitioned into specific environments and habitats by groundwater masses, sediment fluxes (terrestrial versus marine), and subterranean circulation; and that fossil cave foraminifera will be useful proxies for paleohydrogeology, paleoclimatology, and Quaternary sea level.

2.2 Introduction

Even though karst landscape covers nearly ten percent of the globe (Ford and Williams, 1989), underwater (phreatic) coastal cave environments have received very little paleoenvironmental or paleoecological research. Most underwater (phreatic) cave research has focused on biology and hydrogeology, with geologic research generally focused on speleogenesis (e.g., Ford and Ewers, 1978). Investigating marine geology in phreatic caves is a research avenue independent of the geochemical analysis of speleothems for Quaternary climate and sea-level data (Harmon et al., 2007; Dutton et al., 2009; Dorale et al., 2010; Baldini, 2010). Speleothem research only provides information about caves in the vadose zone, but preliminary research indicates that phreatic cave sediments represent an emerging source of paleoclimate and sea-level data (Yamamoto et al., 2009; van Hengstum et al., 2009b, 2010). Despite these efforts, more information on the modern marine geological processes and microfossils in underwater caves is required so their sediments can be confidently applied to Quaternary sea-level and climate problems.

Information on foraminifera in subterranean settings is scarce. The earliest documentation of cave foraminifera, to our knowledge, is by Birnstein and Ljovuschkin (1965). They described a brackish pool (salinity 11 ppt) in Kaptar-Khana Cave (south-western Turkmenistan), which hosts *Borovina* (=*Trochammina*), *Miliammina*, and *Trochamminita*. Whereas cave foraminifera have since been documented elsewhere, there is still no detailed ecological information (e.g., Mikhalevich, 1976; Sket and Iliffe, 1980; Kitamura et al., 2007). Javaux and Scott (2003) completed a preliminary sampling in a few Bermudian caves, and discovered diverse foraminiferal communities different from those of other coastal environments. Only cave entrances were sampled, however, leaving the intrinsic underwater cave habitats unknown. Fossil foraminifera in vadose and phreatic caves have also been documented, but interpreting these foraminifera is challenging without modern ecological studies (e.g., Proctor and Smart, 1991; van Hengstum et al., 2009a). Therefore, this study aims to investigate recent distributions and ecology of foraminifera living throughout an underwater cave, with specific attention given to identifying the differences between anchialine and submarine cave environments.

2.3 Coastal Cave Environments

It is important to consider that coastal caves are not identical, but are classified into specific environments based on inherited geomorphology, hydrogeology, magnitude of terrestrial influence, and coastal position (Fig. 2.1). Coastal aquifers can be grossly divided into two separate groundwater masses, the meteoric lens and saline groundwater separated by a halocline (or mixing zone). The meteoric lens can vary from fresh (e.g., 1.5 ppt salinity inland on the Yucatan) to very brackish (e.g., >20 ppt salinity in some

areas of Bermuda), while saline groundwater is marine (~35 ppt salinity). These groundwater masses flood porous eogenetic coastal karst terrain that often host abundant caves.

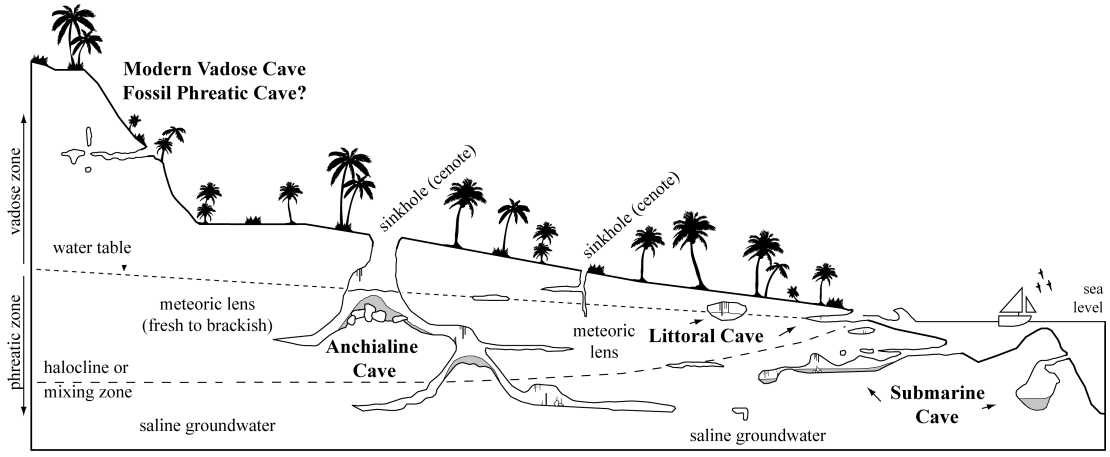

Figure 2.1: Classification of coastal cave environments. On terrestrial karst terrain in the Caribbean region, sinkholes are commonly known as cenotes in Mexico, or blue holes in the Bahamas. Stalactites and stalagmites that formed during Quaternary sea-level lowstands often decorate underwater caves.

Anchialine caves are defined as having restricted atmospheric access, noticeable marine and terrestrial influences, and subterranean connection to the ocean (Fig. 2.1, Stock et al., 1986). Atmospheric access to anchialine caves typically occurs through sinkholes (cenotes), which are often cave passages or fissures that collapsed during previous sea-level regressions. Sinkholes provide physical 'karst windows' to otherwise oligotrophic subterranean habitats, allowing for the influx of terrestrial nutrients, sediments, and non-cave dwelling organisms. Anchialine caves can also transect the meteoric lens and/or the saline groundwater. In contrast, submarine caves are more narrowly defined as having a marine entrance below sea level and cave passages that are only flooded by saline groundwater. Lastly, littoral caves occur at sea level, and typically

contain an air-water interface throughout most of the cave system, caused by the cave passage lying at the water table. Littoral caves that open directly to the sea can have increased water currents and waves originating from outside the cave (Denitto et al., 2007), but when an air-water interface exists deeper in a cave, often the only evidence of its occurrence is speleothem formations or calcite raft deposition (Taylor and Chafetz, 2004; Dorale et al., 2010). At the present time, reef caves are considered a specialized form of submarine caves, which are cavities beyond the coastline in the limestone reef framework (e.g., De Goeij and Van Duyl, 2007; Kitamura et al., 2007).

A few limitations of this classification scheme include: (1) a single cave system can simultaneously host more than one type of cave environment, (2) cave environments are defined based at one point in time, and thus are theoretically evolving with Quaternary sea-level changes, and (3) the classification of coastal cave environments is *independent* of speleogenesis. Furthermore, superimposed upon this classification is that each cave environment contains spatially variable habitats arising from local physico-chemical gradients (e.g., attenuation in organic matter inward from the cave entrance: Fichez, 1990).

Despite the wide usage of this classification scheme, many questions remain about the detailed boundary conditions between cave environments and habitats. For example, because anchialine and submarine caves can equally exist in saline groundwater, what distinguishes anchialine versus submarine cave environments in saline groundwater? What is the relative impact of terrestrial versus marine organic matter on cave benthos? How much bulk organic matter is generally present in submarine cave environments? Is there an ecological response to littoral conditions created deeper in the cave when cave passages intersect the water table? Because foraminifera are sensitive to physical and

chemical variables in other coastal systems (salinity, organic matter, pH), we hypothesize that they would be useful for delineating habitat variability in underwater caves and testing some of these questions.

2.4 Study Site: Geology and Hydrogeology

Bermudian caves can be summarized as collapsed karst features in a Carbonate Cover Island, according to the Carbonate Island Karst Model (Mylroie and Mylroie, 2007). This is because Bermudian geology is characterized by a basalt core overlain by alternating eolianites and paleosols that reflect sedimentary deposition during late Quaternary sea-level highstands and lowstands, respectively (Land et al., 1967; Gees and Medioli, 1970; Hyndman et al., 1974; Vacher et al., 1989, 1995; Hearty, 2002). Bermudian caves have formed by three primary processes: (a) vadose dissolution concentrated at the basalt-eolianite contact during Quaternary sea-level lowstands, (b) further modification and enlargement by phreatic dissolution during Quaternary sea-level highstands, and (c) subsequent collapse events triggered by glacial regressions (Palmer et al., 1977; Mylroie et al., 1995). These processes have created modern caves characterized by large chambers connected by fissures and tunnels. The Bermudian caves re-flooded by the rising groundwater with Holocene sea-level rise are modern underwater caves. Five freshwater lenses (i.e., meteoric lenses with salinity <1 ppt) characterize Bermudian hydrogeology, but late Quaternary speleogenesis has been focused in the northeast of Bermuda where these freshwater lenses are absent (e.g., Vacher, 1978; Mylroie et al., 1995; Vacher and Rowe, 1997).

Green Bay Cave System was selected as the study site because it contains both anchialine and submarine cave environments as described by Stock et al. (1986), and is

located in the north side of Harrington Sound transecting the Lower Town Hill and Belmont Formations (Fig. 2.2). The anchialine cave environment begins at Cliff Pool Sinkhole and transects both groundwater masses in the coastal aquifer (meteoric lens and saline groundwater). Cliff Pool Sinkhole has physical characteristics typical of other Bermudian anchialine ponds: a very narrow tidal range (<0.5 m) with ubiquitous algae and the anchialine gastropod *Cerithium lutosum* (Thomas et al., 1991). In contrast, the submarine cave environment begins at the cave entrance opening into Harrington Sound below sea level. The Trunk Passage connects these two different cave entrances, thereby providing opportune geomorphology to investigate the boundary between anchialine versus submarine cave environments.

Modern groundwater flooding of Green Bay Cave is typical of most Bermudian caves where a thin brackish meteoric lens (< 0.6 m, salinity > 20 ppt) is buoyed on saline groundwater (e.g., Sket and Iliffe, 1980). The submarine cave entrance opening into Harrington Sound allows for tidally forced circulation between coastal ocean water and saline groundwater in the cave (Fig. 2.2, Morris et al., 1977; Cate, 2009). Only ~60% of water flowing into the submarine cave entrance during a tidal cycle returns as outflow into Harrington Sound, indicating a daily diffuse outflow of saline groundwater through the limestone (Cate, 2009). Groundwater current velocities are low throughout internal cave passages, but flow velocities can reach a maximum of 1.5 m s^{-1} in the submarine cave exit during tidal peaks from the restricted geomorphology at the entrance (Cate, 2009).

2.5 Methods

All ecological interpretations herein are based on *total assemblages* (rose Bengal

stained plus non-stained individuals) because: (a) annual-monitoring experiments on total versus living wild populations indicate that total assemblages better represent average environmental conditions (Buzas et al., 1977; Scott and Medioli, 1980b; Redois, 1996); (b) total assemblages provide an averaged taxonomic perspective, which is most directly applicable to paleoecological research (Buzas, 1968; Debenay et al., 2001; Debenay and Guillou, 2002; Osterman, 2003; Melis and Violanti, 2006); and (c) it is widely appreciated that rose Bengal stains both living and recently-dead cellular protoplasm, requiring a conservative approach for its application (Bernhard, 1988; Bernhard et al., 2006). Rose Bengal is still required, however, to verify that total populations are actually representative of modern fauna because phreatic caves can experience low sedimentation rates (van Hengstum et al., 2009a).

Seventy-five surface sediment samples (<4 cm sediment depth, ~ 35 cm^3) were collected by researchers using self-contained underwater breathing apparatus (SCUBA) throughout Green Bay Cave (Fig. 2.2). For foraminiferal analysis, a sediment sub-sample (5 cm^3) was wet-sieved through a 45 μm screen and stored in a rose Bengal solution until further analysis (1 g l^{-1} of 4% buffered formalin). As an a priori requirement for this study, at least one stained individual from each taxonomic unit in each sample required categorical observation (in the bulk sedimentary sample or enumerated subsample) for that species to be reported as part of the modern total assemblage and included in further multivariate analysis. This approach allows for (a) verification that foraminifera recovered from Green Bay Cave are actually living in those passages, as opposed to only transported into the cave, and (b) the identification of any possible fossil taxa. Using this method, van Hengstum et al. (2009a) successfully differentiated a Pleistocene foraminiferal assemblage in Aktun Ha Cave (Mexico) from the modern cave foraminifera

and thecamoebians, so this approach was employed again in Green Bay Cave, Bermuda. For the sake of completeness, rose Bengal-based estimates for absolute abundance of living foraminifera are presented, but all analyses and discussion herein remain concentrated on total assemblages, and relative abundances to avoid bias from time averaging.

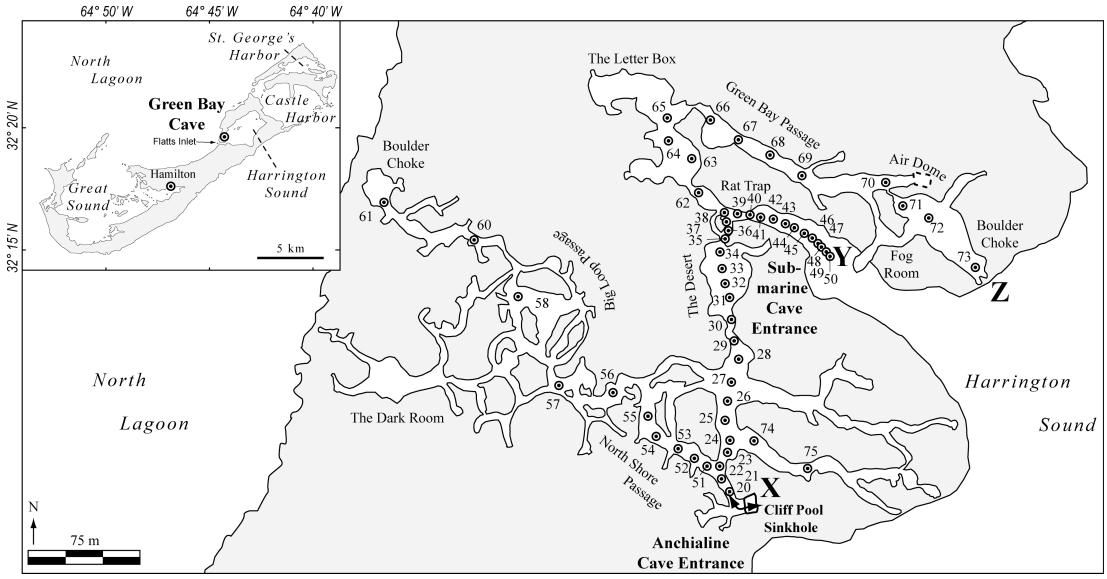

Figure 2.2: Location of Green Bay Cave on Bermuda with a detailed cave survey depicting all the sample locations. Cliff Pool Sinkhole provides the only subaerial access into the cave, the Trunk Passage provides a physical link between the anchialine and submarine cave entrances (Stock et al., 1986), and the Air Pocket is the only location with an air-water interface in the cave. The arrow near Cliff Pool Sinkhole represent the distribution of samples 1 to 19, which are too close together to illustrate with individual markers. Cave map adapted from after original survey sketch by Robert Power, as explored by founding members of the Bermuda Cave Diving Association.

Samples were wet-split, wet-picked, sorted into species, and taxonomically enumerated to create an original data matrix of 75 samples (N) × 136 variables (or species; Scott and Hermelin, 1993, Scott et al., 2001; Appendix 2). The only rose Bengal-stained planktic microfossil observed was tintinnids, a marine ciliate that is a useful proxy for water column particulates (Scott et al., 1995). As such, they were also enumerated to obtain information about the water column throughout the cave. Each sample contained a

minimum count of 233 individuals, but on average achieved a census of 337 individuals. After calculating the relative abundance and standard error for each species in every sample according to Patterson and Fishbein (1989), 30 statistically insignificant species were omitted from further multivariate analysis (standard error greater than relative abundance in all samples, species represented in only 1 sample). Samples in the final data matrix (75 samples × 106 observations) were then compared through Q-mode cluster analysis using a Euclidean similarity measure and Ward's Method of minimum variance in the freeware package *PAST* (Hammer et al., 2001). Two metrics of alpha diversity were also calculated for each sample (Fisher alpha: F_{α}, Shannon-Wiener Diversity Index: *H*).

The sediment properties examined were: mean grain-size, bulk organics (wt. %), calcium carbonate content ($CaCO_3$), $\delta^{13}C_{org}$, and C:N. Grain-size (particle size) was determined to identify the maximum influence of wave action and tidal currents at the submarine cave entrance (up to 1.5 m s^{-1}) because low hydrogeologic current velocities dominate the cave interior. Undigested cave sediment was analyzed to retain a complete signature of localized sedimentary processes (Donnelly and Woodruff, 2007; Donato et al., 2009), on a Beckman Coulter LS 230, which has a precision better than ± 2 μm on replicate samples and standards (15 μm garnet, van Hengstum et al., 2007). Bulk organic matter and $CaCO_3$ (wt. %) were determined on dried ~1.5 g sediment sub-samples by Loss on Ignition (LOI) for 4.5 hrs at 550ºC and 2 hrs at 950ºC, respectively. Analytical precision on replicate LOI samples (n = 19) was better than ± 1.7%, which is typical precision for the method (Heiri et al., 2001). Lastly, $\delta^{13}C_{org}$ and C:N were measured to differentiate sources of organic matter at sampling stations (Lamb et al., 2006, Perdue and

Koprivnjak, 2007; Diz and Francés, 2008; Weijers et al., 2009). Bulk sediment was first treated with a 10% HCl carbonate digestion, followed by a rinse to neutrality, desiccation, and grinding to a homogeneous powder. $\delta^{13}C_{org}$ and C:N determination of the bulk organic residue was performed on sub-samples with a Costech elemental analyzer connected to a Thermo-Finnigan DeltaPlus XP mass spectrometer. Carbon isotope ratios were measured against several international and internal standards, and expressed in the standard delta (δ) notation in per mil (‰) against Vienna PeeDee Belemnite (VPDB) with an analytical precision on replicates of ± 0.2‰. Sediment variables for each sampling station are included in Appendix 2.

Hydrogeologic properties (dissolved oxygen, salinity, pH, temperature) in the cave were measured with an independent submersible multi-parameter probe (YSI 600XLM). The probe was carried in front of the lead diver in a two-person dive team to measure the benthic hydrologic variables in an undisturbed water column, just above the sediment-water interface.

2.6 Results

2.6.1 Environmental Variables

2.6.1.1 Hydrogeological Variables

Two different groundwater masses are discernible at Cliff Pool Sinkhole: a shallow (0.6 m) meteoric lens of brackish water and saline ground water (Fig. 2.3). Salinity in the meteoric lens is ~24 ppt, pH is equal to 7.6, and the temperature is slightly cooler than the saline groundwater (~19°C). Below the halocline, the saline groundwater is marine (salinity 35.5 ppt, pH 8.1), and slightly warmer than the meteoric lens (>20°C). The

thermal warming just below the halocline at Cliff Pool is likely a result of heliothermic heating on the day of measurement. The entire cave system is oxic, as dissolved oxygen in the meteoric lens is 3 mL L^{-1}, >5 mL L^{-1} throughout the saline groundwater, and 6.1 mL L^{-1} in Harrington Sound. The salinity and pH of the saline groundwater in the cave approached oceanic conditions in Harrington Sound on the day of measurement, within instrumental precision.

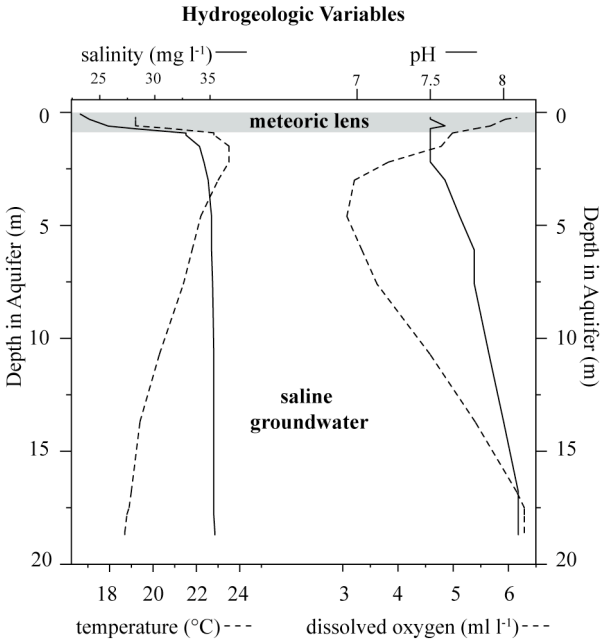

Figure 2.3: Hydrologic variables through the aquifer at Cliff Pool Sinkhole as measured in January 2009. Salinity crosses an important ecological threshold for benthic foraminifera.

2.6.1.2 Sediment Grain-size, Bulk Organic Matter, And $CaCO_3$

Overall, coarse-grained and organic-rich sediment is accumulating near the cave entrances, whereas fine-grained carbonate mud with less organic matter characterizes the cave interior. Starting at Cliff Pool Sinkhole, a poorly sorted diamict with mean grain-size of 255 μm is accumulating down the slope into the cave with abundant terrestrial material (sticks, leaves, livestock bones), fossil marine bivalves (*Arca* sp.) and limestone fragments (sand grains to cobbles). The coarse grained terrestrial sediment accumulating

near Cliff Pool Sinkhole transitions in the Trunk Passage (S20 to S22), from (a) grain-size of 225 μm to ~10 μm, (b) a light brown to grayish color, (c) bulk organic matter decreases from over 10% to less than 8%, and (d) $CaCO_3$ increases to ~50%. After this transition, fine-grained carbonate mud with a mean grain-size of <15 μm (fine silt) dominates the cave passage, which accumulates as infill between boulders in areas with previous ceiling collapses in distal cave passages (Green Bay Passage, Fig. 2.2)

Another sedimentary change occurs in the Trunk Passage from The Desert into the Rat Trap, as carbonate mud in the cave interior transitions into a coarse sandy-shell hash. Mean grain-size shifts from ~9 μm (S32) to 221 μm (S40), and bulk organic matter increases from <5% to a maximum of 20%. Overall, a fine to medium sand sediment (mean 218 – 356 μm) with abundant shell material is accumulating in the cave entrance from Harrington Sound down into the Rat Trap. Occasional coral fragments are also present, indicating that waves and tidal currents are depositing lagoonal sediments into the entranceway of the submarine cave.

There are two notable cave-specific sedimentary observations worth noting. First, some locations in the distal cave passages contained orange- to yellow-hued sediment. Similar hued sediments occur in eastern Yucatan and Mallorcan caves, but the coloration and sedimentary geochemistry is not yet attributed to a marine geologic or hydrogeologic process (van Hengstum et al., 2009a; Fornós et al., 2009). One sample of this sediment (S71) was examined and found to contain modern foraminifera consistent with individuals recovered in the carbonate mud (discussed further below). Second, calcite rafts are in S70, which are a calcite precipitate that forms at the water table in caves (Taylor and Chafetz, 2004; Fornós et al., 2009). Finding calcite rafts in S70 was expected

considering there is a water table almost directly above this sample station in the Air Pocket. No other places in the modern cave contain an air-water interface. Calcite rafts were not laterally transported away from the direct vicinity of the Air Pocket, which is to be expected considering the limited groundwater current velocities in the cave (except at the submarine cave entrance).

2.6.1.3 $\delta^{13}C_{org}$ And C:N

A typical average $\delta^{13}C_{org}$ value for terrestrial organic matter is -26‰, with C:N ratios exceeding 10 (Lamb et al., 2006). This represents detritus of terrestrial plants using the C_3-photosynthetic pathway, which create carbon-isotopically depleted and nitrogen-poor plant tissues (e.g., Lamb et al., 2006). The most $\delta^{13}C_{org}$-depleted sediment sample is located at a depth of 0.6 m in Cliff Pool Sinkhole (S03: -26.7‰), which also has the highest C:N ratio (15.1, Fig. 2.4). This geochemical result is in good agreement with the sample location, as the highest input of terrestrial organic matter into the cave is expected in the shallow sinkhole beside the land surface. In contrast, the most isotopically-enriched sample is S72 (-16.8‰), which is located almost at the terminus of the Green Bay Passage (Fig. 2.2). The isotopic signature of marine organic matter is significantly more carbon isotopically-enriched than terrestrial organic matter, with higher nitrogen content (see fig. 2 in Lamb et al., 2006). The geochemical signature of the organic matter in S72 is consistent with a marine origin, as the inherited geomorphology provides little opportunity for the influx of terrestrial organic matter at the sample site (Fig. 2.2). Beyond these two carbon isotopic end members, the rest of the samples plot in two general clusters in the biplot (Fig. 2.4). Therefore, the more carbon isotopically-depleted

and nitrogen-depleted group (n = 21, mean $\delta^{13}C_{org}$ = -23.9, C:N =11.2) represents samples where the bulk organic matter is predominantly derived from terrestrial sources (Meteoric Lens and Anchialine Cave assemblages, Fig. 2.5). In contrast, the more isotopically- and nitrogen-enriched group (n = 53, $\delta^{13}C_{org}$ = -18.4, C:N =8.3) represents samples where the bulk organic matter is predominantly derived from marine sources (all other foraminiferal assemblages).

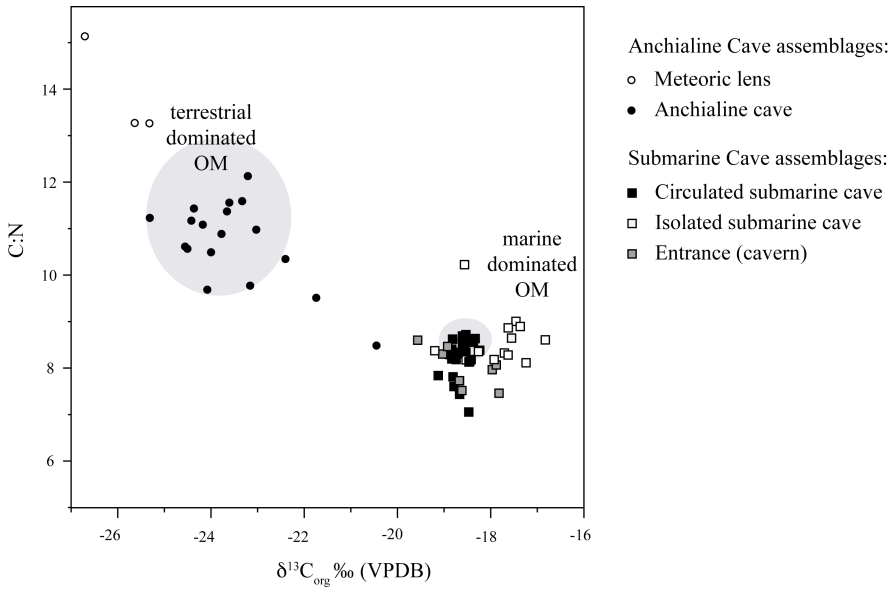

Figure 2.4: A biplot of C:N and $\delta^{13}C_{org}$ indicates that two different sources of organic matter (OM) influence the sediment in Green Bay Cave. Sample stations that are dominated by the flux of terrestrial organic matter are colonized by the ML and AC assemblages; whereas, stations that are dominated by marine organic matter are colonized by the CSC, ISC, E assemblages. The shaded area represents 2σ about the mean (see results).

2.6.2 Foraminiferal Assemblages

Abundant benthic foraminifera (living and dead) are present in Green Bay Cave sediments with a mean of 2492 individuals per cm^3 (min. 106, max. 6822). No endemic cave species of foraminifera were discovered, but three assemblages (anchialine cave, circulated submarine cave, and isolated submarine cave; see below) are specifically cave-

based assemblages in Bermuda, and many taxa that comprise those assemblages were not described in Bermudian coastal environments (Javaux, 1999). In general, benthic foraminifera employing photosynthetic symbionts were not in the cave except rare individuals at the submarine cave entrance, not a surprising result considering the lack of photosynthetically active radiation in dark underwater caves.

The use of rose Bengal ensured that all foraminifera reported in the total assemblages are actually living in the modern cave. Rare infilled (molds or steinkerns) and degraded foraminifera eroding out of the host lithology were easily identifiable and not included in the total assemblages (Appendix 2). This is common in underwater caves because active speleogenesis can cause limestone erosion (van Hengstum, 2008; see fig. 10 in Fornós et al., 2009). However, two samples (S61, S63) had non-infilled fossil lagoonal taxa, which were mostly *Archaias* (Appendix 2) and were excluded from the total assemblage because: (1) the dark cave is not optimal for a taxon that uses photosymbionts, (2) none of these individuals were stained with rose Bengal, and (3) all individuals exhibited characteristics of transport (greater than stage 2-3 abrasion and breakage as per Cottey and Hallock, 1988) despite limited water movement at the sample stations (S61, S63).

The dendrogram produced by the Q-mode cluster analysis on the resultant total assemblages indicates five clusters at a Euclidean Distance of 100, which are interpreted as unique foraminiferal assemblages colonizing distinct habitats in the cave: meteoric lens, anchialine cave, circulated submarine cave, isolated submarine cave, and the entrance (cavern) assemblage (Fig. 2.5):

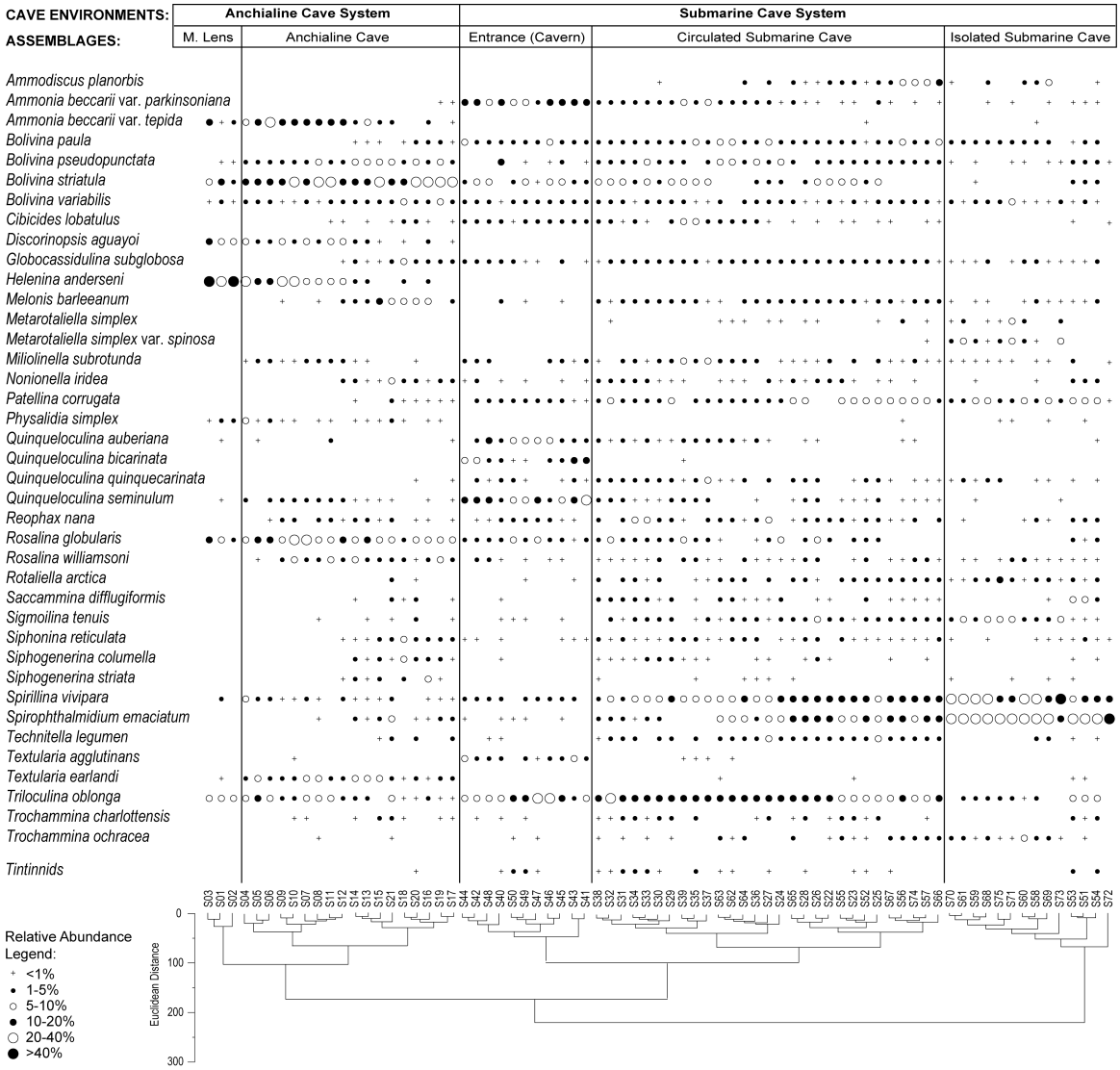

Figure 2.5: Five foraminiferal assemblages can be identified on the dendrogram produced by Q-mode cluster analysis on the statistically significant taxonomic observations in Green Bay surface sediment samples (Euclidean distance = 100). Furthermore, a three-cluster interpretation of the dendrogram (Euclidean distance = 150) distinguishes the different coastal cave environments: anchialine versus submarine. Only taxa that achieve at least >5% in at least a single sample are illustrated to emphasize dominant taxa. ML: Meteoric Lens. See Fig. 2.2 for sample locations in Green Bay Cave.

These five assemblages are in spatial agreement with the measured sedimentologic, organic geochemical, and hydrogeologic variables throughout the cave, and so the foraminifera were assigned into assemblages named after their locality of origin. As such, these 5 clusters are interpreted as colonizing specific habitats in the cave, and all samples

have been categorized into these different environments (Appendix 2). However, a three-cluster interpretation of the dendrogram can also be considered (Euclidean distance = 150), which precisely coincides with the supraclassification between the anchialine versus submarine cave environments described by Stock et al. (1986, Fig. 2.1). The similarities and differences between these five assemblages are described in detail below.

2.6.2.1 Meteoric Lens (ML) Assemblage

The ML assemblage has the lowest alpha diversity (mean $H = 1.7$) and absolute abundance (mean 133 individuals cm^3) of the entire cave system. Only three samples make up this assemblage (S01, S02, S03), which are all located in the meteoric lens of Cliff Pool Sinkhole (<0.6 m deep) in brackish water (mean salinity 24.6 ppt). Bulk organic matter (OM) content is the highest of all assemblages (mean OM 23.5%), which the carbon isotope value (mean -24.4‰) and C:N ratio (mean 12) indicates is derived from terrestrial sources (Lamb et al., 2006; Fig. 4). Euryhaline and stress-tolerant foraminifera dominate this assemblage, such as *Helenina anderseni* (mean 50.9%), *Bolivina striatula* (mean 7.9%), *Discorinopsis aguayoi* (mean 8.8%), and *Ammonia beccarii var. tepida* (mean 5%, Table 2.1). This is also the only assemblage where *Haplophragmoides wilberti* (max. 2.6%), *Trochammina macrescens* (max. 2%), *T. inflata* (max. 3.2%), and *Miliammina fusca* (max. 1.5%) form a statistically significant proportion of the assemblage (Appendix 2).

Table 2.1: Average environmental variables and dominant foraminifera (relative percent) in each total assemblage. See Appendix 2 for complete analytical results.

	Anchialine Cave Environment		**Submarine Cave Environment**		
	Meteoric lens	Anchialine cave	Circulated submarine cave	Isolated submarine cave	Entrance
Hydrogeological variables					
salinity (ppt)	24.6	34.5	35.5	35.5	35.5
pH	7.5	7.8	8.1	8.1	8.1
dissolved oxygen (mL L^{-1})	6.1	5.2	6.2	6.2	6.3
temperature (°C)	19.2	20.7	19.1	19	18.8
Sediment properties					
mean grain-size (μm)	224.8	225	14.6	7.1	302.7
OM (wt %)	23.5	14.0	8.0	6.9	9.8
$CaCO_3$ (wt %)	35.2	37.0	50.9	50.8	51.6
C:N	12.0	11.0	8.2	8.6	8.0
$\delta^{13}C_{org}$ (VPDB)	-24.4	-23.8	-18.7	-17.8	-18.6
Foraminifera					
Total foraminifera per cm^3	133	887	3209	2849	3390
Living foraminifera per cm^3	8	20	132	62	210
Shannon-Wiener index (H)	1.7	2.8	3.3	2.4	3.2
Fisher alpha index	4.1	9.2	16.8	9.4	16.9
Helenina anderseni	**50.9**	7.4			
Discorinopsis aguayoi	**8.8**	**9.9**			
Bolivina striatula	**7.9**	**18.5**	3.7	<1.0	4.0
Rosalina globularis	2.9	**9.2**	2.5	<1.0	3.8
Triloculina oblonga	<1	5.2	**13.4**	1.8	**11.9**
Spirillina vivipara	1.1	1.3	**11.3**	**22.0**	1.2
S. emaciatum		1.0	**7.4**	**30.7**	<1.0
Patellina corrugata		<1.0	4.5	**5.2**	1.5
Quinqueloculina spp.	<1.0	1.4	4.0	<1.0	**26.0**
Ammonia beccarii var. *parkinsoniana*			2.0	<1.0	**10.0**

2.6.2.2 Anchialine Cave (AC) Assemblage

The Anchialine Cave (AC) assemblage is located below the halocline in the saline groundwater in cave passages proximal to Cliff Pool Sinkhole. Foraminiferal alpha diversity increases (*H* 1.7 to 2.8) below the halocline in the saline groundwater (34.5 mL L^{-1}). *Bolivina striatula* (mean 18.5%), *Rosalina globularis* (mean 9.2%), and *Discorinopsis aguayoi* (mean 9.9%) dominate the AC assemblage, with *Ammonia beccarii* var. *tepida* (mean 8.2%) and *Textularia earlandi* (max. 9.6%) also common. Deeper into the cave from Cliff Pool Sinkhole, other shelf and coastal taxa increase in relative abundance, such as: *Melonis barleeanum* (max. 10%), *Siphogenerina striata* (max. 9%), *Hopkinsina atlantica* (max. 4%), *Nonionella iridea* (max. 5.5%), and *Fursenkoina compressa* (max. 4.7%). Many taxa reach their highest relative abundance in the AC assemblage when compared with the other assemblages. The AC assemblage is in finer-grained sediment (mean ~225 μm) with less bulk organic matter (mean OM 14%) than the ML assemblage, and the organic geochemical proxies indicate that the bulk organic matter is primarily derived from terrigenous sources (Fig. 2.4; $\delta^{13}C_{org}$ -23.8‰, C:N ratio 11). Miliolids are present in the AC assemblage, but they do not form a significant fraction of the assemblage (e.g., *Quinqueloculina* spp. mean 1.4%). *Physalidia simplex*, a common taxon in the Yucatan anchialine caves (Mexico), also occurs in Green Bay Cave, dominantly in the AC assemblage (Gabriel et al., 2009; van Hengstum et al., 2009a). Interestingly, tintinnids were observed with the AC assemblage, but they are only suitable for a presence/absence interpretation because they always represent <2% of the total assemblage (Patterson and Fishbein, 1989).

2.6.2.3 Circulated Submarine Cave (CSC) Assemblage

This assemblage has the highest alpha diversity of any recovered from Green Bay Cave (H = 3.3, F_{α}=16.8) and is dominated by *Triloculina oblonga* (mean 13.4%), *Spirillina vivipara* (11.3%), and *Spirophthalmidium emaciatum* (7.4%; Table 2.1). Minor species in the assemblage include *Technitella legumen* (max. 5.8%), *Bolivina striatula* (mean 3.7%), and *Patellina corrugata* (mean 4.5%). Of all the assemblages in Green Bay Cave, the CSC assemblage had the most frequent occurrence of tintinnids, indicating sufficient particulate is present to in the water column to support these planktic ciliates (Fig. 2.5, Garrabou and Flos, 1995; Scott et al., 1995). Measured hydrogeologic variables in the saline groundwater approach oceanic conditions, meaning that oxygen, pH, and salinity are not stressors to the foraminiferal populations (means: 8.1 pH, 19.1°C, dissolved oxygen: 6.2 mL L^{-1}). The substrate for this assemblage is typically carbonate mud (fine silt, mean grain-size 14.6 μm, mean $CaCO_3$ = 50.9%), with lower organic matter content (mean 8.2%). The bulk organic matter associated with the CSC assemblage is more isotopically enriched (mean -18.7‰) than assemblages in the anchialine cave environment (ML, AC), indicating predominantly marine sources (Fig. 2.4). Furthermore, the C:N ratio indicates more nitrogen-rich plant tissues present in the sediment than either the AC or ML assemblage (mean 8.2), which confirms the $\delta^{13}C_{org}$ result (Lamb et al., 2006).

2.6.2.4 Isolated Submarine Cave (ISC) Assemblage

The ISC assemblage is dominated by *Spirophthalmidium emaciatum* (mean 30.7%), reaching as high as 80% (S72). Other significant taxa include *Patellina corrugata* (mean

5.2%) and *Spirillina vivipara* (mean 22%), with lesser contributions from other taxa such as *Rotaliella arctica* (max. 13%) and *Bolivina variabilis* (max. 7%). Overall, this assemblage is less diverse than the CSC (mean *H* of 2.4). Tintinnids were observed in only two samples (S53, S54), which are located directly adjacent to samples belonging to the CSC assemblage (Fig. 2). Tintinnids were never observed further into the cave than these positions. Sedimentary conditions were similar to the CSC assemblage with white carbonate mud, mean 7.1 μm, mean $CaCO_3$ 50.8%; except for S71 which is orange-hued. Bulk organic matter is slightly lower in the ISC assemblage (mean 6.9%), and comprises the most carbon isotopically-enriched and nitrogen-enriched samples (mean: $\delta^{13}C_{org}$ 17.8‰ and C:N 8.6). The organic geochemical proxies indicate that the bulk organic matter is predominantly derived from marine sources (Fig. 2.4). As with the CSC assemblage, conditions in the saline groundwater are close to ocean values and are not ecologically restrictive to foraminifera (means: 8.1 pH, 18.8°C, 6.3 mL L^{-1} dissolved oxygen).

2.6.2.5 Entrance (Cavern) Assemblage

The Entrance assemblage is located ~60 m into the cave from submarine cave entrance at the northwestern end of Harrington Sound (samples: S41 to S50). The light-limited, or 'twilight' zone, of an underwater cave entrance is colloquially referred to as the 'cavern'. However, the Entrance assemblage is present in the light-limited areas at the cave entrance to the completely dark Rat Trap (Fig. 2.2). This assemblage is dominated by *Quinqueloculinia* spp. (mean 26%), *Triloculina oblonga* (mean 11.9%), and *Ammonia beccarii var. parkinsoniana* (mean 10%). Foraminiferal diversity is as high as the CSC

assemblage (H = 3.2), and comprises typical lagoonal foraminifera. Similarly to the ISC and CSC assemblages, the mean hydrogeologic variables approach oceanic values and are not ecologically limiting to foraminifera. Four samples were actually derived from open water lagoon in Harrington Sound, just outside the cave (S47, S48, S49, S50). These lagoonal samples cluster with the Entrance assemblage in the dendrogram (Fig. 2.5), indicating that the entrance to the submarine cave is lagoonal in character. The substrate typically consists of poorly-sorted, medium sand, shell hash (302 μm mean grain-size) that contains a bulk organics content of 9.8%. The carbon isotopes and C:N ratio are similar to the ISC and CSC assemblages (mean: $\delta^{13}C_{org}$ 18.6‰, C:N 8), indicating a dominantly marine origin for the bulk organic matter.

2.7 Discussion

2.7.1 Taphonomy: Are Cave Foraminifera Transported Or In Situ?

A limitation of using total assemblages to derive ecological information is that one must consider possible taphonomic effects on the final assemblages. After several lines of reasoning, however, we argue that the foraminiferal assemblages recovered from Green Bay Cave are representative of long-term, average conditions at the sampling sites. In a previous study of cave foraminifera and thecamoebians, van Hengstum et al. (2009a) found late Pleistocene foraminifera in the surface sediments of Aktun Ha cave (Mexico) because of very low (to non-existent) sedimentation rates in the distal cave passages. This is why rose Bengal is helpful for cave studies: to verify that foraminifera reported in the total assemblages are at least living (or recently living) in the cave. Our approach required all foraminifera reported as part of the total assemblages to be observed as stained in the

processed surface sediment samples at each sample station. Because sedimentation rates throughout the cave are unknown, the degree of time averaging is also unknown. The rose Bengal treatment, however, provides strong evidence that the total assemblages reported herein are representative of the recent (not Pleistocene) conditions in Green Bay Cave (except samples S73 and S61, discussed below).

Cave entrances that are physically open to the ocean will inevitably be influenced by wave action, and in the case of Green Bay Cave, strong tidal currents. These physical processes (waves, currents) will transport sediment, nutrients and foraminifera from the lagoon into the submarine cave, and are responsible for generating the shell hash in the first 50 m of the cave adjacent to Harrington Sound. With increasing distance into the cave, rapidly attenuating current velocities facilitate a grain-size shift to fine carbonate mud (with little shell fragments), precisely with a change from the Entrance to CSC assemblage. The infrequency of foraminifera with photosymbionts in the Entrance assemblage indicates that wholesale transport of lagoonal foraminifera into the cave is not occurring, because photosymbiotic taxa are quite common in Bermudian lagoons (Javaux, 1999) and would be expected in the cave if mass transport were occurring. Furthermore, stained foraminifera were still found throughout the Entrance assemblage that are consistent with the total assemblage, providing strong evidence that foraminifera are actually living in the cave benthos. Therefore, although the Entrance assemblage may be incorporating some tests transported into the submarine cave, the total assemblage is still interpreted as representing the summation of physical processes impacting the habitat at the submarine cave entrance. Similarly, some gravity-derived transport of shallower water taxa from the sinkhole into the deeper underwater cave is likely occurring, but this is likely minor because sinkhole taxa (e.g., *Trochammina inflata*) are not present at the base

of Cliff Pool Sinkhole. Lastly, although most foraminifera were previously known to Bermuda, several taxa in Green Bay Cave have never before been reported from Bermuda (e.g., *Ammodiscus planorbis, Labrospira evoluta*, *Parvigenerina* spp.), and the community of foraminifera forming the Anchialine Cave assemblage had never before been documented in any Bermudian coastal environment. The combination of evidence indicates that the recovered foraminifera are indeed living in the cave and representative of the different cave habitats.

2.7.2 The Anchialine Cave Environment

Salinity, dissolved oxygen and food resources (quantity and source of organic matter) are perhaps the most important variables influencing benthic foraminiferal ecology (e.g., Jorissen et al. 1995; Jorissen and Witting, 1999; Morigi et al., 2001; Scott et al., 2001; Debenay and Guillou, 2002; Murray, 2006). Dissolved oxygen in the groundwater is not controlling foraminifera in Green Bay Cave because dissolved oxygen is only ecologically-limiting to foraminifera if <2 mL L^{-1} and the groundwater is completely oxic (Fig. 2.3, Bernhard and Sen Gupta, 1997; Osterman et al., 2008). By definition, anchialine cave environments can be located in both the meteoric lens and saline groundwater (Fig. 2.1). Two different habitats belong to the anchialine cave environment in Green Bay Cave, which are occupied by different foraminiferal assemblages: the meteoric lens (ML) and anchialine cave (AC). Both the ML and AC assemblages have similar C:N and $\delta^{13}C_{org}$ values indicating the terrestrial surface is the dominant source of sedimentary OM (Fig. 2.3, Table 2.1). The major environmental difference between the two habitats is salinity: the brackish meteoric lens is divided from the saline groundwater by a halocline. Therefore, groundwater salinity is interpreted as

dividing the anchialine cave environment into two separate habitats that are colonized by different benthic foraminiferal communities.

Euryhaline foraminifera dominated by *Helenina anderseni* and *Ammonia beccarii* var. *tepida* are common in the brackish meteoric lens (mean salinity 24.6 ppt), which is the assemblage with the lowest diversity (mean *H* 1.7). *Helenina anderseni* is described as nearly obligate brackish by Debenay and Guillou (2002), and found globally in tropical and sub-tropical brackish habitats such as mangroves and at marine to freshwater transitions (e.g., Scott et al., 1991; Hayward and Hollis, 1994; Debenay et al., 1998). *Discorinopsis aguayoi* is also a typical inhabitant of tropical brackish ponds and mangroves (Javaux and Scott, 2003). Other diagnostic brackish water indicators in ML assemblage are common salt marsh taxa, such as *Trochammina inflata*, *T. macrescens*, *Miliammina fusca*, and *Haplophragmoides wilberti* (Scott and Medioli, 1980a; Horton and Edwards, 2006). Only salinity crosses an ecological threshold for benthic foraminifera in the meteoric lens (Murray, 2006; Table 2.1), indicating that this groundwater mass provides stressed habitats for euryhaline taxa abundant in other salinity-stressed marginal marine settings (e.g. Scott and Medioli, 1980a; Javaux and Scott, 2003; Horton and Edwards, 2006). Therefore, the meteoric lens is a specific habitat that is part of the anchialine cave environment of Stock et al. (1986) because it is terrestrially-influenced by (a) hydrogeology in the meteoric lens and (b) sedimentology from high quantities of terrestrial organic matter eroding into Cliff Pool Sinkhole.

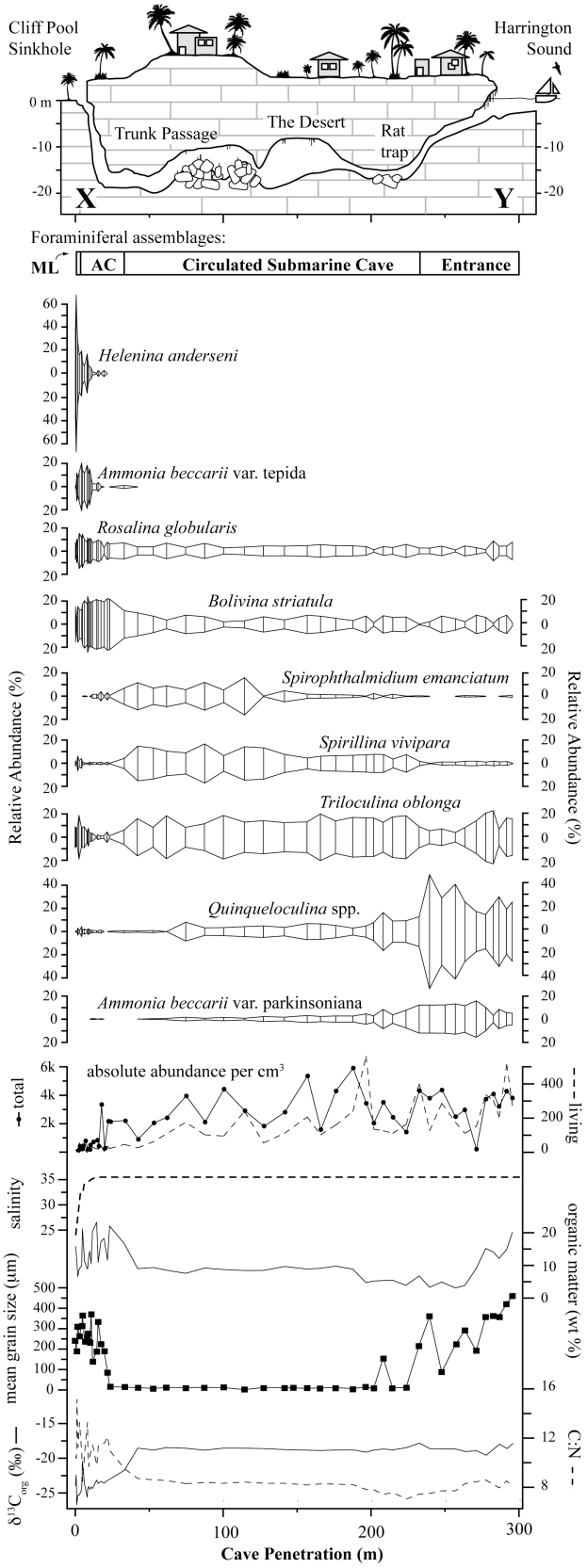

Figure 2.6: Relative abundance of dominant foraminifera along a linear transect from Cliff Pool Sinkhole (X) to Harrington Sound (Y) illustrating dominant foraminiferal, hydrogeological, and sedimentological changes through the cave. This transect (along the Trunk Passage) contains the boundary between the anchialine and submarine cave environments due to the loss of terrestrial-influence, which is indicated by precise shifts in foraminiferal assemblages and geochemical proxies (see Table 2.1). ML: meteoric lens assemblage, AC: anchialine cave assemblage.

The fauna colonizing the meteoric lens in Green Bay Cave, Bermuda, also share comparisons with available results on the brackish (oligohaline) meteoric lens fauna in Yucatan cenotes (Mexico; van Hengstum et al., 2008). However, the Mexican sites are fresher than in Bermuda, giving rise to notable faunal differences. Euryhaline taxa such as *Miliammina fusca* and *Trochammina* spp. are common in both regions, but in the oligohaline Yucatan cenotes *Ammonia beccarii* var. *tepida* is abundant instead of *Helenina anderseni*. This is likely related to salinity because *Ammonia beccarii* var. *tepida* commonly occurs in salinity <15 ppt, and Bradshaw (1961) could not determine the lethal minimum salinity for *A. beccarii* var. *tepida* in culturing experiments. The fresher Mexican cenotes also allow thecamoebians (testate amoebae) to colonize when salinity is below 3.5 ppt (i.e., *Centropyxis*, *Arcella*; van Hengstum et al., 2008).

Foraminifera rapidly diversify below the halocline (mean *H* of 2.8, >0.6 m) in the saline groundwater at Cliff Pool Sinkhole. The Anchialine Cave (AC) assemblage is a previously undocumented community of foraminifera living in the Bermudian coastal waters, dominated by *Bolivina striatula* (mean 18.5%) and *Rosalina globularis* (mean 9.2%). These taxa are also common in the saline habitats flooded by the upper oxic layer above the hydrogen sulphide layer in Mecherchar Jellyfish Lake (Palau), which is an environment some also consider is anchialine (Lipps and Langer, 1999; Kawagata et al., 2005). With increasing depth into the cave, euryhaline taxa decrease (e.g., *Helenina*, *Ammonia, Discorinopsis*) and stenohaline taxa increase (e.g., *Siphogenerina*, *Nonionella iridea*, *Fursenkoina,* Murray, 2006) because the marine conditions in the saline groundwater are more favorable to foraminifera. Hydrogeologic mixing and vertical tidal oscillation of the halocline likely create temporarily brackish conditions to a depth of ~1 m in the saline groundwater where the euryhaline taxa are persisting. The segregation of

foraminiferal assemblages by haloclines in coastal caves and stratified lagoons can be compared (e.g., Debenay et al., 1998). In stratified lagoons, euryhaline foraminifera colonize habitats flooded by the upper brackish water, with stenohaline taxa found below the halocline (Debenay et al., 1998; Debenay and Guillou, 2002). However, foraminifera living both above and below the halocline in stratified lagoons are still considered part of the greater lagoon environment. In contrast, foraminifera living below the halocline in the distal cave may actually be part of the 'submarine cave environment', and not a part of the 'anchialine cave environment' (Fig. 2.1, Stock et al., 1986). This distinction is important because although the halocline is a critical environmental feature in phreatic caves, subterranean habitats flooded by groundwater cannot be simply considered subterranean stratified lagoons or estuaries. In contrast, they are a unique class of coastal environments that give rise to uniquely adapted cave ecosystems and marine geological processes.

By measuring $\delta^{13}C_{org}$ and C:N in the cave sediment, the quality and source (terrestrial vs. marine) of organic matter can be correlated to the assemblages (Fig. 2.4; Lamb et al., 2006). The source of organic matter is an important ecological variable for benthic foraminifera, causing differential resource partitioning, chemical gradients in the sediments, and microhabitat dysoxia (e.g., Jorissen et al., 1995; De Rijk et al., 2000; Morigi et al., 2001; Abu-Zied et al., 2008; Diz and Francés, 2008; Mojtahid et al., 2009). For example, Mojtahid et al. (2009) found that the quality, quantity and source (terrestrial vs. marine) of organic matter in the Rhône River prodelta (France) controlled benthic foraminifera because different taxa colonized the terrestrial (more refectory) versus more marine (more labile) organic matter. Furthermore, Diz and Francés (2008) found that seasonal phytodetritus caused a rapid response from benthic foraminifera in the

shallow Ria de Vigo embayment (<20 m, Spain) as specific taxa adjusted to the availability of a new food resource (labile phytodetritus). Because Cliff Pool Sinkhole is a point source for both abundant terrestrial materials (sediments, OM, etc.) and some primary productivity, organic matter gradients will like be influencing foraminifera in anchialine cave environments.

Overall, the strongly depleted $\delta^{13}C_{org}$ value of organic matter in the anchialine cave habitats (AC and ML assemblages) indicates it is primarily derived from terrestrial sources (Lamb et al., 2006; Mojitahid et al., 2009; Fig. 2.4). The contribution of any aquatic-based plant tissues from the sinkhole also with a depleted $\delta^{13}C_{org}$ value will likely be minor considering both the small size of the aquatic sinkhole and the large quantity of terrestrial sediments eroding into the cave. The $\delta^{13}C_{org}$ value of the AC assemblage (-23.8‰) is slightly more enriched than the ML assemblage (-24.4‰), indicating the AC assemblage is receiving slightly more marine-based organic matter sources (Table 2.1, Fig. 2.6). This is also supported by a lower C:N ratio in the AC assemblage, as marine organic matter is more nitrogen enriched than terrestrial organic matter (Table 2.1). This is an expected result because some primary productivity will occur in the low light areas near Cliff Pool Sinkhole, causing slightly more marine organic matter to accumulate with the AC assemblage. Therefore, the AC assemblage defines a separate habitat within the anchialine cave environment because although it is in the saline groundwater, it remains *dominated* by terrestrial influences (Stock et al., 1986).

The specific foraminifera inhabiting the anchialine cave environment below Cliff Pool Sinkhole will need adaptations to large quantities of terrestrial organic matter (more refectory), with limited supplies of marine phytodetritis (more labile). For example,

Rosalina globularis is a common taxon in the AC assemblage that passively grazes when food availability is high, but becomes an active forager as food resources diminish (Sliter, 1965). *Bolivina striatula* is also common in the AC assemblage, which is eutrophic and co-occurs with *Buliminella elegantissima* in areas with high quantities of terrestrial organic matter (Patterson et al., 2000; Eichler et al., 2003; Abu-Zied et al., 2008). A by-product of abundant organic matter in the habitats of the AC assemblage will be dysoxia within millimeters of the sediment surface (Corliss, 1991; Bernhard and Sen Gupta, 1997; Diz and Francés, 2008), requiring infaunal biserial and triserial taxa to be at least tolerant to intermittent dysoxia. Although dissolved oxygen in the sediments was not measured in this study, infaunal taxa comprising the AC assemblage such as *Fursenkoina*, *Hopkinsina*, *Bolivina* are known to be tolerant to dysoxia (Kaiho, 1994; Bernhard and Sen Gupta, 1997). The high quantity of refectory terrigenous organic matter, pulsed phytodetritus, and likelihood of sedimentary dysoxia would also explain the high relative abundance of *Textularia earlandi* (max. 9.2%) in the AC assemblage, which is found nowhere else in Green Bay Cave. *Textularia earlandi* is a very opportunistic taxon that is highly tolerant to dysoxia (Bernhard et al., 1997; Alve and Goldstein, 2010). Therefore, we interpret the AC assemblage as primarily controlled by the high volume of terrigenous organic matter entering the cave at Cliff Pool Sinkhole.

The effects of terrigenous organic matter is concentrated near the base of the Cliff Pool Sinkhole, however, and not uniform throughout the entire cave system. Terrigenous organic matter and sedimentary character attenuate in Green Bay Cave with increasing distance away from Cliff Pool Sinkhole, which is easily observed using SCUBA (Fig. 2.6). van Hengstum et al. (2009a, fig. 3B) also observed abundant organic matter around cenotes in a Mexican anchialine cave. This process is related to the attenuation of

terrestrial sediments after they are eroded into the sinkholes. Less than 60 m along the Trunk Passage, the Circulated Submarine Cave assemblage begins (Fig. 2.2, Fig. 2.6) synchronous with prominent sedimentary, organic geochemical, and wholesale faunal changes indicative of an environmental change.

2.7.3 The Boundary Between Anchialine And Submarine Cave Environments

The idea that coastal cave environments can be differentiated from each other is an established concept (Stock et al., 1986). However, a general research focus on the marine ecology of macro-invertebrates and prokaryotes, combined with the limited observation/sampling capability of researchers on SCUBA, has precluded quantitative division of anchialine versus submarine cave environments. As a consequence, the nomenclature of coastal cave environments can be confusing.

Stock et al. (1986) stated that terrestrial influence (either hydrogeological, sedimentological, or chemical) is a prerequisite for anchialine cave environments. Habitats flooded by the meteoric lens are easily categorized as anchialine because they are terrestrially influenced by both hydrogeology (flooded by meteoric water) and terrigenous sediment/chemical fluxes. However, a problem arises when classifying coastal caves because both submarine and anchialine cave environments equally occur in the saline groundwater (Fig. 2.1). So, what characteristics then differentiate anchialine and submarine cave environments (and habitats) flooded by saline groundwater? In our view, the dominant manifestations of 'marine versus terrestrial influence' on anchialine ecosystems can be either through (a) hydrogeological impact on the system from the terrestrial-derived meteoric lens versus the oceanic-derived saline groundwater, and/or (b) the flux of chemicals and sediments entering a cave from either terrestrial or marine

sources, often through physical entrances ('karst windows'). Some of these ideas were presented in Stock et al. (1986), but in practice the differentiation of anchialine versus submarine cave environments has never been quantified and remains equivocal. Therefore, we argue that anchialine cave environments develop in saline groundwater when terrestrial influences *dominate* a phreatic cave and marine influences are subsidiary. This new theoretical framework now allows for anchialine and submarine cave environments to be quantitatively distinguished (e.g. with $\delta^{13}C_{org}$ and C:N).

Green Bay Cave is well suited to quantifying the boundary between these two cave environments because of its intrinsic geomorphology: an anchialine sinkhole entrance is separated from a submarine cave entrance by >250 m of flooded cave passage (Fig. 2.5). Precisely at the shift from the AC to the CSC assemblages, (1) the carbon isotopic signature of bulk organic matter shifts from depleted to more enriched values, indicative of a shift from terrestrial to marine organic matter, (2) the C:N ratio changes indicating the presence of more nitrogen-rich marine organic tissues in the sediment, (3) mean grain-size decreases as allogenic cave sedimentation begins, and (4) there is an overall reduction in bulk organic matter. No measured hydrogeologic shift occurs at this transition that is critical to foraminifera, however, the foraminiferal change (AC to the CSC assemblages) indicates the cave habitat is changing. The foraminiferal shift also reflects the totality of environmental parameters in the cave (sedimentology, organic matter sources and fluxes), not just hydrogeologic parameters. Sample 21 reflects the maximum point where the cave benthos is routinely impacted by terrestrial nutrients, sediments, and organic matter entering into the cave from Cliff Pool Sinkhole. Marine processes begin to dominate the cave benthos beyond sample 21 in the Trunk Passage from Cliff Pool Sinkhole to Harrington Sound (Figs. 2.2, 2.6). Based on the quantified

change from a terrestrial-dominated to a marine-dominated cave environment between S20-S22, we argue that this location marks the boundary between the anchialine and submarine cave environment in the Green Bay System, consistent with the definitions proposed by Stock et al. (1986). Therefore, sedimentological, geochemical, and micropaleontological proxies are useful for differentiating coastal cave environments.

2.7.4 The Submarine Cave Environment

Of all the categories of coastal caves, submarine caves have arguably received the most research attention by global marine ecologists because they host intriguing taxonomic gradations within many phylogenetic groups. The submarine cave entrance to Green Bay Cave begins at Harrington Sound, and ambient light attenuates with increasing distance to the Rat Trap (Fig. 2.7). The inability of Q-mode cluster analysis to differentiate the lagoon entrance samples attests to the similarity of foraminifera in the submarine cave entrance and the lagoon (S47-50, Fig. 2.2). *Quinqueloculina* spp. and other miliolids dominate the Entrance assemblage, consistent with foraminiferal assemblages living in global lagoons (e.g., Haig 1988; Javaux and Scott, 2003). *Quinqueloculina* is an epifaunal, to shallow infaunal, miliolid not tolerant to dysoxia (Corliss, 1991), so the waves and currents impacting the submarine cave entrance must keep the upper sediment layers oxygenated to support the high relative abundance of *Quinqueloculina*. There is an overall attenuation in organic matter with distance into the submarine cave from Harrington Sound (Fig. 2.7), similar to a submarine cave in France (Tremies Cave; Fichez, 1990). Based on $\delta^{13}C_{org}$ and C:N, the organic matter throughout all habitats in the submarine cave environment is derived from marine sources (Table 2.1, Fig. 2.4). Grain-size at the submarine cave entrance is also the coarsest in Green Bay

Cave (mean 302 μm), with abundant fractured shells and sand, which is consistent with the coarse substrate at the entrance to a Japanese submarine cave (Daidokutsu Cave: Omori et al., 2010). Because the submarine cave entrance is open to Harrington Sound, waves and tidal currents will transport lagoonal sediments into the cave. Detailed faunal transitions from the cave opening to the Rat Trap are likely caused by attenuating light and marine organic matter (e.g., *Ammonia beccarii* var. *parkinsoniana*), similarly to how foraminifera respond to these gradients in the anchialine cave entrance (Jorrissen et al., 1995). Omori et al. (2010) documented decreasing light conditions within a Japanese submarine cave over the last ~7 ka using algal symbiotic-bearing foraminifera (e.g., *Amphistegina*). However, only rare taxa with photosymbionts (e.g., *Amphistegina*, *Planorbulina*) were recovered in the Entrance assemblage of Green Bay Cave, located nearest to the cave entrance where ambient light is most available. Therefore, the Entrance assemblage occupies a separate habitat within the submarine cave environment because sample sites are completely flooded by saline groundwater and *dominated* by marine processes, but experiences higher current velocities from wave and tides to create a lagoon-like environment for foraminifera.

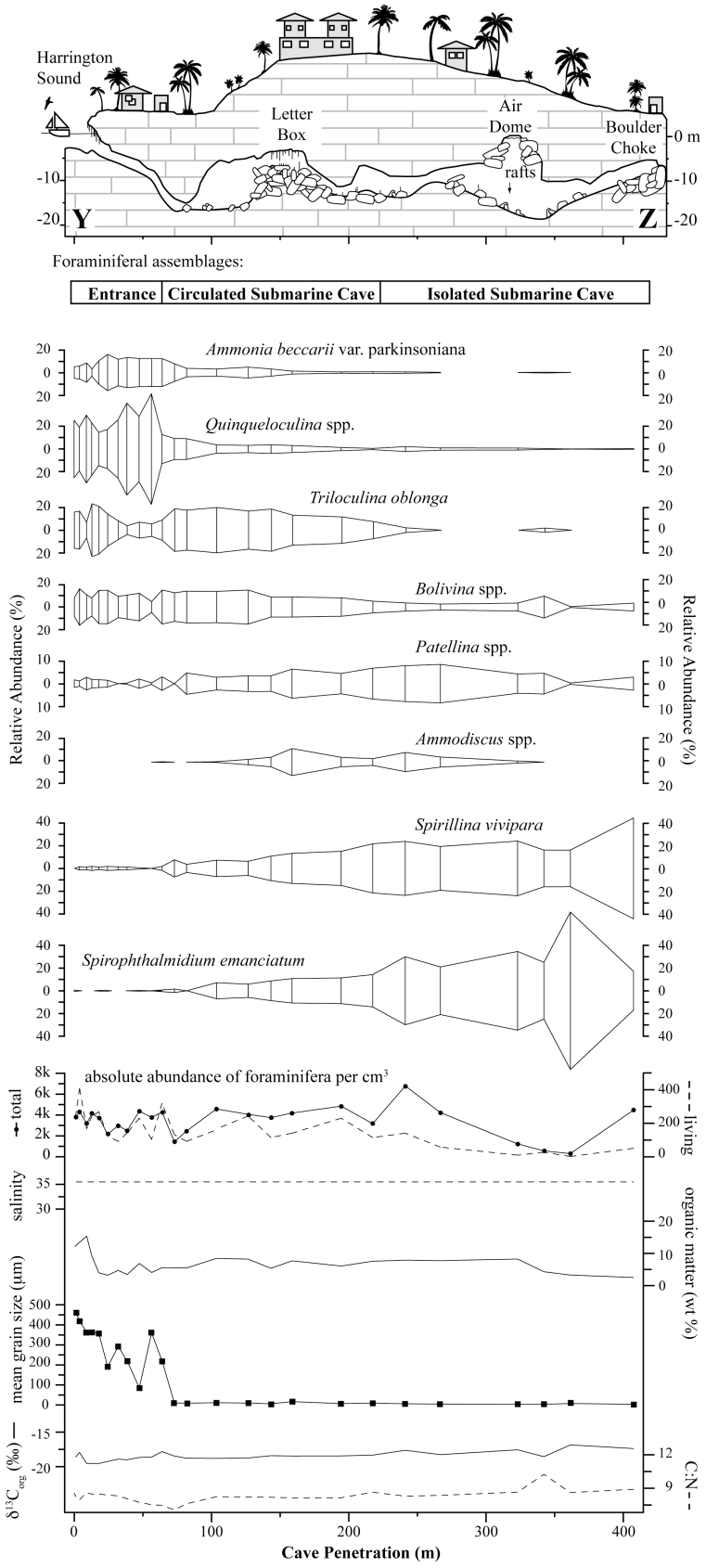

Figure 2.7: Relative abundance of dominant foraminifera along a linear transect from Harrington Sound (Y) to the end of the Green Bay Passage at the boulder choke (Z). This transect emphasizes foraminiferal community structure and environmental parameters with increasing distance from a physical cave exit to the ocean. The abundance of fossil *Archaias* in the sediments at the boulder choke suggests that this cave passage once exited in Harrington Sound (Figure 2.2), but has since been isolated by a historical collapse event.

The Circulated Submarine Cave assemblage begins at the Rat Trap, along with a sedimentological shift from a coarse-grained shell hash to fine-grained carbonate-mud (mean grain-size 14.9 μm), reduced bulk organic matter (mean 8%), and increased $CaCO_3$ (mean 50.9%). Fine carbonate mud also characterizes the inner substrate in Daidokutsu Cave (see fig. 2 in Omori et al., 2010). The most diverse assemblage in Green Bay Cave is the CSC assemblage, which is predominately *Triloculina* and *Spirillina*. Because neither salinity nor dissolved oxygen are ecologically-limiting to foraminifera in the CSC assemblage, and all the OM is derived from nitrogen-rich (labile) marine sources, the CSC assemblage must be responding to some other physical variable. The submarine cave entrance is the main point source for extracaverniculous particulate matter and nutrients entering the cave from Harrington Sound. This is to be expected because tidal circulation daily transports 1960 m^3 of lagoonal (coastal ocean) water into the more distal cave habitats (Cate, 2009), which will contain dissolved nutrients and particulate matter from the ocean (Harrington Sound). Some dissolved nutrients are likely entering the saline groundwater at Cliff Pool Sinkhole, but tidal circulation of the saline groundwater will remain the dominant mechanism for transporting any nutrients up the North Shore Passage (Fig. 2.2). However, both the $\delta^{13}C_{org}$ and C:N ratio indicate that marine organic matter is dominantly fertilizing the CSC assemblage, because marine organic matter is more nitrogen- and carbon-isotopically enriched than terrestrial organic matter (Lamb et al., 2006). As such, the CSC cave assemblage is a part of the submarine cave environment – and not anchialine cave environment – because it is found in passages that are (a) completely flooded by saline groundwater, and (b) marine processes *dominantly* influence the cave benthos (Fig. 2.1, Stock et al., 1986). Therefore, we suggest that the Circulated

Submarine Cave (CSC) assemblage colonizes habitats where the cave benthos and water column receive a constant supply of dissolved nutrients and particulate organic matter from the lagoon through tidally forced saline groundwater circulation.

Tintinnids provide strong supporting evidence that tidally forced saline groundwater circulation of lagoonal nutrients is fertilizing cave habitats where the CSC assemblage is located. The species richness and biomass of plankton is known to decrease with increasing distance into the cave (Garrabou and Flos, 1995), but tintinnids are one of the only planktic ciliates actually preserved in sediment. Although the low number of tintinnids precludes a detailed interpretation of their abundance (Patterson and Fishbein, 1989), they are suitable for an analysis based on presence or absence. Generally, tintinnids are present in The Desert, Trunk Passage, partially up the North Shore Passage, and in the Green Bay Passage (below The Letterbox, Fig. 2.2). Considering that tintinnids feed on particulate matter (Scott et al., 1995), they indicate that the modern water column above the CSC assemblage is regularly supplied with particulate matter to support tintinnid populations. The location of tintinnids in Green Bay Cave (proximal to entrances) also agrees well with sediment trap data from Tremies Cave, a submarine cave in France, where the quantity of particulate matter was found to attenuate with increasing distance into the cave (Fichez, 1990). The only samples containing tintinnids that are not part of the CSC assemblage are S53 and S54, however, these samples alternate with the CSC assemblage indicating at least partial mixing of the water column in that area (Fig. 2.2). Importantly, tintinnids were not recovered in the more distal cave passages (e.g., past the Letter Box) with the ISC assemblage, suggesting nutrients are not being systematically transported there by tidal circulation. However, data on dissolved nutrients distributed throughout Green Bay Cave are needed to test this hypothesis along with the

tintinnid results.

The Isolated Submarine Cave (ISC) assemblage occurs at the most distal passages of the cave, and is dominated by *Spirophthalmidium emaciatum*, *Spirillina vivipara*, *Patellina corrugata*, and bolivinids. Both the ISC and CSC assemblages are dominated by known epiphytic taxa in open water settings (e.g., *Rosalina*, spirillinids: Langer, 1993); but there are no plants in the dark cave because photosynthetically active radiation is non-existent. The lowest quantity of bulk organic matter occurs in the ISC assemblage, which is the most marine-derived organic matter in the entire cave system based on the $\delta^{13}C_{org}$ and C:N (Fig. 2.4). These sediments are even more carbon isotopically enriched than lagoonal sediments in Harrington Sound (Vollbrecht, 1996), which emphasizes the environmental isolation of the ISC assemblage from the lagoon and terrestrial surface. Fine carbonate mud characterizes the substrate in the distal cave, similar to the CSC assemblage. Therefore, the ISC assemblage is colonizing habitats that belong to the submarine cave environment because (a) the cave is completely flooded by saline groundwater and (b) marine processes *dominate* the habitat (Stock et al., 1986).

Foraminifera that favor high organic matter are not abundant in the distal cave with the ISC assemblage. For example, the relative abundance of *Melonis barleeanum* is typically <1% in most sample stations in the ISC assemblage. This is because *M. barleeanum* favors locales receiving abundant organic matter (Caralp, 1989), and so it has the highest relative abundance in cave areas that receive abundant organic matter content (the AC and CSC assemblages, Fig. 2.5). The environmental conditions present in the distal cave likely favor epifaunal and suspension-feeding life modes, or infaunal taxa capable of utilizing and foraging diverse organic matter resources with reduced nutrient availability. *Pattellina* (mean 5.2%) and *Spirillina* (mean 22%) can both adopt epifaunal

suspension-feeding life modes (Langer, 1993), suggesting that they are suited to utilizing suspended food resources transported into the distal cave by circulating saline groundwater. Bolivinds, another common group in the ISC assemblage, are shallow infaunal (0-2 cm) detritivores common in fine-grained sediments (Corliss, 1991; Murray, 2006; Teodoro et al., 2010). The most abundant taxon in the ISC assemblage is *Spirophthalmidium emaciatum* (mean 30.7%), which has only been reported as rare in a few localities, including New Guinea (Haig, 1988), the Mediterranean (Cimerman and Langer, 1991), and in the deep Pacific (Brady, 1884). The poor observational record of this miliolid in open ocean settings is not surprising, considering that it is fragile and likely rapidly degrades in coastal environments. Furthermore, the high relative abundance of *S. emaciatum* in the distal isolated cave indicates it may be an oligotrophic miliolid in its preferred habitat. Decreased nutrient and food resources in the distal cave can be expected to impact foraminiferal diversities because oligotrophy in underwater caves impacts many other faunal groups. The horizontal distance from the cave to the ocean through the eolianite (porous karst) is not impacting the foraminifera, because although the terminus of the North Shore Passage is close to the ocean (<30 m) the foraminiferal diversity remains low and is dominated by *S. emaciatum.* Therefore, dissolved nutrients do not appear to be transported directly through the karst wall from the lagoon, which is consistent with the daily net diffuse outflow of saline groundwater from inside the cave through the porous karst (Cate, 2009). This would further emphasize the control of nutrients (particulate matter, dissolved chemicals, etc.) transported into Green Bay Cave through submarine cave entrance on the cave benthos.

The Air Pocket has no apparent effect on foraminifera, which is caused by the cave intersecting the water table (Fig. 2.2). There is sedimentary evidence for the existence of

the water table, however, because calcite rafts are accumulating below the Air Pocket and not laterally transported in the cave. This occurrence of calcite rafts is expected because they only precipitate at air-water interfaces in caves, a common process observed in Mallorcan littoral caves (Taylor and Chafetz, 2004; fig. 9 in Fornós et al., 2009). According to the classification scheme of Stock et al. (1986), this area may be referred to as littoral cave environment (Fig. 2.1). However, because the Air Pocket is such a spatially limited feature (<2-3 m width) and marine geological processes associated with submarine cave environments remain the dominant influence on the cave benthos, this area remains best described as part of the submarine cave environment.

The *Archaias* tests that were recovered in samples S73 and S61 are not part of the modern total assemblage in the cave because none were ever stained by rose Bengal. The photosymbiotic life mode of *Archaias* is well known, likely explaining the rarity of this taxon in samples near the submarine cave entrance by Harrington Sound. There are no physical exits out to the ocean at these locales, so the question remains as to their origin. These two samples occur at the very back of the cave system up North Shore Passage and Green Bay Passage, the most distal position from any cave opening, in a thin layer of sediment (<3 cm) on a pile of collapsed limestone. Both the North Shore Passage and Green Bay Passage terminate at eolianite breakdown piles, where the cave ceiling has collapsed in the geologic past. The taphonomy of the shells (abraded, fragmented) indicates that they were previously subjected to energetic conditions that are not presently observed in these cave passages where water currents are very minor (Cottey and Hallock, 1988). Based on the collapsed cave ceilings, the lack of *Archaias* in the modern cave environment, and shell taphonomy indicative of transport, we interpret these fauna as related to a time when the cave passages were not collapsed and continued into the

ocean. Under these conditions, the passages would have been ancient submarine cave entrances during previous Late Quaternary sea-level highstands, and photosymbiotic taxa could have been transported into the cave from an adjacent lagoon or reef.

2.7.5 Fossil Cave Foraminifera And Quaternary Sea level

Based on the modern foraminiferal assessment from Green Bay Cave, fossil cave foraminifera can be used as a relative indicator for Quaternary sea level. Pleistocene foraminifera have been found in cave sediments, but confidently interpreting them has been challenging without modern ecologic studies for comparison. Flank margin caves specifically form between the meteoric lens and the saline groundwater from $CaCO_3$-undersaturation at the halocline (Smart et al., 1988; Mylroie and Carew, 1990). Because the halocline is related to the position of sea level, flank margin caves are used as Quaternary sea-level indicators (Mylroie and Carew, 1990; Mylroie, 2008; Mylroie and Mylroie, 2009). Quaternary sea-level highstands, however, have repeatedly flooded coastal caves with groundwater (Ford and Williams, 1989), causing continual reversion of coastal caves to phreatic habitats suitable for aquatic invertebrates and microfossils. This implies that coastal caves can preserve more sea-level information than has been previously inferred, beyond the first-order approximation of determining sea level during flank margin cave formation.

The first step for using microfossils in sea-level analysis will be to associate cave microfossils with a specific category of coastal cave environment (Fig. 2.1). For example, Proctor and Smart (1991) found *Bolivina*, *Ammonia*, *Cibicides*, and *Cassidulina* in Corbridge Cave (UK) sediments at 5.8 m and 7.2 m above modern sea level, which were constrained by U-series dating to 155-116 ka and >210 ka, respectively. By comparison

with foraminifera in Green Bay Cave, the Corbridge Cave microfossils can be attributed to a fossil anchialine cave environment formed during Marine Isotope Stage 5 and 7 sea-level high stands. Similarly, a fossil foraminiferal assemblage in Aktun Ha Cave, Mexico dominated by *Bolivina* and *Rosalina* was attributed to a late Pleistocene anchialine cave habitat by van Hengstum et al. (2009a), which is also consistent with the modern anchialine cave assemblage in Green Bay Cave.

In a more specific scenario, the meteoric lens habitat within the anchialine cave environment can also be detected if diagnostic water brackish indicators are recovered (e.g., *Trochammina inflata, T. macrescens*). Because the elevation of the meteoric lens is very closely related to sea level, fossil meteoric lens fauna can constrain Quaternary sea level. For example, Wilkinson (2006) found fossil *Polysaccammina* and *Pseudothurammina* in elevated marine caves in Bermuda (+21 m) dated to Marine Isotope Stage (MIS) 11; these taxa colonize modern meteoric lens habitats in Bermuda and Mexico (Javaux, 1999; van Hengstum et al., 2008). van Hengstum et al. (2009b) interpreted these taxa and other brackish microfossils as related to +21 m paleo-meteoric lens in Bermuda during MIS 11, which was caused by a sea-level highstand. Lastly, an assemblage of >80% fossil *Helenina anderseni* is present in Maya Blue Cave, Mexico, which is ecologically consistent with the Meteoric Lens assemblage in Cliff Pool Sinkhole, possibly indicates a co-stratigraphic position of a paleo-meteoric lens and sea level (van Hengstum and Reinhardt, unpublished data). Therefore, fossil cave foraminifera will provide no less than a proxy for the minimum position of Quaternary sea level when found in Pleistocene cave sediments.

2.8 Conclusions

1. The anchialine cave environment in Green Bay Cave consists of two habitats colonized by different foraminiferal assemblages: (a) Meteoric Lens assemblage, dominated by euryhaline foraminifera in the brackish meteoric lens in Cliff Pool Sinkhole (e.g., *Helenina*, *Ammonia*, *Trochammina*), and (b) Anchialine Cave assemblage, characterized by a diverse assemblage living below the halocline in saline groundwater near Cliff Pool Sinkhole and dominated by *Rosalina* and *Bolivina*. Salinity differences in the coastal aquifer (meteoric lens versus saline groundwater) are interpreted as the primary ecological control on foraminifera in the anchialine cave environment, secondarily controlled by the sources and flux of terrigenous sediments and organic matter entering the cave.
2. The submarine cave environment consists of three habitats colonized by different foraminiferal assemblages: (a) Entrance assemblage, dominated by typical lagoonal foraminifera (*Quinqueloculina*) on a coarser-grained substrate emplaced by wave action, (b) Circulated Submarine Cave assemblage, characterized by diverse fauna dominated by miliolids and *Spirillinidae* on a carbonate mud substrate that receiving nutrients from tidally-forced saline groundwater circulation, and (c) Isolated Submarine Cave assemblage, dominated by *Spirophthalmidium emaciatum* in the distal cave passages that are most isolated from the tidal supply of nutrient and particulate organic matter.
3. Sedimentological (bulk organics, granulometry) geochemical ($\delta^{13}C_{org}$, C:N), and foraminiferal proxies can define the boundary between the anchialine and submarine cave environment (AC to CSC assemblages, S20-S22). Using these proxies, anchialine cave environments could be faithfully distinguished as where

terrestrial processes dominated the cave, whereas, submarine cave environments were distinguished where marine processes dominated the cave (as per Stock et al., 1986). This addresses the problem of what differentiates anchialine versus submarine cave environments in saline groundwater.

4. These results provide a framework for interpreting Pleistocene cave foraminifera related to previous Quaternary sea-level highstands. However, it remains critical to first establish the specific type of coastal cave environment being addressed—in both modern and ancient scenarios.

2.9 Taxonomy

The following is a list of species, primary references, and any important remarks for taxa from the Bermudian caves. The scanning electron micrographs reflect the emphasis of this study on the cave fauna, for which this represents the first detailed taxonomic investigation. Where appropriate, important synonymies are listed (limited geographic distribution, scarce literature or a rather significant reference). Generic foraminiferal names follow Loeblich and Tappan (1964, 1988), and are all verified in the Ellis and Messina Catalogue of Foraminifera or primary references from the literature. Tintinnid taxonomy follows the exhaustive work of Kofoid and Campbell (1929), upon which modern tintinnid taxonomy is based (e.g., Shackleton and Moore, 1954). All the described characteristics of tintinnid loricae can be observed with standard stereo light microscope at a magnification of 80x.

2.9.1 Foraminifera

Abditodentrix rhomboidalis (Millet)

Figs. 2.8.1-2

Textularia rhomboidalis Millet, 1899, p. 559, Plate 7, Fig. 4a-b.

Bolivina rhomboidalis (Millet) Cushman, 1927, p. 138, pl. 18, fig. 7.

Abditodentrix rhomboidalis (Millet) Cimerman and Langer, 1991, p. 60, pl. 63, figs. 10-11.

Allogromia spp. Rhumbler 1904 p. 206

Remarks: A few rose Bengal stained individuals were recovered in sediment samples saturated by the brackish meteoric lens in Cliff Pool Sinkhole. These were also found in the meteoric lens of Deep Blue Sinkhole (Walsingham Cave System).

Ammobaculites foliaceus (Brady)

Fig. 2.8.3

Lituola (*Haplophragmium*) *foliaceum* Brady, 1881, p. 50, pl. 33, figs. 20-25.

Ammobaculites foliaceus Cushman and McCulloch, 1939, p. 65, figs. 9-10.

Ammobaculites catenulatus Cushman and McCulloch, 1939, p. 65, pl. 7, figs. 11-14.

Ammodiscus planorbis Höglund, 1947

Figs. 2.8.4-5

Ammodiscus planorbis Höglund, 1947, p. 125, pl. 8, fig. 4, pl. 28, figs. 13-16.

Remarks: This species is easily differentiated from *A. tenuis* by its highly-polished brownish test, which is different from *A. planus.* SEM observations of the aperture indicate the test is agglutinated.

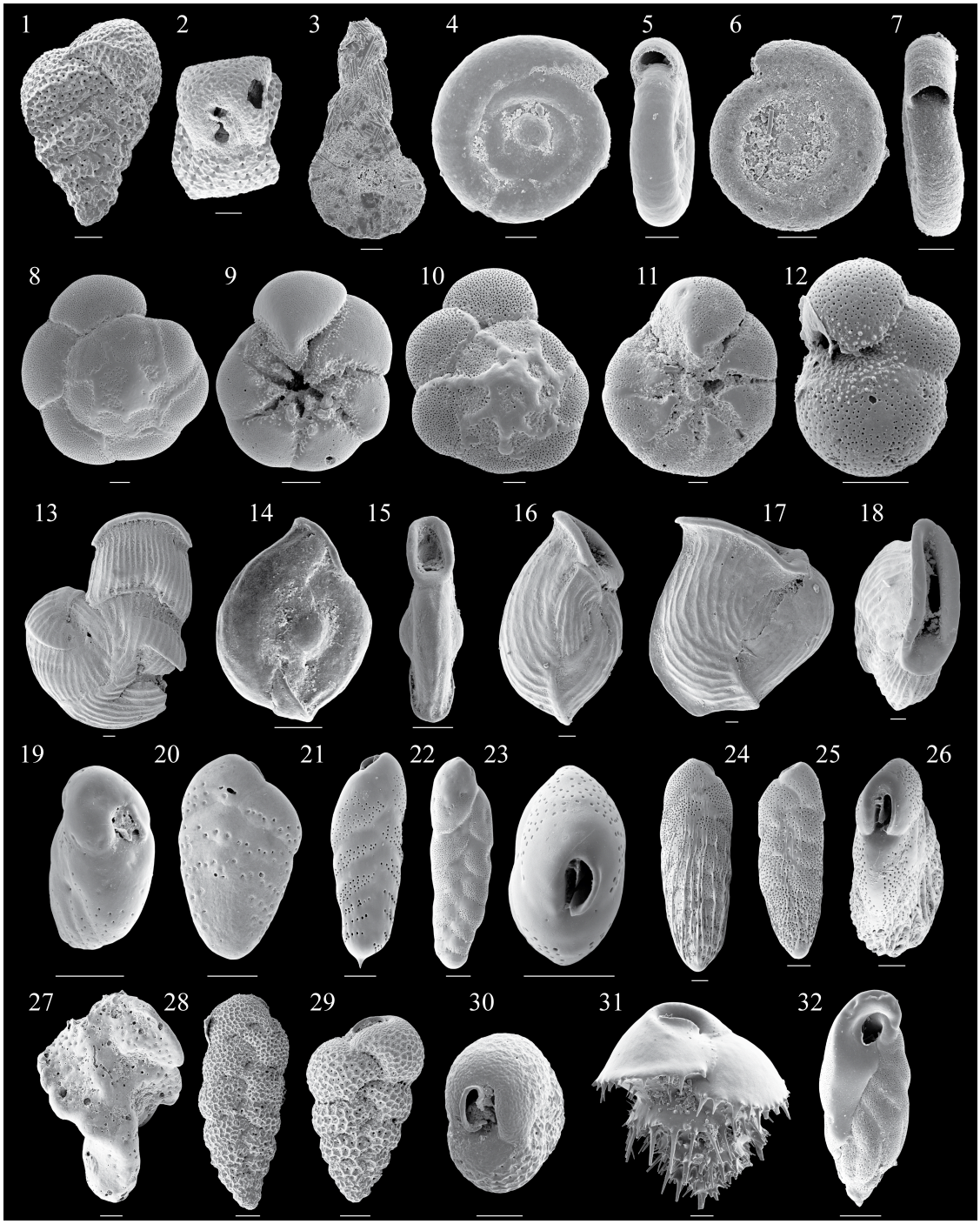

Figure 2.8 (Following page): 1, 2 *Abditodentrix rhomboidalis*; **3** *Ammobaculites foliaceus*; **4, 5** *Ammodiscus planorbis*; **6, 7** *Ammodiscus tenuis*; **8, 9** *Ammonia beccarii* var. *tepida*; **10, 11** *Ammonia beccarii* var. *parkinsoniana*; **12** juvenile *Ammonia beccarii*; **13** *Articulina lineata*; **14, 15** *Articulina multilocularis*; **16** *Articulina pacifica*; **17, 18** *Articulina sagra*; **19, 20** *Bolivina paula*; **21-23** *Bolivina pseudopunctata*; **24-26** *Bolivina striatula*; **27** *Bolivina tortuosa*; **28-30** *Bolivina variabilis*; **31** *Bulimina marginata*; **32** *Buliminella elegantissima*. Scale bar represents 50 μm.

Ammodiscus tenuis Brady, 1847

Figs. 2.8.6-7

Ammodiscus tenuis Brady 1884, p. 332, pl. 38, figs. 4-6.

Ammonia beccarii var. *parkinsoniana* d'Orbigny, 1839a

Figs. 2.8.10-11

Rosalina parkinsoniana d'Orbigny, 1839a, Plate 4, figs. 25-27

Ammonia beccarii (Linné, 1758) var. *parkinsoniana* d'Orbigny, 1839a

Ammonia beccarii var. *tepida* Cushman, 1926a

Figs. 2.8.8-9

Rotalia beccarii var. *tepida* (Cushman, 1926a)

Ammonia beccarii (Linné, 1758) forma *tepida* (Cushman, 1926a; imaged in Hayward et al., 2003, p. 353, pl. 1, figs. 1-8.)

Remarks: Despite the intergradation between phenotypes in the genus *Ammoina* (Schnikter, 1971; Walton and Sloan, 1990), two distinct ecophenotypes of *A. beccarii* can be observed in Bermudian caves. The *A. beccarii* forma *tepida* is found in the anchialine cave environment, characterized by a larger test, more lobed periphery, and typically lacks an umbilical plug.

Amphistegina lessonii d'Orbigny, 1826

Amphistegina lessonii d'Orbigny, 1826, p. 304, no. 3, pl. 17, figs. 1-4.

Archaias angulatus (Fichtel and Moll, 1798)

Nautilus angulatus Fichtel and Moll, 1798 (1803 - 2nd edn.), p. 112, pl. 21, 23.

Archaias angulatus Cushman, 1928, p. 218, pl. 31.

Articulina lineata Brady, 1884

Fig. 2.8.13

Articulina lineata Brady, 1884, p. 183, pl. 12, fig. 19-21.

Articulina carinata Cushman, 1944a, p. 15, pl. 3, figs, 18-20.

Articulina multilocularis Brady, Parker and Jones, 1888

Figs. 2.8.14-15

Articulina multilocularis Brady, Parker and Jones, 1888, p. 215, pl. 40, fig. 10.

Articulina pacifica Cushman, 1944

Fig. 2.8.16

Articulina pacifica Cushman, 1944a, p. 17, pl. 14-18, figs. 15-16.

Articulina sagra d'Orbigny, 1839a

Figs. 2.8.17-18

Articulina sagra d'Orbigny, 1839a, p. 160, pl. 9, figs. 23-26.

Asterigerina carinata d'Orbigny, 1839a

Asterigerina carinata d'Orbigny, 1839a, p. 118, pl. 5, fig. 25; pl. 6, figs. 1-2.

Bolivina paula Cushman and Cahill, 1932

Figs. 2.8.19-20

Bolivina paula Cushman and Cahill, 1932, p. 84, pl. 12, fig. 6.

Bolivina pseudopunctata Höglund, 1947

Figs. 2.8.21-23

Bolivina pseudopunctata Höglund, 1947, p. 273, pl. 24, fig. 5a-b; pl. 32, figs. 23-24.

Bolivina striatula Cushman, 1922

Figs. 2.8.24-26

Bolivina striatula Cushman, 1922, p. 27, pl. 3, fig. 10.

Remarks: There is wide variability in number and development of striations on the test. Some tests can even appear almost devoid of striations under light microscopy, but are clearly striated when observed with scanning electron microscopy.

Bolivina tortuosa Brady, 1881

Fig. 2.8.27

Bolivina tortuosa Brady, 1881, p. 57, pl. 52, figs. 31-34.

Bolivina variabilis (Williamson)

Figs. 2.8.28-30

Textularia variabilis Williamson, 1858, p. 76, pl. 6, figs. 162-163.

Bolivina subexcavata Cushman and Wickenden, 1929, p. 9, pl. 4, figs. 4a-b.

Remarks: Some authors consider the *B. variabilis* (Williamson), *B. subexcavata* Cushman and Wickenden, and *Abditodentrix rhomboidalis* (Millet) intragradational morphotypes of the same species. At the present time, I consider *B. variabilis* (Williamson), *B. subexcavata* Cushman and Wickenden intragradational, and use the senior synonym of Williamson (1858).

Broeckina orbitolitoides (Hofker)

Praesorites orbitolitoides Hofker, 1930, p. 149, pl. 55, figs. 8, 10, 11, pl. 57, figs. 1-5, pl. 61, figs. 3, 14.

Broeckina orbitolitoides (Hofker) Munier-Chalmas, 1882

Bulimina consectata (McCulloch, 1977)

Figs. 2.9.1-2

Neobulimina consectata McCulloch, 1977, p. 242, pl. 106, figs. 1a-b.

Bulimina consectata (McCulloch) van Hengstum and Scott, 2011, figs 2.9.1-2.

Bulimina marginata d'Orbigny, 1826

Fig. 2.8.31

Bulimina marginata d'Orbigny, 1826, p. 269, pl. 12, figs. 10-12.

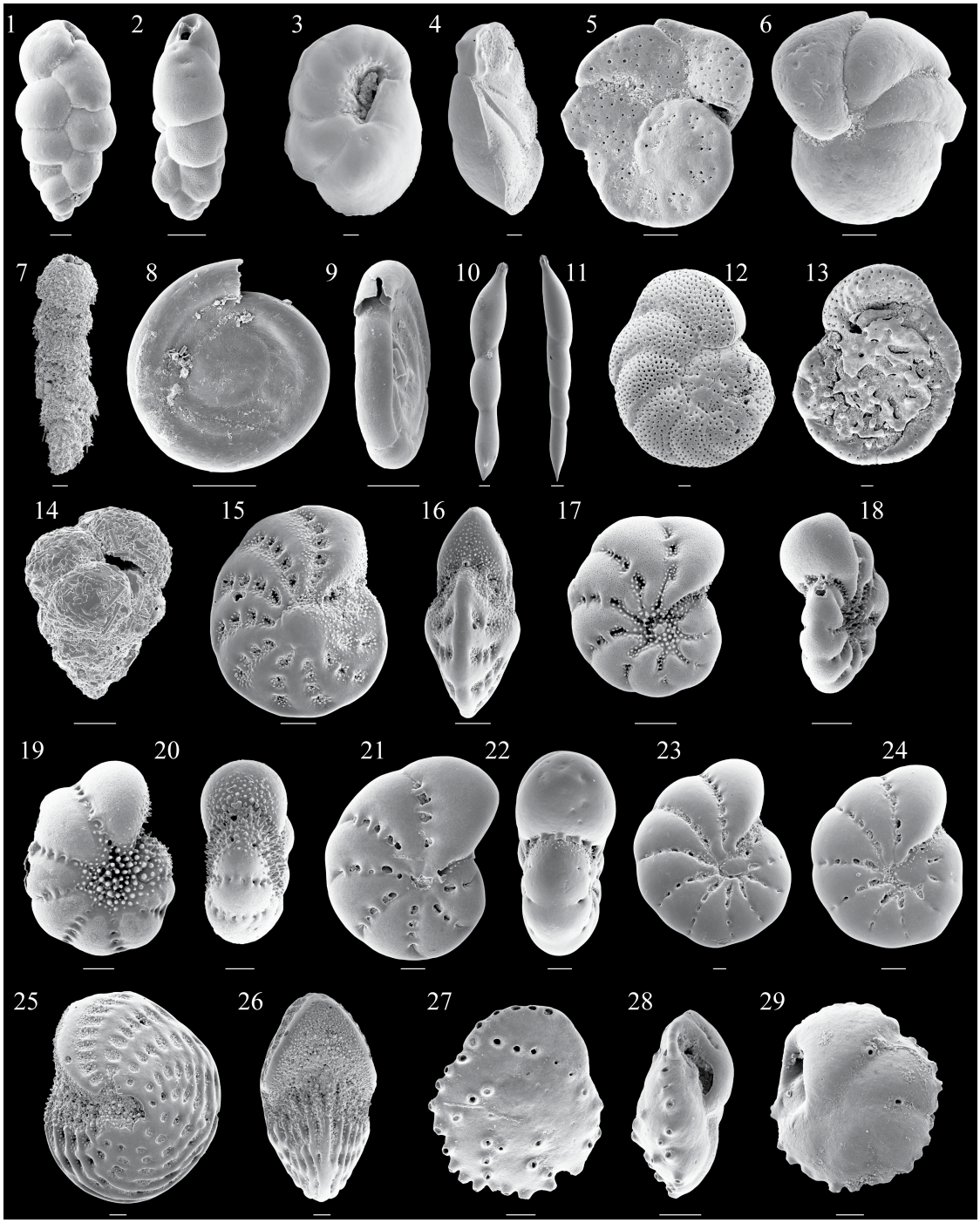

Figure 2.9: 1, 2 *Bulimina consectata*; **3, 4** *Cancris sagra*; **5, 6** *Cibicides lobatulus*; **7** *Clavulina tricarinata*; **8, 9** *Cyclogyra involvens*; **10, 11** *Dentalina communis*; **12, 13** *Discorinopsis aguayoi*; **14** *Eggerella scabra*; **15, 16** *Elphidium advenum*; **17, 18** *Elphidium frigidum*; **19, 20** *Elphidium norvangi*; **21-24** *Elphidium excavatum*; **25, 26** *Elphidium sagra*; **27-28** *Epistominella pulchra*. Scale bar represents 50 μm.

Buliminella elegantissima (d'Orbigny)

Fig. 2.8.32

Bulimina elegantissima d'Orbigny, 1839b, p. 51, pl. 7, figs. 13-14.

Buliminella elegantissima (d'Orbigny) Cushman, 1919, p. 606

Cancris sagra (d'Orbigny) Figs. 2.9.3-4

Rotalina sagra d'Orbigny, 1839a, p. 77, pl. 5, figs. 13-15.

Cancris sagra (d'Orbigny) Parker, 1954, pl. 10, fig. 15, fig. 21.

Cibicides lobatulus (Walker and Jacob)

Figs. 2.9.5-6

Nautilus lobatulus Walker and Jacob, 1798, p. 642, pl. 14, fig. 36.

Cibicides lobatulus (Walker and Jacob) Cushman, 1927, p. 170, pl. 27, figs. 12-13.

Clavulina tricarinata d'Orbigny, 1839a

Fig. 2.9.7

Clavulina tricarinata d'Orbigny, 1839a, p.111, pl. 2, figs. 16-18.

Cyclogyra involvens (Reuss)

Figs. 2.9.8-9

Operculina involvens Reuss, 1850, p. 370, pl. 46, fig. 20.

Cyclogyra involvens (Reuss) Bock, 1971, p. 12, pl. 3, fig. 2.

Cymbaloporetta squammosa (d'Orbigny)

Rosalina squammosa d'Orbigny, 1839a, p. 91, pl. 3, figs. 12-14.

Cymbaloporetta squammosa (d'Orbigny) Cushman, 1922, p. 41, pl. 6, figs. 4-6.

Dentalina communis (d'Orbigny)

Figs. 2.9.10-11

Nodosaria (*Dentaline*) *communis* D'Orbigny, 1826, pl. 1, fig. 4.

Discorinopsis aguayoi (Bermúdez)

Figs. 2.9.12-13

Discorbis aguayoi Bermúdez, 1935, p. 204, pl. 15, figs. 10-14.

Discorinopsis aguayoi (Bermúdez) Phleger, Parker, and Peirson, 1953, p. 7, pl. 4, figs. 23-24.

Eggerella scabra (Williamson)

Fig. 2.9.14

Bulimina scabra Williamson, 1858, pl. 5, figs. 136-147.

Eggerella scabra (Williamson) Daniels, 1970, p. 70, fig. 46, pl. 2, fig. 5.

Elphidium advenum (Cushman)

Figs. 2.9.15-16

Polystomella advena Cushman 1922, p. 56, pl. 9, figs. 11-12.

Elphidium advenum Cushman, 1930, p. 25, pl. 10, figs. 1-2.

Elphidium crispum (Linné)

Nautilus crispus Linné, 1758, p. 709, pl. 1, figs. 2d-f.

Polystomella crispa d'Orbigny 1846, p. 125, pl. 6, figs. 9-14.

Elphidium crispum (Linné) Cushman and Grant, 1927, p. 73, pl. 7, figs. 3a-b.

Elphidium excavatum

Figs. 2.9.21-24

Polystomella excavata Terquem, 1876, p. 429, pl. 2, figs. 4a-b.

Elphidium excavatum (Terquem) Cushman, 1930, p. 21, pl. 8, figs.1-7.

Elphidium c.f. *frigidum* Cushman, 1933b

Figs. 2.9.17-18

Elphidium frigidum Cushman, 1933b, p. 5, pl. 1, figs. 8a-b.

Elphidium norvangi Buzas, Smith, and Beam, 1977

Figs. 2.9.19-20

Elphidium norvangi Buzas, Smith, and Beam, 1977, p. 96, pl. 7, figs. 1-4.

Elphidium oceanicum (Cushman) Kawagata et al., 2005, pl. 3, figs. 10-11.

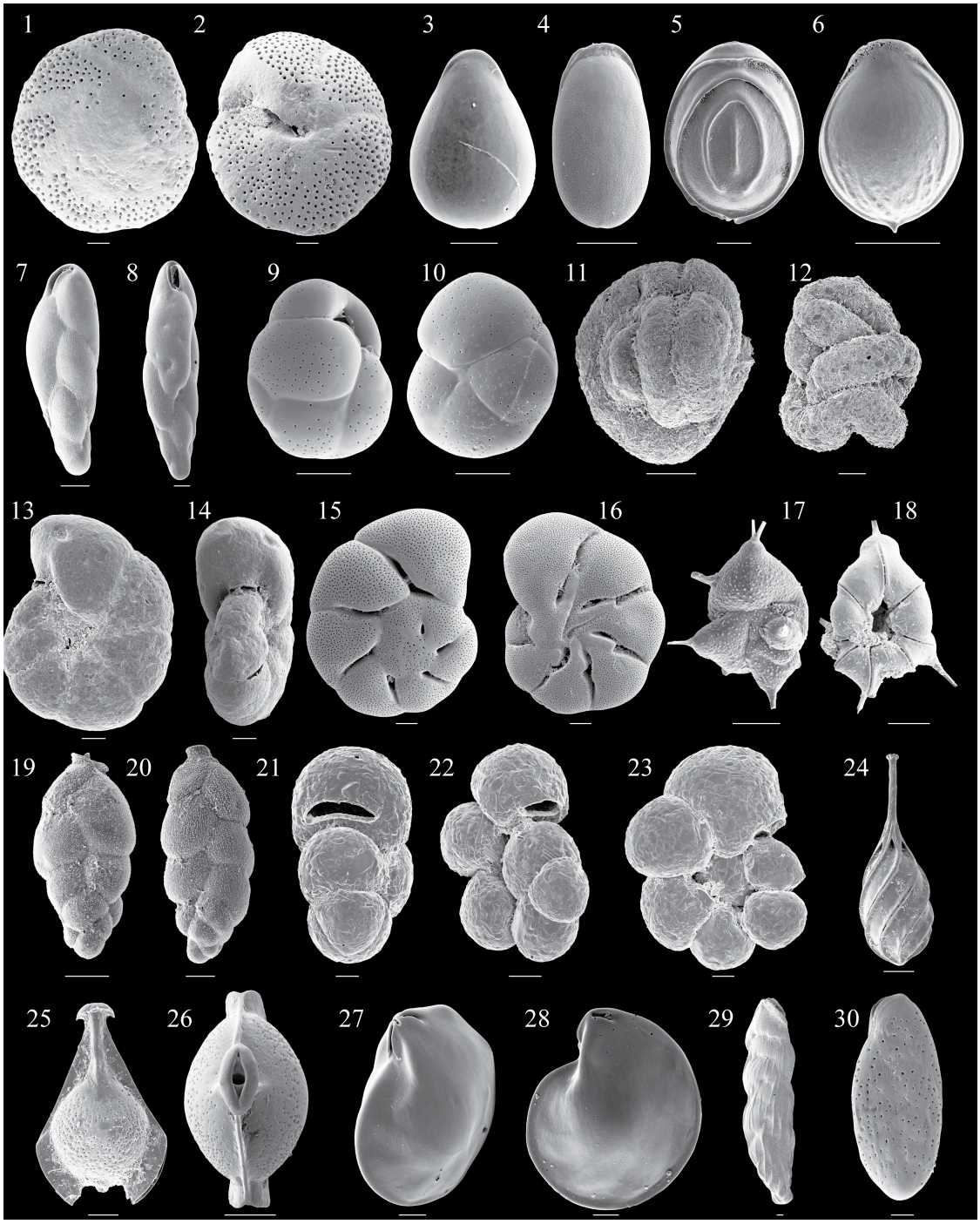

Figure 2.10: 1, 2 *Eponides antillarum*; **3, 4** *Fissurina lucida*; **5** *Fissurina* sp; **6** *Fissurina evoluta*; **7, 8** *Fursenkoina compressa*; **9, 10** *Globocassidulina subglobosa*; **11** *Glomospira charoides*; **12** *Glomospira irregularis*; **13, 14** *Haplophragmoides wilberti*; **15, 16** *Helenina anderseni*; **17, 18** *Rotaliella arctica*; **19, 20** *Hopkinsina pacifica*; **21-23** *Labrospira evoluta*; **24** *Lagena spiralis*; **25, 26** *Lagenosolenia* sp.; **27, 28** *Lenticulina iota*; **29** *Loxostoma mayori*; **30** *Loxostoma rostrum*. Scale bar represents 50 μm.

Elphidium sagra (d'Orbigny)

Figs. 2.9.25-26.

Polystomella sagra d'Orbigny, 1839a, p. 55, pl. 6, figs. 19-20.

Elphidium sagrum Cushman, 1930, p. 24, pl. 9, figs 5-6.

Epistominella pulchra (Cushman)

Figs. 2.9.27-29

Pulvinulina pulchra Cushman, 1933a, p. 92, pl. 9, fig. 19.

Eponides antillarum (d'Orbigny)

Figs. 2.10.1-2

Rotalina antillarum d'Orbigny, 1839a, p. 75, pl. 5, figs. 4-6.

Eponides antillarum (d'Orbigny) Parker, 1954, p. 528, pl. 9, figs. 14-15.

Eponides spp.

Remarks: These rare individuals were not identified to the species level.

Fissurina lucida (Williamson)

Figs. 2.10.3-4

Entosolenia marginata (Montagu) var. lucida Williamson, 1848, p. 17, pl. 2, fig. 17.

Entosolenia lucida (Williamson) Cushman and Gray, 1946, p. 30, pl. 5, figs 16-18.

Fissurina lucida (Williamson) Loeblich and Tappan, 1953, p. 76-77, pl. 14, fig. 4.

Fissurina evoluta McCulloch, 1977

Fig. 2.10.6

Fissurina evoluta McCulloch, 1977, p. 104-105, pl. 58, figs. 11-12, 18.

Fissurina sp.

Fig. 2.10.5

Remarks: This individual was unidentified to the specific level.

Fursenkoina compressa (Bailey)

Figs. 2.10.7-8

Bulimina compressa Bailey 1851, p. 12, pl. 12, figs. 35-37.

Virgulina compressa (Bailey) Phleger and Parker, 1951, p. 49, pl. 9, figs. 4-5.

Fursenkoina compressa (Bailey) Loeblich and Tappan, 1961, p. 314.

Globocassidulina subglobosa (Brady)

Figs. 2.10.9-10

Cassidulina subglobosa Brady, 1881, p. 60, pl. 54, figs. 17a-c.

Cassidulina subglobosa (Brady) Bock et al., 1971, p. 64, pl. 23, fig. 12; Javaux, 1999, p. 314, pl. 2, fig. 10.

Globocassidulina subglobosa (Brady) Jones, 1994, p. 60, pl. 54, figs. 17a-c.

Glomospira charoides (Jones and Parker)

Fig. 2.10.11

Trochammina squamata Jones and Parker var. *charoides* Jones and Parker, 1860, p. 304, (not imaged).

Glomospira charoides (Jones and Parker) Höglund, 1947, p. 129, pl. 3, fig. 11.

Glomospira irregularis (Grzybowski)

Fig. 2.10.12

Ammodiscus irregularis Grzybowski, 1898, p. 285, pl. 11, figs. 2-3.

Glomospira irregularis (Grzybowski) Geroch, 1960, pl. 8, figs. 11-12.

Haplophragmoides wilberti Anderson, 1953

Figs. 2.10.13-14.

Haplophragmoides wilberti Anderson, 1953, p. 21, pl. 4, fig. 7.

Helenina anderseni (Warren)

Figs. 2.10.15-16

Pseudoeponides anderseni Warren, 1957, p. 39, pl. 4, figs. 12-15.

Helenina anderseni (Warren) Saunders, 1961, p. 148.

Homotrema rubra (Lamarck)

Milipora rubra Lamarck, 1816, p. 202.

Homotrema rubra Hickson, 1911, p. 445, pl. 30, fig. 2.

Hopkinsina pacifica Cushman, 1933a

Figs. 2.10.19-20

Hopkinsina pacifica Cushman, 1933a, p. 86, pl. 8, fig. 16.

Labrospira evoluta (Natland)

Figs. 2.10.21-23

Haplophragmoides evoluta Natland, 1938, p. 138, pl. 3, figs. 5-6.

Labrospira evoluta (Natland) van Hengstum and Scott, figs. 2.10.21-23.

Remarks: This individual is placed within the genus *Labrospira* Höglund because it is partially evolute with a single areal aperature, not at the base of apertural face as in *Haplophragmoides* Cushman; and without a row of areal apertural openings characteristic of *Cribrostomoides* Cushman (as per Loeblich and Tappan, 1987).

Lagena spiralis Brady, 1884

Fig. 2.10.24

Lagena spiralis Brady, 1884, p. 448, pl. 114, fig. 9.

Lagenosolenia sp.

Figs. 2.10.25-26

Lenticulina iota (Cushman)

Figs. 2.10.27-28

Cristellaria iota Cushman, 1923, p. 111, pl. 70, figs. 4-6.

Lenticulina iota (Cushman) Barker, 1960, pl. 60, figs. 4-6.

Loxostoma mayori (Cushman)

Fig. 2.10.29

Bolivina mayori Cushman 1922, p. 40, pl. 3, figs. 5-6.

Loxostoma mayori (Cushman) Bermudéz, 1935, p. 197; Javaux, 1999, pl. 6, fig. 21 (sideview; Not pl. 3, fig. 20)

Loxostoma rostrum Cushman, 1933a

Fig. 2.10.30

Loxostoma rostrum Cushman, 1933a, p. 82, pl. 8, figs. 13a-b,

Loxostomum porrectum (Brady) Javaux, 1999, p. 335, pl. 3 fig. 21

Melonis barleeanum (Williamson)

Figs. 2.11.1-2

Nonionina barleeana Williamson, 1858, p. 32, pl. 3, figs. 68-69.

Melonis barleeanum (Williamson) Corliss, 1991, p. 2, figs. 9-10.

Metarotaliella simplex (Grell)

Figs. 2.11.3-5

Rotaliella simplex Grell, 1979, p. 11, pl. 2, figs. 1-4.

Metarotaliella sp. Pawlowki and Lee, 1991, p. 153, pl. 2, fig. 5.

Metarotaliella simplex (Grell) Loeblich and Tappan, 1987, p. 564, pl. 616, figs. 1-3

Metarotaliella simplex (Grell) Usera et al., 2002, p. 145, fig. 3 (7).

Metarotaliella simplex (Grell) var. *spinosa* van Hengstum and Scott, n. var.

Figs. 2.11.6-7

Remarks: The spinose and non-spinose variants always co-existed, therefore we are not confident this represents a new species at this stage. The characteristics of the aperture are identical to *M. simplex*.

Miliammina fusca (Brady)

Figs. 2.11.8-9

Quinqueloculina fusca Brady, 1870, p. 286, pl. 11, figs. 2-3.

Miliammina fusca (Brady) Phleger and Walton, 1950, p. 280, pl. 1, figs. 19a-b.

Miliolinella circularis (Bornemann)

Figs. 2.11.10-11

Triloculina circularis Bornemann, 1855, p. 349, pl. 19, figs 4a-c.

Miliolinella circularis (Bornemann) Brady, 1884, p. 169, pl. 4, fig. 3; pl. 5, figs. 13-14.

Miliolinella subrotunda (Montagu)

Figs. 2.11.12-13

Vermiculum subrotundum Montagu, 1803, p. 521.

Miliolinella subrotunda (Montagu) Haynes, 1973, p. 36, pl. 5, figs. 5-6; pl. 32, figs. 8-9.

Figure 2.11: 1, 2 *Melonis barleeanum*; **3-5** *Metarotaliella simplex*; **6, 7** *Metarotaliella simplex* var. *spinosa*; **8, 9** *Miliammina fusca*; **10, 11** *Miliolinella circularis*; **12, 13** *Miliolinella subrotunda*; **14, 15** *Mychostomina revertens*; **16-18** *Nonion pauperata*; **19-21** *Nonionella atlantica*; **22, 23** *Nonionella iridea*; **24, 25** *Parvigenerina arenacea*; **26, 27** *Parvigenerina bigenerinoides*. Scale bar represents 50 μm.

Mychostomina revertens (Rhumbler)

Figs. 2.11.14-15

Spirillina vivipara (Ehrenberg) var. revertens Rhumbler, 1906, p. 32, pl. 2, figs. 8-10.

Mychostomina revertens (Rhumbler) Loeblich and Tappan, 1994, p. 36, pl. 52, figs. 1-13.

Nonion pauperata Balkwill and Wright, 1885

Figs. 2.11.16-18

Nonion pauperata Balkwill and Wright, 1885, p. 353, pl. 13, figs. 25-26.

Nonionella atlantica Cushman, 1947

Figs. 2.11.19-21

Nonionella atlantica Cushman, 1947, p. 90, pl. 20, figs. 4-5.

Nonionella iridea Heron-Allen & Earland, 1932

Figs. 2.11.22-23

Nonionella iridea Heron-Allen and Earland, 1932, p. 438, pl. 16, figs. 14-16.

Parvigenerina arenacea (Heron-Allen and Earland)

Figs. 2.11.24-25

Bifarina porrecta (Brady) var. *arenacea* Heron-Allen and Earland, 1922, p. 132, p. 4, figs. 23-26.

Parvigenerina arenacea (Heron-Allen and Earland) Loeblich and Tappan, 1987, p. 68, pl. 123, 13-16.

Parvigenerina bigenerinoides (Lacroix)

Figs. 2.11.26-27

Textularia bigenerinoides Lacroix, 1932, p. 24, pl. 24, fig. 27; pl. 25, figs. 28-31.

Parvigenerina bigenerinoides (Lacroix) Seiglie, 1974, (not imaged).

Remarks: Seiglie (1974) considered *P. bigenerinoides* (Lacroix) a junior synonym of *Textularia fusiformis* Chaster (1892), and placed them all under *P. fusiformis*. There is no evidence of the later uniserial phase in the hypotype in the Ellis and Messina catalgue, or description by Chaster of a later uniserial stage characteristic of *Parvigenerina*. As such, *Textularia fusiformis* Chaster (1892) likely belongs in the genera *Pseudobolivina*, and *P. bigenerinoides* (Lacroix) stands.

Patellina corrugata Williamson, 1958

Figs. 2.12.1-3

Patellina corrugata Williamson, 1958, p. 46, pl. 3, figs. 86-89.

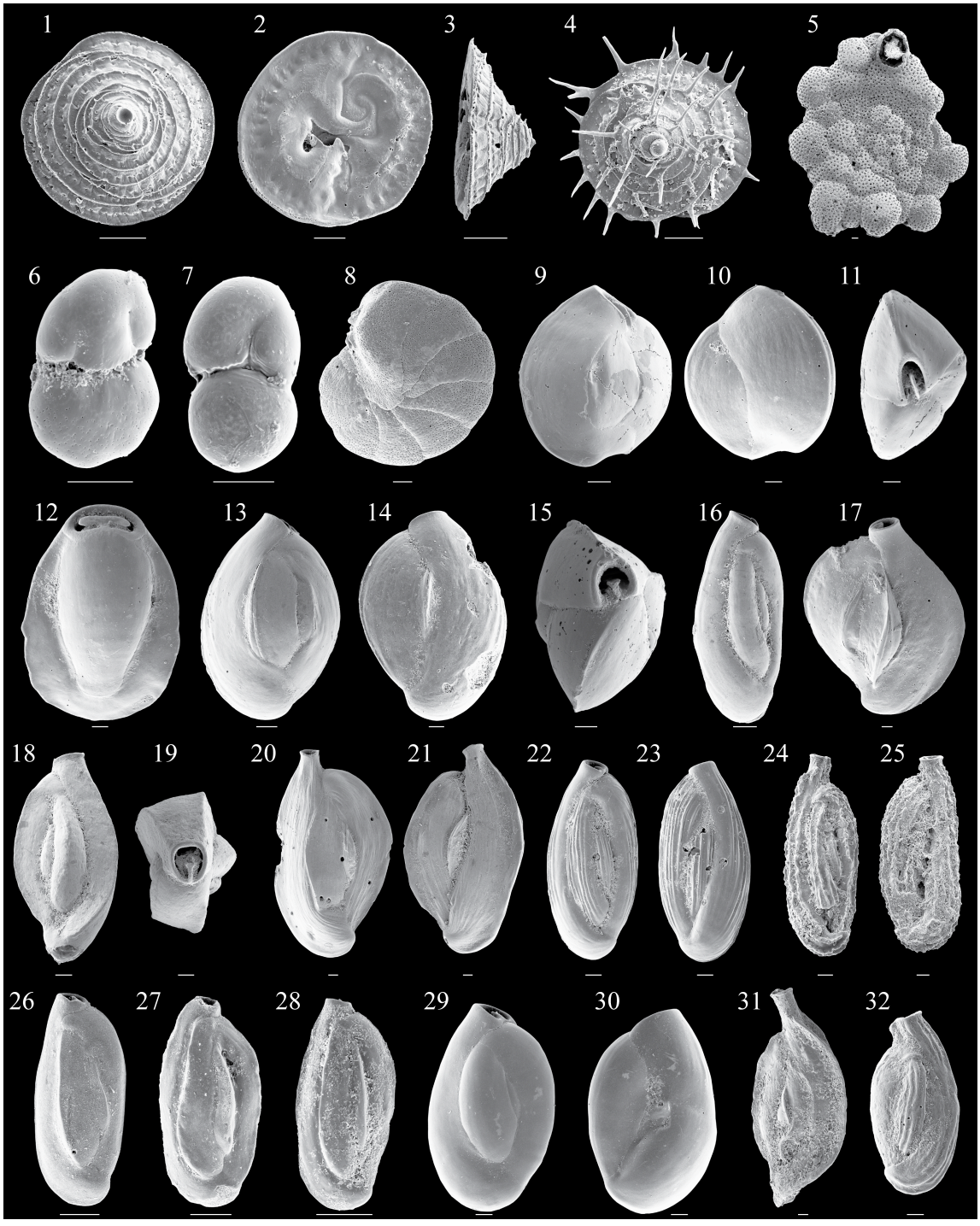

Figure 2.12: 1-3 *Patellina corrugata*; **4** *Patellina corrugata* var. *spinosa*; **5** *Planorbulina mediterranensis*; **6, 7** *Physalidia simplex*; **8** *Peneroplis pertusus*; **9-11** *Quinqueloculina auberiana*; **12** *Pyrgo denticulata*; **13-15** *Q. bicarinata*; **16** *Q. bosciana*; **17** *Q. candeiana*; **18, 19** *Q. contorta*; **20, 21** *Q. candeiana*; **22, 23** *Q. laevigata*; **24, 25** *Q. subpoeyana*; **26-28** *Q. quinquecarinata*; **29, 30** *Q. seminulum*; **31** *Q. polygona*; **32** *Q. tenagos*. Scale bar represents 50 μm.

Patellina corrugata Williamson, 1958 var. *spinosa* Zheng, 1979

Fig. 2.12.4

Patellina corrugata Williamson, 1958, p. 46, pl. 3, figs. 86-89.

Patellina spinosa Zheng, 1979, p. 177-178, pl. 21, figs. 12a-c.

Remarks: Although this form was given species status, spines are not a taxonomic feature. We suspect the spines are simply an adaptation, as spines were also observed on *Spirillina vivipara* in Walsingham Cave (Bermuda), where one side was completely ornamented, but the other remained smooth. The aperture is identical in both forms

Peneroplis carinatus d'Orbigny, 1839b

Peneroplis carinatus d'Orbigny, 1839b, p. 33, pl. 3, figs. 7-8.

Peneroplis pertusus Forskål, 1775

Fig. 2.12.8

Peneroplis pertusus Forskål, 1775, p. 125 (not figured).

Peneroplis pertusus (Forskål) Brady, 1884, pl. 13, figs. 16-17.

Peneroplis proteus (d'Orbigny)

Peneroplis protea d'Orbigny, 1839a, p. 60, pl. 7, figs. 7-11.

Physalidia simplex Heron-Allen and Earland, 1928

Figs. 2.12.6-7

Physalidia simplex Heron-Allen and Earland, 1928, p. 288, pl. 1, figs. 1-2.

Physalidia simplex (Heron-Allen and Earland) Loeblich and Tappan, 1964, fig. 462-2, Loeblich and Tappan (1988), p. 547, pl. 592, figs. 7-8.

Ammonia tepida var. juvenile van Hengstum et al. 2008, p. 314, pl. 1, fig. 13; van Hengstum, 2008, fig. 3-S3.18; Gabriel et al., 2009 (not figured); van Hengstum et al., 2009a (not figured).

Remarks: This individual is common in both Mexican (Yucatan) and Bermudian anchialine caves, colonizing both the meteoric lens and saline groundwater. It is quite euryhaline, as rose Bengal stained individuals have been recovered from a wide salinity range (1.5 - 35 ppt; van Hengstum et al., 2008, 2009a, this paper, Guillem, 2007). Howevever, they seem to be most abundant in the oligohaline to polyhaline range (see discussion in Chapter 6). In Mexico, sub-fossil assemblages of almost 100% *P. simplex* were recovered by Gabriel et al., (2009) and were originally identified as juvenile *Ammonia beccari* var. tepida. Guillem (2007) also suspected they were juveniles, and came to the same conclusion here that these represent the morphology of the species. However, these individuals are planispiral and evolute (never trochospiral), only ever attain three chambers, with an interiomarginal aperture. Our specimens are identical to the figured specimen of Loeblich and Tappan (1988) and Guillem (2007).

Planorbulina mediterranensis d'Orbigny, 1826

Fig. 2.12.5

Planorbulina mediterranensis d'Orbigny, 1826, p. 280, pl. 14, figs. 4-6.

Planulina exorna Phleger and Parker, 1951

Planulina exorna Phleger & Parker, 1951, p. 32, pl. 18, figs. 5-7; 8a-b.

Planulina wuellerstorfi (Schwager)

Anomalina wüellerstorfi Schwager, 1866, p. 258, pl. 7, figs. 105, 107.

Planulina wuellerstorfi (Schwager) Cushman, 1929, p. 104, pl. 15, figs. 1-2.

Pyrgo denticulata (Brady)

Fig. 2.12.12

Biloculina ringens (Lamarck) var. *denticulata* Brady, 1884, p. 143, pl. 3, figs. 4-5.

Pyrgo denticulata (Brady) Cushman, 1929, p. 80, pl. 33, fig. 1; Bock et al. 1971, p. 23, pl. 8, fig. 11.

Pyrgo elongata (d'Orbigny)

Biloculina elongata d'Orbigny, 1826, p. 298, (not figured).

Pyrgo elongata (d'Orbigny) Cushman, 1929, p. 70, pl. 19, figs. 2-3; Bock, 1971, p. 23, pl. 8, fig. 12.

Quinqueloculina auberiana d'Orbigny, 1839a

Figs. 2.12.9-11

Quinqueloculina auberiana d'Orbigny, 1839a, p. 193, pl. 12, figs. 1-3.

Quinqueloculina compressiostoma Zheng, 1988, p. 197, pl. 5, fig. 6, pl. 30, figs. 7-9.

Quinqueloculina bicarinata d'Orbigny, 1826

Figs. 2.12.13-15

Quinqueloculina bicarinata d'Orbigny, 1826, p. 136, pl. 7, figs. 3a-c; Haig, 1988, p. 233, pl. 5, figs. 1-5.

Quinqueloculina bosciana d'Orbigny, 1839a

Fig. 2.12.16

Quinqueloculina bosciana d'Orbigny, 1839a, p. 191, pl. 11, figs. 22-24.

Quinqueloculina candeiana d'Orbigny, 1839a

Fig. 2.12.17

Quinqueloculina candeiana d'Orbigny, 1839a, p. 199, pl. 12, figs. 24-26.

Quinqueloculina collumnosa Cushman, 1922

Quinqueloculina collumnosa Cushman, 1922, p. 571, pl. 10, fig. 10.

Quinqueloculina contorta d'Orbigny, 1846

Figs. 2.12.18-19

Quinqueloculina contorta d'Orbigny, 1846, p. 298, pl. 20, figs. 4-6.

Quinqueloculina exsculpta (Heron-Allen and Earland)

Miliolina exsculpta Heron-Allen and Earland, 1915, p. 567, pl. 42, figs. 23-26.

Quinqueloculina exsculpta (Heron-Allen and Earland) Haig, 1988, p. 233, pl. 6, figs. 8-10.

Quinqueloculina funafutiensis (Chapman)

Figs. 2.12.20-21

Miliolina funafutiensis Chapman, 1901, p. 178, pl. 19, figs. 6-6a.

Quinqueloculina funafutiensis (Chapman) Cushman, 1929, p. 30, pl. 4, figs. 4a-b.

Quinqueloculina laevigata d'Orbigny, 1826

Figs. 2.12.22-23

Quinqueloculina laevigata d'Orbigny, 1826, p. 143, pl. 3, figs. 31-33.

Quinqueloculina poeyana d'Orbigny, 1839a

Quinqueloculina poeyana d'Orbigny, 1839a, p. 191, pl. 11, figs. 25-27.

Quinqueloculina poeyana (d'Orbigny) Cushman, 1929, p. 31, pl. 5, figs. 2a-b.

Quinqueloculina polygona d'Orbigny, 1839a

Fig. 2.12.31

Quinqueloculina polygona d'Orbigny, 1839a, p. 198, pl. 12, figs. 21-23.

Quinqueloculina quinquecarinata Collins, 1958

Figs. 2.12.26-28

Quinqueloculina quinquecarinata Collins, 1958, p. 360, pl. 2, figs. 8a-c.

Quinqueloculina seminulum (Linné)

Figs. 2.12.29-30

Serpula seminulum Linné, 1758, p. 786.

Quinqueloculina seminulum (Linné) Cushman, 1929, p. 24, pl. 2, figs, 1-2.

Quinqueloculina spp.

Remarks: In practice, rare (e.g., *Q. funafutiensis*) and identifiable juvenile individuals were grouped together and not identified to the species level.

Quinqueloculina subpoeyana Cushman, 1922

Figs. 2.12.24-25

Quinqueloculina subpoeyana Cushman, 1922, p. 66 (not figured).

Quinqueloculina subpoeyana (Cushman), Cushman, 1929, p. 31, pl. 5, figs. 3a-b.

Quinqueloculina sulcata d'Orbigny, 1826

Quinqueloculina sulcata d'Orbigny, 1826, p. 301, (not figured).

Quinqueloculina sulcata (d'Orbigny) Fornasini, 1900, p. 364, p. 363 (holotype).

Quinqueloculina tenagos Parker, 1953

Fig. 2.12.32

Quinqueloculina tenagos (new name) Parker, 1962.

Quinqueloculina rhodiensis Parker et al. (not Wiesner) 1953, p.12, pl. 6, figs. 3a-c.

Reophax nana Rhumbler, 1911

Figs. 2.13.1-2

Reophax nana Rhumbler, 1911, p. 182, pl. 8, figs. 6-12.

Reophax nanus (Rhumbler) Lankford and Phleger, 1973, p. 127, pl. 1, fig. 4. *Reophax scottii* Chaster, 1892

Figs. 2.13.3-4

Reophax scottii Chaster, 1892, p. 57, pl. 1, fig. 1.

Reophax subfusiformis Earland, 1933

Figs. 2.13.5-6

Reophax subfusiformis Earland, 1933, p. 74, pl. 2, figs. 16-19.

Reussella atlantica Cushman, 1947

Reussella spinulosa var. atlantica Cushman, 1947, p 91, pl. 20, figs. 6-7.

Reussella atlantica Cushman, Bock et al., 1971, p. 48, pl. 17, fig. 10

Rosalina spp.

Remarks: These were rare rosalinids not identified to the specific level.

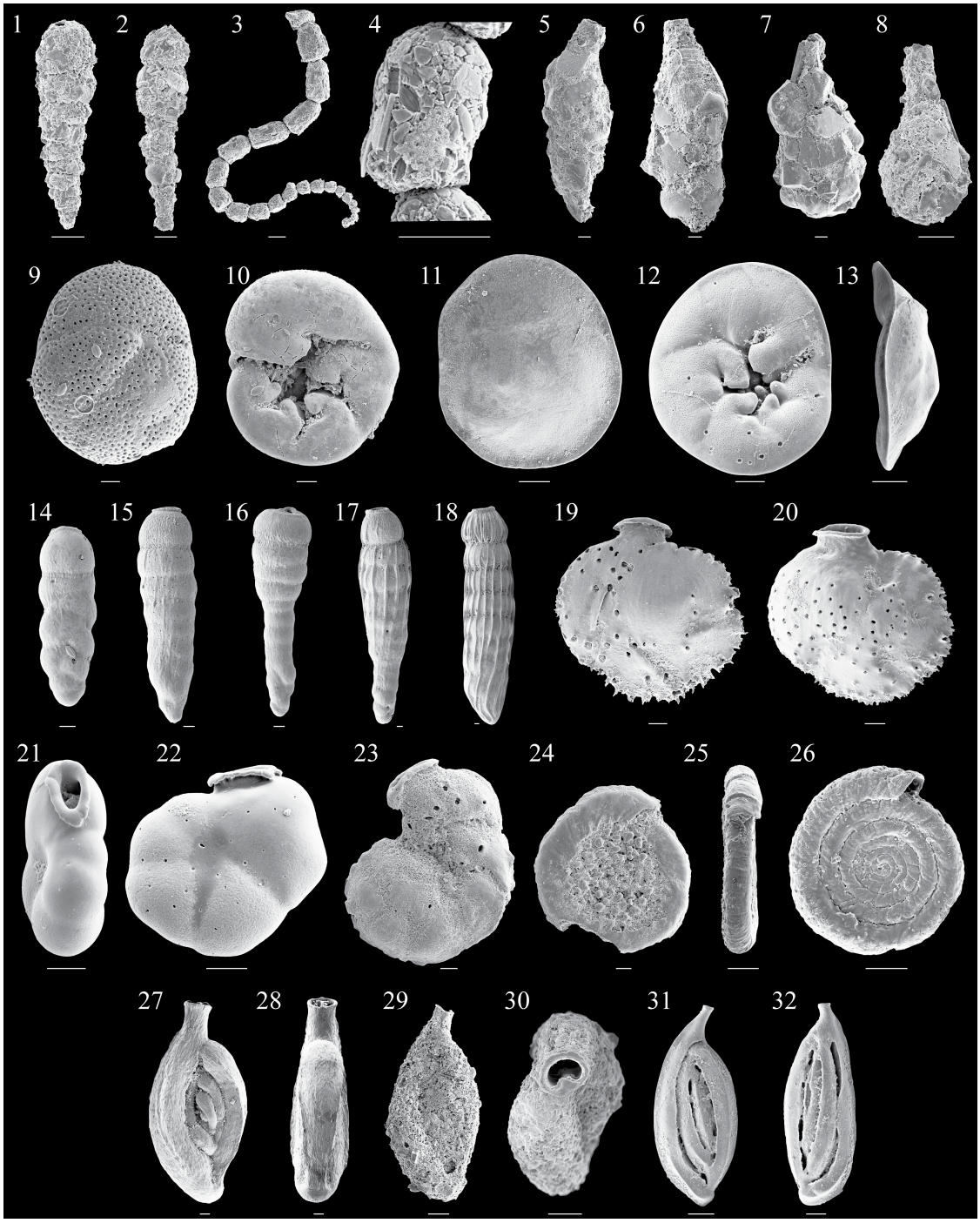

Figure 2.13: 1, 2 *Reophax nana*; **3** *Reophax scottii*; **4** magnified chamber of *R. scottii* emphasize diatoms in shell structue; **5, 6** *Reophax subfusiformis*; **7, 8** *Saccammina difflugiformis*; **9, 10** *Rosalina globularis*; **11-13** *Rosalina williamsoni*; **14, 15** *Siphogenerina columellaris*; **17, 18** *Siphogenerina striata*; **19, 20** *Siphonina reticulata*; **21, 22** *Siphonina temblorensis*; **23** *Siphoninella soluta*; **24** *Spirillina tuberculata*; **25, 26** *Spirillina vivipara*; **27, 28**; *Spiroloculina antillarum* **29, 30**; *Spiroloculina arenata* **31, 32** *Sigmoilina tenuis*. Scale bar represents 50 μm.

Rosalina globularis d'Orbigny, 1826

Figs. 2.13.9-10

Rosalina globularis d'Orbigny, 1826, plate 13, figs. 1-4.

Rosalina subaraucana (Cushman) van Hengstum et al., 2009a (not imaged), van Hengstum, 2008, Fig. 3-S3.30.

Rosalina vilardeboana d'Orbigny, 1839

Rosalina vilardeboana d'Orbigny, 1839, p. 44, pl. 6, figs. 13-15.

Rosalina williamsoni (Parr)

Figs. 2.13.11-12

Discorbis williamsoni Parr, 1932, p. 226, pl. 21, fig. 25.

Rotalina nitida Williamson (not Reuss), 1858, p. 54, pl. 4, figs. 106-108.

Discorbis parkeri Natland, 1950, p. 27, pl. 6, figs. 11a-c.

Rosalina parkerae (Natland), Parker, 1954, p. 525, pl. 8, figs. 24-25.

Rotaliella arctica (Scott and Vilks)

Figs. 2.10.17-18

Glabratella arctica Scott and Vilks, 1991, p. 30, pl. 2, figs. 10-12.

Rotaliella keigwini Pawlowski, 1991, p. 169-170, pl. 2, figs. 2a-d.

Saccammina difflugiformis (Brady)

Figs. 2.13.7-8

Reophax difflugiformis Brady, 1879a, p. 51, pl. 4, figs. 3a-b.

Saccammina difflugiformis (Brady) Thomas, Medioli, Scott, 1990, p. 234, pl. 2, figs. 10-12.

Sigmoilina tenuis (Czjzek)

Figs. 2.13.31-32

Quinqueloculina tenuis Czjzek, 1848, p. 149, pl. 13, figs. 31-34.

Spiroloculina tenuis Brady (Czjzek), 1884, pl. 10, fig 8.

Spiroloculina gradeloupi (d'Orbigny) Javaux, 1999, p. 366, pl. 7, fig 8.

Siphogenerina columellaris (Brady)

Figs. 2.13.14-16

Uvigerina columellaris Brady, 1881, p. 64pl. 75; figs. 15-17.

Siphogenerina columellaris Cushman, 1926b, p. 12, pl. 2, figs. 4, 11; pl. 3, figs. 1-4.

Siphogenerina striata (Brady)

Figs. 2.13.17-18

Sagrina striata Brady (not Schwager), 1884, p. 584, pl. 75, figs. 25-26.

Siphogenerina striata var. curta Cushman, 1926b, p. 8, pl. 2, fig. 5; pl. 5, figs. 5-6.

Siphonina reticulata (Czjzek)

Figs. 2.13.19-20

Rotalina reticulata Czjzek, 1848, p. 145, pl. 13, figs. 7-9.

Siphonina reticulata (Czjzek) Cushman, 1929, p. 7, pl. 1, figs. 1-2, pl. 3, fig. 4.

Siphonina temblorensis Garrison, 1959

Figs. 2.13.21-22

Siphonina temblorensis Garrison, 1959, p. 669, pl. 86, figs. 4a-c.

Remarks: All individuals are small and never developed an acute periphery or keel.

Siphoninella soluta (Brady)

Fig. 2.13.23

Planrbulina (*Truncatulina*) *soluta* Brady, 1881; 1884, p. 66, pl. 96, fig. 4.

Siphoninella soluta (Brady) Cushman, 1927.

Sorites marginalis (Lamarck)

Orbutiles marginalis Lamarck, 1816, p. 196.

Sorites marginalis (Lamarck) Cushman, 1930, p. 49, pl. 18, figs. 1-4.

Spirillina tuberculata Brady, 1879b

Fig. 2.13.24

Spirillina tuberculata Brady, 1879b, p. 279, pl. 8, figs. 28a-b.

Spirillina vivipara Ehrenberg, 1843

Figs. 2.13.27-28

Spirillina vivipara Ehrenberg, 1843, p. 422, pl. 3, fig. 41.

Spiroloculina antillarum d'Orbigny, 1939a

Figs. 2.13.29-30

Spiroloculina antillarum d'Orbigny, 1939a, p. 166, pl. 9, figs. 3-4.

Spiroloculina arenata Cushman, 1921a

Figs. 2.13.25-26

Spiroloculina arenata Cushman, 1921a, p. 63, pl. 14, fig. 17.

Spiroloculina sp.

Remarks: These uncommon individuals were not identified to the specific level.

Spirophthalmidium emaciatum Haynes, 1973

Figs. 2.14.1-5

Spirophthalmidium acutimargo (Brady) var. *emaciatum* Haynes 1973

Spiroloculina acutimargo Brady 1884, pl. 10, figs. 14 (not figs. 12, 13, or 15).

Remarks: Brady (1884) described the fig. 14 (pl. 10) with the phialine lip as an immature individual, and the figures lacking the phialine lip as adults. Haynes (1973) attributed Brady's fig. 14 to just a variant of *S. acutimargo.* All cave phenotypes had an aperture on an elongated neck (of variable length) bordered by a fragile phialine lip. However, cave individuals never intergrade into specimens without a phialine lip. Therefore, Haynes' variant warrants elevation to the specific level.

Svratkina australiensis (Chapman, Parr, and Collins)

Figs. 2.14.9-11

Discorbis tuberculata var. australiensis Chapman, Parr, and Collins, 1934, p. 169, pl. 8, fig. 9.

Svratkina bubnanensis McCulloch, 1977, p. 409, pl. 153, figs. 3, 11.

Svratkina bubnanensis (McCulloch) Loeblich and Tappan 1994, p. 161, pl. 353, figs. 10-11.

Svratkina sp. A Hottinger, Halicz, Reiss, 1993, p. 138, pl. 196, figs. 7-10.

Baggina sp. Lankford and Phleger, 1973, p. 115, pl. 4, fig. 22.

Technitella legumen Norman, 1878

Figs. 2.14.6-7

Technitella legumen Norman, 1878, p. 279, pl. 16, figs. 3-4.

Textularia agglutinans d'Orbigny 1839a

Fig. 2.14.8

Textularia agglutinans d'Orbigny 1839a, p. 144, pl. 1, figs. 17-18 and 32-34.

Textularia earlandi Parker, 1952

Figs. 2.14.13-14

Textularia earlandi Parker, 1952 (new name)

Textuarlia tenuissima Earland (not Häusler), 1933, p. 95, pl. 3, figs. 21-30.

Textularia elegans Lacroix (not Hantken), 1931, p. 14, pl. 3, figs. 21-30.

Textularia sp.

Figs. 2.14.15-16

Remarks: This species differed from *T. earlandi* in being smaller, a golden brownish color, and prevalent in the submarine cave environment. The aperture was a small opening within a minute depression on the apertural face.

Trifarina occidentalis Cushman, 1923

Fig. 2.14.12

Trifarina occidentalis Cushman, 1923, p. 169 (not figured).

Uvigerina angulosa Cushman 1922, p. 34, pl. 5, figs. 3-4.

Triloculina bermudezi Acosta, 1940

Fig. 2.14.21

Triloculina bermudezi Acosta, 1940, p. 37, pl. 4, figs. 1-5.

Triloculina carinata d'Orbigny, 1839a

Triloculina carinata d'Orbigny, 1839a, p. 158, pl. 10, figs. 15-17.

Triloculina nasuta Cushman, 1935

Fig. 2.14.17

Triloculina nasuta Cushman, 1935, p. 5, pl. 2, figs. 1-3.

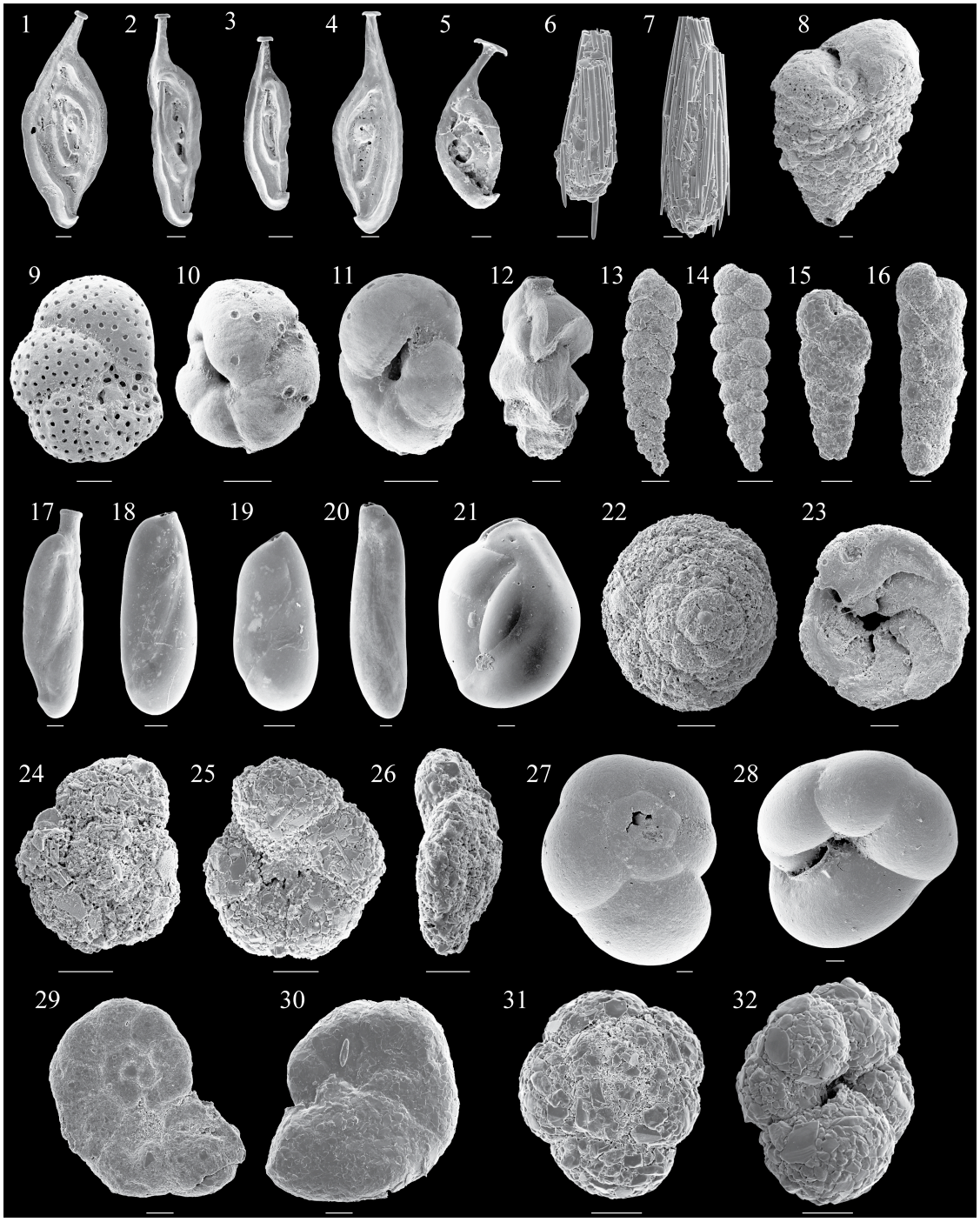

Figure 2.14: 1-5 *Spirophthalmidium emaciatum*; **6, 7** *Technitella legumen*; **8** *Textularia agglutinans*; **9-11** *Svratkina australiensis*; **12** *Trifarina occidentalis*; **13, 14** *Textularia earlandi*; **15, 16** *Textularia* sp.; **17** *Triloculina nasuta*; **18-20** *Triloculina oblonga*; **21** *Triloculina bermudezi*; **22, 23** *Trochammina ochracea*; **24-26** *Trochammina charlottensis*; **27, 28** *Trochammina inflata*; **29, 30** *Trochammina macrescens*; **31, 32** *Trochammina quadriloba*. Scale bar represents 50 μm.

Triloculina oblonga (Montagu)

Figs. 2.14.18-20

Vermiculum oblongum Montagu, 1803, p. 522, pl. 14, fig. 9.

Triloculina oblonga (Montagu) d'Orbigny, 1826, p. 300, no. 16; Javaux, 1999, p. 372, pl. 8, figs. 6-8; Bock, 1971, p. 27, pl. 11, figs. 2-4.

Remarks: This species exhibited high intraspecific variation (size and shape), but could easily be differentiated from the similar-sized *Q. quinquecarinata* (has acute chamber margins).

Triloculina rotunda d'Orbigny, 1826

Triloculina rotunda d'Orbigny, 1826, p. 299.

Triloculina suborbicularis d'Orbigny, 1839a

Triloculina suborbicularis d'Orbigny, 1839a, p. 177, pl. 10, figs. 9-10.

Trochammina charlottensis Cushman, 1925

Figs. 2.14.24-26

Trochammina charlottensis Cushman, 1925, p. 39, pl. 6, fig. 4.

Trochammina inflata (Montagu)

Figs. 2.14.27-28

Nautilus inflatus Montagu, 1808, p. 81, pl. 18, fig. 3.

Trochammina inflata (Montagu) Parker and Jones, 1859, p. 347, Brady 1884, p. 338, pl. 91, fig. 4a-c.

Trochammina macrescens Brady

Figs. 2.13.29-30

Trochammina inflata (Montagu) var. *macrescens* Brady, 1870, p. 290, pl. 11, fig. 5.

Trochammina macrescens Brady, Scott and Medioli, 1980, p. 44, pl. 3, figs. 1-8.

Trochammina ochracea (Williamson)

Figs. 2.13.22-23

Rotalina ochracea Williamson, 1858, fig. 112-113.

Trochammina ochracea (Williamson) Cushman, 1920, p. 75, pl. 15, fig. 3, Scott and Medioli, 1980, p. 45, pl. 4, figs. 4-5.

Trochammina quadriloba Höglund, 1948

Figs. 2.13.31-32

Trochammina pusilla Höglund (not Geinitz), 1947, pl. 17, figs. 4a-c.

Trochammina quadriloba Höglund, 1948, (new name, not figured), p. 48.

Tubinella funalis (Brady)

Articulina funalis Brady, 1884, p. 185, pl. 13, figs. 6-11.

Tubinella funalis (Brady) Rhumbler, 1906.

Wiesnerella auriculata (Egger)

Planispirina auriculata Egger, 1893, p. 245, pl. 3, figs. 13-15.

Wiesnerella auriculata (Egger) Cushman, 1933c, p. 33, pl. 3, figs. 7-9.

2.9.2 Tintinnida

Codonella acuta Kofoid and Campbell, 1929

Fig. 2.15.1

Codonella acutula Kofoid and Campbell, 1929, p. 52, fig. 104.

Description: A small (<55 μm) cup-shaped lorica with a collar that is not spiral or hyaline; lorica is well defined by a nuchal restriction; aboral end is acute, yet not pointed or developing into a horn. The length of the lorica is only slightly greater than the width.

Codonella elongata Kofoid and Campbell, 1929

Fig. 2.15.4

Codonella elongata Kofoid and Campbell, 1929, p. 59, fig. 102.

Description: A small (<55 μm), elongate cup-shaped lorica with a collar that is not spiral or hyaline; lorica is well defined by a nuchal restriction; aboral end is acute, yet not pointed or developing into a horn. The lorica length is notably greater than the width.

Remarks: This species differs from *Codonella* sp. 1 in the length of the lorica, which is caused by a well-developed and elongated collar.

Codonellopsis americana Kofoid and Campbell, 1929

Fig. 2.15.2

Codonellopsis americana Kofoid and Campbell, 1929, p. 75, fig. 159.

Description: Lorica shaped like a toy gyroscope; tall, hyaline collar with spiral turns and perforated by fenestrae positioned at ~90º to each other, aboral end rounded to acute and never developing into a horn. Genera is common in warm waters.

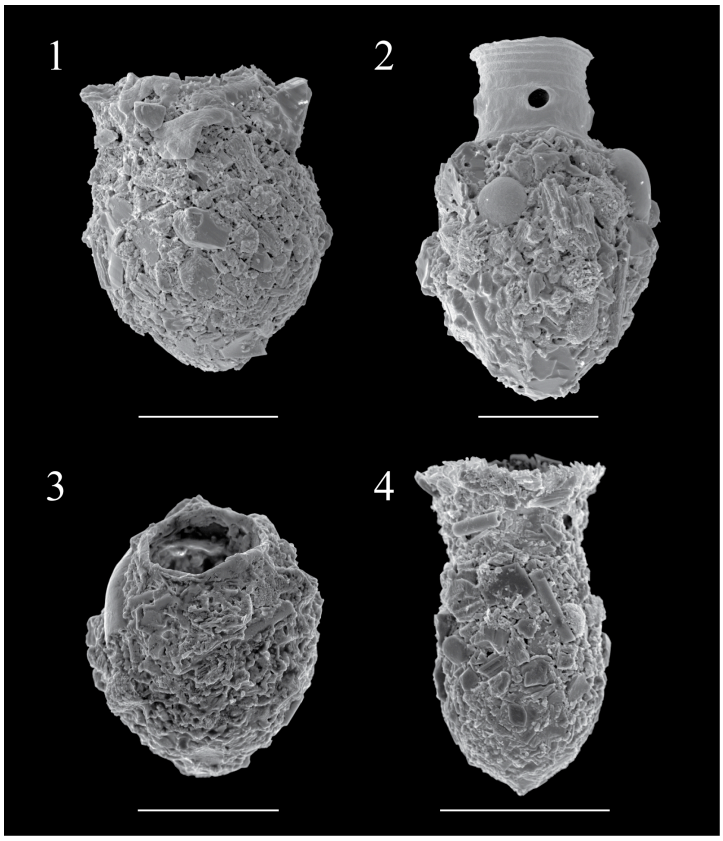

Figure 2.15: 1 *Codonella acutula*; **2** *Codonellopsis americana*; **3** *Stenosemella avellana*; **4** *Codonella elongata*. Scale bar represents 50 μm.

Stenosemella avellana (Meunier).

Fig. 15.3

Tintinnopsis avellana Meunier, 1919, p. 30, pl. 22, fig. 37.

Stenosemella avellana (Meunier) Kofoid and Campbell, 1929, p. 69, fig. 134.

Description: Oval- or olive-shaped lorica with a short, hyaline collar devoid of spiral turning, aboral end acute, but never developing into a horn. Differs from others in the genus by having the greatest width near the middle and in sloping shoulders from the aperture.

PART II: Sea-level Signatures in Phreatic Coastal Caves

Chapter 3: Glacioeustacy Controls Sedimentation and Environments in Coastal Caves and Sinkholes

Peter J. van Hengstum[1], David B. Scott[1], Darren R. Gröcke[2], Matthew A. Charette[3]

1. Centre for Environmental and Marine Geology, Dalhousie University,

Halifax, Nova Scotia, B3H 4J1, Canada

2. Department of Earth Sciences, Durham University, South Road, Durham,

UK, D1H 3LE

3. Department of Marine Chemistry and Geochemistry, Woods Hole Oceanographic

Institution, Woods Hole, MA, USA

Status of manuscript: In preparation for *Marine Geology.*

3.1 Abstract

The oscillation of speleogenetic karst basins (caves, sinkholes) between the phreatic and vadose zone during Quaternary sea-level change is an important process impacting coastal cave and karst science because groundwater and sea level oscillate in synchrony. However, the transition of a coastal cave from vadose through all phreatic environmental conditions (littoral, anchialine, submarine) has actually never been evidenced, despite the hypothesized likelihood of this relationship. Twelve sediment cores constrained with nineteen radiocarbon dates were collected from a Bermudian phreatic cave (underwater) to test this hypothesis, affording the first complete Holocene succession from a phreatic cave (13 ka ago to present). The sedimentary successions were characterized with X-radiography, microfossil content, bulk organic matter, organic geochemistry ($\delta^{13}C_{org}$, C:N), and grain-size. Four depositional environments (facies) can be isolated in that strata that are composed of one or more lithofacies: (a) Vadose Facies (> 7.6 ka, calcite rafts), (b) Littoral Facies (7.6 – 7.9 ka: calcite rafts and muds), (c) Anchialine Facies (~7 – 1.6 ka: slackwater and diamict lithofacies), and (d) Submarine Facies (<1.6 ka: carbonate mud and shell hash). The timing of these depositional environments can be directly correlated to eustatic sea-level rise in the North Atlantic over the Holocene, indicating that glacioeustatic sea-level change controls the evolution of coastal cave and karst environments. These results provide a framework for interpreting sedimentary and paleontological remains in global coastal cave environments, and likely implicate sea level as contributing to the biological development of modern endemic cave ecosystems.

3.2 Introduction

Sea level is a critical factor affecting coastal cave and karst science because groundwater and sea level oscillate in near synchrony in the coastal zone. For example, previous Quaternary sea-level highstands elevated the mildly acidic halocline, and created globally elevated caves (Mylroie and Carew, 1988; Smart et al., 1988; Mylroie and Carew, 1990; Florea et al., 2007; Mylroie, 2008; Mylroie and Mylroie, 2009). After formation, however, coastal caves have been repeatedly flooded and drained from oscillating sea level, which forces environmental evolution in the cave itself. Biogenic overgrowths on stalagmites detect the switch between phreatic and vadose conditions from sea-level change (Surić et al., 2005, 2009; Dutton et al., 2009), but they provide no information on how cave environments have evolved with sea-level change.

Different cave environments exist in the vadose (unsaturated) versus phreatic (saturated) zone. Any speleogenetic karst basin in the unsaturated vadose zone can be described as being a *vadose* environment. Modern phreatic coastal caves were originally classified as littoral, anchialine, or submarine by Stock et al. (1986), but were subtly expanded upon by van Hengstum and Scott (2011). All phreatic cave environments have broad subterranean connection to the ocean because they are open-systems, flooded by a circulating coastal aquifer, but they can now be quantitatively differentiated based on sedimentological and geochemical proxy evidence (van Hengstum and Scott, 2011). In short, *littoral* environments are created when the water table or sea level is within the cave passage (e.g., Mallorca: Fornós et al., 2009; Dorale et al., 2010). *Anchialine* environments are dominated by terrestrial influences, chemical, hydrogeological, or sedimentological (i.e., Yucatan: van Hengstum et al., 2008, 2010). *Submarine* environments dominated by marine processes, are complelely filled with saline

groundwater or seawater, and typically have entrances flooded by sea level (i.e., France: Fichez, 1990, Italy: Airoldi and Cinelli, 1996). This classification scheme is independent of cave speleogenesis (e.g., Ford and Ewers, 1978; Smart et al., 2006; Ginés and Ginés, 2007), and focuses solely on the environmental conditions in speleogenetic karst basin. Vadose and phreatic (littoral, anchialine, submarine) environments can be observed with respect to sea level along global karst coastlines, but they have never been linked in a succession.

Its been previously proposed that glacioeustatic sea-level oscillations control sedimentation patterns in coastal karst basins (Fig. 3.1, Fornós et al., 2009; Gabriel et al., 2009, van Hengstum et al., 2010). We additionally hypothesize, however, that glacioeustatic sea-level oscillations control the environmental evolution of coastal karst basins between: vadose (during sea-level lowstands), littoral, anchialine, and finally submarine conditions (during sea-level highstands). This conceptual framework allows for each cave environment to retain spatially variable and dynamic depositional settings, but sea level becomes the external forcing mechanism driving coastal cave evolution. The purpose of this study is to test this hypothesis using successions from a modern phreatic coastal cave, which has inevitably been flooded by Holocene eustatic sea-level rise.

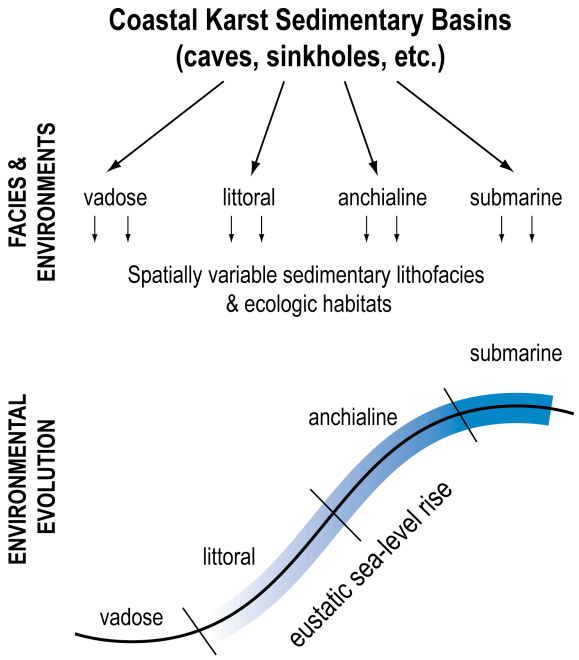

Figure 3.1: Environments and facies in speleogenetic karst basins, and their evolution during a transgressive systems tract.

3.3 Regional Setting

Bermuda is ideal for testing this hypothesis because it contains abundant phreatic and vadose caves. Bermuda can be considered a Carbonate-Cover Island according to the Carbonate Island Karst Model because it contains a basalt core overlain with alternating eolianite (~90%) and paleoesols (~10%) that developed during late Quaternary sea-level highstands and lowstands, respectively (Bretz, 1960; Land et al., 1967; Gees and Medioli, 1970; Hyndman et al., 1974; Vacher et al., 1989, 1995; Mylroie et al., 1995; Mylroie and Mylroie, 2007). Caves are found in most Bermudian eolianite formations, but are most abundant in the diagenetically mature Walsingham Formation on the isthmus between Castle Harbor and Harrington Sound (Land et al., 1967; Mylroie et al., 1995; Hearty, 2002). It is generally thought that three primary processes formed Bermuda's laterally-extensive caves: (a) phreatic dissolution in a paleo-meteoric lens during sea-level

highstands, (b) vadose dissolution concentrated at the basalt-eolianite contact during sea-level lowstands, and (c) subsequent modification from collapse events (Palmer et al., 1977; Mylroie et al, 1995). These processes generated the current geomorphology of large cave chambers connected by fissures (e.g., Walsingham Cave System; Iliffe, 1987). Sedimentary infill has since accumulated on cave floors, which can reach several meters in structural depressions.

This study focuses on Green Bay Cave (GBC), which is located on the northeastern shore of Harrington Sound. The entire cave system is currently underwater, necessitating the use of SCUBA (self-contained underwater breathing apparatus) for all collections. Preliminary sediment probing indicated that several meters of sediment was present suitable for a coring survey in the main passages. GBC contains two connected cave entrances by almost 300 m of phreatic cave passage: an anchialine sinkhole entrance (Cliff Pool Sinkhole) and a submarine cave entrance opening below sea level into Harrington Sound. van Hengstum and Scott (2010) documented the boundary between the modern anchialine and submarine cave environment in GBC using micropaleontological, sedimentological, and organic geochemical proxies, indicating these proxies are suitable for differentiating coastal cave environments in the stratigraphic record.

Green Bay Cave is almost entirely flooded by saline groundwater. A thin, brackish meteoric lens is buoyed on the saline groundwater within 60 cm of sea level in Cliff Pool Sinkhole, with saline groundwater below throughout the entire cave passages (salinity >20 ppt, van Hengstum and Scott 2010). The saline groundwater is tidally circulated through the submarine cave entrance at Harrington Sound, where maximum current velocity reaches 1.5 m s^{-1} during peak tidal flow. However, low groundwater flow velocities persist in the cave (Cate, 2009; van Hengstum and Scott, 2011). Lastly, GBC

and Harrington Sound experience diminished tidal amplitudes in comparison to the rest of Bermuda because water oscillating between Harrington Sound and the ocean is strongly restricted through the narrow Flatts Inlet, which has a sill at ~2.25 m (Morris et al., 1977; Vollbrecht 1996).

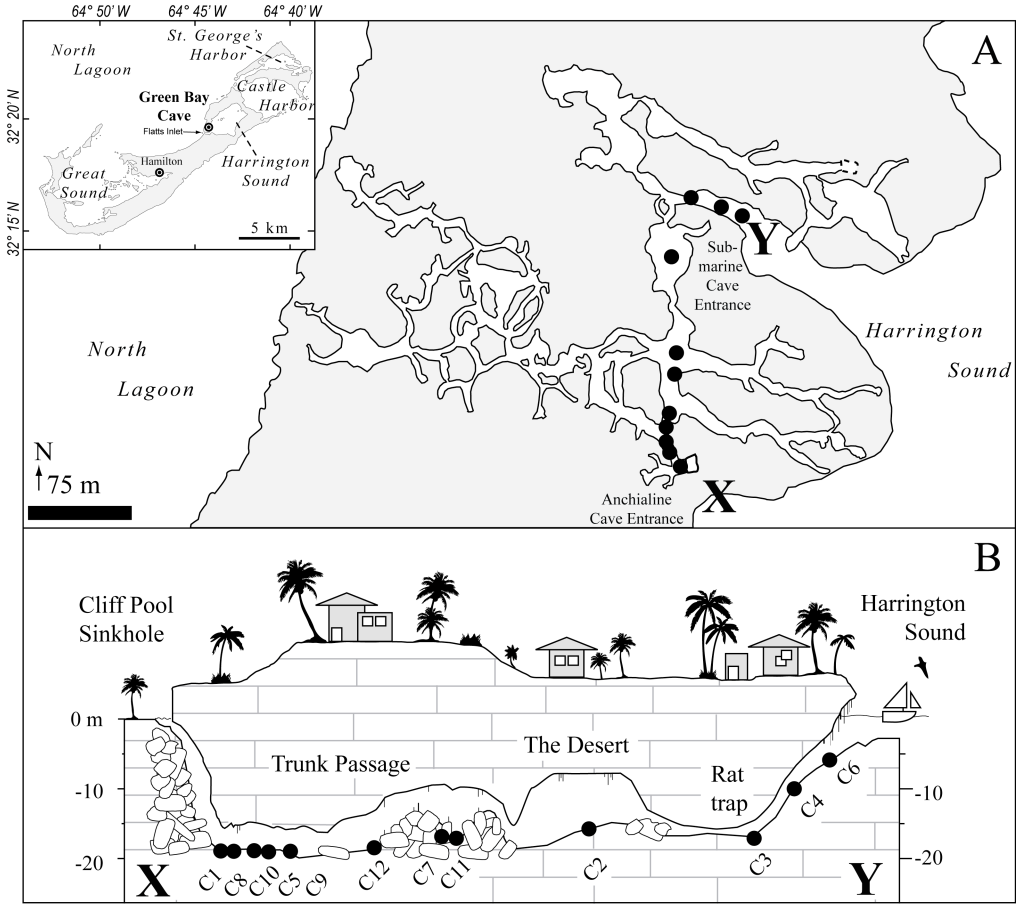

Figure 3.2: A: Primary cave passages in Green Bay Cave, Bermuda. Twelve cores were collected on the X-Y transect encompassing the anchialine to submarine cave environmental transition. B: Location of cores collected on SCUBA along the X-Y transect.

3.4 Methods

Twelve push cores (5 cm diameter) were extracted in Green Bay Cave along the transect from the submarine cave entrance in Harrington Sound to the anchialine cave entrance and Cliff Pool Sinkhole (Fig. 3.2). Polycarbonate tubes were percussed into the

sediment using a stage bottle (extra scuba tank), which were plugged with a rubber stopper and capped at maximum penetration to generate suction in the core tube for sediment withdrawal. Original sediment columns were measured underwater to allow estimates of total compaction introduced by the coring method.

All cores were extruded, logged, and sampled at 5-10 mm intervals; however, cores 1 to 5 were shipped back to the laboratory for X-radiography before sampling at the Bedford Institute of Oceanography. Nineteen (19) radiocarbon dates on organics (wood, bulk organics) and biogenic carbonates (shells) provided age constraint for the successions, which were converted to calibrated dates using IntCal09 and Marine09 (Reimer et al., 2009) with Calib 6.0 (Appendix 1). A local ΔR value of -48 ± 40 was applied to biogenic carbonates where necessary (Druffel, 1997), and multiple ^{14}C ages were obtained where possible at similar stratigraphic contacts in different cores to duplicate the age constraint.

A Beckman Coulter LS 230 employing the Fraunhofer optical model was used for particle size analysis, allowing for particle size determination between 0.04 and 2000 μm (Murray, 2002; Eshel et al., 2004). An analysis of bulk sediments was favored over analysis of individual sedimentary constituents (e.g., carbonates, organic fraction) to retain a complete signature of environmental processes (Donnelly and Woodruff, 2007; Donato et al., 2009). Each core was sampled at 5 to 10 mm intervals, each sample of which was analyzed for particle size distributions. Downcore particle size distributions (PSDs) were then log transformed (to the phi-scale), interpolated, and plotted as a color surface plot (Beierle et al., 2002). Interpolated PSDs often allow for better characterization of subtle changes in downcore grain-size distributions and lithofacies

than standard particle-size statistics alone (mean, median, mode, standard deviation; van Hengstum et al., 2007, 2010; Donato et al., 2009; Reinhardt et al., 2010). Lastly, replicate sediment samples in the resultant lithofacies were inspected with a stereomicroscope (up to 40X) to determine the presence or absence of microfossils (gastropods, bivalves, microfossils, etc.).

Sedimentary organic matter (source, quantity, quality) is important to characterize in phreatic cave sediments because organic matter is often a limiting resource in the dark cave, and therefore exerts significant environmental control on phreatic caves (Fichez, 1990; Panno et al., 2004; van Hengstum et al., 2009a, 2010; van Hengstum and Scott, 2011). The quantity of sedimentary organic matter (weight %) was estimated in all cores by loss on ignition at 550°C for 4.5 hours (every sample PSD were measured on). Error on replicate samples was less than ± 2%, which is typical precision for the method (Heiri et al., 2001). Isotopic ($\delta^{13}C_{org}$) and elemental (C:N) analyses of bulk organic matter were completed to identify the changes in the dominant source of organic matter through time from cores 1, 2, 3, 5, and 9 (source and quality, Lamb et al., 2006). Sediment samples were first subjected to a 10% HCl carbonate digestion for 24 hours, rinsed to neutrality, then dried and powdered. Stable carbon isotopes were then compared against international standards, with reproducibility on replicates equal to ±0.2‰, and expressed in the standard delta (δ) notation in per mil (‰) against Vienna PeeDee Belemnite (VPDB). Previous measurements of $\delta^{13}C_{org}$ in surface sediment samples collected throughout Green Bay Cave (n = 74) indicated that two dominant sources for the organics in Green Bay Cave: terrestrial and/or marine. This sampling survey indicated that the terrestrial endmember (δX_t) was -26.7‰, and that the marine endmember (δX_m) had a

value of -16.8‰ (van Hengstum and Scott, 2011). As such, the relative contribution (as a percent) of terrigenous (F_t) versus marine (F_m) organic matter in the cave sediment can be evaluated using traditional isotopic mass balance mixing equations (e.g., Thornton and McManus, 1994; Voβ and Struck, 1997; Ogrinc et al., 2005):

$$(1)\ \delta X = F_m * \delta X_m + F_t * \delta X_t$$

$$(2)\ 1 = F_t + F_m$$

3.5 Lithofacies

A total of 5.82 m of core was recovered, originally representing 14.4 m of sediment after an average compaction of 58.5% (Table 3.1). High rates of compaction were expected because carbonate mud is the dominant sediment, which can have up to 80% porosity (Enos and Sawatsky, 1981). All radiocarbon dates are stratigraphically ordered, and sequentially date correlative lithofacies in the succession. The oldest radiocarbon date measured is on a *Poecilozonites* shell (terrestrial gastropod) at the base of core 5, which is dated to 12.9 ka (Appendix 1). Therefore, the recovered successions began during the earliest Holocene, and the dates indicate that we recovered the first succession from a phreatic cave that spans the entire Holocene. Six lithofacies were defined in the cores based on organic matter quantity (OM wt. %), organic matter source ($\delta^{13}C_{org}$, C:N) granulometry (PSDs), X-radiographs, and microfossils. In general, a basal calcite raft lithofacies, which is devoid of microfossils, initiates the cave succession and passes up into a calcite raft and mud, which contains abundant aquatic microfossils and fish remains. This is followed by organic-rich diamict and slackwater deposits

(microfossil-poor), which are finally succeeded by carbonate mud and shell hash, as described in detail below.

Table 3.1: Water depth, core recovery, and compaction of push cores.

Core	Water Depth (m)	Recovery (m)	True Thickness (m)	Compaction (%)
C1	18.9	0.74	1.94	61.9
C2	15.8	0.44	1.08	59.3
C3	16.5	0.5	1.7	70.6
C4	12.2	0.23	1.01	77.2
C5	19.5	0.68	1.33	48.9
C6	10.7	0.42	0.92	54.3
C7	19.6	0.41	0.85	51.8
C8	20.1	0.42	1.29	67.4
C9	19.8	0.65†	1.25	48
C10	19.8	0.5	1.34	62.7
C11	19.6	0.49	1.09	55
C12	19.3	0.34	0.62	45.2

† Basal ~4 cm was observed before falling back into hole.
Error of ±0.3 m on depth measurements from gauges.
Note: The cores appear as *GBC1* in Appendix 1 to denote core 1 in this table.

3.5.1 Calcite Rafts

This sedimentary unit is dominated by calcite rafts, which are a common autochthon in caves. Calcite rafts have a distinctive morphology with a completely flat surface on one side, and calcite rhombohedra on the opposing side (Fig. 3.3). Calcite rafts precipitate at an air-water interface (puddle, water table) because groundwater is often carbonate-saturated, and the cave atmosphere is typically pCO_2-depressed, resulting in groundwater off-gassing and precipitation of calcite at the interface (Taylor and Chafetz, 2004; Taylor et al., 2004). This causes the mineral side in contact with the atmosphere to remain flat (planar), whereas, the downward crystal growth into groundwater occurs on

the opposite mineral face. Eventually, floating calcite rafts sink when gravitational forces on the calcite raft overtake surface tension. The calcite raft lithofacies is the coarsest unit in the recovered strata (mean 433.5 μm), and contains the lowest bulk organic matter content (mean 2.9%). The sedimentary organic matter at the base core 5 is dominantly derived from terrestrial sources based on the depleted $\delta^{13}C_{org}$ values, but some is derived from marine sources. However, $\delta^{13}C_{org}$ values become increasingly enriched in the upper part of the unit indicating that another source of organic matter is present (Lamb et al., 2006). No aquatic invertebrates were observed in the sediment, except the terrestrial gastropod *Poecilozonites* that is endemic to Bermuda (Hearty and Olson, 2010). This confirms that the cave was in the unsaturated zone during deposition of this unit, and that the calcite raft lithofacies is part of the vadose facies. The entire lithofacies has a distinctive orange hue, similar to the orange-hued sediment recovered in phreatic Aktun Ha Cave in Mexico (van Hengstum et al., 2009). Preliminary evidence suggests the coloring is from matured iron-oxide that precipitated from groundwater either at the time of cave flooding, or sometime in the Holocene history of the cave (van Hengstum and Charette, unpublished data; Charette and Sholkovitz, 2002). Further geochemical analysis and longer term groundwater sampling is required to ascertain the source and timing of this post-depositional feature.

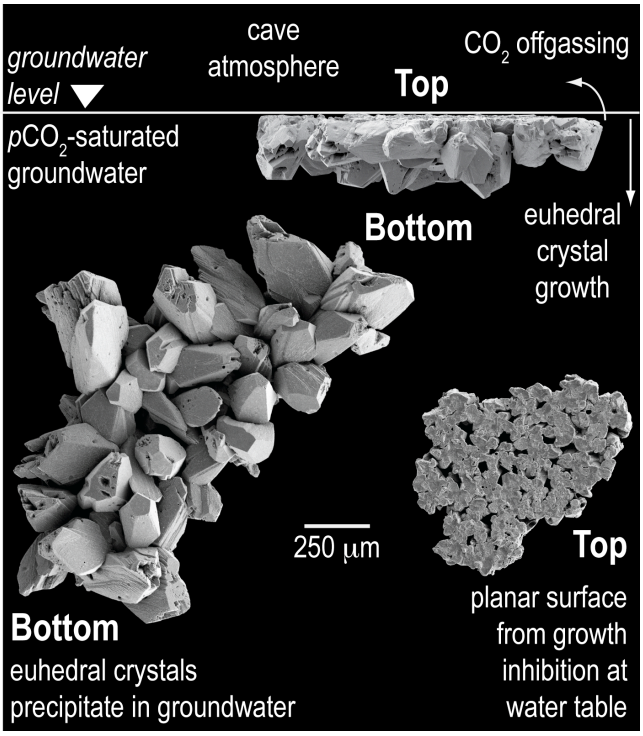

Figure 3.3: Scanning electron micrographs of calcite rafts from Green Bay Cave. Note the top, flat side that was in contact with an atmosphere, versus the bottom side that precipitated in the groundwater and promoted growth of euhedral calcite crystals.

Fig. 3.4: Small fish bones recovered from the calcite rafts and mud lithofacies in core 11, which are older than 7.56 ka. Upper: hemitrich of a soft fin ray fish. Lower: possibly a spinous ray.

3.5.2 Calcite Rafts And Mud

This lithofacies is thickest in core 5 (12.5 cm), but is also present at the base of cores 9, 12, 7, and 11. The mean particle size in the lithofacies is 5.4 μm, with a mean organic matter content of 8.4%. The $\delta^{13}C_{org}$ values in core 5 oscillate between approximately -25‰ to -19‰, indicating that the dominant source of organic matter oscillates between terrestrial and marine sources (Lamb et al., 2006). A fine carbonate mud matrix in addition to calcite rafts uniquely characterizes this lithofacies, whereas calcite rafts are the only sedimentary constituents in the basal lithofacies. Abundant marine microfossils are in the unit, along with brachiopods and bryozoans. The ostracod *Paranesidea sterreri* was observed in all cores and the gastropod *Caecum caverna* was observed in core 12, both of which are Bermudian cave endemics (Maddocks and Iliffe, 1986; Moolenbeek et al., 1988; Table 3.2). Interestingly, two small fish bones were recovered from core 11 (47 to 47.5 cm, Fig. 3.4). The calcite rafts and mud lithofacies that accumulated directly above basement eolianite (cores 12, 7 and 11) also exhibited basal orange-hued staining, which is likely related to the same unresolved ground-water derived mechanism affecting the calcite raft lithofacies. The combination of microfossils and calcite rafts indicates that GBC was a littoral environment during the accumulation of this unit, and the calcite raft and mud lithofacies is part of the littoral facies.

Table 3.2: Arithmetic average for sedimentological and geochemical characteristics in the six lithofacies.

	Granulometry				Organic Matter (OM) Geochemistry					Fossils
Lithofacies	Mean (μm)	Median (μm)	Mode (μm)	Standard Deviation (μm)	Bulk OM (wt %)	C:N	$\delta^{13}C_{org}$ (‰)	Percent Terrestrial OM (F_t)	Percent Marine OM (F_m)	
calcite rafts	433.5	254.4	420	436.8	2.9 ± 0.9	14.2 ± 1.7	-22.2 ± 3.3	54.2	45.8	*Poecilozonites*
calcite rafts and mud	5.4	4.7	9.2	3.8	8.4 ± 2.4	15.1 ± 3.2	-21.8 ± 2.8	48.2	51.8	f, sw, o, sp, br, fish bones
slackwater	18.6	12.7	23.3	19.2	21.7 ± 3.6	17.8 ± 4	-25.9 ± 2.3	87.2	12.8	Brackish foraminifera, rare o Except: f, 0 at tops of cores 1 and 8
diamict	197.8	80.4	394.4	255.1	22.0 ± 9.0	29.6 ± 9.6	-27.3 ± 0.8	98.6	1.4	Brackish foraminifera, rare o
shell hash	270.1	98.1	626.8	357.5	5.6 ±1.7	10.5 ± 1.9	-19.7 ± 1.3	28.9	71.1	f, sw, o, sp
carbonate mud	9.4	7.7	16.6	7.2	9.7 ± 3.1	12.1 ± 1.5	-21.1 ± 1.1	43.7	56.3	f, sw, o, sp, br, *Barbatia* and corralites

Microfossils: serpulid worm tubes (sw), marine foraminifera (f), marine ostracods (o), sponge spicules (sp), brachiopods (br)
Note: C:N and $\delta^{13}C_{org}$ only completed on cores: 1, 2, 3, 5, 9.

3.5.3 Diamict

Diamicts are sedimentary units characterized by chaotic, poorly sorted sediments derived from various sources. Cores close to Cliff Pool Sinkhole contain the diamict lithofacies in GBC, which is characterized by a poorly-sorted, coarse-grained sediment matrix (mean 197.8 μm, mean standard deviation 255.1 μm) that alternates with framework-supported cobbles and woody fragments (e.g., core 1: 21-28 cm). The sediments contain a mean of 22% organic matter, which is 98.6% terrigenous based on $\delta^{13}C_{org}$ mass balance (Table 3.2). *Poecilozonites* shells are common in core 8 below 30 cm and at the base of core 10, intervals that are characterized by very poorly sorted, broad particle size distributions (Fig. 3.6). These terrestrial *Poecilozonites* shells are not in situ because eustatic sea-level rise flooded the cave passage floor at -20 m below sea level by ~5 ka (Blanchon and Shaw, 1995; Siddall et al., 2003; Toscano and McIntyre, 2003).

Aquatic microfossils are rare in the diamict lithofacies in comparison to the calcite rafts and mud lithofacies (Table 3.2). The brackish foraminifera *Physalidia simplex* and *Conicospirillina* sp. is the most common microfossil, known from oligohaline to polyhaline Mediterranean and Mexican restricted coastal environments (Usera et al., 2002; Guillem, 2007; van Hengstum et al., 2008, 2010). We infer that the diamict is part of the anchialine facies because the cave was in the phreatic zone during its deposition and dominated by terrestrial sedimentary processes (see introduction).

3.5.4 Slackwater

The slackwater lithofacies is a well-sorted, organic-rich unit (mean 21.7% organic matter) characterized by silt- to clay-sized particles (mean particle size 18.6 μm) quantified by strongly unimodal grain-size distributions (Fig. 3.4). Organic matter in the slackwater lithofacies is derived from terrestrial sources based on the depleted $\delta^{13}C_{org}$ values, which equates to approximately 87.2% terrestrial sources. By corollary, more marine organic matter is present in the slackwater lithofacies than the diamict lithofacies, with mean C:N ratio of 17.8. Fine laminae can be observed in the X-radiograph of C5 (46 to 50 cm) in the slackwater lithofacies (Fig. 3.5), indicating little, if any, bioturbation occurred during this interval.

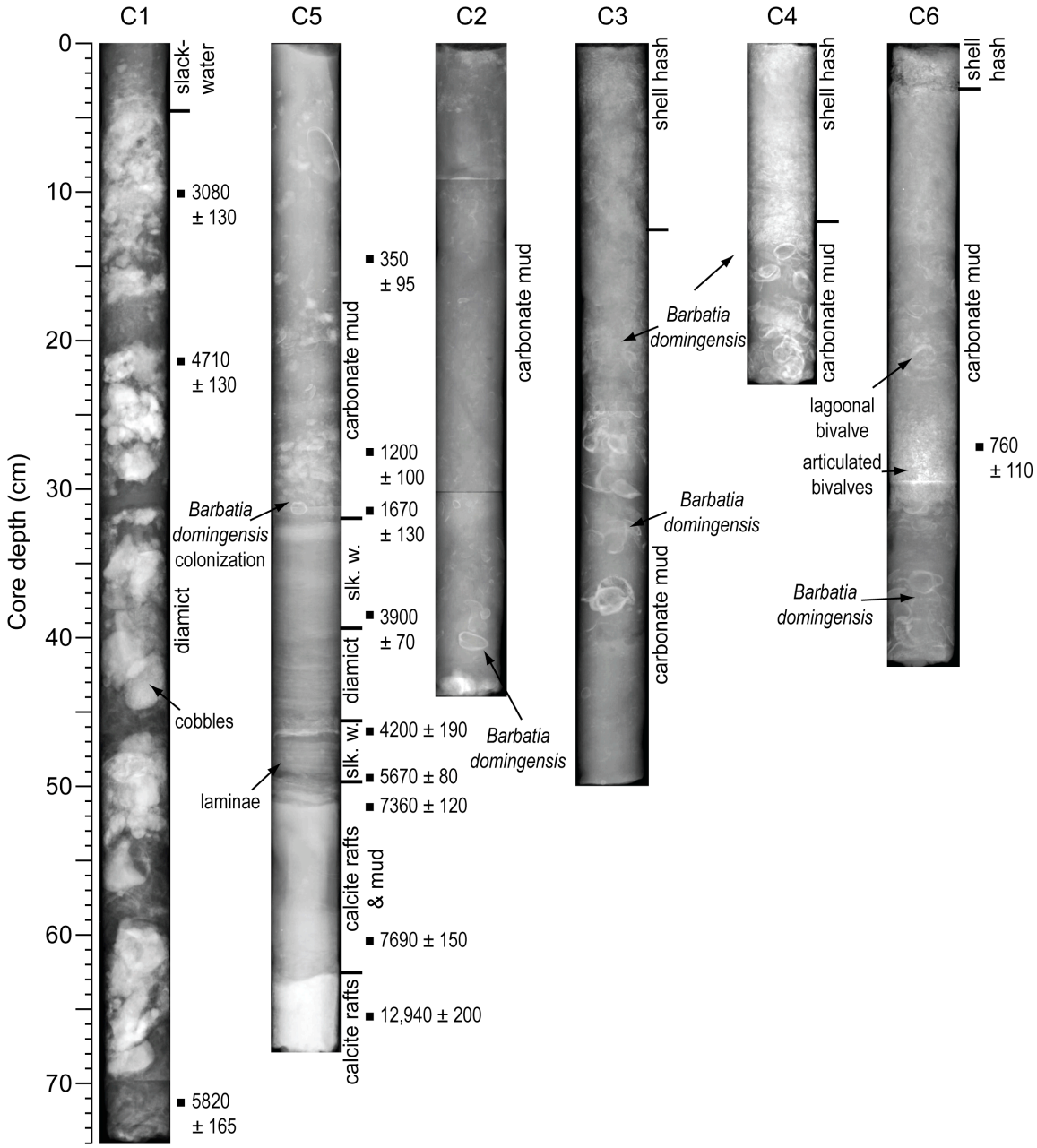

Figure 3.5: X-radiographs of selected cores, with lithofacies and important sedimentological characteristics annotated (slk. wtr.: slackwater).

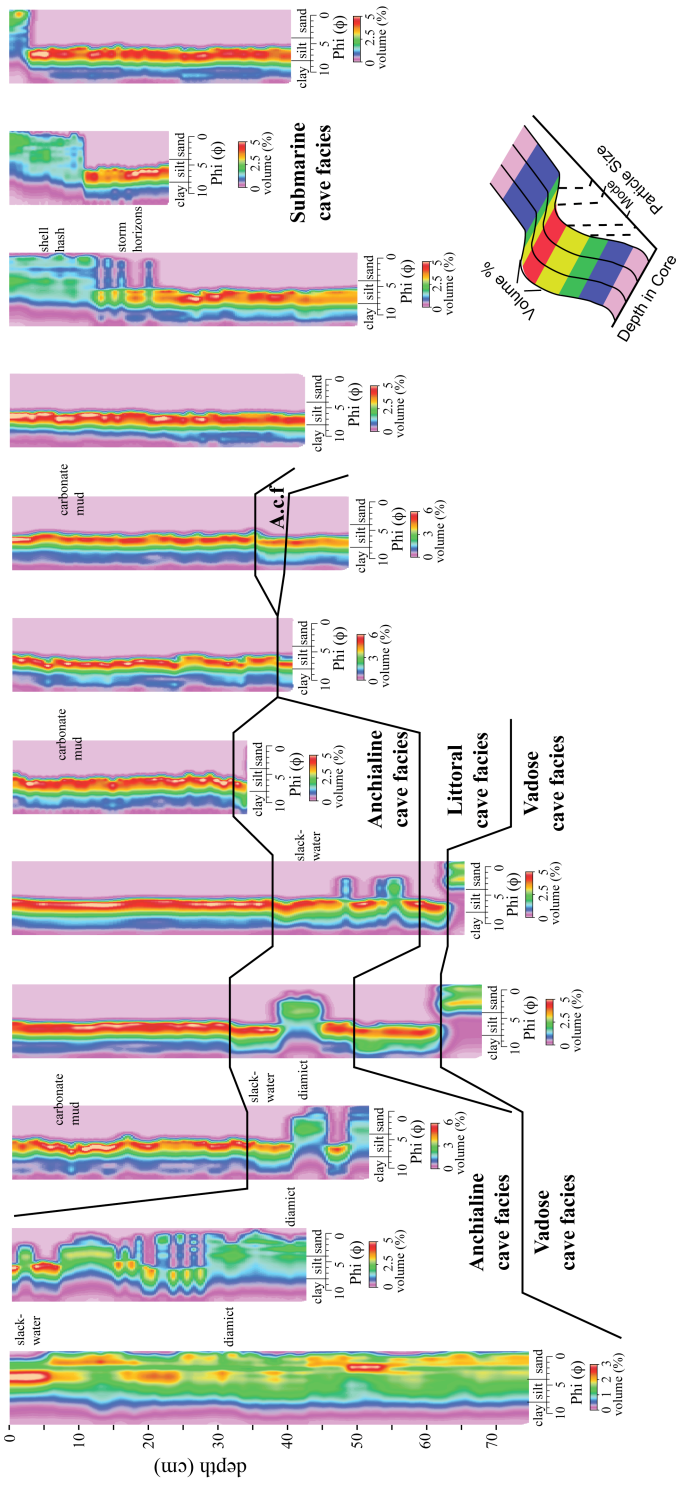

Figure 3.6: Color-contoured, interpolated, particle size distributions (PSDs) from 0.4 to 2000 μm (1.3 to -10.9 ϕ), based on every downcore sediment sample (5 mm to 10 mm sampling interval) in all cores.

Few microfossils are present in the slackwater lithofacies, which is dominated by the brackish foraminifers *Physalidia simplex*, *Conicospirillina* sp., and a few ostracods. The tops of cores 1 and 8, however, have abundant saline foraminifera consistent with the modern anchialine cave assemblage in the surface sediment (Table 3.2, van Hengstum and Scott, 2011). This indicates that the slackwater lithofacies present at the top of cores 1 and 8 accumulated under different hydrogeologic conditions than those at the other core sites. The slackwater lithofacies is considered part of the anchialine facies because the cave was in the phreatic zone during its deposition and dominated by terrestrial sedimentary processes (see introduction).

3.5.5 Carbonate Mud

A condensed unit of serpulid worm tubes and the bivalve *Barbatia domingensis* demarcates the base of the carbonate mud lithofacies, both of which are present throughout the lithofacies in all cores (Appendix 1, Figs. 3.6, 3.7). A well-sorted carbonate mud (mean 9.4 μm) with a mean of 9.7% organic matter characterizes the unit, which is easily correlated through the cave system with a strong unimodal PSD in the coarse clay to fine silt sized-fraction (Fig. 3.6). The lithofacies resembles the modern surface sediments documented by van Hengstum and Scott (2010) throughout the majority of GBC. $\delta^{13}C_{org}$ values and the C:N ratio indicate the organic matter in the carbonate mud lithofacies is dominantly derived from nitrogen-rich marine sources, estimated as 56.3% from mass balance. Abundant marine microfossils (sponge spicules, diverse benthic foraminifera, bryozoans, etc.) are present throughout the unit, along with *Barbatia domingensis* and brachiopods. Corallites of the Bermudian cave coral

Coenocyanths goreaui are present only in this lithofacies, which have been previously documented in the modern environment of GBC (see discussion in Cairns, 2000). Therefore, the carbonate mud lithofacies is considered part of the submarine facies because GBC was a phreatic cave during its deposition and dominated by marine sedimentary processes.

Two interesting minor types of sediment occur within the carbonate mud lithofacies, specifically at the submarine cave entrance. Firstly, three coarser-grained (sand) units are present in core 3 at a depth of 12 to 20 cm, each of which is only 1 cm thick. Secondly, a layer of monospecific, imbricated and articulated lagoonal bivalves was found in core 6 at ~35 cm deep, which is inconsistent within a context of the recovered strata from GBC. The PSDs indicate that carbonate mud is the sedimentary matrix for both of these minor sediment types, suggesting that background environmental conditions were briefly interrupted by some external event, such as a storm.

3.5.6 Shell Hash

This lithofacies occurs in cores 3, 4 and 5 near the submarine cave entrance to Harrington Sound. The thickest sequence (13 cm) occurs at the top of core 3. Heavily fractured and angular lagoonal bivalve shells and debris (e.g., coral fragments) are abundant in the unit, which is clast-supported with a lagoonal carbonate sand matrix. Additional shell material includes lagoonal foraminifera, ostracods, bryozoans, and general shell debris, all of which have been transported into the submarine cave entrance from the open lagoon (Harrington Sound). The mean $\delta^{13}C_{org}$ values (-19.7‰) and C:N ratio (10.5) indicate that sedimentary organics are derived from marine sources, which contain more nitrogen-rich plant tissues (Lamb et al., 2006). The lithofacies is present in

surface sediment samples from Harrington Sound to the Rat Trap (van Hengstum and Scott, 2011), which resembles the tops of cores 3, 4 and 5 (Figs. 3.5, 3.6). Therefore, the shell hash lithofacies is part of the submarine facies because GBC was a phreatic cave during its deposition and dominated by marine sedimentary processes.

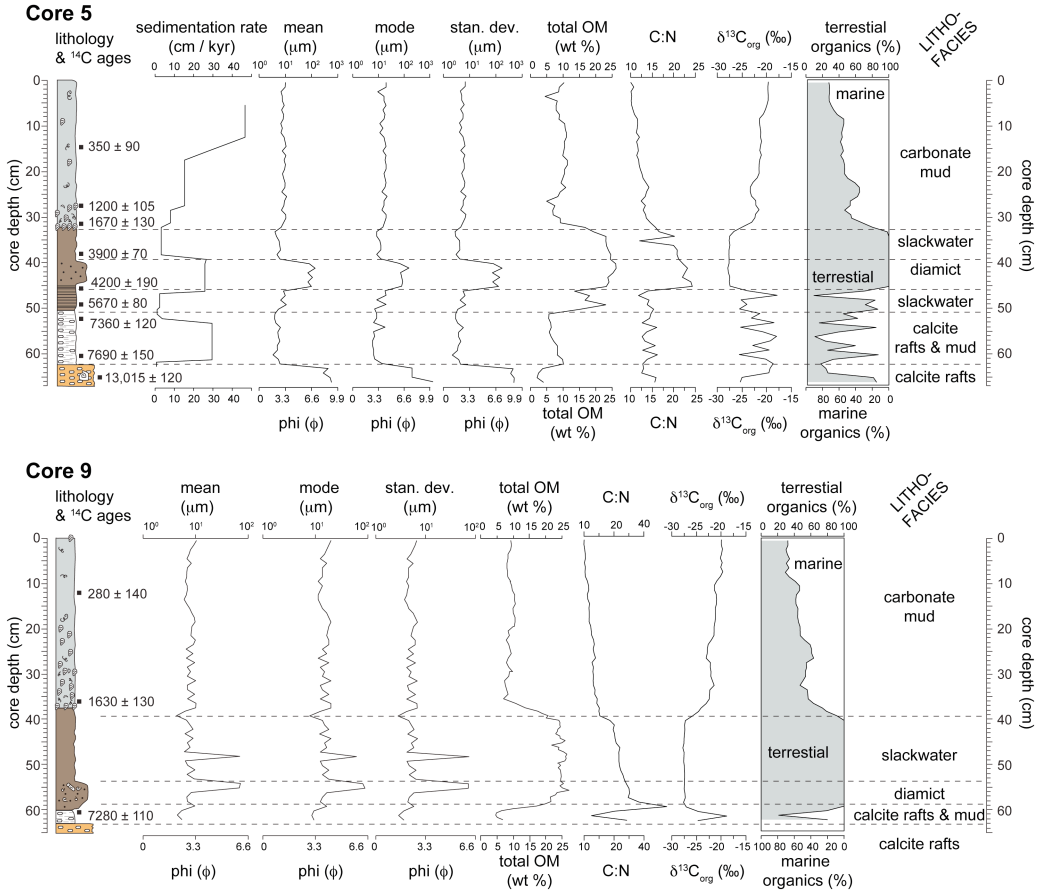

Figure 3.7: Downcore sedimentological and geochemical variables from cores 5 and 9, which span the Holocene. Sedimentation rates were calculated only on core 5 because it had the best age control, which were calculated by linear interpolation between radiocarbon ages.

3.5.7 Correlation And Age

Nineteen radiocarbon dates from the different cores provide confident age constraint for the contacts and timing of different sedimentary facies (Fig. 3.8). Only one radiocarbon date was available for the vadose facies because of the lack of shell or organic matter recovered in the calcite raft lithofacies. However, one *Poecilozonites* shell provides a basal date on the succession dated to 12.9 ka (Index No. 28 - Appendix 1). The contact between the vadose and littoral facies was dated in cores 5 and 11, providing a replicate age of ~7.7 ka on biogenic carbonate. The contact between the littoral and anchialine facies was dated in cores 5, 9, and 11, but the youngest age for the contact was on core 5 dated to 7.3 ka. We infer that the littoral facies rapidly accumulated in ~400 years, and deposition of the anchialine facies began at 7.3 ka ago. The contact between the anchialine and submarine facies was dated in three cores (5, 9, and 11), all of which replicated the result of 1.6 ka. Bivalves from slightly above this contact (1 cm) in core 12 and core 5 (2 cm) replicated a slightly younger result of 1.2 ka, perhaps indicating that sedimentation rates were low at the onset of the submarine facies. As such, the anchialine facies accumulated in the center of GBC over 5.7 ka, from 7.3 to 1.6 ka.

The radiocarbon dates also indicate variable sedimentation rates in the succession, and the presence of condensed horizons (low sedimentation rates) in the anchialine facies. For example, in core 5, 38–46 cm accumulated in 0.3 ka, whereas 46–50 cm accumulated in 1.5 ka (Fig. 3.7), based on linear interpolation between radiocarbon ages. Similar condensed and expanded horizons were found in the anchialine facies in Aktun Ha Cave (Mexico, van Hengstum et al., 2010). Based on estimates from core 5, the sedimentation rates for the carbonate mud lithofacies shift from approximately 15 to 40 cm ka^{-1}. This

sedimentation rate is comparable to the changing sedimentation rate for carbonate mud lithofacies in a Japanese submarine cave (21-42 cm ka^{-1}: Omori et al., 2010). Two dates from the carbonate mud lithofacies at similar positions in the cores 5 and 9 also give similar ages of ~0.4 ka ago, within radiocarbon uncertainties. The contact below the shell hash lithofacies is not constrained, but the unit began accumulation after 0.76 ka based on dated articulated bivalve horizon in core 6.

3.6 Discussion

Ford and Williams (1989) consider cave entrance deposits separate from cave interior deposits, and organize cave sediments as allogenic or autogenic deposits. This classification system is limited for comparing both vadose and phreatic sediments within a context of their depositional environments through geologic time, and limits inter-site comparability from geographically distributed karst basins. In our view, four main environments can be observed in coastal cave and karst basins: vadose, littoral, anchialine, and submarine, which contain spatially variable lithofacies (i.e., from the cave entrance to interior). This natural organization of cave facies harmonizes the interpretation of karst basin sediments akin to other coastal environments (e.g., deltas, lagoons, river systems). This framework is applied to the Holocene successions from Green Bay Cave, and provides a model for linking the evolution of karst basins under glacioeustatic sea-level forcing.

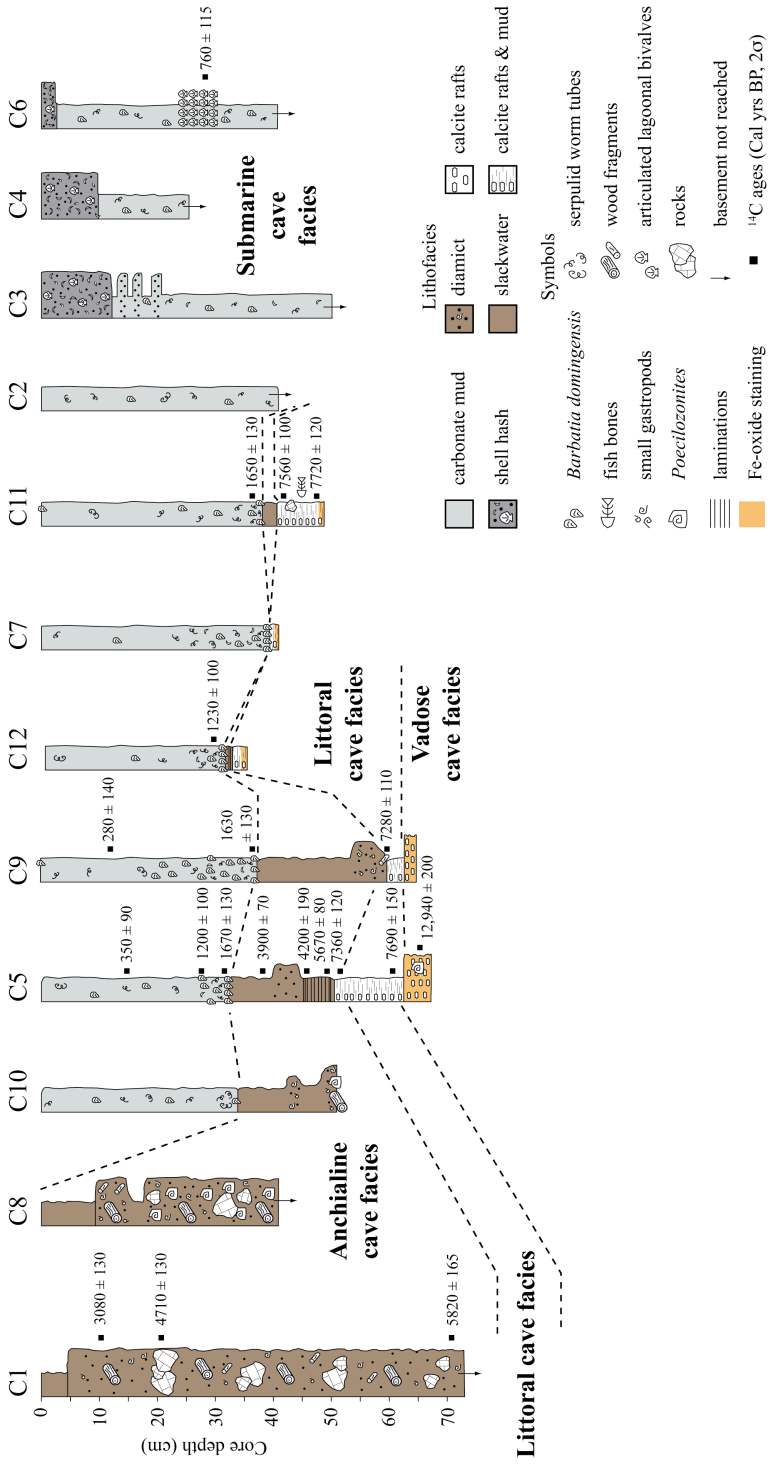

Figure 3.8: Correlation and facies analysis for Green Bay Cave succession.

3.6.1 Green Bay Cave (GBC) Evolution

3.6.1.1 GBC Vadose Facies

Green Bay Cave was in the vadose zone at the onset of the calcite raft lithofacies because at 12.9 ka, eustatic sea level was at approximately -65 m (Blanchon and Shaw, 1995; Siddall et al., 2003), which is far below the cave floor (-21 m). Thus, GBC was in the vadose (unsaturated) zone above the water table, which allowed a vadose facies to develop (Fig. 3.8). The vadose facies in GBC is dominated by calcite rafts, which are unambiguously indicative of standing water in a cave (Taylor and Chafetz, 2004; Taylor et al., 2004; Kolesar and Riggs, 2007). Standing water, however, was likely transient as indicated by the lack of aquatic microfossils and low accumulation rate of the lithofacies. These pools were perhaps derived from meteoric water dripping into the cave, forming small $CaCO_3$-saturated pools. The calcite raft lithofacies, however, only represents one possible unit in the GBC vadose facies prior to 7.9 ka (discussed further below, Fig. 3.9). The open atmosphere within the cave likely allowed *Poecilozonites* to crawl or wash into the cave, as has been observed in other Bermudian speleogenetic karst basins in the vadose zone (Hearty et al., 2004; Hearty and Olson, 2010).

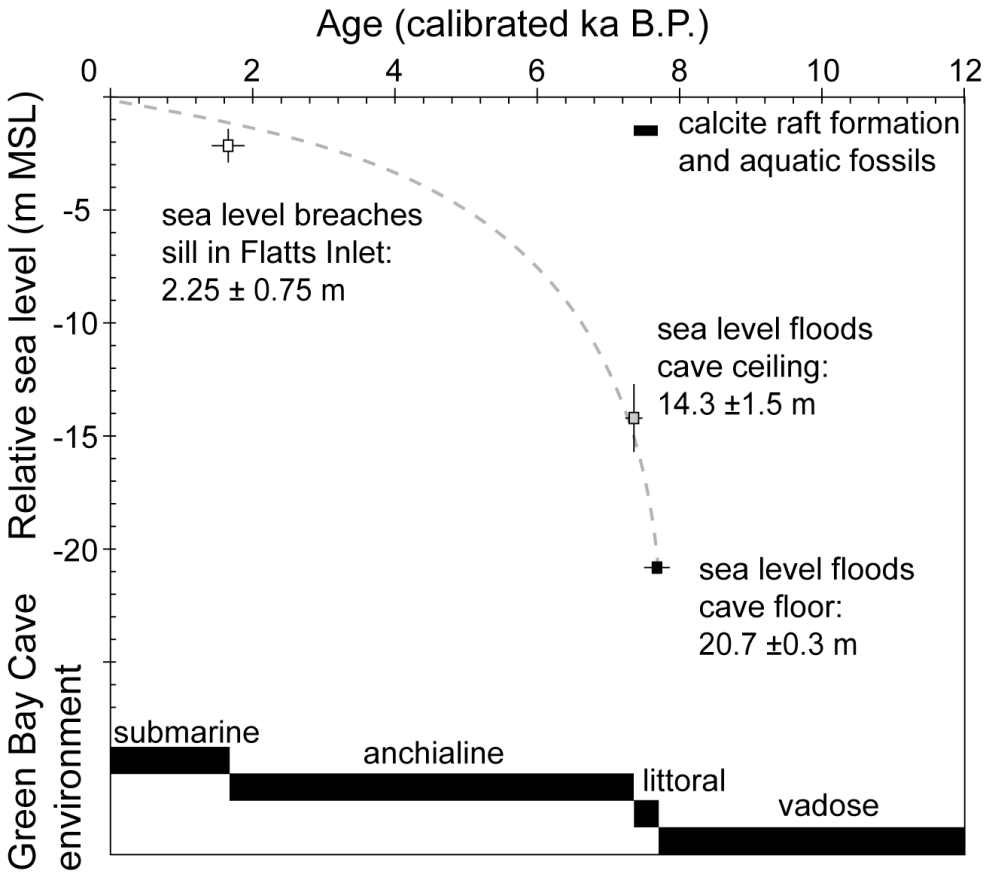

Figure 3.9: The impact of Holocene eustatic sea-level rise on facies development and environmental change in Green Bay Cave, Bermuda. Bar below the upper abscissa represents the only interval when calcite rafts and a marine ecosystem occur synchronously in the cave sediment.

3.6.1.2 GBC Littoral Facies

Sea level was within GBC to create a littoral cave environment 7.7 ka ago. This is evidenced by calcite raft precipitation that indicates an air-water interface was in the cave, coeval with marine microfossils indicative of a permanent aquatic habitat. Calcite rafts are one of many types of speleothem, which are reputable sea-level indicators and index points (Harmon et al., 1981; Richards et al., 1994; Vesica et al., 2000; Dutton et al., 2009; Dorale et al. 2010). The onset of calcite rafts also provides a sea-level index point in GBC

because they can only form when the water table is in a cave, once the effects of hydraulic head (gradients) are removed from elevation estimates (e.g., 5-10 mm km^{-1} in eastern Yucatan: Marin and Perry, 1994). Calcite rafts are currently forming in Mallorcan littoral caves (Spain), providing a modern analog for Green Bay Cave conditions from 7.9 - 7.6 ka ago (see figs. 9, 11 in Fornós et al., 2009). The presence of the endemic Bermudian cave ostracod *Paranesidea sterreri* and gastropod *Caecum caverna* indicate that the preserved microfossils are *in situ* and indicative of an aquatic habitat, and not merely transported into the passage from the lagoon. The fish bones in core 11 also suggest a marine ecosystem was present in the cave. Occasional high influx events of terrigenous organic matter (e.g., eolian, washover) likely caused the alternation between marine versus terrigenous organic matter preserved in core 5. Based on coeval calcite rafts and marine microfossils, Green Bay Cave was definitively flooded by Holocene sea-level rise ~7.7 ka ago, which formed an aquatic littoral cave environment. The floor of Green Bay Cave is located at –20.7 m below modern sea level, which the sedimentary evidence indicates was flooded by Holocene sea-level rise at 7.7 ka (Fig. 3.9). The position and timing of Green Bay flooding by sea-level rise is consistent with estimates of eustatic sea level rise in early-mid Holocene eustatic sea-level rise (Blanchon and Shaw, 1995; Siddall et al., 2003). Therefore, eustatic sea-level rise forced environmental evolution in Green Bay Cave System at 7.7 ka from a vadose to littoral cave environment.

3.6.1.3 GBC Anchialine Facies

The anchialine facies in Green Bay Cave is composed of two lithofacies, the diamict and slackwater, both of which are coeval and dominated by terrestrial sediment (Table 3.2). Cave diamicts typically form anywhere there is haphazard influx of poorly

sorted sediment into a cave entrance, or fluvial mass entrainment and re-deposition of cave sediment (Ford and Williams, 1989; Bosch and White, 2007; White, 2007). In contrast, slackwater lithofacies are fine-grained sedimentary units typically deposited distal to cave entrances and composed of clays and silts settling out of suspension (Ford and Williams, 1989; Bosch and White, 2007). The modern diamict lithofacies in GBC is at the sediment surface from Cliff Pool Sinkhole down into the cave, which attenuates in grain-size with increasing distance into the cave (van Hengstum and Scott, 2011). The modern diamict comprises sandy carbonate sediment, terrestrial plant (from wood to leaves) and animal remains (gastropod shells to livestock bones), and aquatic debris (mussel shells, algae, etc., van Hengstum and Scott, 2011). Terrestrial sediments and organic matter entering GBC at Cliff Pool Sinkhole are the obvious source of the poorly sorted, terrestrial-dominated diamict lithofacies in cores 1, 8, and 10. The diamict lithofacies is envisaged as laterally pinching out into the slackwater lithofacies because coarser grained sediment will be deposited near the sinkhole as bed load, whereas, finer-grained sediment will be transported further into the cave as suspended load (Ford and Williams, 1989). This mechanism is consistent with modern sedimentary patterns in GBC (van Hengstum and Scott, 2011), and explains both (a) the pinching out of the slackwater lithofacies in the distal successions (e.g., cores 12, 11 and 7), and (b) the attenuation in the cave of particle size distributions of the diamict lithofacies. Although the slackwater lithofacies in GBC is dominantly terrigenous, some uncertainty may be introduced to the $\delta^{13}C_{org}$ values from the transport of some fine-grained aquatic-derived organics from Cliff Pool Sinkhole into the cave (algae, phytoplankton: Schmitter-Soto et al. 2002; Sánchez et al., 2002; van Hengstum et al., 2010). This is because some lacustrine to brackish aquatic

organic matter can have similar depleted $\delta^{13}C_{org}$ values as terrigenous plants (Lamb et al., 2006). However, this is likely a minor process in GBC because of the small size of the aquatic environment in the sinkhole, and $\delta^{13}C_{org}$ remains a reliable proxy for differentiating marine versus terrestrial organic matter in coastal environment (e.g., Voβ and Struck, 1997; Lamb et al., 2006; Kemp et al., 2010). Based on the successions near Cliff Pool Sinkhole, the anchialine facies is perhaps also at the base of cores 3, 4, and 6, pre-dating when sea level flooded the entrance to GBC that opens into Harrington Sound.

Intervals of high (versus low) sedimentary influx into the cave (e.g., storminess, land disturbance, climate-forced precipitation changes) would provide increased (or decreased) sediment supply into the anchialine cave environment. This is perhaps the explanation for the variable sedimentation rates and condensed horizons observed in the anchialine cave facies in core 5 (Fig. 3.7). A similar pattern of condensed versus expanded horizons were described in the anchialine Aktun Ha Cave (Mexico), which were also related to changing terrigenous sedimentary influx into sinkholes (cenotes, van Hengstum et al., 2010).

3.6.1.4 GBC Submarine Facies

Theoretically, saline groundwater will completely flood a cave, or any speleogenetic karst basin, at some point during sea-level rise, and the predominance of marine processes will create submarine environments (Stock et al., 1986; van Hengstum and Scott, 2011). The onset of the carbonate mud lithofacies at 1.65 ka ago indicates the onset of the submarine cave environment in GBC, when well-oxygenated saline groundwater began to flood the cave (Fig. 3.9). Based on the onset of carbonate mud

lithofacies, tidally forced circulation throughout GBC was established by ~1.65 ka. In open ocean lagoons, carbonate mud deposition is initiated by oceanic circulation, which is linked to eustatic sea-level rise flooding the lagoon (Gischler, 2003; Zinke et al., 2005). Brachiopods, *Barbatia domingensis*, corals, and saline foraminifera also colonize the cave at 1.65 ka. *Barbatia domingensis* is an epifaunal suspension feeder ubiquitous in the modern caves of Bermuda, which is more commonly found attached to cavities in corals and reefs in Florida, Bermuda and Bonaire, which is also found in lagoonal sediments (Bretsky, 1967; Logan et al., 1984; Choi and Ginsburg, 1983; Kobluk et al., 1986; Sterrer, 1986; see fig. 9 in Zinke et al., 2005). Corallites of *Coenocyanthus goreaui* are also present in the carbonate mud lithofacies, which is a cave-adapted coral previously described from GBC and indicative of an oxygenated marine environment (Cairns, 2000). The sand horizons indicated by the PSDs in the carbonate mud lithofacies of core 3 likely relate to storm activity. However, the imbricated, monospecific, articulated bivalves in core 6 (0.76 ka) are suggestive of an Atlantic tsunami event (Reinhardt et al., 2006; Donato et al., 2008), but a more extensive coring survey in the cave entrance is needed to evaluate this hypothesis.

Modern coastal circulation between Harrington Sound and the ocean in Bermuda has only been achieved in the late Holocene when the sill in Flatt's Inlet (2.25 m ±0.5 m) was breached by Holocene sea-level rise (Vollbrecht, 1996). Tidally forced saline groundwater circulation in GBC, which occurs presently (Cate, 2009), is also linked to this event, because only an isolated marine basin existed in Harrington Sound prior to the sill being breached. Therefore, the transition to the carbonate lithofacies indicates the onset of modern circulation between Harrington Sound, the ocean, and GBC because (a) core lithofacies and surface sediments are equivalent, (b) *B. domingensis* is a

paleoenvironmental indicator of circulated marine conditions, and (c) coral only recently colonized Harrington Sound after it became circulated with North Lagoon (Vollbrect, 1996). Sea level breaching a 2-3 meter sill at 1.6 ka is within analytical error for the timing of Holocene sea-level rise in Bermuda (Ellison, 1993; Javaux, 1999), and indicates the change from the anchialine to submarine cave environment was forced by glacioeustatic sea-level rise. As a consequence, the anchialine facies laterally back-stepped towards Cliff Pool Sinkhole, as indicated by diversification of saline microfossils in a slackwater lithofacies overlying the diamict lithofacies in cores 1 and 8, as previously discussed (Fig. 3.8).

3.6.2 Spatial-variability In Global Karst Lithofacies

More broadly in global caves during sea-level lowstands, or if a cave is never flooded by sea level, spatially-variable sedimentary processes will give rise to site-specific lithofacies (Fig. 3.9, e.g., lacustrine, thalweg, guano, calcite rafts, entrance talus: Gospodarič, 1988; Ford and Williams, 1989; Gilbertson et al., 2005; Woodward and Goldberg, 2001; Bosch and White, 2007; White, 2007). Woodward and Goldberg (2001, table 3) provide a good summary of the dominant physical sedimentary processes that generate different vadose lithofacies, which readers are directed to for a more thorough analysis. An important distinction for vadose facies, however, is that pedogenic processes are often overprinted if the vadose lithofacies is never flooded by groundwater or sea level. It may be considered intuitive that the vadose facies comprises spatially variable lithofacies accumulating in global karst basins in the vadose zone; however, this provides a necessary framework for considering the entire geologic history of coastal karst basins.

Karst basin geomorphology and coastal position will likely remain significant factors influencing the lateral accretion, spatial variability, and vertical development of lithofacies in littoral environments. With the flooding by sea level and the local groundwater, permanent water flow through and open-system and aquatic ecosystems are established in littoral cave environments (Fig. 3.10). As such, sediments entering littoral cave environments can be eroding into the karst basin from terrestrial or marine sources, derived from any in situ aquatic ecosystems, or speleogenetic and/or hydrogeologic precipitates (e.g., calcite rafts). A modern littoral cave environment in Bermuda (Castle Grotto) is directly open to a lagoon, so waves and storms regularly transport sandy sediments from the lagoon into the cave. Similar basin morphology describes Blue Marino Cave, Italy, which opens directly to the ocean and is only partially flooded by sea level (Adriatic coast, see fig. 1B in Corriero et al., 2000). Attenuating wave action will therefore influence lateral lithofacies development in littoral caves opening directly to the ocean, which will not be a factor influencing lithofacies in karst basins protected from the ocean (e.g., unbreached flank margin caves). For example, Fornós et al. (2009) recovered terrestrial-influenced lithofacies (among others) from littoral caves set back from the coastline in Mallorca, with no lagoonal sand lithofacies characteristic of Castle Grotto, Bermuda. Although not observed in cores, we speculate that a diamict lithofacies was accumulating near the

Figure 3.10: (Following Page) Conceptual model of glacioeustatic-forced environmental evolution and facies development in coastal karst basins (caves, sinkholes) during a transgressive systems tract. Note that the boundary between anchialine and submarine caves in Stage 3 can now be quantified (see Chapter 2, this dissertation, van Hengstum and Scott, 2011).

1. Sea-level lowstand

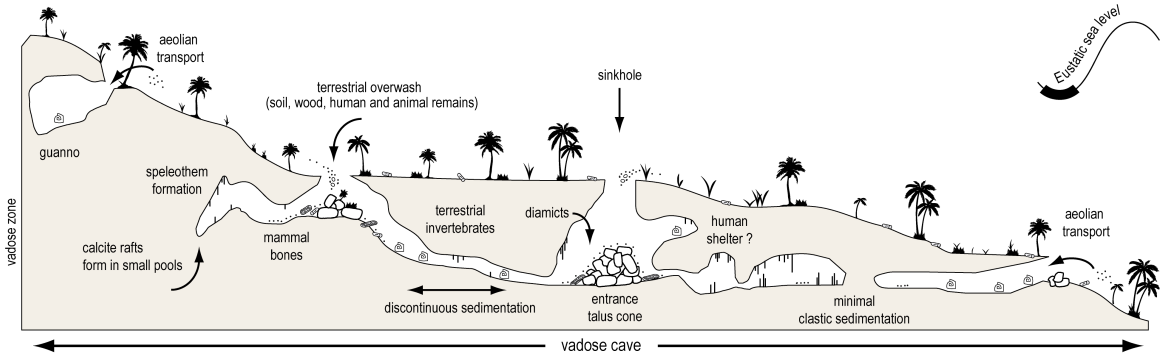

2. Early sea-level rise

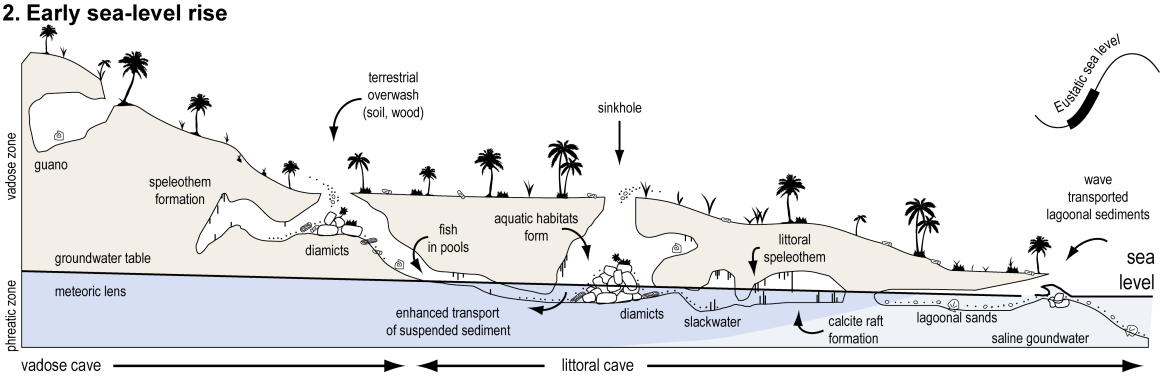

3. Late sea-level rise

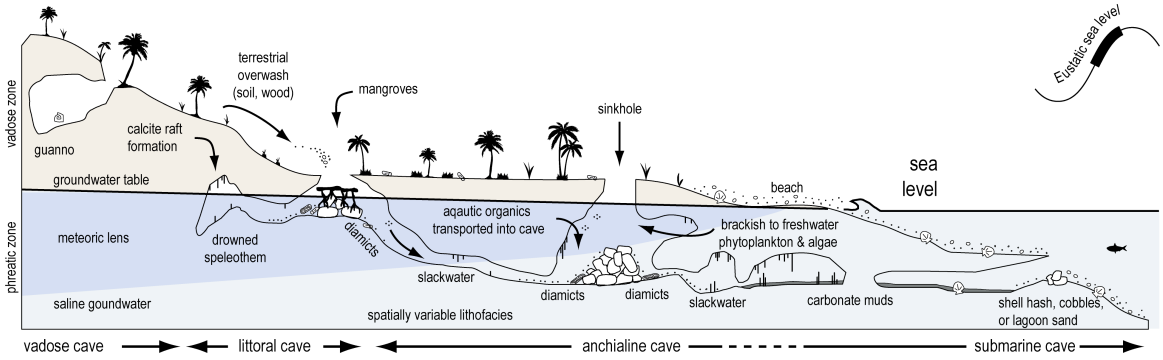

4. Sea-level highstand

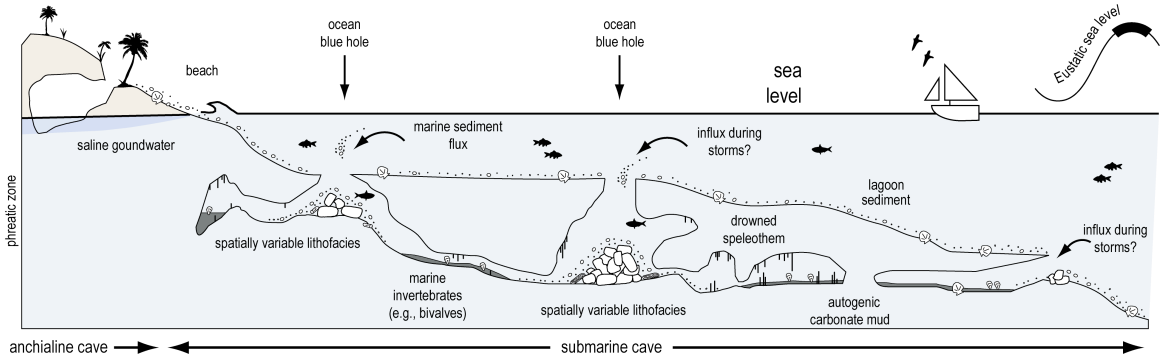

entrances to GBC when it was a littoral cave environment. Therefore, at least four factors influence the lithofacies that develop in littoral cave environments: coastal position, basin geomorphology, hydrodynamics, and water source (groundwater versus ocean). However, when sea level begins to flood a speleogenetic karst basin, all sedimentary units developing within them can be organized into a littoral facies.

Lateral lithofacies development can also occur in anchialine and submarine cave environments, although far less research has been conducted on these sedimentary facies. In the modern environment of the anchialine Aktun Ha Cave (Mexico), the sinkhole is an aquatic-based lithofacies, which transitions into an entrance diamict in the proximal cave, which finally transitions into a slackwater lithofacies deeper in the cave (Gabriel et al., 2009; van Hengstum et al., 2010). In the modern submarine environment in GBC, the shell hash lithofacies in cores 3, 4 and 6 attenuates into carbonate mud lithofacies deeper in the cave. The lateral lithofacies development in the submarine Daidokutsu Cave (Japan), are also comparable to GBC. Herein, a marine-based diamict with cobbles is accumulating at the cave entrance to Daidokutsu Cave that attenuates into carbonate mud the cave interior (see fig. 2 in Omori et al., 2010). The accumulation of coarse-grained sediment at the submarine cave entrance appears largely linked to the influence of waves and tidal currents, whereas coarse-grained diamicts at the entrance to anchialine caves appear largely related to gravitational transport of eroded aquatic and terrestrial sediments. Although more sites are needed to qualify these relationships, it is apparent that spatially variable lithofacies also develop in anchialine and submarine caves, which can be organized into the anchialine or submarine facies, respectively.

3.6.3 Research Applicability of Cave Facies

Vadose facies are extremely valuable in multiple disciplines (e.g., paleoclimate, paleoanthropology, paleogeography; Woodward and Goldberg, 2001; Courty and Vallverdu, 2001; Hearty et al., 2004). Karst basins essentially function as sediment traps that are protected from most subariael erosive processes. Therefore, it is not surprising that some of the most important paleoanthropologic finds (e.g., hominids and Paleolithic archaeological sites) are from vadose facies. Fossil records of invertebrates are also preserved in vadose facies. A 500 ka old vadose diamict lithofacies from Admiral's Cave (Bermuda) was used by Hearty and Olson (2010) to re-examine the punctuated theory of evolution using *Poecilozonites* shells, a theory originally based on the Bermudian endemic *Poecilozonites*. Although not recovered, we speculate a vadose diamict lithofacies likely accumulated at the base of Cliff Pool Sinkhole in GBC before 7.9 ka ago, coeval with the calcite raft lithofacies forming in the distal cave (core 5). In a Florida karst sinkhole, Hansen et al. (2001) recovered a late Pliocene (~2.8 to 1.8 Ma) succession preserving a regional palynological record that accumulated during a eustatic sea-level lowstand. Lastly, the geochemical signals preserved in vadose facies also contain also provide paleoclimate records (Panno et al., 2004; Polk et al., 2007; Wurster et al., 2008). It is well understood that cave sediments from the vadose zone have immense research value, but the advance presented here is that these separate lithofacies can all be organized into a greater vadose facies.

Littoral facies from karst basins (caves, sinkholes) appear useful to Quaternary sea-level research. This is because groundwater and sea level oscillate in synchrony once the effects of hydraulic head (gradients) are taken into account. In a subaerial

speleogenetic karst basin (i.e., sinkhole), Gabriel et al. (2009) recovered a *Rhizophora* peat lithofacies in the main sinkhole (cenote) of Aktun Ha Cave System (Mexico), which coincided with sea-level rise in the Yucatan karst platform. More distally positioned in a cave, co-stratigraphic calcite rafts and mud lithofacies in Green Bay Cave demarcate sea level flooding the cave floor at 7.9 ka (previously discussed). In a fossil example, littoral cave deposits preserved in small, elevated (+ 21 m) caves in Bermuda have been attributed to a co-stratigraphic position of sea level during Marine Isotope Stage 11 (Olson and Hearty, 2009; van Hengstum et al., 2009b). Importantly, these examples indicate that the applicability of the littoral facies to Quaternary sea-level research is quite promising.

Different anchialine facies have been successfully used in Quaternary Science (paleoclimate, paleohydrogeology, and paleoecology). Steadman et al. (2007) used sediments that can be described as an entrance diamict lithofacies from Sawmill Sink (Abaco, Bahamas) to reconstruct the paleoecology of the Pleistocene terrestrial landscape in the Bahamas, although the owl roost is part of a vadose facies. Although not originally identified as such, the slackwater lithofacies accumulated in Aktun Ha Cave (Mexico) records the paleoclimate influences on the eastern Yucatan meteoric lens (van Hengstum et al., 2010). Lastly, Alverez Zarikian et al. (2005) used ostracod paleoecology and $\delta^{18}O_{carb}$ to reconstruct long-term paleohydrogeological and paleoclimate changes in a sediment core recovered from Little Salt Spring (Florida), beginning with synchronous rise of the meteoric lens (local aquifer) and eustatic sea-level rise in the mid-Holocene, and eventual flooding of the sinkhole. When utilizing anchialine facies in paleoenvironmental research, it remains important to disentangle the effects of

hydrogeology versus climate on investigated proxies (sediments, microfossils; e.g., Alverez Zarikian et al., 2005; van Hengstum et al., 2010).

Only recently have submarine facies been explored for paleoclimate and/or paleoceanographic records. In the most complete example, a 7000-year paleoceanographic record of the East China Sea was obtained from Daidokutsu Cave (Japan, Yamamoto et al., 2010). Daidokutsu Cave is a submarine cave located offshore in a fore reef slope that is tidally circulated with the ocean water (Kitamura et al., 2007; Yamamoto et al., 2008, 2010). This allows microfossils preserved in the carbonate mud lithofacies to record oceanic conditions over Holocene time scales. Inland karst basins that are submarine environments can also preserve paleoclimate records if the saline groundwater mass flooding the karst basin is circulated with the ocean (Chapter 6, this dissertation). Because Walsingham Cave (Bermuda) is circulated with the ocean, this allowed van Hengstum (Chapter 6, this dissertation) to reconstruct the late Holocene paleoclimate of Bermuda using $\delta^{18}O_{foram}$ preserved in the carbonate mud lithofacies. From the limited case studies available, it appears that open-system saline groundwater circulation is a prerequisite for unbioturbated submarine facies to archive paleoclimate signals.

3.6.4 Sea level Forces Environmental Evolution in Speleogenetic Karst Basins

After comparing the complete Holocene successions in Green Bay Cave to sedimentary observations in other global coastal karst basins, we argue that glacioeustatic sea-level change controls the evolution of karst basins, which in turn effects the sedimentary deposits that can develop (Fig. 3.9). Overall, the Green Bay Cave succession is similar to Holocene transgressive sequences in lagoons (e.g., Gischler, 2003; Zinke et

al., 2005). However, instead of basal palesols and *Rhizophora* peat lithofacies observed in lagoons, Green Bay Cave accumulates calcite raft (vadose facies) followed by calcite rafts and mud lithofacies (littoral facies), which are loosely the cave-equivalent of lowstand and intertidal scenarios. During a lowstand, spatially variable sedimentary environments comprise the vadose facies, which transition to littoral facies when sea level first floods a carbonate platform (Fig. 3.10). As sea level continues to rise with complex groundwater relationships, anchialine environments first form that will eventually become completely submerged submarine facies when a karst platform becomes completely flooded. In the modern world, ocean blue holes represent the final phase of environmental development in karst basins, which often have entrances to submarine cave systems (e.g., Blue Hole, Belize; Fig. 3.6).

Sea-level change will also impact the ecosystems and organisms capable of living in a karst basin through time. In Green Bay Cave, the groundwater salinity shifted from marine, to brackish, and back to marine, which required invertebrates to adapt to changing hydrogeological conditions (e.g., emigration). Sea-level forced environmental evolution can also impact megafauna. For example, fossil seal skeletons in Bel Torrente Cave (Sardinia, Italy) indicate that the cave was likely a Monk Seal calving ground and nursery ~6.5 ka ago when sea-level was ~10 m lower and Bel Torrente Cave was a littoral cave environment. Since this time, however, sea-level rise has created the modern anchialine environment in the distal cave, which is currently not suitable for monk seal calving due to the lack of sufficient air pockets (De Waele et al., 2009). In contrast, sea-level regressions will force endemic aquatic cave crustaceans (stygobites) to vertically migrate as to remain in suitable groundwater habitats, whereas endemic vadose cave arthropods (troglobites) will expand into new vadose habitats. The true impact of sea-

level change on the evolution and development of endemic cave fauna and ecosystems remains yet to be fully appreciated.

A simplified expression of Johannes Walther's Law of the Correlation of Facies is that continuous sedimentary facies observed laterally in modern space should equally be developed in stratigraphic succession (Middleton, 1973)—a principle not demonstrated in global karst basins. Inherited geomorphology will be the dominant control for the development of facies in karst speleogenetic basins, but unlimited space for sediments to accumulate is a prerequisite in the conceptual application of Walther's Law. This principle requires that vadose (e.g., Admiral's Cave), littoral (e.g., Castle Grotto), submarine (e.g., Green Bay Cave), and anchialine facies and environments (e.g., Deep Blue Cavern) are equally represented respect to modern sea level and in succession. Based on the successions in GBC, this principle can be extended to karst basin facies because all these environments and facies occur in succession as a response to glacioeustatic sea-level rise.

3.7 Conclusions

The successions recovered from Green Bay Cave, Bermuda, track Holocene sea-level rise and document all facies and environments in response to glacioeustatic sea-level rise (vadose, littoral, anchialine, submarine). Through the Holocene transgressive sea-level cycle, vadose conditions existed in the cave until sea level flooded the cave floor at ~ 7.6 ka to create a littoral cave environment, promoting concurrent calcite raft precipitation (water table proxy) and a marine benthic habitat. Concurrently rising sea and groundwater levels eventually flooded Green Bay Cave causing a terrestrially dominated anchialine environment to develop. Sea-level rise eventually breeched a local sill at 1.65

ka and initiated (a) coastal circulation between Green Bay Cave, Harrington Sound, and the open ocean, and (b) submarine cave environments. Post-depositional alteration to the sediment column also appears plausible from saline groundwater upwelling. The succession in Green Bay Cave provides an evolutionary model for interpreting sediments in speleogenetic karst basins (caves, sinkholes) can be interpreted over geologic time scales.

Chapter 4: Foraminifera In Elevated Bermudian Caves Provide Further Evidence For +21 m Eustatic Sea Level During Marine Isotope Stage 11

Peter J. van Hengstum[1], David B. Scott[1], Emmanuelle J. Javaux[2]

1. Dalhousie University, Department of Earth Sciences, Halifax, Nova Scotia, Canada,

B3H 4J1, Tel: 1.902.494.3604, Fax: 1.902.494.6889

2. University of Liège, Research unit of Paleobotany-Paleopalynology-Micropaleontology, Geology

Department, 4000 Sart-Tilman Liège, Belgium

This manuscript is currently published:

van Hengstum, P.J., Scott, D.B., Javaux, E.J., 2009. Foraminifera in elevated Bermudian caves provide further evidence for +21 m eustatic seal level during Marine Isotope Stage 11. *Quaternary Science Reviews*, 28, 1850-1860, doi: 10.1016/j.quascirev.2009.05.017.

4.1 Abstract

Two hypotheses have been proposed to explain the origin of marine isotope stage (MIS) 11 deposits in small Bermudian caves at +21 m above modern sea level: (1) a +21 m MIS 11 eustatic sea-level highstand, and (2) a MIS 11 mega-tsunami event. Importantly, the foraminifera reported in these caves have yet to be critically evaluated within a framework of coastal cave environments. After statistically comparing foraminifera in modern Bermudian littoral caves and the MIS 11 Calonectris Pocket A (+21 m cave) to the largest available database of Bermudian coastal foraminifera, foraminiferal assemblages in modern littoral caves – and Calonectris Pocket A – cannot be statistically differentiated from lagoons. This observation is expected considering littoral caves are simply sheltered extensions of a lagoon environment in the littoral zone, where typical coastal processes (waves, storms) homogenize and rework lagoonal, reefal, and occasional planktic taxa. Fossil protoconchs of the Bermudian cave stygobite *Caecum caverna* were also associated with the foraminifera. These results indicate that the MIS 11 Bermudian caves are fossil littoral caves (breached flank margin caves), where the total MIS 11 microfossil assemblage is preserving a signature of coeval sea level at +21 m. Brackish foraminifera (*Polysaccammina*, *Pseudothurammina*) and anchialine gastropods (~95%, >300 individuals) indicate a brackish anchialine habitat developed in the elevated caves after the prolonged littoral environmental phase. The onset of sea-level regression following the +21 m highstand would first lower the ancient brackish Ghyben-Herzberg lens (< 0.5 m) and flood the cave with brackish water, followed by drainage of the cave to create a permanent vadose environment. These interpretations of the MIS 11 microfossils (considering both taphonomy and paleoecology) are congruent with the

micropaleontological, hydrogeological and physical mechanisms influencing modern Bermudian coastal cave environments. In conclusion, we reject the mega-tsunami hypothesis, concur with the +21 m MIS 11 eustatic sea-level hypothesis, and reiterate the need to resolve the disparity between global marine isotopic records and the physical geologic evidence for sea level during MIS 11.

4.2 Introduction

The proposed MIS 11 (400 ka) +21 m eustatic sea-level highstand has been debated since geologic evidence was first marshaled by Hearty et al. (1999) and supported by reports from other widespread localities (Kaufman and Brigham-Grette, 1993; Lundberg and McFarlane, 2002; Roberts et al., 2007). Problems arose when the physical geologic evidence for a MIS 11 highstand could not be reconciled with marine stable isotopic or atmospheric CO_2 records that suggest sea level during MIS 11 should be homologous to more recent interglacials due to similar oceanic water volumes (i.e., MIS 5e: +4-6 m; Hodell et al., 2000; Karner et al., 2002; Raynaud et al., 2005; Rohling et al., 2008). The islands of Bermuda are ideally suited for sea-level research, because they have remained tectonically and glacio-isostatically stable during the Quaternary (Vacher and Rowe, 1997). To date, Bermudian evidence for the MIS 11 highstand are marine-to-brackish sediments and fossils in karst caves, exposed in four elevated caves surrounding Government Quarry: Calonectris (+21.3 m), UGQ4 (+21 m), UGQ5 (+18 m), and the Land et al. site (~ +21; Land et al., 1967; McMurtry et al., 2007). These deposits are fossiliferous, containing: molluscs, vertebrates, echinoderms, red algae, coral fragments, and foraminifera. Numerous age determinations (U-series dating on flowstone, amino acid racemization on *Poecilozonites* and *Glycymeris*) from independent laboratories

confirm an MIS 11 age for the sediments and fossils in question (Hearty and Olson, 2008; McMurtry et al., 2008; Olson and Hearty, 2009).

Recently, McMurtry et al. (2007) proposed that the sediments were not developed *in situ*, but were transported into the caves from lower elevations by a mega-tsunami. Their arguments are based on: (1) the range of elevations for the deposits, (2) re-interpretation of isopachous cements as multi-generational and developed in multiple environments—not solely through speleogenesis, (3) generating additional variable U-series ages on the calcite flowstone (although still indicating a MIS 11 age for the sediments), and (4) the occurrence of several species of benthic foraminifera that were interpreted as having been transported by a mega-tsunami because they are supposedly atypical of other Bermudian coastal environments (i.e., lagoons, beaches). Arguments for and against the first three main points have been extensively discussed in publications debating the mega-tsunami hypothesis (i.e., Hearty and Olson, 2008; McMurtry et al., 2007, 2008; Olson and Hearty, 2009), however, the foraminifera have until now received incomplete assessment. The objective of this study is to compare modern Bermudian cave microfossils to those preserved in the MIS 11 elevated caves. This comparison will test whether or not the foraminifera found by McMurtry et al. (2007) were transported by mega-tsunami or if in fact are consistent a MIS 11 sea-level highstand. Without this analysis, the debate surrounding the origin of sedimentary deposits in the elevated Bermudian caves is currently incomplete.

4.3 Coastal Cave Environments And Foraminifera

There are several different types of coastal cave environments and habitats that require consideration before investigating geological remains in caves (Fig. 4.1).

Importantly, cave environments are not static, but constantly change in response to external and internal factors, such as ongoing speleogenesis (both phreatic and vadose) or sea-level change. In coastal carbonate terrain, local hydrogeology is arguably the greatest ecological control on ecosystems in different coastal cave systems. The groundwater flooding a cave passage is either part of the Ghyben-Herzberg (GH) lens (fresh to brackish water) or basal marine groundwater that is intruding from the coast (Vacher, 1988; Whitaker and Smart, 1990). The GH lens contains meteoric water that is flowing coastward, whereas the basal marine water exhibits more complex subterranean circulation patterns (Moore et al., 1992; Whitaker and Smart, 1990; Vacher, 1988). The interface between these two water masses is the halocline or mixing zone, which is (1) a slightly acidic region, dominantly responsible for phreatic cave dissolution, and (2) strongly controlled by sea level (see theoretical and practical discussions in: Smart et al., 1988; Vacher and Rowe, 1997; Schneider and Kruse, 2003). Arising from the strong environmental gradients between these two separate water masses (salinity, dissolved oxygen, etc), different aquatic invertebrates have habitats in different passages and areas of coastal caves, depending upon which water mass is currently saturating a specific cave passage (e.g., Pohlman et al., 1997).

The Stock et al. (1986) classification of coastal cave environments, and elaborated on herein, is most frequently used to describe the phreatic (flooded) cave habitats of modern aquatic cave fauna (stygobites and stygophiles). First, reef caves are void spaces below modern sea level in modern reef environments. They range in size from small void spaces to dominant cave passages, and are hydrologically dominated by coastal oceanography (e.g., Kitamura et al., 2007).

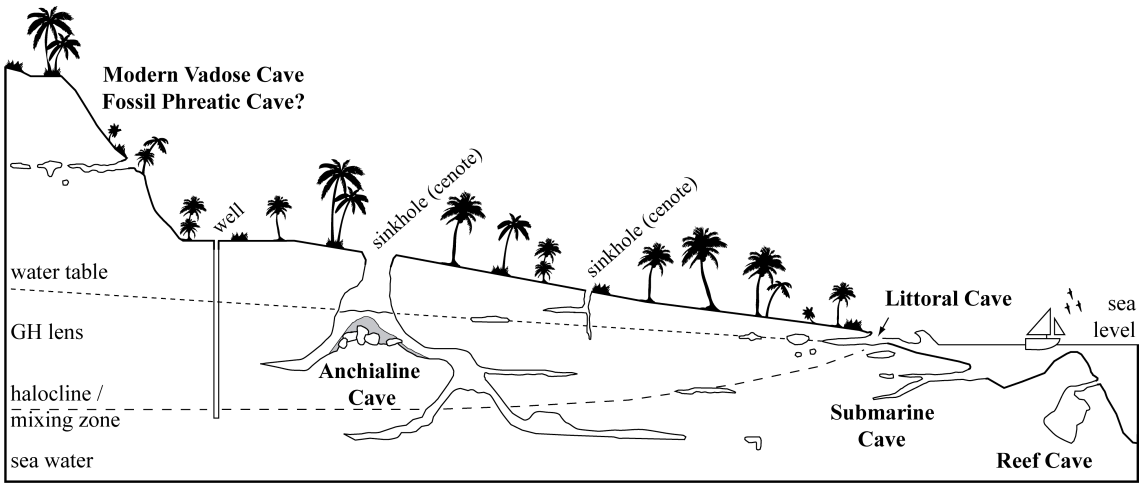

Figure 4.1: Classification of coastal cave environments. Note that sinkholes are commonly known as cenotes in Mexico, and this nomenclature is often extended to other global locales.

Anchialine caves have a recognizable terrestrial and marine influence, and typically intersect (or are within) the Ghyben-Herzberg (GH) lens. Anchialine caves can have either sub-aerial access through a sinkhole (cenote), or subterranean access by a cave passage meandering from the basal saline groundwater into the GH lens (Fig. 4.1). In contrast, submarine caves have entrances that are below sea level, their passages are completely flooded with saline water, yet they receive active continental influence, not from the terrestrial surface, but through subterranean saline groundwater circulation (i.e., Whitaker and Smart, 1990). These caves retain a significant marine character at their entrance, and have arguably received the majority of marine ecological attention. Next, littoral caves occur at sea level in the littoral zone, and are human-accessible from outside the cave environment. They often contain the air-water interface, which can continue for some distance into the cave. Within a geologic framework, littoral cave environments can be sea caves, or breached flank margin caves—where speleogenesis and wave action have collectively breached a flank margin cave wall. The breaching of a flank margin cave wall is an important environmental event, as the cave habitat instantly evolves from a

dark and isolated subterranean void space, to a protected enclosure along a coastline with physical oceanic communication. Because many flank margin caves form significantly close to sea level, they have received considerable geologic attention as a Pleistocene sea-level proxy (Mylroie and Carew, 1990; Labourdette et al., 2007 Mylroie et al., 2008). This classification of coastal cave environments provides a simplified – yet necessary – framework for evaluating cave micropaleontological remains, as sea level and hydrogeological changes will have concomitant impacts on how specific habitats in a phreatic cave evolve.

An important limitation of this scheme is that not all cave environments are adequately described *sensu stricto* by this classification. For example, large solitary coastal cave systems may contain several types of cave environments; such as Ox Bel Ha in Mexico that hosts anchialine and submarine environments. Furthermore, other types of coastal environments can potentially overprint cave habitats, especially when the cave entrance has evolved into another coastal system (e.g., from a sinkhole into a mangrove swap or lagoon). This classification scheme also omits the relationships between the present cave environment and the geologic mechanisms responsible for cave formation. For example, many modern submarine cave environments are historical former flank margin caves. Despite these caveats, this classification scheme provides a necessary environmental framework for understanding the origin of ancient cave deposits.

Benthic foraminifera (unicellular marine to brackish protists) are particularly important environmental proxies across coastal environments, owing to the excellent preservation potential of their tests in the sedimentary record, and their ecologic sensitivity to critical environmental parameters (e.g., pH, dissolved oxygen, temperature). The sensitivity of foraminifera to salinity has caused specific species to evolve ecological

niches at specific elevations relative to modern sea level in salt marshes, which is widely used as an accurate tool for demarcating former sea levels (Scott and Medioli, 1980a, 1978; Scott et al., 1981; Horton and Edwards, 2005). In contrast to their widespread application in coastal research, there has been very little systematic investigation of foraminifera in caves. Documentation of foraminifera in subterranean settings is typically limited to mentioning their sedimentary contribution within the context of a broader analysis, or just documenting their existence (Fig. 4.2).

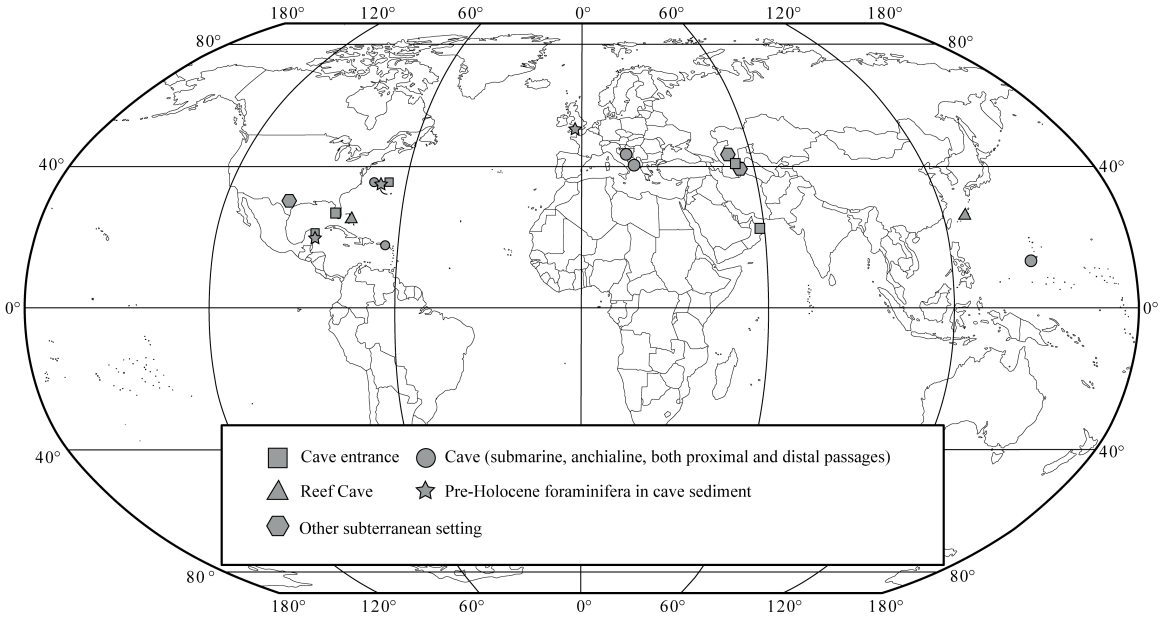

Figure 4.2: Global subterranean locations where foraminifera have been recovered. As reported by: Birstein and Ljovuschkin (1965), Mikhalevich (1976), Sket and Iliffe (1980), Reiswig (1981), Rasmussen and Brett (1985), Longly (1986), Proctor and Smart (1991), Novosel et al. (2002), Javaux and Scott (2003), McMurtry et al. (2007), Kitamura et al. (2007), Denitto et al. (2007), Lewis and Tichenor (2008), E. Reinhardt (Oman - Pers. Com., 2009), van Hengstum et al. (2008, 2009). Foraminifera have yet to be documented in southern hemisphere coastal cave environments.

van Hengstum et al. (2009), however, demonstrated that benthic foraminifera are capable of discriminating historical vertical displacements of the halocline and GH lens in coastal cave environments. Microfauna in phreatic caves respond to the evolving cave habitats caused by sea-level change. Most importantly, euryhaline foraminifera and testate amoebae can colonize cave passages saturated by the GH lens (fresh to brackish water), which are different from the marine taxa living below the halocline in the saline groundwater (Bermuda: Sket and Iliffe, 1980; Javaux, 1999; Mexico: van Hengstum et al., 2008, 2009).

4.4 Regional Setting

The origin of foraminifera in the MIS 11 elevated Bermudian caves (Calonectris, UGQ4, UGQ5, Land et al. 1967 site) will only be deciphered after they have been compared with all natural Bermudian coastal environments, including coastal caves (Fig. 4.3A). In 1993 and 1995, over 170 surface sediment samples (upper 5 cm) were collected from across Bermudian coastal environments: mangroves (Hungry Bay, Mill Share), reefs (Hog Breaker reefs, Twin Reefs, North Lagoon traverse), lagoons (North Lagoon off Devonshire dock, Harrington Sound), protected lagoons with peripheral mangroves (Walsingham Bay, Mangrove Bay), and the entrance to anchialine caves (Leamington Cave, Walsingham Cave System – entrances: Walsingham and Crystal caverns; Javaux, 1999). All of the sampling sites were typically in one environmental category, except a transect that was sampled in the North Lagoon (from the lagoon, into the reef). In addition, two samples were collected in early 2009 from a modern littoral cave. This sample collection provides the necessary framework to examine the similarity between

fossil and modern assemblages of Bermudian coastal foraminifera. Based on the mega-tsunami hypothesis, there should be minimal congruency between the foraminiferal assemblages in modern Bermudian coastal environments and the foraminiferal assemblages in the MIS 11 elevated caves (McMurtry et al., 2007).

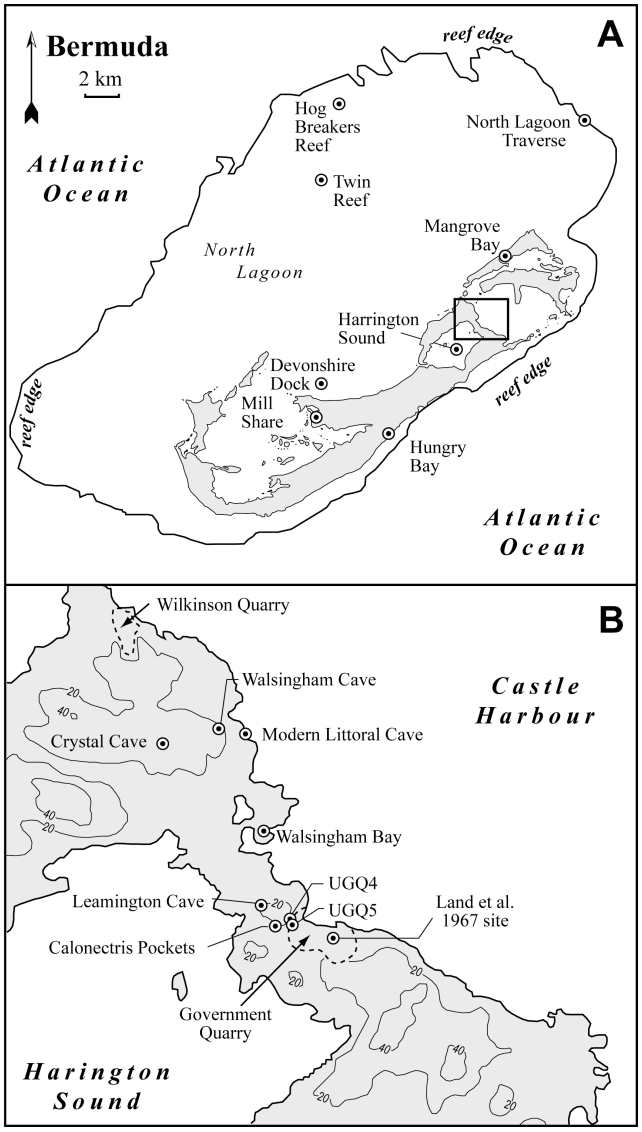

Figure 4.3: Surface sediment locations across Bermuda (A) and along the Walsingham Tract (B). Base map and contours (20 m interval) after Vacher et al. (1989), square in (A) is magnified in (B).

The MIS 11 fossil caves are all located in the vicinity of Government Quarry, Bermuda, on the isthmus separating Harrington Sound and Castle Harbor (Fig. 4.3B). Geologically, this area is commonly referred to as the Walsingham Tract, after the Walsingham Formation. This limestone bedrock is the oldest and most diagenetically mature eolianite on Bermuda (Land et al., 1967) and is famous for both vadose and phreatic caves. Sediment no longer exists in outcrop for either the Land et al. (1967) or the Calonectris sites, however, representative sediment samples from Calonectris Pocket A and Pocket B (< 50 cm apart) were obtained from the Smithsonian Institution for analysis (see Olson and Hearty, 2009 for detailed outcrop descriptions). Wilkinson (2006) discovered that only very rare foraminifera are preserved in the other elevated MIS 11 caves (UGQ4, UGQ5, Land et al. 1967 site), which are only suitable for a presence/absence-based interpretation (McMurtry et al., 2007). Although foraminifera from every cave are unavailable and unsuitable for multivariate statistical treatment, we re-summarize all the microfossils preserved in the Bermudian MIS 11 cave sediments to allow for a holistic interpretation of the foraminifera in question.

4.5 Methods

Surface sediment samples (10 cm^3, upper 5 cm) were washed over a 63 μm sieve, and approximately 300 foraminifers were wet-enumerated where possible in petri dishes (Javaux, 1999). Approximately 271 separate taxonomic units were originally identified in the surface samples, collectively forming the largest available database of Bermudian coastal foraminifera. For the MIS 11 Calonectris Pockets, only Calonectris Pocket A contained abundant foraminifera suitable for multivariate statistics analysis, not Pocket B. However, all foraminifera observed from Calonectris Pocket B were noted for their

presence, similarly to the other elevated cave sites. Only total assemblages of foraminifera were considered in this analysis (thanatocoenosis), which includes the bias introduced by typical taphonomic processes at each sample site, such as coastal re-working. However, the thanatocoenosis is thought to better characterize average environmental conditions at a sample locale (Scott and Medioli, 1980b) and allows for the inclusion of fossil material into a statistical investigation with the modern samples.

After manually entering the original database from Javaux (1999) into a personal computer, statistically insignificant samples (n = 25) were omitted from the analysis (where: <300 individuals were enumerated, abundances of taxonomic units grossly did not total 100%, insignificant sampling of a separate environmental settings). The original 271 taxonomic units (species) were then amalgamated into genera to smooth any taxonomic inconsistencies (especially in the miliolid group) and create a more robust comparison between environments by desensitizing the analysis to micro-environmental effects within individual ecotopes. Of the original 128 different genera (variables) identified, 38 genera were deemed statistically insignificant and omitted from the final multivariate analysis due to the estimated standard error for the genera being greater than the abundance in all samples (Patterson and Fishbein, 1989). This resulted in a final data matrix of 102 samples, each with 90 variables. Samples were then compared using a Euclidean distance coefficient and amalgamated into clusters using Ward's method of minimum variance and displayed in an hierarchical dendrogram, using the software package *PAST* (Paleontological Statistics, Hammer et al., 2001), which approaches the method of Fishbein and Patterson (1993). Finally, representative microfossil specimens from the modern littoral cave and MIS 11 Calonectris Pockets were imaged using scanning electron microscopy (SEM) to confirm taxonomy, examine shell exteriors, and

make detailed visual comparisons.

4.6 Results

4.6.1 Modern Bermudian Coastal Foraminifera

The dendrogram produced through the Q-mode cluster analysis indicates five distinct clusters that are interpreted as different assemblages of coastal foraminifera in Bermuda: Mangrove Assemblage, Reef Assemblage, Lagoon Assemblage, Anchialine Cave Assemblage, and the Protected Lagoon Assemblage (Fig. 4.4). Only a brief overview of these assemblages is provided here, as all the major and subtle ecological and taxonomic nuances of this dataset are provided in Javaux (1999) and Javaux and Scott (2003).

The Mangrove Assemblage contains samples from Mill Share and Hungry Bay and has the lowest diversity of all the assemblages. The dominant genus is *Trochammina*, with *Polysaccammina*, *Miliammina*, *Pseudothurammina,* and *Discorinopsis* present in lower abundances. The Reef Assemblage is dominated by *Homotrema rubrum* at Hog Breaker Reef, Twin Reef, and North Lagoon Reef and has significantly increased diversity in the miliolid and rotalid groups as compared with the Mangrove Assemblage. The Reef Assemblage and the Mangrove assemblage are both very well defined by the cluster analysis, owing largely to the significant overall contribution of *Trochammina* and *Homotrema* to their respective assemblages.

The most diverse samples are in the Lagoon Assemblage, where miliolid genera are dominant. Samples from Devonshire Dock, Harrington Sound, the modern littoral cave, Calonectris Pocket A, and two samples from a protected lagoon (Mangrove Bay) are included in this assemblage. Many characteristic reef (*Homotrema*, *Asterigerina*,)

mangrove (*Polysaccammina*, *Pseudothurammina*), and planktic taxa are commonly encountered in the lagoons, indicating that coastal processes are constantly reworking foraminiferal tests from across the Bermudian platform. The inclusion of two samples from a protected lagoon site is therefore not surprising, considering the size of the database and that locations within a protected lagoon may actually be more comparable to an open lagoon site, such as the entrances to more open water. The Protected Lagoon Assemblage contains samples from both Walsingham Bay and Mangrove Bay, which are protected by mangroves (*Rhizophora* spp.) around the lagoon periphery. *Discorinopsis*, *Helenina*, *Triloculina*, and *Trochammina* are the most dominant genera in the Protected Lagoon Assemblage, with overall decreased diversity as compared with the open lagoons (Harrington Sound, North Lagoon). Three mangrove swamp samples are similar to the Protected Lagoon Assemblage based on the Q-mode cluster analysis (MA-MS2, MA-HB3, MA-HB4). All of these samples are < 30 cm deep in the water and have increased abundances of *Triloculina oblonga* (opportunistic subtidal taxon), *Discorinopsis,* and *Helenina*—common higher-salinity mangrove species. In such shallow settings, evaporation may cause increased salinity (albeit still euhaline) in smaller pools, environmentally creating a protected lagoon microenvironment within a larger mangrove setting.

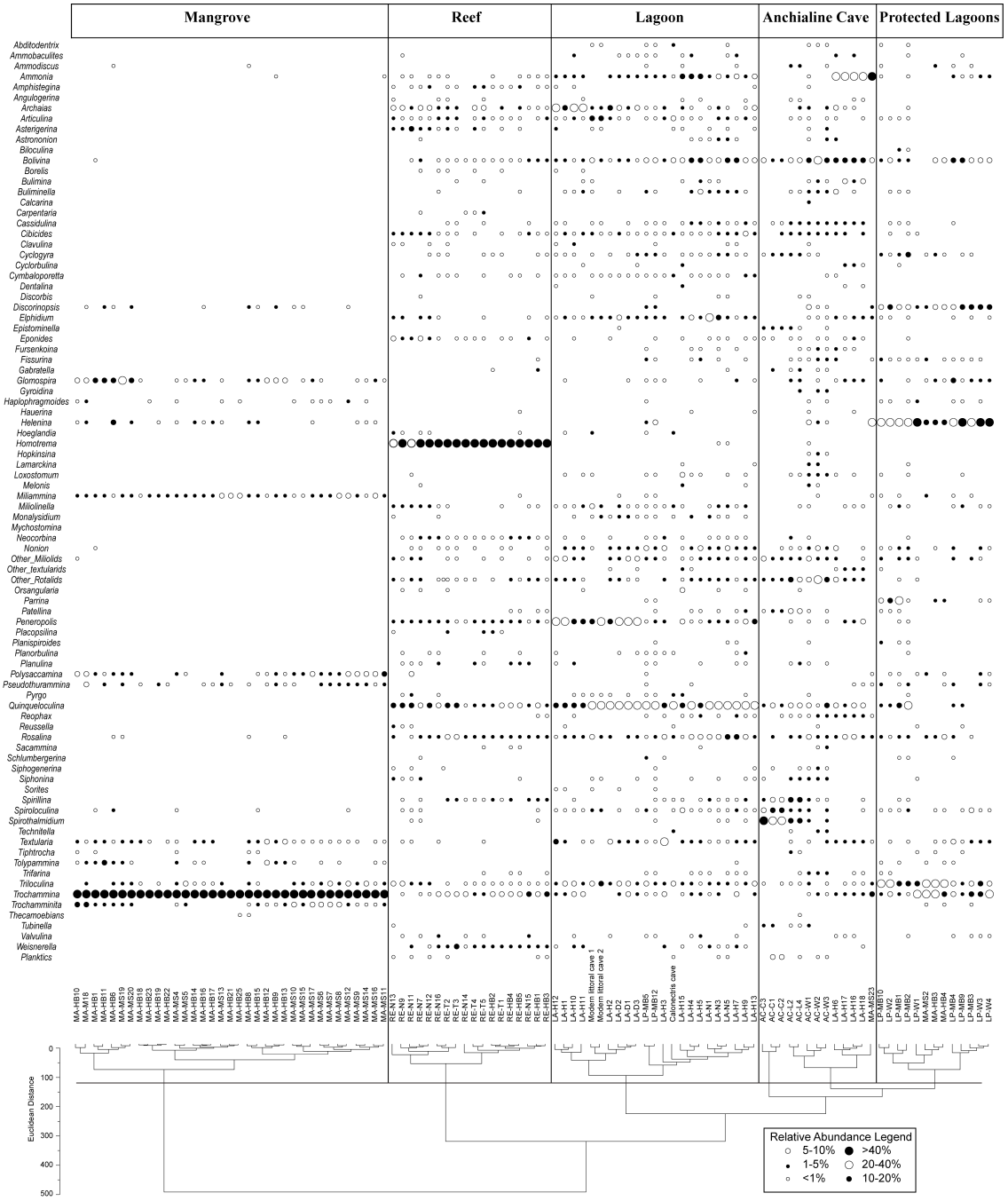

Figure 4.4: The dendrogram produced through Q-mode cluster analysis indicates five separate assemblages of coastal foraminifera in Bermuda. In the Lagoon Assemblage, note the similarity between the modern littoral cave and Calonectris Pocket A to other lagoon samples. Sample label prefixes (environment): MA-mangrove, RE-reef, LA-lagoon, AC-anchialine cave, LP-protected lagoon. Sample label suffixes (locale): HB-Hungry Bay Marsh, H-Harrington Sound lagoon, MS-Mill Share, N-North Lagoon traverse, MB-Mangrove Bay, HB-Hog Breaker Reef, T-Twin Reef, D-Devonshire dock, C-Crystal Cave, L-Leamington Cave, W-Walsingham Cave, W-Walsingham Bay.

The Anchialine Cave Assemblage is best characterized by elevated abundances of *Spirophthalmidium* sp., a taxon that is rarely encountered (< 1%) outside the phreatic cave environment (Javaux, 1999). Five samples from outside the cave environment (LA-H16, LA-H17, LA-H18, LA-H6, MA-M23) are most similar to Bermudian anchialine cave samples, all which have the highest abundances of *Ammonia* in the whole database. This preliminary investigation of Bermudian phreatic caves was limited to only the entrances of the larger subterranean cave systems, and did not sample through the full range of environmental variables that exist in a phreatic cave (light gradients, salinity gradients, etc.). This factor explains why the anchialine cave samples share similarity to other open water sample locales. However, this limited sampling of the anchialine caves recovered different living foraminifera in the brackish GH lens than in marine conditions below the halocline (based on rose Bengal staining, Javaux, 1999). *Polysaccammina* and *Pseudothurammina* were found living in the brackish GH lens, although only in samples requiring omission from multivariate statistics because insufficient individuals were originally counted in those samples (Javaux, 1999). These species are diagnostic brackish taxa and only form small populations in marshes, brackish ponds, and the GH lens in Bermuda and Mexico (van Hengstum et al., 2008; Roe and Patterson, 2006; Javaux and Scott, 2003; Scott, 1976). However, despite the removal of these samples from the database, typical marsh foraminifera *Trochammina*, *Polysaccammina*, and *Pseudothurammina* are living in the modern GH lens in the Walsingham Tract (< 30 cm thick GH lens - Iliffe et al., 1983; Javaux, 1999). Below the halocline in full marine salinity, typical lagoon taxa fauna are living (*Quinqueloculina*, *Rosalina, Triloculina*). Lastly, minor abundances of reef, lagoon, and planktic foraminifera are present at the

sediment-water interface in the anchialine caves. *Archaias angulatus* and *Articulina* tests were often fractured, and edge rounding and abrasion were common on *Amphistegina* and *Asterigerina* tests. Furthermore, *Homotrema rubrum*, a diagnostic reef taxon, was found inland within the cavern of Walsingham Cave, several hundred meters away from the modern coastline, and several kilometers from the reef. The absence of rose Bengal staining indicates these taxa are not living in modern anchialine caves (Javaux, 1999). Their transport into the cave is attributed to typical coastal processes (waves, hurricanes) reworking these taxa from adjacent coastal environments into the caves.

Most relevant to this study is that neither the samples from the modern littoral cave, nor samples from Calonectris Pocket A, can be statistically differentiated from the modern lagoon based on foraminifera alone. The modern littoral cave samples are statistically most similar to samples collected from Harrington Sound lagoon and the North Lagoon (sample sites off Devonshire dock). Fractured, dead specimens of *Archaias angulated* and *Articulina mucronata* were present in the modern littoral cave, along with reef taxa *Amphistegina lessoni* and *Asterigerina carinata*. Therefore, typical coastal processes (waves and storms) are responsible for transporting material from the reefs and lagoons into the modern littoral cave, demonstrating how littoral caves act as mere sheltered extensions of lagoons with respect to foraminifera. Typical coastal foraminifera dominated the modern littoral cave assemblage (*Quinqueloculina*, *Triloculina*, other rotalids), with lower abundances of *Textularia agglutinans* and stygophilic ostracods (*Loxoconcha oculocrista, Paranesidea sterreri*). However, the modern littoral cave is also the habitat for the endemic cave gastropod *Caecum caverna*—which does not live in lagoons—and provides a diagnostic paleoenvironmental marker for a phreatic cave. Many foraminiferal tests have surficial pitting (Plate 1 - M3, M7, M9, M12), not a surprising

characteristic because mildly acidic conditions can occur in littoral caves from the mixing of meteoric water in the GH lens with saline marine water (Smart et al., 1988; Mylroie et al., 2008).

4.6.2 Microfossils In MIS 11 Caves

Microfossils preserved in the sediment of MIS 11 Calonectris Pockets included foraminifera, rare ostracods, and rare bryozoan fragments (Fig. 4.5). Statistically insignificant quantities of foraminifera were preserved in Calonectris Pocket B, but typical coastal taxa were observed, including: *Amphistegina*, a sole fractured specimen of *Archaias, Asterigerina, Bolivina*, *Quinqueloculina*, *Rosalina*, and *Triloculina* (Table 4.1). Ostracods and other microfossil remains were absent from Pocket B. In contrast, a high abundance of foraminifera (~832 cm^{-3}) were preserved in Pocket A, including all the taxa from Pocket B, except *Archaias angulatus*, as well as a two planktic foraminifers. The only agglutinated taxon recovered from the Calonectris site was *Textularia agglutinans* (Fig. 4.5 – F10). After examining Calonectris foraminifera with SEM, several tests contained fractured chambers (Fig. 4.5 – F5, F10) as well as dissolution pitting (Fig. 4.5 – F7)—characteristics also observed in foraminiferal tests from the modern littoral cave (M9, M12). Secondary calcite overgrowth was also observed on the foraminifer tests (Fig. 4.5 – F8), and on the interior of ostracod valves.

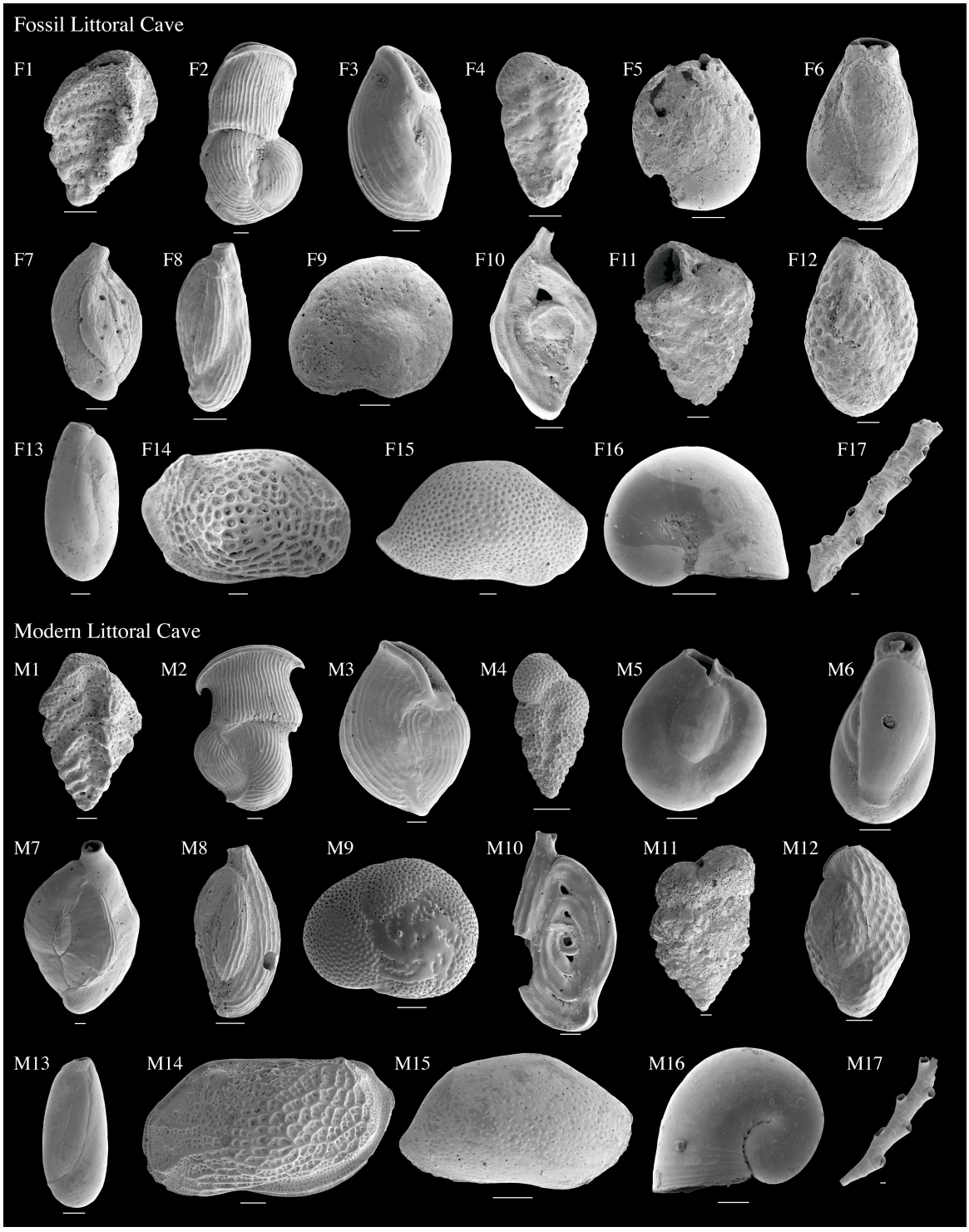

Figure 4.5: A comparison of MIS 11 littoral cave (Calonectris) microfossils (top half) to the microfossils in the modern littoral cave (bottom half). Foraminifera: **F1, M1**: *Abditodentrix rhomboidalis* (Millett) 1899; **F2, M2**: *Articulina spp.* (d'Orbigny) 1826; **F3, M3**: *Articulina mexicana* Cushman 1944a; **F4, M4**: *Bolivina variabilis* (Williamson) 1858; **F5, M5**: *Miliolinella subrotunda* (Montagu) 1803; **F6, M6**: *Pyrgo elongata* d'Orbigny 1826; **F7, M7**: *Quinqueloculina candeiana* d'Orbigny 1839a; **F8, M8**: *Quinqueloculina poeyana* d'Orbigny 1839a; **F9, M9**:

Rosalina subaraucana (Cushman) 1922; **F10, M10**: *Spiroloculina antillarum* d'Orbigny 1839; **F11, M11**: *Textularia agglutinans* d'Orbigny 1839a; **F12, M12**: *Triloculina carinata* d'Orbigny 1839a; F13, M13: *Triloculina oblonga* (Montagu) 1803. Ostracods: **F14, M14**: *Loxoconcha oculocrista* Teeter 1975; **F15, M15**: *Paranesidea sterreri* Maddocks and Iliffe, 1986. Troglobytic gastropod: **F16, M16**: *Caecum caverna* Moolenbeek, Faber, and Iliffe, 1988. Bryozoan fragment: **F17, M17**. Scale bars represent 50 μm.

Additionally, all of the foraminifera documented from the Calonectris Pockets also are present in modern Bermudian caves (Table 4.1). Pocket A also contained the ostracods *Loxoconcha oculocrista* and *Paranesidea sterreri* (articulated and disarticulated specimens), which are common taxa in modern Bermudian anchialine and littoral caves, and capable of withstanding mesohaline conditions (5 – 18 ppt, Maddocks and Iliffe, 1986). Notably, the genus *Loxoconcha* especially favors littoral environments (Van Morkhoven, 1963). Finally, two specimens of the gastropod *Caecum caverna* were found in Calonectris Pocket A, a protoconch (Fig. 4.5 – F16) and a protoconch with part of the secondary growth stage attached. This gastropod is an aquatic, Bermudian endemic cave taxon (stygobite) that can tolerate salinity from 20 – 35 ppt (Moolenbeek et al., 1988). The recovery of this taxon is significant by providing strong evidence that Calonectris Pockets were once phreatic cave environments.

Foraminifera preserved in the other Bermudian MIS 11 caves (UGQ5, UGQ4, Land et al. 1967 site) were previously presented by McMurtry et al. (2007). The only taxon preserved in all the MIS 11 caves is the robust foraminifer *Amphistegina lessoni*. The Land et al. (1967) site (+21 m) is the most diverse, containing a planktic foraminifer, reworked *Homotrema rubrum* fragments, *Gypsina* sp., *Quinqueloculina* spp., and very rare *Archaias*, *Asterigerina*, *Textularia*, *Polysaccammina*, and

	Modern Caves				MIS 11 Caves		
	Anchialine	Littoral	C. Pocket A	C. Pocket B	UGQ4	Land site	UGQ5
Stygobites							
Caecum caverna (gastropod)	●	●	●				
Stygophiles							
Abditodentrix rhomboidalis	●	●	●				
Bolivina spp.	●	●	●	●			
Cibicides sp.	●	●	●				●
Cymbaloporetta squamosa	●	●	●				
Milionella subrotunda	●	●	●				
Hoeglundina c.f. *elegans*	●	●	●	●	●		
Quinqueloculina candeiana	●	●	●			●	
Quinqueloculina lamarckiana	●	●	●	●			●
Quinqueloculina poeyana	●	●	●				●
Quinqueloculina seminulum	●	●	●			●	
Quinqueloculina vugaris	●	●	●			●	●
Quinqueloculina spp.	●	●	●	●			
Planorbulina sp.	●	●	●				
Pyrgo elongata		●	●				
Pyrgo subsphaerica		●	●				
Polysaccammina ipohalina	●					●	
Pseudothurammina limnetis	●					●	
Reophax sp.	●						●
Rosalina spp.	●	●	●	●			
Spiroloculina antillarum	●	●	●				
Textularia agglutinans	●	●	●			●	
Triloculina carinata	●	●	●				
Triloculina oblonga	●	●	●				
Triloculina spp.	●	●	●	●			
Loxoconcha sp.	●	●	●			●	
Paranesidea sterreri	●	●	●				
Bryozoan fragments		●	●		●	●	●
Transported							
Amphistegina lessoni	●	●	●	●	●	●	●
Archaias angulatus	●	●		●		●	
Articulina spp.	●	●	●				
Articulina pacifica	●	●	●	●			
Asterigerina carinata	●	●	●	●		●	
Gypsina vesicularis	●					●	●
Homotrema rubrum	●	●		●		●	●
Planktic foraminifera	●	●	●			●	
Coral fragments		●					

Table 4.1: Shared microfossils between the MIS 11 deposits and modern cave environments. Data for UGQ5 (+18 m), UGQ4 (+21 m), and the Land et al., (1967) site (~+21 m) from Wilkinson (2006).

Pseudothurammina. UGQ5 (+18 m) contained only *Gypsina*, *Quinqueloculina*, and reworked *Homotrema rubrum.* In contrast to the other MIS 11 caves, where typically several taxa are preserved, only one taxon was preserved in UGQ4 (+21 m; *Amphistegina lessoni*). The lack of diversity preserved in UGQ4 is not surprising, as neither diverse nor abundant microfossils were preserved in Calonectris Pocket B, which is < 50 cm away from the abundant assemblages in Calonectris Pocket A. Considering subterranean geochemical processes are not spatially or temporally constant in vadose cave environments, the differential preservation of microfossils between caves sites likely reflects the different taphonomic history endured by microfossils in different cave locales. Importantly, all the microfossils preserved in the MIS 11-aged sediments are deposited or living in modern Bermudian cave environments (Table 4.1).

4.7 Discussion: Sea level Or Mega-tsunami?

Based on several independent lines of micropaleontological evidence, we must reject the mega-tsunami hypothesis because the MIS 11 foraminifera in the elevated Bermudian caves cannot be attributed solely to a mega-tsunami event. Diverse foraminifera from coastal and pelagic sources are known to characterize modern tsunami deposits (Hawkes et al., 2007). However, Hawkes et al. (2007) were able to statistically differentiate a tsunami foraminiferal assemblage from background foraminiferal assemblages in different coastal environments, across a spatially extensive area, from the same tsunami (2004 Indian Ocean event). In contrast, the MIS 11 foraminifera from Calonectris Pocket A are statistically similar to the expected background microfossil

assemblage in a littoral cave environment. Bermudian paleotopography during a +21 m sea-level highstand would have just been several small emergent islands with a shoreline quite proximal (< 50 m, Fig. 4.3) to entrance(s) of the Government Quarry caves, where typical wave and storm activity cannot be ignored as mechanisms for transporting robust calcite grains (reef foraminifera and coral fragments) and pelagic taxa into MIS 11 coastal caves. Considering the foraminifera preserved in Calonectris Pocket A are most statistically similar to modern lagoons, and by corollary to modern littoral cave environments, the vast majority of the foraminifera preserved in Calonectris Pocket A are interpreted as an *in situ* MIS 11 littoral cave assemblage (thanatocoenosis). Despite the lack of statistically significant populations of foraminifera in the other elevated cave sites, all the foraminifera ever recovered in these sites can be accounted for in modern Bermudian coastal cave environments (Javaux, 1999; Wilkinson, 2006; Table 4.1). Therefore, we interpret all the Bermudian +21 m caves (UGQ4, UGQ5, Calonectris Pockets, Land et al. 1967 site) as recording a micropaleotological signature of a co-stratigraphic sea level – dated to MIS 11.

Morphologically, shell fragmentation and surface dissolution occur equally on foraminiferal tests from the modern littoral cave and the Calonectris Pockets (Fig. 4.5). The observed shell fragmentation is taphonomically consistent with shells being reworked in the littoral zone, and minor acidity is common at the halocline in modern phreatic caves. This provides supporting evidence for an *in situ* interpretation of these foraminiferal assemblages, as opposed to transport by a mega-tsunami. However, fragmentation can also occur through other transport mechanisms, and acidic conditions can also occur in vadose caves from percolating environmental acids or organic acids derived from the breakdown of organic matter. Regardless of the mechanism that

deposited the microfossils, vadose conditions have occurred in the elevated caves since the microfossils were emplaced (e.g., MIS 2). During these times, non-spatially consistent, mildly acidic conditions can help explain the differential preservation of microfossils between the different Bermudian elevated caves, as robust foraminifer tests clearly have the greatest preservation potential (*Amphistegina* – Table 4.1). Therefore, because the shell taphonomy and the selective preservation of microfossils between the caves can equally be attributed to phreatic cave (speleogenic) and high-energy (i.e., tsunami) environmental histories, these characteristics cannot be used as diagnostic evidence for either the MIS 11 +21 m highstand or mega-tsunami hypothesis, as previously argued (McMurtry et al., 2007).

Despite the ambiguous shell characteristics, other micropaleontological evidence recovered from the elevated Bermudian caves unequivocally supports the interpretation of *in situ* phreatic cave environments caused by +21 m sea level. The most convincing evidence is the recovery of the aquatic gastropod *Caecum caverna* (stygobite) in Calonectris Pocket A (Fig. 4.5). *Caecum caverna* (gastropod) are common in the sediment of modern Bermudian caves, either solely as the protoconch or with the secondary growth stage attached (Moolenbeek et al., 1988). Considering only one specimen was found in the modern littoral cave sediment (Fig. 4.5), the littoral caves are likely the seaward extension of this stygobite in subterranean environments. However, they are relatively abundant in Bermudian anchialine caves, possibly reflecting this is their optimal habitat. The recovery of this stygobite in Calonectris indicates that marine water once flooded this elevated cave. Littoral and cave-tolerant (stygophiles) ostracods (*Loxoconcha oculocrista* and *Paranesidea sterreri*) were preserved in Calonectris Pocket A, and *Loxoconcha* sp. was recovered from the Land et al. (1967) site (Fig. 4.5). These

ostracods currently live in modern Bermudian coastal cave environments, and suggest the littoral zone was once present in the elevated caves (Van Morkhoven, 1963; Maddocks and Iliffe, 1986). Lastly, bryozoan skeletal fragments were present in both the modern littoral cave and in Calonectris Pocket A. Living bryozoans and their skeletal remains are quite common in coastal caves, and even stygobitic cave taxa have been described (e.g., Silén and Harmelin, 1976). We find it challenging to envisage how a mega-tsunami coincidently eroded, transported, and deposited (a) cave stygobites, (b) littoral, cave-adapted ostracods, (c) bryozoans, and (d) an assemblage of foraminifera statistically and taphonomically consistent with a littoral cave environment, all into elevated caves during MIS 11. The comprehensive micropaleontological evidence preserved in the elevated Bermudian caves is consistent with the simple explanation that littoral cave environments did exist at +21 m in Government Quarry, Bermuda during MIS 11.

Interestingly, *Polysaccammina ipohalina* and *Pseudothurammina limnetis* were preserved in carbonate clasts from archived museum samples belonging to the destroyed cave of Land et al. (1967; Wilkinson, 2006). This is a surprising recovery in sediments dated to MIS 11, considering these taxa are individually not significantly abundant in modern brackish environments (salt marshes, ponds). Furthermore, due to the largely organic makeup of their tests, these marsh taxa are rarely preserved outside of their usual anoxic marsh environments because their shells easily oxidize or are consumed by bacteria. We find it pressing to believe *Polysaccammina* and *Psuedothurammina* have remained taxonomically identifiable since MIS 11 after enduring: mechanical homogenization in a tsunami, energetic deposition into a vadose cave, subsequent desiccation—but not oxidation or bacterial consumption, and encasement by calcite cements. Although common marsh foraminifera have been previously found in tsunami

deposits (*Haplophragmoides*, Hawkes et al., 2007), this example was from an open coastline, not a cave. To our knowledge, there are currently no documented descriptions of the foraminiferal characteristics of known recent tsunami deposits in caves, providing no comparative data. Furthermore, if a tsunami entrained Bermudian mangrove or salt marsh taxa and deposited them into a cave, we would expect to recover *Trochammina* and *Discorinopsis*, which are common Bermudian mangrove genera, similarly to *Haplophragmoides* of Hawkes et al. (2007), not coincidently two extremely rare foraminifers. Therefore, we favor an *in situ* origin for these fragile marsh foraminifera, as this interpretation is taphonomically more plausible.

At the onset of sea-level regression following the MIS 11 highstand, the original littoral cave environments would become saturated by brackish water from the concomitant vertical lowering of the GH lens (Fig. 4.6). The limited spatial extent of coeval Bermudian paleotopography likely favored the formation of a very thin GH lens during MIS 11 (< 0.5 m), analogous to modern hydrogeological conditions along the modern Walsingham Tract (Iliffe et al., 1983). Considering, the strong control of sea level on the absolute elevation of a GH lens on small islands (Schneider and Kruse, 2003), an MIS 11 GH lens <0.5 m thick on Bermuda perched at +21 m also reflects a very similar eustatic sea-level position (Fig. 4.6). This brackish water would create an anchialine habitat in the elevated Bermudian caves, which would have been particularly suitable to *Polysaccammina* and *Psuedothurammina,* consistent with modern conditions in Bermudian coastal caves (Fig. 4.5). The recent documentation of a ~95% anchialine gastropod assemblage (>300, only ~5% marine individuals) in the Calonectris cave (+21 m) further corroborates the marsh foraminiferal paleoecology where an anchialine environment developed after a littoral cave environment (Olson and Hearty, 2009).

Continual sea-level regression would have ultimately drained the elevated caves to create a vadose cave environment, suitable for the precipitation of speleothem deposits (flowstone) above the MIS 11 cave sediments, which have been repeatedly dated to late MIS 11 or early MIS 10 (McMurtry et al., 2008; Olson and Hearty, 2009).

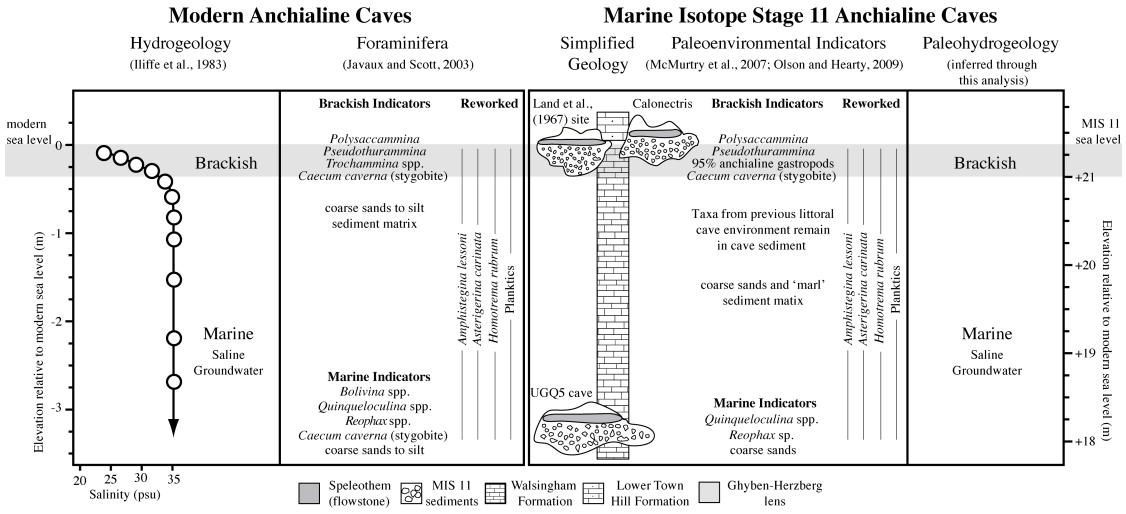

Figure 4.6: Diagrammatic representation of the MIS 11 cave environment (microfossils, sediments, groundwater, and GH lens) and MIS 11 sea-level position during development of anchialine environmental conditions. Note the striking similarity between modern and MIS 11 micropaleontological, hydrogeological, and coastal variables in Bermudian coastal caves. Modern salinity data after Iliffe et al. (1983).

4.8 Conclusions

After comparing modern and fossil Bermudian cave foraminifera, the microfossil evidence can no longer support the mega-tsunami hypothesis because they are not unequivocally diagnostic of tsunami. In contrast, the MIS 11 microfossils preserved in the Bermudian elevated caves provide striking evidence for a MIS 11 +21 m sea-level highstand, as tectonic and glacio-isostatic sea-level changes are not major geologic factors contributing to sea-level change in Bermuda. Considering the microfossils within a taphonomic and paleoecologic framework, we conclude: (1) that the Government Quarry Caves were indeed MIS 11 coastal cave environments; (2) typical assemblages of

in situ littoral cave foraminifera developed due to a co-stratigraphic sea level (+21 m); and (3) sea-level regression following the MIS 11 highstand flooded the caves with a brackish GH lens – creating a suitable habitat for marsh foraminifera and anchialine gastropods. These results indicate that modern cave environments cannot be ignored in any interpretation of sea level or tsunami history in Bermuda, and demonstrate that foraminifera in coastal cave environments have a wider potential as sea-level markers than previously appreciated. Although the risk of tsunami events in the Caribbean is becoming increasingly apparent (Ward and Day, 2001; Teeuw et al., 2009), microfossil evidence for ancient tsunamis still requires stringent evaluation. Lastly, because the Bermudian microfossil evidence in the elevated Government Quarry Caves corroborates the previously presented geologic evidence for a MIS 11 +21 m eustatic sea-level highstand, we suggest a greater focus on resolving the disparity between global marine isotopic records and the physical geologic evidence for sea level during MIS 11.

Chapter 5: North Atlantic Cave Succession Documents Abrupt Eustatic Sea-level Event At 7.6 ka Ago

Peter J. van Hengstum and David B. Scott

Dalhousie University, Centre for Environmental and Marine Geology

Halifax, Nova Scotia, B3H 4J1, Canada

Note: This manuscript is prepared for a short-style publication venue.

5.1 Abstract

Evidence for the purported sea-level rise at 7.6 ka ago is needed from tectonically and glacio-isostatically stable areas like Bermuda. Green Bay Cave, Bermuda, affords the first underwater cave sedimentary succession spanning the Holocene and documents local sea-level rise. Calcite rafts precipitate at cave air-water interfaces, and can provide a sea-level proxy in coastal phreatic caves when an aquatic ecosystem is coeval with calcite raft formation. Flooding of the -20.7 m cave floor 7.6 ka ago created a littoral cave environment suitable for benthic foraminifera and calcite raft precipitation. Sea level reached the cave ceiling elevated to -14.3 m by 7.3 ka ago, causing calcite raft precipitation to cease, and foraminiferal assemblages document the onset of anchialine conditions. Finally, sea level breached a local sill at -2.25 m below sea level at 1.65 ka ago, which initiated the modern submarine cave environment. The timing of the littoral cave environment provides a robust 'sea-level window' for tracking sea-level change, and indicates a ~6.4 ±1.7 m sea-level fluctuation on Bermuda over ~300 years. This result corroborates global sea-level evidence for an abrupt eustatic sea-level rise at this time, and is most likely related to final collapse of the Labrador sector of the Laurentide Ice Sheet.

5.2 Introduction

Bermuda is well suited to investigating sea-level problems because it has remained tectonically and glacio-isostatically stable over the Quaternary (Vacher and Rowe, 1997, Olson and Hearty, 2009). Basal brackish peat is a classic proxy for generating sea-level curves because brackish marshes and mangroves form only at sea level. Problematically, salt marshes and mangroves only became established in Bermuda

~5 ka ago (Ellison, 1993, 1996; Javaux, 1999), hindering the availability of basal brackish peat for sea-level research before this time.

Freshwater peat is widely available in the Holocene stratigraphic record of Bermuda, which has been used to generate sea-level curves (e.g., Redfield, 1967; Neumann, 1971; Vollbrect, 1996). However, this proxy is a *maximum* sea-level proxy only, meaning that sea-level curves using freshwater peat are unreliable for discerning rapid sea-level changes. For example, Blanchon and Shaw (1995) documented reef drowning in the Caribbean Sea at 7.6 ± 0.1 ka ago due to an abrupt 6.5 ± 2.5 m eustatic sea-level rise. Debate ensued regarding this event when other Caribbean and Pacific coral data were used to challenge this hypothesis (Hubbard et al., 1997; Bard et al. 1996; Toscano and Lundberg, 1998), but recent evidence from the Red Sea, Swedish Baltic Sea, and elsewhere has drawn renewed attention to a eustatic event at 7.6 ka (i.e., Siddall et al., 2003; Yu et al., 2007; Bird et al., 2010). Such a eustatic sea-level event would have impacted Bermuda, but sea-level proxies other than basal peat is needed to test the hypothesis in Bermuda.

Here we present robust evidence (sedimentologic, geochemical, microfossil) for the rapid flooding of Green Bay Cave (GBC) at 7.6 ka ago, an underwater cave in Bermuda (Fig. 5.1). Underwater caves provide independent accommodation space for sediments and aquatic ecosystems that can archive sea-level changes. Quaternary sea-level oscillations have repeatedly flooded and drained speleogenetic karst basins (caves, sinkholes) because sea and groundwater levels oscillate in synchrony (van Hengstum et al., 2009a,b). During a relative sea-level rise, coastal caves transition through vadose, littoral, anchialine, and finally into submarine caves, leaving a unique signature of each

phase in the sediment record (reviewed in: van Hengstum et al., 2009b; van Hengstum and Scott, 2011; Chapter 5).

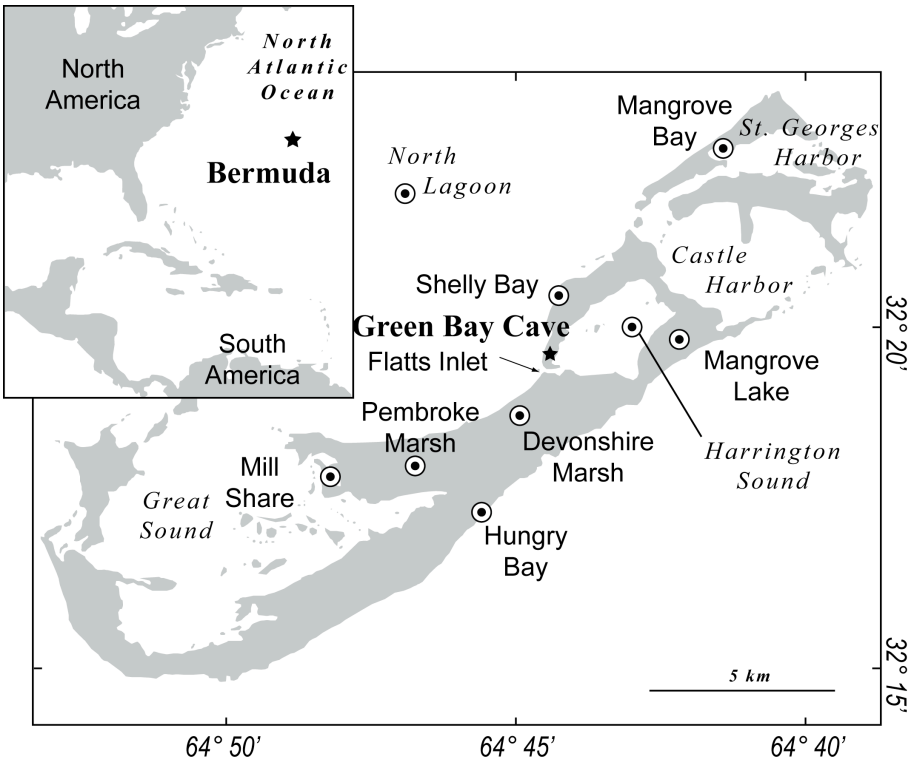

Figure 5.1: Location of Green Bay Cave and marsh sampling sites from the literature.

Importantly, a littoral cave environment is created when sea level (adjusted for groundwater hydraulic head) is within a cave passage creating conditions suitable for aquatic invertebrates and calcite raft precipitation. Calcite rafts are a common morphology of microcrystalline calcite that precipitate at air-water interfaces in caves (Fig. 5.2, Taylor and Chafetz, 2004). When found in the sediment record, calcite rafts provide diagnostic evidence for a paleo-water table. Our approach employs using calcite rafts and marine microfossils to bracket the littoral cave environment phase in GBC, thereby tracking sea-level flooding of the cave. Considering the ubiquity of karst

platforms and caves in tropical and subtropical basins, this approach opens new avenues for precisely tracking global sea-level change.

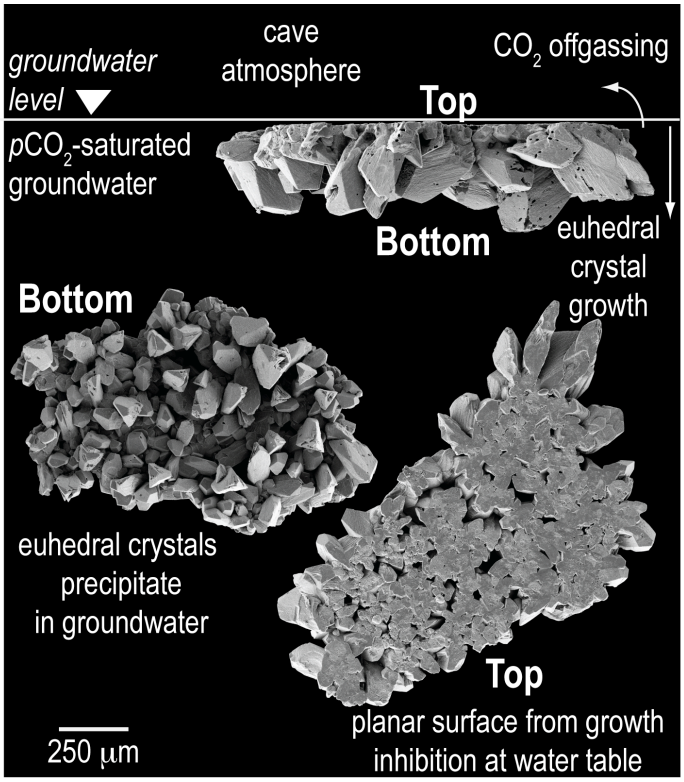

Figure 5.2: Scanning electron micrographs of calcite rafts from GBC, with annotations to explain conditions of formation.

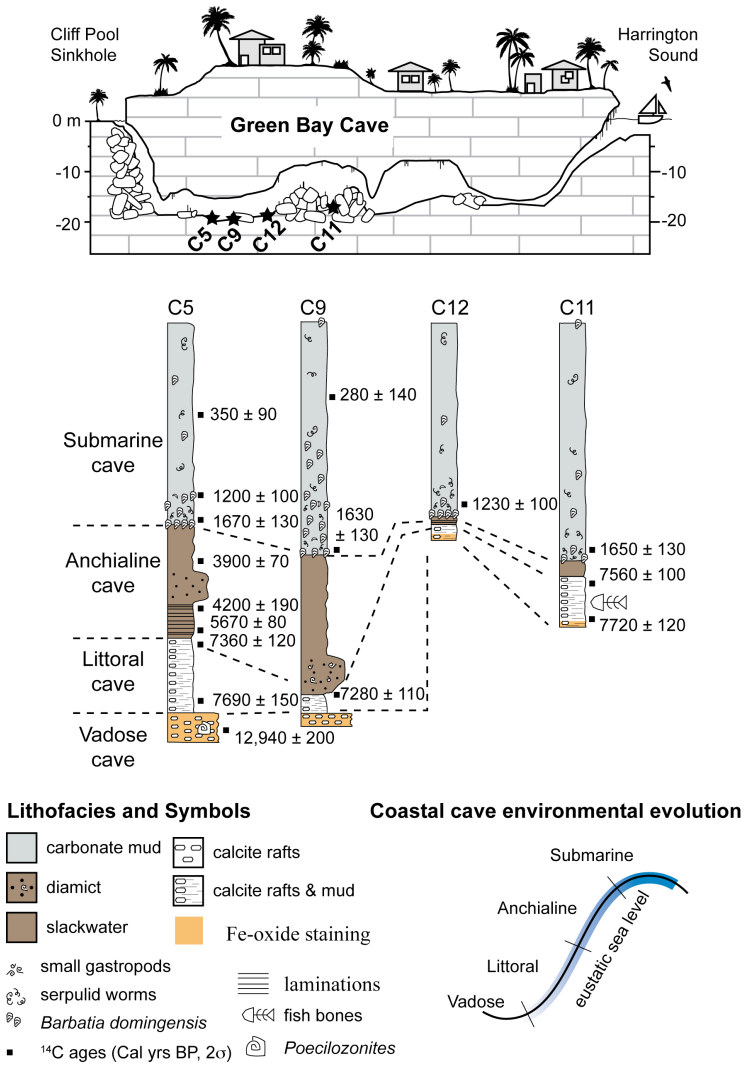

Figure 5.3: Cross section through Green Bay Cave with sample sites, and core logs with ^{14}C ages (2σ error).

5.3 Study Area And Methods

The Holocene flooding history of GBC, located on the northwest coast of Harrington Sound, was reconstructed using sedimentology, micro- and macrofossils, stable carbon isotopes ($\delta^{13}C_{org}$) and radiocarbon dating. GBC consists of an anastomosing network of passages with an anchialine sinkhole entrance and a submarine cave entrance

opening into Harrington Sound. Ocean water from Harrington Sound flows into the cave under tidal-forcing (1.5 m s^{-1} at peak flow, Cate, 2009), which becomes slow moving saline groundwater under the karst platform in the cave interior. Four sediment cores were obtained from GBC using self-contained underwater breathing apparatus (SCUBA) and numerous levels were dated with ^{14}C, which indicated complete recovery of a Holocene succession (13 ka ago to present, Fig. 5.3). After examining stratigraphic and faunal successions throughout GBC, it is evident that these cores were not impacted by waves or tidal currents and represent in situ sedimentation and ecosystems (Chapter 4). Paleoecological analyses with foraminifera were completed on the most expanded records in cores 5 and 9 to serve as independent proxies of salinity and hydrogeologic circulation (van Hengstum and Scott, 2011). Foraminifera were concentrated by wet sieving (~1.25 cm^3) sediment samples (0.5 to 1 cm interval) over a 45 μm mesh, every 1 - 2 cm downcore. Taxa were identified and counted wet in petri dishes (van Hengstum and Scott, 2011) to achieve a census of >300 per sample, to provide a reasonable standard error on dominant taxa (Patterson and Fishbein, 1989; Fatela and Taborda, 2002).

Two original data matrices of foraminiferal counts were produced for cores 5 and 9, totaling 95 samples and 96 different taxonomic units (observations). However, 31 observations were deemed statistically insignificant because the units are present in only one sample or because the estimated standard error for the observation was greater than the relative abundance in all samples (Patterson and Fishbein, 1989; Appendix 6). The final data matrices (C5: 52 samples × 65 variables, C9: 43 samples × 64 variables) were then square-root transformed and subjected to stratigraphically constrained Paired Group Q-mode cluster analysis for biofacies identification.

Primary productivity in caves is significantly limited due to the lack of light, a characteristic that causes the quantity and provenance of sedimentary organic matter to be a dominant abiotic control on cave environments (van Hengstum and Scott, 2011; van Hengstum et al. 2010; Chapter 4). The quantity of bulk sedimentary organic matter was estimated downcore by loss on ignition at 550°C for 4.5 hours. Analytical error on replicates every 5 to 10 cm in all cores was ± 2%, which is typical for the method (Heiri et al., 2001). $\delta^{13}C_{org}$ and C:N were determined on bulk sediments, proxies that provide a method for determining whether terrestrial or marine sources of organic matter are entering the cave after applying simple mass balance mixing equations (e.g., Thornton and McManus, 1994). Samples were first subjected to a 10% HCl carbonate digestion, rinsed to neutrality, then dried residues were powdered using a mortar and pestle. $\delta^{13}C_{org}$ measurements are compared against international standards and expressed in the standard delta (δ) notation in per mil (‰) against Vienna PeeDee Belemnite (VPDB).

A framework for local Holocene sea-level rise was developed from published peat proxies, together with additional marsh peat samples collected for this study (Hungry Bay Mangrove, Bermuda; Appendix 5). Botanical remains (Ellison, 1996; Vollbrecht, 1996) or marsh foraminifera (Javaux, 1996; this study) were used to verify the peats were brackish. All ^{14}C ages (new and previously published) were calibrated using the radiocarbon curves of Reimer et al. (2009) in Calib 6.0, using a $\Delta R = -48 \pm 40$ where appropriate on biogenic carbonates (Druffel, 1997).

5.4 Results

The succession in GBC can be divided into four separate lithofacies with different sedimentologic and microfossil characteristics (Fig. 5.3, Table 5.1). The vadose facies accumulated prior to 7.7 ka ago, which passes up into the littoral facies that accumulated in ~300 years from 7.7 to 7.3 ka ago. The anchialine facies is the longest duration of 5.7 ka, accumulating from ~7.3 ka to 1.6 ka. Finally, the transition to the submarine facies at 1.6 ka ago represents the onset of the submarine environment in the cave, conditions that are consistent with modern environmental conditions in GBC (van Hengstum and Scott, 2011).

Table 5.1: Facies characteristics and timing within GBC.

Cave Facies	Sediments	Origin of organic matter	Paleontological remains
1. Vadose >7.7 ka	calcite rafts	terrestrial	terrestrial gastropods (*Poecilozonites*)
2. Littoral 7.7 - 7.3 ka	calcite rafts and carbonate mud	terrestrial and marine	All marine: cave gastropods & ostracods, oligotrophic cave foraminifera, sponges
3. Anchialine 7.3 - 1.6 ka	fine grained, organic rich mud	terrestrial	marine fauna passing into low diversity brackish foraminifera
4. Submarine <1.6 ka	fine grained, carbonate mud	marine	All marine: bivalves, diverse foraminifera, cave coral, sponges

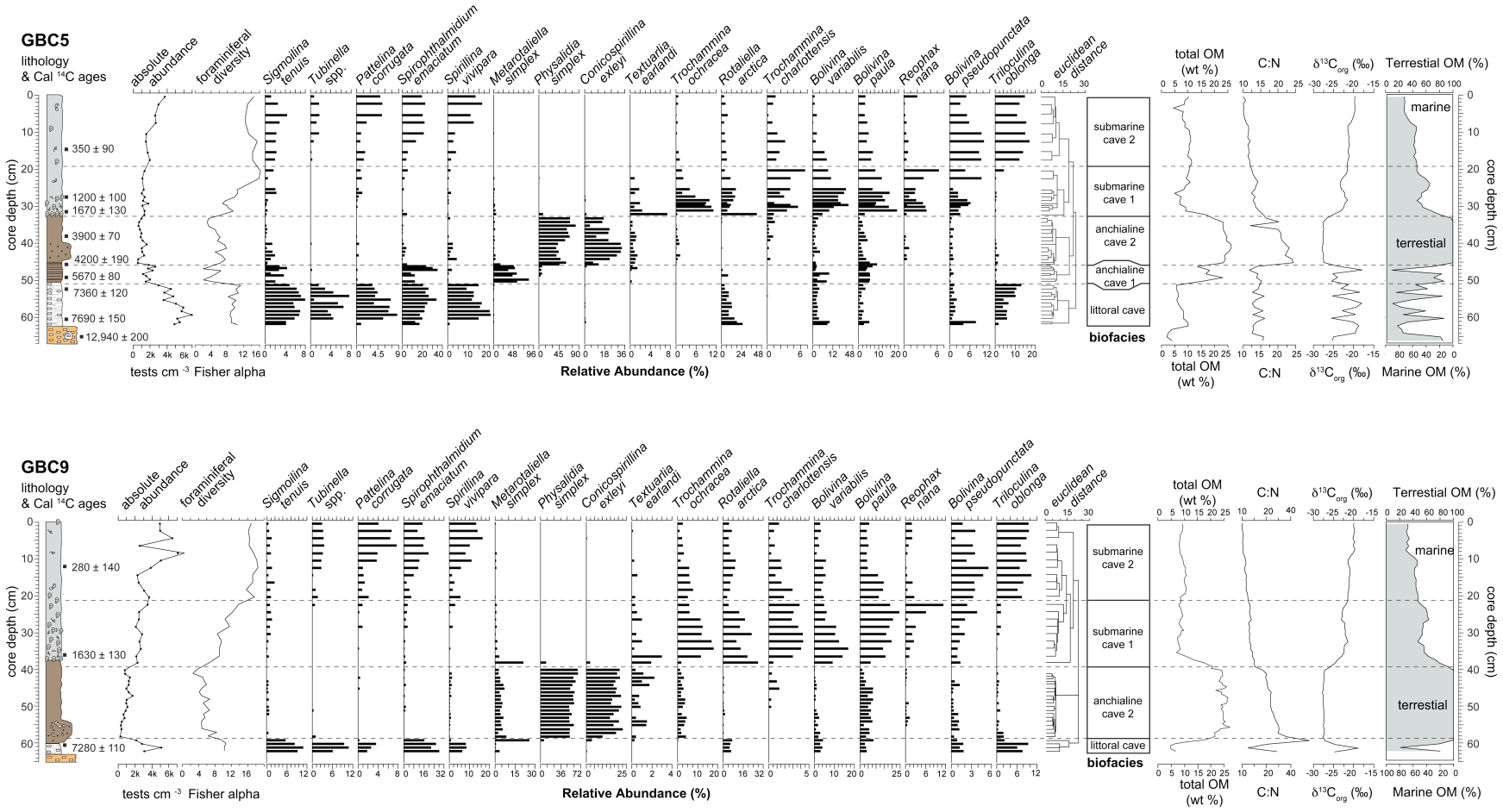
GBC5
lithology
& Cal ¹⁴C ages
absolute abundance
foraminiferal diversity
Sigmoilina tenuis
Tubinella spp.
Pattelina corrugata
Spirophthalmidium emaciatum
Spirillina vivipara
Metarotaliella simplex
Physalidia simplex
Conicospirillina exleyi
Textularia earlandi
Trochammina ochracea
Rotaliella arctica
Trochammina charlottensis
Bolivina variabilis
Bolivina paula
Reophax nana
Bolivina pseudopunctata
Triloculina oblonga
euclidean distance
total OM (wt %)
C:N
δ¹³C_org (‰)
Terrestrial OM (%)
core depth (cm)
350 ± 90
1200 ± 100
1670 ± 130
3900 ± 70
4200 ± 190
5670 ± 80
7360 ± 120
7690 ± 150
12,940 ± 200
submarine cave 2
submarine cave 1
anchialine cave 2
anchialine cave 1
littoral cave
biofacies
marine
terrestial
tests cm ⁻³ Fisher alpha
Relative Abundance (%)
total OM (wt %)
C:N
δ¹³C_org (‰)
Marine OM (%)
GBC9
lithology
& Cal ¹⁴C ages
280 ± 140
1630 ± 130
7280 ± 110
submarine cave 2
submarine cave 1
anchialine cave 2
littoral cave
biofacies
marine
terrestial

Figure 5.4 (Preceding page): Micropaleontological, sedimentological, geochemical, and ^{14}C dates from cores 5 and 9.

5.4.1 Vadose Cave Facies

Calcite rafts dominate the vadose facies, and are post-depositionally coated with Fe-oxide precipitates from upwelling anoxic saline groundwater. The vadose facies contain no foraminifera, because the cave was in the vadose zone prior to 7.7 ka according to regional sea-level estimates (e.g., Blanchon and Shaw, 1995; Toscano and McIntyre, 2003), and thus too elevated for marine incursions. The only invertebrate recovered from the vadose cave facies was the endemic terrestrial gastropod *Poecilozonites*, providing a basal ^{14}C age of 13 ka ago.

5.4.2 Littoral Cave Facies

Accumulation of the littoral facies was short-lived from 7.7 – 7.3 ka, based on radiocarbon-dated microfossils at the stratigraphic contacts in multiple cores. Carbonate mud provides matrix support to calcite rafts, which contain abundant microfossils, bryozoans, fish remains, and the Bermudian endemic cave ostracod *Paranesidea sterreri* (Maddocks and Iliffe, 1986, Chapter 4). Foraminifera immediately colonized the cave at 7.6 ka, coincident with the onset of the littoral cave facies. *Spirophthalmidium emaciatum* (~23%) dominated the facies, accompanied by *S. vivipara* and *T. oblonga* (Table 5.1). Because (a) calcite rafts only form at an air-water interface, and (b) the microfossils indicate that a marine ecosystem was present, the onset of the littoral facies demarcates initial flooding of the cave floor by sea-level rise (-20.7 ± 0.3 m) at ~7.7 ka.

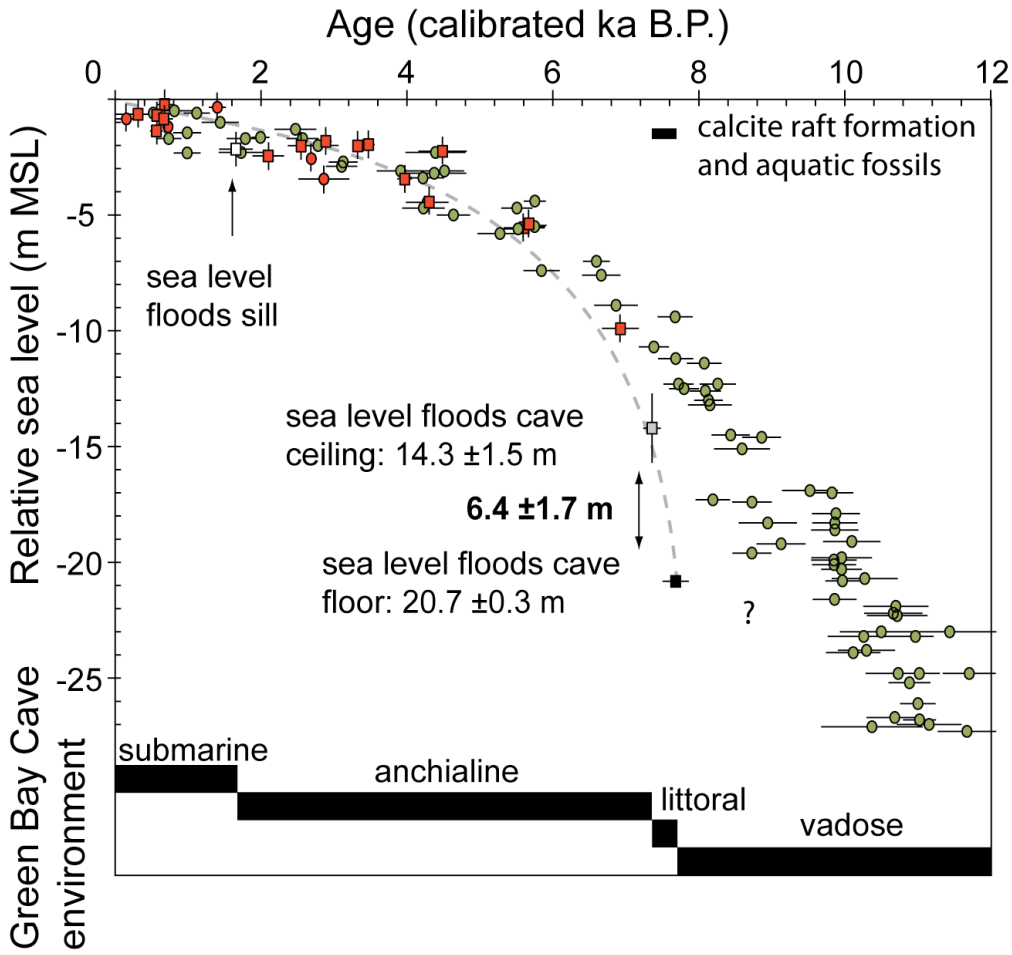

Figure 5.5: Holocene sea-level proxies for Bermuda. Appendix 5 indicates original citation of peat data, recalibrated for this study. Proxies: green circles are maximum sea-level indicators from freshwater peat, red circles are brackish peat, red squares are sea-level index points from basal brackish peat. Vertical uncertainty in brackish peats from the maximum tidal range observed in Bermuda (± 1.2 m, Morris et al., 1977).

Spirophthalmidium emaciatum is dominant in modern GBC passages that are most oligotrophic and hydrogeologically isolated from the ocean (van Hengstum and Scott, 2011), and the GBC littoral cave facies probably represents a similar setting. No basal brackish peat in Bermuda is dated to the early Holocene, so the elevation of the cave floor combined with evidence for the onset of the littoral cave facies provides a new sea-level index point. Water table elevations derived from GBC are co-stratigraphic with sea level

because negligible vertical error is introduced by small hydraulic gradients on Bermuda in comparison with sampling errors associated with depth gauges (± 0.3 m).

5.4.3 Anchialine Cave Facies

The anchialine facies consists of the diamict and slackwater lithofacies, which contain terrigenous sediment (depleted $\delta^{13}C_{org}$ values, high C:N ratio) that entered the cave from 7.3 to 1.6 ka ago. No calcite rafts are observed in this facies or any thereafter, indicating that an air-water interface no longer existed in the cave. The oldest basal brackish peat sea-level index point from Bermuda is –9.9 ± 1.2 m dated at 6.9 ka, followed by two closely positioned index points (–5.5 and 5.4 m below sea level) dated to 5.6 ka (Fig 5.5). Multiple basal brackish peat dates from 0 to 4 ka ago combined with the other dates confidently place the GBC in the phreatic zone during deposition of the anchialine facies and thereafter.

Two foraminiferal assemblages (or biofacies) characterize the anchialine facies (Fig. 5.4). The anchialine 1 biofacies is only present in core 5, likely a result of a condensed horizon caused by low sedimentary influx into the cave, a known process characterizing anchialine cave facies elsewhere (van Hengstum et al., 2010). A lower diversity assemblage with *S. emaciatum* and *M. simplex* dominates the biofacies, indicating normal salinity conditions that are less ecologically favorable to foraminifera in comparison with the littoral biofacies.

Impoverished foraminifera characterize the anchialine 2 biofacies, which is dominated by the brackish water indicators *Physalidia simplex* (57%) and *Conicospirillina* sp. (Guillem, 2007; van Hengstum et al., 2008, 2010). Data is currently sparse regarding the modern ecology of either *Physalidia simplex* of *Conicospirillina* sp..

In the most important study to date on these taxa, Guillem (2007) sampled living and dead benthic foraminifera living in Cabanes-Torreblanca Coastal Lagoon (Spain). This site is a grouping of shallow coastal ponds ranging in salinity from 6.6 to 13.4 ppt, which were excavated in a salt marsh for peat extraction. The eight sites sampled over a 12 month period contained abundant living and dead salt marsh foraminifera, including *Trochammina inflata*, *T. macrescens*, and *Haplophragmoides* (Guillem, 2007). However, the perennial ponds also contained abundant *P. simplex* (dead and stained) and to a lesser extent *Conicospirillina* sp., which were most abundant in the higher-salinity sampling sites (salinity >9 ppt, Guillem, 2007). *Physalidia simplex* was also present (stained) in the most polyhaline pond (13 ppt) in August 1993, when seasonal suboxic conditions characterized the benthic water mass (1.12 mL/L). Elsewhere, van Hengstum et al. (2008) found rose Bengal stained *P. simplex* in oligohaline cenotes (sinkholes) in Mexico, however, *Conicospirillina* sp. was not documented. Rose Bengal-stained *P. simplex* was also encountered in Aktun Ha Cave System (salinity 1.5 ppt; van Hengstum et al., 2009a), and in the cavern of Maya Blue Cave (salinity 1.9 ppt, van Hengstum and Reinhardt, unpublished data). The modern ecological evidence indicates that *P. simplex* occupies at least low oligohaline to polyhaline habitats, and appears unaffected by suboxia, whereas, *Conicospirillina* sp. colonizes at least polyhaline habitats. Therefore, the anchialine 2 biofacies indicates very brackish conditions persisted in Green Bay Cave from ~4.1 to 1.6 ka with possible intermittent dysoxia, likely from a paleo-mixing zone developed between saline groundwater and a paleometeoric lens.

5.4.4 Submarine Cave Facies

Accumulation of the submarine cave facies began at 1.6 ka ago, indicated by carbonate mud and marine organic matter deposition with colonization by *Barbatia domingensis* (mussel), juvenile corals, brachiopods, and saline microfossils. The rapid change in the cave to marine conditions (from brackish) at 1.6 ka ago can be attributed to sea level breaching the sill located in Flatts Inlet (-2.25 ± 0.75 m). This caused open circulation between Harrington Sound and the ocean, allowed *Oculina* coral to colonize Harrington Sound (Vollbrecht, 1996), and the onset of tidally forced saline groundwater circulation in GBC. The sill elevation and timing of its breaching are consistent with local sea-level estimates derived from basal brackish peats.

Foraminiferal diversity rapidly increased at 1.65 ka ago to form the submarine cave 1 biofacies, dominated by bolivinids and *R. arctica*. This biofacies passes up into the submarine cave 2 biofacies that is dominated by fauna of *S. emaciatum* and *T. oblonga*, which characterizes surface assemblages at the core sites (van Hengstum and Scott, 2011). The foraminiferal change indicates an immediate shift to normal marine conditions favoring increased foraminiferal diversity. Submarine biofacies 1 comprises predominantly opportunists and detritivores (*Bolivinia*, *Trochammina*, *Reophax*: Murray, 2006) that initially colonized the cave during the submarine cave 2 biofacies. The transition from the submarine 1 to submarine 2 biofacies is interpreted ecological succession in the cave as nutrients were continually supplied to the site from tidally forced hydrogeologic circulation.

5.5 Discussion And Conclusions

We argue that the succession from GBC provides a robust flooding history in response to Holocene sea-level rise, consistent with available basal brackish peat proxies. Earlier than 6.9 ka ago, however, the cave succession provides the only available sea-level index points on Bermuda. Sea level was within the cave passage during deposition of the littoral cave facies because: (1) calcite rafts precipitated at a paleo-water table, and (2) a marine ecosystem provided habitat to diverse microfossils. Based on this evidence, sea level flooded the cave floor (–20.7 ± 0.3 m) at 7.7 ka ago (Fig. 5.5).

The elevation of the cave ceiling combined with the stratigraphic evidence can be used to obtain a second sea-level index point. The stratigraphic contact between the littoral and anchialine facies dates the time when the water level reached the cave ceiling and calcite rafts could no longer form. However, extracting a precise sea level index point for a cave ceiling is hampered by irregularity in ceiling height. There is very little lateral transport of calcite rafts in modern cave passages due to negligible saline groundwater currents in the distal cave (van Hengstum and Scott, 2011), so we assume the calcite rafts formed in the immediate vicinity, if not above, the core sites in GBC. Above core 5 where the transition from the littoral to anchialine facies is well constrained, the ceiling elevation ranged from -13.1 to -15.5 m (± 0.3 m), which provides a conservative estimate for an upper sea level index point at -14.3 m ± 1.5 m. Therefore, based on ~400 yrs for the littoral facies to form while the cave was flooding – from floor to ceiling – there was an abrupt 6.4 ± 1.7 m sea-level rise in Bermuda between 7.7 and 7.3 ka ago.

A eustatic event is the likely explanation for the rapid flooding of GBC because Bermuda has remained tectonically and glacio-isostatically stable over the Holocene. Some argue that Bermuda has been slowly subsiding (Vogt and Jung, 2007), with

estimated subsidence rates of 0.6 to 1.2 cm ky^{-1} (Liu and Chase, 1989). This maximum estimated rate, however, can only account for a maximum of ~15 cm of relative sea-level change over the whole Holocene, and insufficient to explain the ~6.4 m rise documented in the cave succession.

Bermudian estimates for the 7.7 ka event are similar to: (a) Caribbean coral drowning events (6.5 ± 2.5 m, 7.6 ka: Blanchon and Shaw, 1995); (b) Cayman Island tidal notch (-18.5 m) and reef drowning (7.6 ka, Blanchon et al., 2002); (c) North Sea coast (~4 m, 7.9-7.6 ka: Behre, 2007), (d) Baltic Sea (~6 m, 8.0-7.7 ka: Lemke, 2004); (e) Sweedish silled basins (~4.5 m, 7.6 ka, Yu et al., 2007); (f) rapid sea-level rises in the Red Sea (Siddall et al., 2003), Sunda Shelf (Bird et al., 2010) and western Australia (Larcomb et al., 1995). The regional variability has been attributed to localized tectonics or isostasy (Yu et al., 2007), which likely acted in concert to amplify apparent sea-level rise along eastern North America (e.g., >10 m in Maine, 7.5-6.5 ka ago: Kelley et al., 2010).

Final demise of the Laurentide Ice Sheet (LIS) remains the probable source of water for the 7.7 ka event. The LIS contributed 9.2 ± 1.1 m of sea-level rise after 8.5 ka BP over the following 1.7 ka (Carlson et al., 2008) from accelerated retreat and melting of a ~600 km remnant of the Labrador ice sheet occurred at ~7.6-6.8 ka (Carlson et al., 2007). In Bermuda, rates of sea level rise of 1.6 cm yr^{-1} can be estimated from a 6.4 m sea-level jump in ~400 years. These rates are higher than those indirectly estimated by Carlson et al., (2008) from $\delta^{18}O$ on planktic foraminifera from the Labrador Sea (~1 cm yr^{-1}), but are consistent with direct evidence for sea-level forced drowning of Caribbean reefs at 7.6 ka (>1.4 cm yr^{-1}: Blanchon and Shaw, 1995) and preclusion of mangrove development in Bermuda prior to 6.5 ka ago (> 1.2 cm yr^{-1}: Ellison, 1993).

Dating the flooding history of an underwater cave in Bermuda provides strong evidence for the 7.7 ka eustatic sea-level event (timing and magnitude), representing a new approach for tracking Quaternary sea-level change (as in van Hengstum et al., 2009b). The ~6 m contribution to eustatic sea-level rise from the remnants of the Laurentide Ice Sheet is especially concerning with regard to uncertainties regarding the contribution of the Greenland Ice Sheet to future sea-level rise. Densely populated, low-lying karst islands abound in global tropical and sub-tropical oceanic basins—a troubling combination if any rapid ice sheet disintegration re-occurs.

Part III: Climate Signatures In Phreatic Coastal Caves

Chapter 6: Underwater Cave Sediments Indicate 3200 Years of Ocean-atmospheric Forcing Of Bermudian Climate With A Cold and Stormy Onset To The Little Ice Age

Peter J. van Hengstum[1], Andrew W. Kingston[2], David B. Scott[1], William P. Patterson[2], Bruce Williams[3]

1. Centre for Environmental and Marine Geology, Dalhousie University,

Halifax, Nova Scotia, B3H 4J1, Canada

2. Department of Geological Sciences, University of Saskatchewan, 114 Science Place,

Saskatoon, Saskatchewan, S7N 5E2, Canada

3. Bermuda Institute of Ocean Sciences, 17 Biological Station, Ferry Reach, St. George's,

GE 01, Bermuda

Note: This manuscript is prepared for a longer-style publication venue.

6.1 Introduction

Feedbacks between ocean circulation and Holocene climate variability remain poorly understood because so few long-term, high-resolution oceanic records of paleoclimate change are available. For example, in a recent global analysis of 1209 proxy records examining the drivers of the Medieval Warm Period-Little Ice Age transition, only 25 records covered the last 2000 years with better than decadal resolution, and only three were marine sediment series (Mann et al., 2008). New locations for highly resolved, marine-based proxy records of paleoclimate have been repeatedly called for (e.g., Jones, 2001; Keigwin and Boyle, 2000). Sediments in underwater caves represent an emerging cache of paleoclimate data, which may help to redress the problem (Kitamura et al., 2007; Yamamoto et al., 2010; van Hengstum et al., 2010).

Underwater caves are ubiquitous on karst platforms, and may (a) be open systems because groundwater is constantly circulating through the environment, and (b) contain repositories of unbioturbated sediment preserving shells of carbonate-secreting organisms (e.g., bivalves, foraminifera: Kitamura et al., 2007, van Hengstum and Scott, 2011). In short, the coastal aquifers that flood underwater caves are stratified into two water masses, each with individual circulation and hydrographic properties. The meteoric lens is the upper water mass of variable salinity (fresh to brackish), derived from precipitation and any saline groundwater absorbed during groundwater mixing events. Preliminary research by van Hengstum et al. (2010) indicates that underwater caves flooded by the meteoric lens preserve proxy records of precipitation-related climate changes. In Aktun Ha Cave (northeastern Yucatan, Mexico), changing storm activity and salinity in the meteoric lens caused by Holocene southern migration of the Intertropical Convergence Zone was archived in underwater cave sediments (van Hengstum et al., 2010).

Importantly, circulation in the meteoric lens is not directly connected with regional oceanography.

The lower saline groundwater mass, however, is directly connected with the ocean. Shallow saline groundwater circulation is tidally forced (Beddows et al., 2005; 2007), and deep circulation is driven by thermohaline and/or geothermal convection cells (Whitaker and Smart, 1990; Moore et al., 1992; reviewed in van Hengstum et al., 2010). Using these principles, Yamamoto et al. (2010) demonstrated that active circulation of water from the East China Sea into Daidokutsu Cave (Okinawa, Japan) afforded preservation of a 7 ka climate record in the cave sediment. The preservation of saline groundwater-ocean circulation relationships in underwater cave sediments requires further testing to evaluate its global applicability to paleoceanography and paleoclimatology.

This study presents new thermal and surficial erosion reconstructions from cores extracted from an underwater cave in Bermuda, containing sediment deposited over the last 3.2 ka. Walsingham Cave is an open system, where saline groundwater is directly circulating with the ocean. These results are compared with other proxy records from the North Atlantic to understand regional and local climate variability. This work is an important developmental step to guide future cave research, and indicates that paleoclimate records in Caribbean-Atlantic underwater caves warrant further attention.

6.2 Regional Setting

6.2.1 Oceanography And Climate

The islands of Bermuda are located in the North Atlantic subtropical gyre (64ºW, 32ºN), with different oceanographic conditions over the shallow carbonate platform as

compared with open-ocean conditions in the Sargasso Sea (Fig. 6.1). The open ocean is characterized by a deep mixed layer (>200 m) below a shallow surface layer that develops a seasonal thermocline at ~ 10 m (Morris et al., 1977; Goodkin et al., 2008a). Results of temperature monitoring at Hydrostation "S" (30 km southeast, 32º10'N, 64º30'W) since 1954 indicate that mean monthly sea surface temperatures (SST) ranged from 18.3ºC to 28.9ºC (<16 m), with a mean annual variation of 22.4ºC to 24.3ºC (Goodkin et al., 2008a). Such warm temperatures are maintained in Bermuda by the poleward transport of heat via the Gulf Stream, which also introduces local thermal variability from eddy activity (Sweeney et al., 2003).

In contrast to the open-ocean, shallow coastal waters in Bermuda experience greater seasonality. Monthly SST data have been recorded in St. Georges Harbour (Higgs Bay) continually since January 2000, with data only missing for March 2004 (32º22'13"N, 64º40'40"W). Monthly SST range from 15.9ºC to 29.8ºC, with annual variation of 22.8ºC to 23.5ºC, consistent with previous intermittent measurements (Morris et al., 1977). Inshore temperature variability is also a function of the connectivity of specific lagoons to the open ocean. For example, oceanic communication to Harrington Sound is restricted by Flatts Inlet, whereas the North Lagoon is directly open to the ocean (Morris et al., 1977). Long-term summer temperatures are comparable between Hydrostation "S" in the Sargasso Sea and coastal water in St. Georges Harbour, but winter temperatures are on average 2.4ºC cooler in the coastal water than in the open ocean.

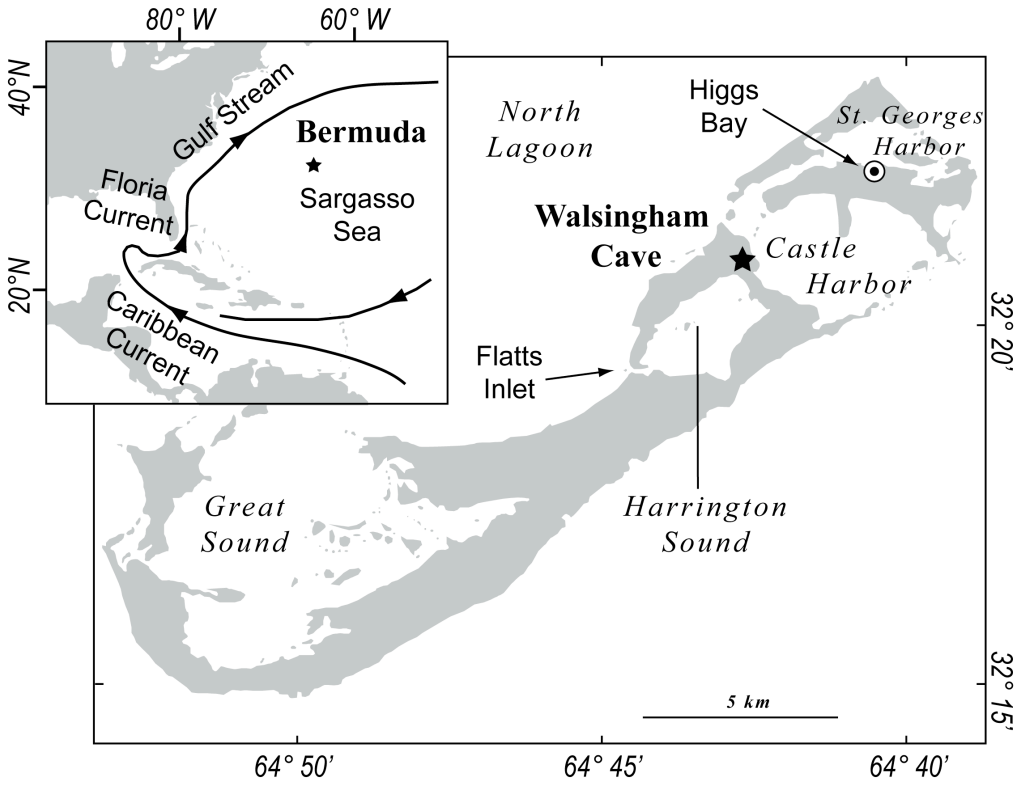

Figure 6.1: Regional oceanographic currents and site locations on Bermuda discussed in text.

Bermuda is proximal to the southern dipole of the North Atlantic Oscillation (NAO), the winter atmospheric pressure difference between the Bermuda/Azores high and the Icelandic low, which is arguably the predominant mode of climate variability in the Northern Hemisphere (Hurrell and Deser, 2009). Coral proxies (Sr/Ca, $\delta^{18}O_{aragonite}$) indicate that NAO activity can account for most of Bermuda's winter SST temperature variability over the last 55 years (Kuhnert et al., 2005), but changes in ocean circulation cannot be dismissed as impacting both annual and winter temperatures (Kuhnert et al., 2005; Goodkin et al., 2008a). Therefore, proxy reconstructions of Bermudian climate are especially sought to investigate North Atlantic climate in response to ocean-atmospheric forcing (e.g., NAO, Gulf Stream; Keigwin, 1996; Draschba et al., 2000; Kuhnert et al., 2005; Goodkin et al., 2008a), especially within a framework of millennial-scale climate

change through the Holocene (Bond et al., 2000; deMenocal et al., 2000; Cronin et al., 2005).

Based on Sargasso Sea planktic foraminifera and Bermudian coral, Bermuda was 1-2ºC cooler than present during the Little Ice Age (LIA, Keigwin, 1996; Goodkin et al., 2008a), and ~1ºC warmer during the Medieval Warm Period (Keigwin, 1996). The climate shift to cooler Little Ice Age conditions at 1400 AD has recently been associated with a change from a persistent positive phase of the NAO to a variable phase at ~1450 AD (Troulet et al., 2009), with increased NAO multidecadal variability since the late eighteenth century (Goodkin et al., 2008b). A reconstruction of Gulf Stream transport by Lund et al. (2006) indicates: (a) a decrease of ~3 Sv from 0.6 to 1.1 ka ago, (b) reduced transport compared to present from 0.6 to 0.2 ka ago coinciding with the Little Ice Age, and (c) an ~3 Sv increase from 0.2 ka ago to present. The effects of reduced heat flux to Bermuda during the LIA are not yet documented in a Bermudian paleoclimate record because multi-millennial scale climate records are unavailable from the islands.

6.2.2 Cave Geology And Hydrogeology

Bermudian caves can be summarized as collapsed karst features in a Carbonate Cover Island, according to the Carbonate Island Karst Model (Mylroie and Mylroie, 2007). This is because Bermudian geology is characterized by a basalt core overlain by alternating eolianites and paleosols that developed during late Quaternary sea-level highstands and lowstands, respectively (Land et al., 1967; Vacher et al., 1989, 1995; Hearty, 2002). Bermudian caves have formed by three primary processes: (a) vadose dissolution concentrated at the basalt-eolianite contact during Quaternary sea-level lowstands, (b) further modification and enlargement by phreatic dissolution during

Quaternary sea-level highstands, and (c) subsequent collapse events triggered by glacial regressions (Palmer et al., 1977; Mylroie et al., 1995). These processes have created caves characterized by larger chambers connected by fissures and tunnels. Superimposed upon this inherited geomorphology, Holocene sea-level rise created abundant underwater (phreatic) cave environments in Bermuda, providing sea-level independent accommodation space for sedimentary infill (Chapter 4).

Caves are abundant in the Walsingham Formation, which is the oldest and most diagenetically mature Bermudian eolianite (38% porosity) located on the isthmus between Castle Harbour and Harrington Sound (Fig. 6.1; Land et al., 1967; Mylroie et al., 1995; Hearty and Olson, 2010). Walsingham Cave is in the Idwal Hughes Nature Preserve (32º20’53”N, 64º42’37”W), and groundwater is encountered at sea level because negligible hydraulic gradients are present on such a small land area. The groundwater flooding the cave is characterized by a thin meteoric lens of brackish water (<0.5 m, salinity >20 ppt) buoyed on saline groundwater, which characterizes hydrogeology in most of the regional underwater caves (Maddocks and Iliffe, 1986). There is no large passage connecting Walsingham Cave to the ocean, precluding lagoonal bioturbators from entering the cave (e.g., sea cucumbers). This also forces saline groundwater to migrate between the cave and the ocean through the porous karst during tidal cycles, causing detectable oscillations to groundwater levels in caves (Maddocks and Iliffe, 1986; Cate, 2009). Several sinkhole (fissure-collapse) entrances provide subaerial access into Walsingham Cave, with the largest opening modified with a cement stairway down to the cave pool. Average water depth to the carbonate mud sediment surface is 18 m below sea level.

6.3 Material And Methods

6.3.1 Thermal Monitoring Of Saline Groundwater

Saline groundwater temperature was monitored in Walsingham Cave during 2010 because temperature is a groundwater circulation proxy (Whitaker and Smart, 1990; Beddows et al., 2005, 2007; Kitamura et al., 2007; Yamamoto et al., 2010). An independent probe monitoring depth and temperature was deployed at 8.95 m below sea level (1 minute sampling interval), allowing determination of temperature variation in relation to regional oceanography and tidal cycles. This sampling depth is below hydrographic influence of the ~50 cm meteoric lens, which is thermally impacted by precipitation, because tides only oscillate groundwater elevation a mean 0.75 m on Bermuda (1.2 maximum: Morris et al., 1977). Precision and accuracy on depth measurements is 1.3 cm and 30.5 cm, respectively, with 0.01ºC and 0.8ºC on temperature. Daily measurements (1440 samples) provided the daily temperature minimum and maximum, and were averaged to provide the daily mean.

Cave temperature data were compared to both coastal temperatures measured in 2010 (Higgs Bay), and Sargasso Sea surface temperatures (SST) measured at Hydrostation "S" in 2009. Daily temperature measurements of coastal SST were downloaded from Bermuda weather (http://www.weather.bm/). 2009 Sargasso Sea SST data from Hydrostation "S" were downloaded from the Bermuda Institute of Ocean Sciences (http://bats.bios.edu/).

Annual SST variation (cave, coastal, Sargasso Sea) was then compared with the two dominant sources of heat in Bermuda, the Gulf Stream and solar radiation. The National Oceanic and Atmospheric Administration's Western Boundary Time Series Project measures the volume of the Florida Current (in Sv, measurement error ± 0.2 Sv),

which is the portion of the Gulf Stream passing through the Florida Straits (http://www.aoml.noaa.gov/phod/floridacurrent/data_access.php). Daily measurements from 2000-2007 were averaged and smoothed with a 30-day low-pass filter to obtain the mean annual cycle of the Florida Current (Meinin et al., 2010). Monthly averaged solar insolation for a 22-year period (July 1983 to June 2005) over a 1º × 1º grid centered at 32.5ºN 63.5ºW was obtained from National Aeronautics and Space Administration's Surface Meteorology and Solar Energy Program (http://eosweb.larc.nasa.gov/PRODOCS/sse/table_sse.html).

6.3.2 Sedimentology And Chronology

Three push cores (5 cm diameter) were extracted with SCUBA (self-contained underwater breathing apparatus) in Walsingham Cave at 18 m below sea level. A stage bottle (extra scuba tank) was used to percuss 3 m polycarbonate tubing (5 cm diameter) into the sediment, which was rubber-stoppered and capped at maximum penetration to generate core tube suction for sediment withdrawal. All cores were extruded, logged, and sampled at 5 mm intervals in the field. Age constraint on the successions was provided by 16 radiocarbon dates on both organics (wood, bulk organics) and biogenic carbonates (foraminifera, ostracods) in cores 1 and 3. All conventional radiocarbon ages were converted to calibrated ages using IntCal09 and Marine09 (Reimer et al., 2009) with Calib 6.0, with a local ΔR value of -48 ± 40 applied to biogenic carbonates (Druffel, 1997; Appendix 1).

Particle size analysis was completed on a Beckman Coulter LS230 employing the Fraunhofer optical model, providing particle size determination between 0.04 – 2000 μm

(Murray, 2002; Eshel et al., 2004). An analysis of bulk sediments was favored over analysis of individual sedimentary constituents (e.g., carbonates, organic fraction) to retain a complete signature of environmental processes (Donnelly and Woodruff, 2007; Donato et al., 2009). Downcore particle size distributions (PSDs) were then log transformed (to the phi-scale), interpolated, and plotted as a color surface plot (Beierle et al., 2002). Interpolated PSDs often allow for better recognition of subtle changes in downcore distributions and more detailed characterization of the lithofacies than standard particle-size statistics alone (mean, median, mode, standard deviation). Bulk sedimentary organic matter (wt. %) was estimated by loss on ignition at 550°C for 4.5 hours. Replicate samples in all cores provided error generally less than ± 2%, which is typical precision for the method (Heiri et al., 2001).

6.3.3 $\delta^{18}O_c$ On Triloculina oblonga

Stable oxygen isotope geochemistry of foraminiferal calcite ($\delta^{18}O_c$) was sought to complement the sedimentological methods for understanding how the cave environment has varied in response to North Atlantic climate change. We hypothesize that if a cave is flooded by saline groundwater circulated with the ocean, then climate-forced changes to regional oceanography should be preserved in cave sedimentary biogenic $\delta^{18}O$ (e.g., Yamamoto et al., 2010). Oxygen isotopes are useful because there is temperature-dependant fractionation between water and calcite, resulting in a 0.2‰ increase in $\delta^{18}O$ for every 1ºC decrease in temperature (Epstein, 1953; Emiliani, 1955; Schackleton, 1974; Erez and Luz, 1983; Kim and O'Neil, 1997; Bemis et al., 1998). Therefore, provided the oxygen isotope composition of seawater is known, $\delta^{18}O_c$ values can be used for

paleothermometry. The use of oxygen isotope paleothermometry is hampered, however, because $\delta^{18}O_c$ is also related to the oxygen isotope composition of seawater ($\delta^{18}O_w$), which varies linearly with salinity (Bemis et al., 1998; Katz et al., 2010). Specifically, there is a 0.5‰ decrease in $\delta^{18}O$ per 1 ppt salinity decrease. Despite these limitations, the $\delta^{18}O$ from foraminiferal and coral $CaCO_3$ has repeatedly detected thermal changes associated with North Atlantic climate change during the LIA in Bermuda because this event caused robust oceanic temperature change with very little overall salinity changes (<0.6 ppt, Keigwin, 1996; Draschba et al., 2000; Kuhnert et al., 2005; Goodkin et al., 2008a,b). Therefore, even after considering the limitations imposed by the potentially variable $\delta^{18}O_w$ values through time, oxygen isotope analysis provides a simple, first-order test of the climate records preserved in Walsingham Cave.

Insufficient classical foraminiferal paleothermometers (e.g., *Cibicides*) live in the miliolid-dominated underwater caves of Bermuda, and some cave habitats are completely dominated by *Triloculina oblonga* (van Hengstum and Scott, 2011). Therefore, $\delta^{18}O_c$ was determined on monospecific samples of *T. oblonga* (~40 individuals per analysis) from core 2. Admittedly, *Triloculina oblonga* is an unconventional paleothermometer because the few tested miliolids are not in direct isotopic equilibrium with their water mass (e.g., *T. trigonula, Q. vulgaris, Pyrgo*: Grossman, 1984; Grossman, 1987; Langer, 1995). The $\delta^{13}C$ from miliolid shells is not secreted in equilibrium with $\delta^{13}C_{DIC}$ due to multiple effects, including vital and endosymbionts, and as such, is not well suited as an environmental proxy at this time (Grossman, 1984). However, the $\delta^{18}O$ disequilibria observed in *T. trigonula* was consistent between replicates (Grossman, 1984), suggesting that *Triloculina* disequilibria effects would impart a systematic offset between the $\delta^{18}O_c$-

derived and actual temperatures, similar to that documented for *Uvigerina* and other rotalids (Bemis et al., 1998; Fontanier et al., 2006). In another miliolid, a systematic offset from *Cibicides* was also observed in downcore $\delta^{18}O_c$ records of *Pyrgo* in deep-sea cores (Duplessy et al., 1970), and core top samples of *Pyrgo* have exhibited systematic $\delta^{18}O_c$ offsets from *Uvigerina* (Woodruff, 1980). Therefore, we hypothesize that rapid calcification in a smaller (shorter-lived) epifaunal triloculininid combined with running multiple individuals (~40) per sample, would provide a homogenized $\delta^{18}O$ isotopic signal from the cave with a constant offset from isotopic equilibrium. Estimates of paleotemperature anomaly about the long-term mean were calculated using the temperature equation of Bemis et al. (1998), which is arguably the most suitable for benthic foraminifera after calibration using culture-based studies (Fillipsson et al., 2010):

$$T\ (^{o}C) = 16.5 - 4.80\ (\delta^{18}O_c - \delta^{18}O_w)$$

We stress that these results are presented solely for comparing relative temperature change presumably recorded by *Triloculina* with other records, not to provide a definitive quantification of absolute temperature change in light of the uncertainty discussed above. The resultant $\delta^{18}O$ signal was also smoothed with a 100-yr moving average to focus on the most significant environmental perturbations in comparison to the long-term trends.

Triloculina oblonga has a highly-variable external morphology (elongated versus compressed) that some would argue is better described as the confusing *T. oblonga*-group, representing a small, widely-distributed coastal miliolid with a triloculine chamber arrangement. Our view is that *T. oblonga* is a highly adaptable and diverse miliolid that exhibits significant intergradations within its species concept. Advantageously, pristine *T. oblonga* shells are typically thin-walled and translucent (e.g., Goldstein, 1997). This

enables omission of any infilled individuals (with pyrite, sediment), or any with suspicious overgrowths. This is in contrast to opaque walls of larger miliolids (e.g., *T. trigonula, T. carinata, T. lineata, Q. vulgaris, Pyrgo)*, which may be infilled and subsequently bias isotopic results. Scanning electron microscopy revealed pristine porcelaneous *T. oblonga* tests throughout the core; original three-dimensional random array of calcite needles forms the test wall with a two-dimensional array of calcite needles randomly position on the surface (Fig. 6.2; Haake, 1971; Angell, 1980).

6.3.4 Isotope Ratio Mass Spectrometry

Foraminifera were transferred into stainless steel cups and roasted *in vacuo* at 200°C for one hour to remove water and volatile organic contaminants that may interfere with the isotopic values of carbonates. All stable isotope analyses were obtained using a Finnigan Kiel-IV carbonate preparation device directly coupled to a dual-inlet Finnigan MAT 253 isotope ratio mass spectrometer (Saskatchewan Isotope Laboratory, University of Saskatchewan). Twenty to fifty micrograms of carbonate (~40 *T. oblonga* individuals) are reacted at 75°C with three drops of anhydrous (100%) phosphoric acid for seven minutes. The evolved CO_2 was then cryogenically purified before being passed to the mass spectrometer for analysis. Isotope ratios are corrected for acid fractionation and ^{17}O contribution using the Craig correction (Craig, 1957). Data is directly calibrated against internal and national standards (NBS-19), with precision on $\delta^{18}O$ values of 0.11‰, respectively, and reported in standard delta notation (δ) relative to VPDB:

$$\delta^{18}O_c = 1000 * [(^{18}O/^{16}O)_{sample} - (^{18}O/^{16}O)_{standard}] / (^{18}O/^{16}O)_{sample}$$

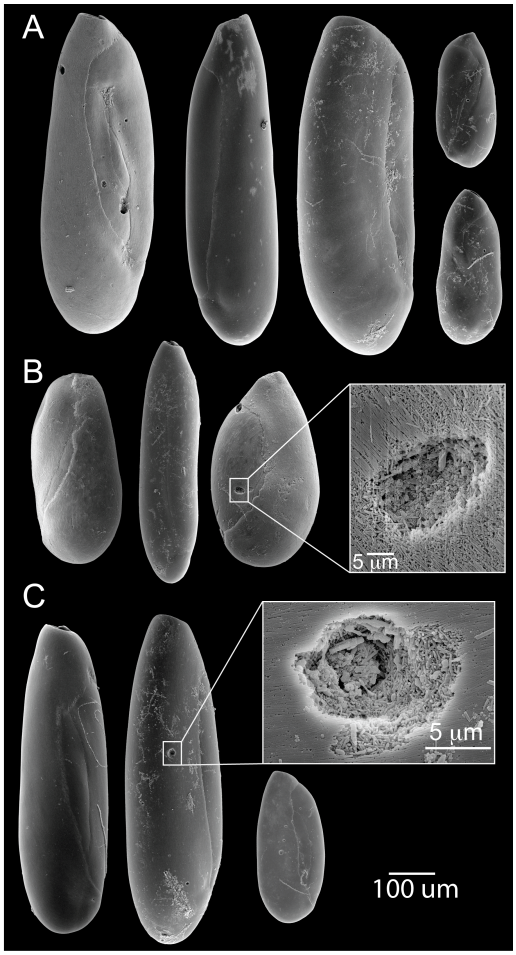

Figure 6.2: Downcore scanning electron micrographs of *Triloculina oblonga* from before (A: 5.75 cm), during (B: 22.75 cm), and after (C: 4.25 cm) prominent positive excursion in the $\delta^{18}O_c$, indicating pristine shell preservation.

6.4 Modern Cave Circulation And Foraminifera

Walsingham Cave is an open-system environment because saline groundwater is well circulated through the porous karst with two regional sources of water: the coastal (lagoonal) water and the Sargasso Sea. Coastal water was ~6ºC cooler than the Sargasso Sea in January-February of 2010, with saline groundwater temperature (SGT) in the cave diurnally fluctuating through 3.5ºC. Coldest daily cave temperatures occurred just after high tides in the winter, as cooler coastal water moved into the cave under tidal forcing (Fig. 6.3). However, cave temperatures increased throughout the tidal cycle as warmer

Sargasso Sea water became incorporated into saline groundwater through active circulation. Both coastal SST and SGT increase in early February, which corresponds to a brief ~1 Sv increase in Gulf Stream transport at the beginning of the seasonal cycle (Fig. 6.3, Meinen et al., 2010).

In the late spring, saline groundwater temperatures increase with thermal convergence between coastal water and the Sargasso Sea (March/early April). The rapid synchronous increase in cave, coastal, and Sargasso Sea temperatures in March 2010 indicates a low residence time for shallow saline groundwater in the cave. The timing of this convergence corresponds to the annual seasonal ~2 Sv increase in Gulf Stream transport, as measured through the Florida Straits (Anderson and Corry, 1985; Hamilton et al., 2005; DiNezio et al., 2009; Meinen et al., 2010), and seasonal increases in solar radiation. However, cave temperatures are ~2ºC cooler throughout the summer with little thermal variability, suggesting that the saline groundwater remains protected from direct solar insolation.

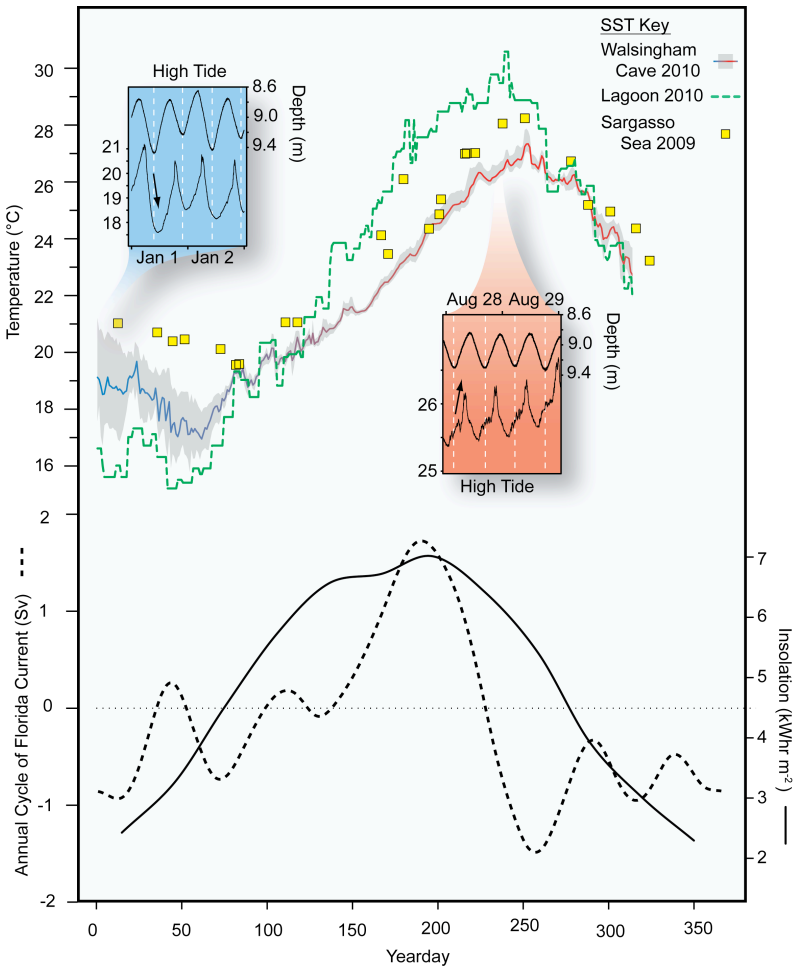

Figure 6.3: Comparison of temperatures in Walsingham Cave (2010), coastal water (2010), and Sargasso Sea (2009) with seasonal variability in regional heat supply related to Gulf Stream transport (2000-2007, Meinen et al., 2010) and mean annual solar radiation in Bermuda (see methods).

Regional maximum temperatures (coastal and Sargasso Sea SST, SGT) occur in late August, lagging behind peak insolation and Gulf Stream transport as a result of the heat capacity of seawater. As such, ocean heat storage from summer insolation prevents an immediate signature of reduced heat supply associated with Gulf Stream transport reductions in August. In summary, saline groundwater in Walsingham Cave experiences thermal seasonality because it is actively circulated with two sources (coastal water and Sargasso Sea), but SGT is annually cooler than both the coastal and open ocean due to a

lack of direct solar insolation. Therefore, cave sediments can be explored for long-term paleoclimate records because any changes to regional ocean temperatures would also force temperature change in the cave.

6.5 Results

6.5.1 Chronology And Sedimentation

The oldest date for the recovered successions in Walsingham Cave is at the base of core 2 on biogenic carbonate, dated to 3.15 ka (Fig. 6.4). Considering sea level has risen only ~3 m over the last 3.2 ka (this dissertation), proxy-records from cave cores collected from 18 m below sea level will largely reflect climatic and hydrogeologic changes—not sea-level change. Overall, the four dates from sedimentary organic matter were slightly younger (< 200 years) than the biogenic carbon dates (core 2). As such, only biogenic carbonate proxies were used in deriving linear age-depth models for consistency (Fig. 6.4).

Throughout the recovered successions, similar sedimentary processes are operating basin wide in the cave based on sedimentation rates, particle size analysis, and bulk sedimentary organic matter (wt. %). The recovered cave succession can be generally described as an allogenic carbonate mud lithofacies deposited in a submarine cave environment with increasing organic matter content and coarser particle sizes upcore. Sedimentation rates were higher prior to 2 ka (> 54. 1 cm kyr^{-1}), coinciding with predominantly carbonate mud deposition and <10% organic matter content. Carbonate mud in submarine cave environments in Bermuda typically has 9.7 ± 3.1% organic matter (van Hengstum and Scott, 2011), which is consistent with the Walsingham cores and indicates that predominantly in situ organic matter production occurred in Walsingham

cave prior to 2 ka. This interval is also characterized by well-sorted particle size distributions, with a mode of <10 μm (6.6-6.9 ϕ). However, sedimentation rate decreases in the basin after 2 ka (core 2: 15.9 cm kyr^{-1}, core 4: 28.9 cm kyr^{-1}), with little change in either bulk organic matter or particle size distributions (Fig. 6.5).

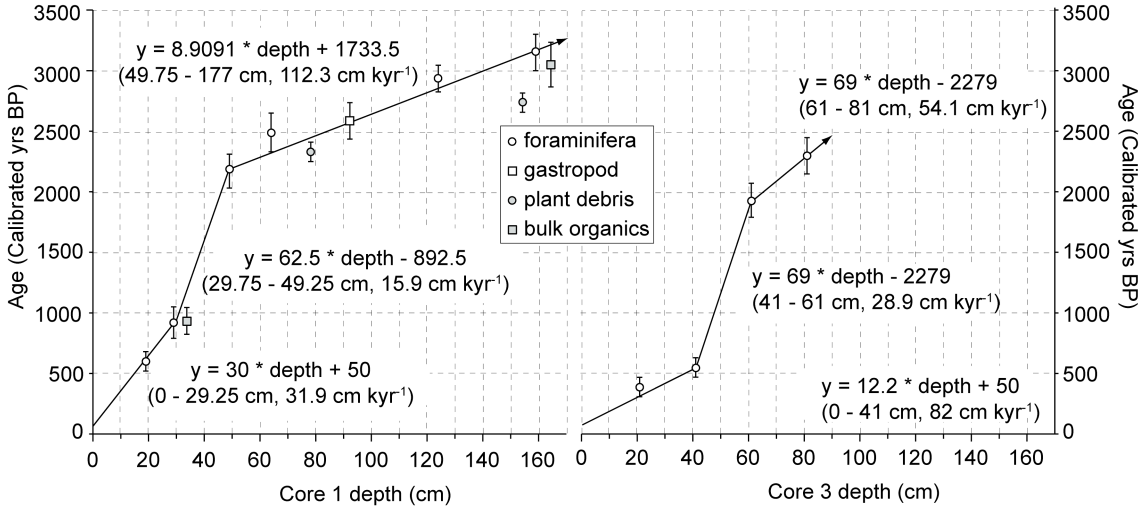

Figure 6.4: Downcore age models and sedimentation rates based on linear interpolation between ^{14}C ages. Note synchronous sedimentation change basin wide at ~2.0 ka ago, and spatial relationships between core sites and the more recent sedimentary shift.

The sediment in all cores can be described as a marine carbonate mud, but shifts in color from a basal grayish-white carbonate mud, to light brown carbonate mud by 2 ka, and finally brown carbonate mud at ~0.6 ka. The final brown carbonate mud contains obvious terrestrial organic matter fragments, such as small twigs, which are absent in the white carbonate mud. The sediment includes only rare fragments of detrital limestone, and negligible siliciclastic content. Core 4 is near the sinkhole entrance and has a higher sedimentation rate (83 cm kyr^{-1}) and coarser particle sizes (20 to >60 μm) than core 2 (31.9 cm yr^{-1}, 18 μm), which is located furthest into the cave. The spatial pattern of sedimentation indicates that areas closest to the sinkhole entrance (core 4) receive the

highest sediment volume and coarsest particles compared with areas deeper in the cave (core 2). Synchronous with increasing sedimentation rates, bulk organic matter and particle sizes increase in all cores (Fig. 6.5). Bulk organic matter in all cores exceeds 12%, with a maximum of 20% in core 2 at ~0.65 ka. Sediments in Bermudian underwater caves achieve a high bulk organic matter (>13%) and coarse particle sizes (>15 μm) in caves that receive a constant flux of terrestrial sediments, such as near sinkholes (van Hengstum and Scott, 2011). Considering Walsingham Cave has no direct underwater cave passage to Castle Harbour, the increasing sedimentation rates, bulk organic matter, and particle sizes indicates that increasing quantities of terrestrial sediment have been deposited into the cave over the last millennia.

More specifically, although increased terrestrial erosion began at 0.9 ka, as evidenced in core 2, peak erosion did not occur until after 0.65 ka, after which particle size increases in cores 2 and 4, and likely in core 3 (Fig. 6.5). Peak organic matter influx, however, appears concentrated at 0.65 ka, coinciding with peak flux of organic matter transported to the distal cave (core 2). Land-use changes are not responsible for these sedimentary changes because (a) the cave entrance remains on an unspoiled nature reserve, and (b) deforestation post-dated island colonization in 1609 AD (Rueger and von Wallmenich, 1996), which is beyond 2σ radiocarbon error of the peak at 0.65 ka.

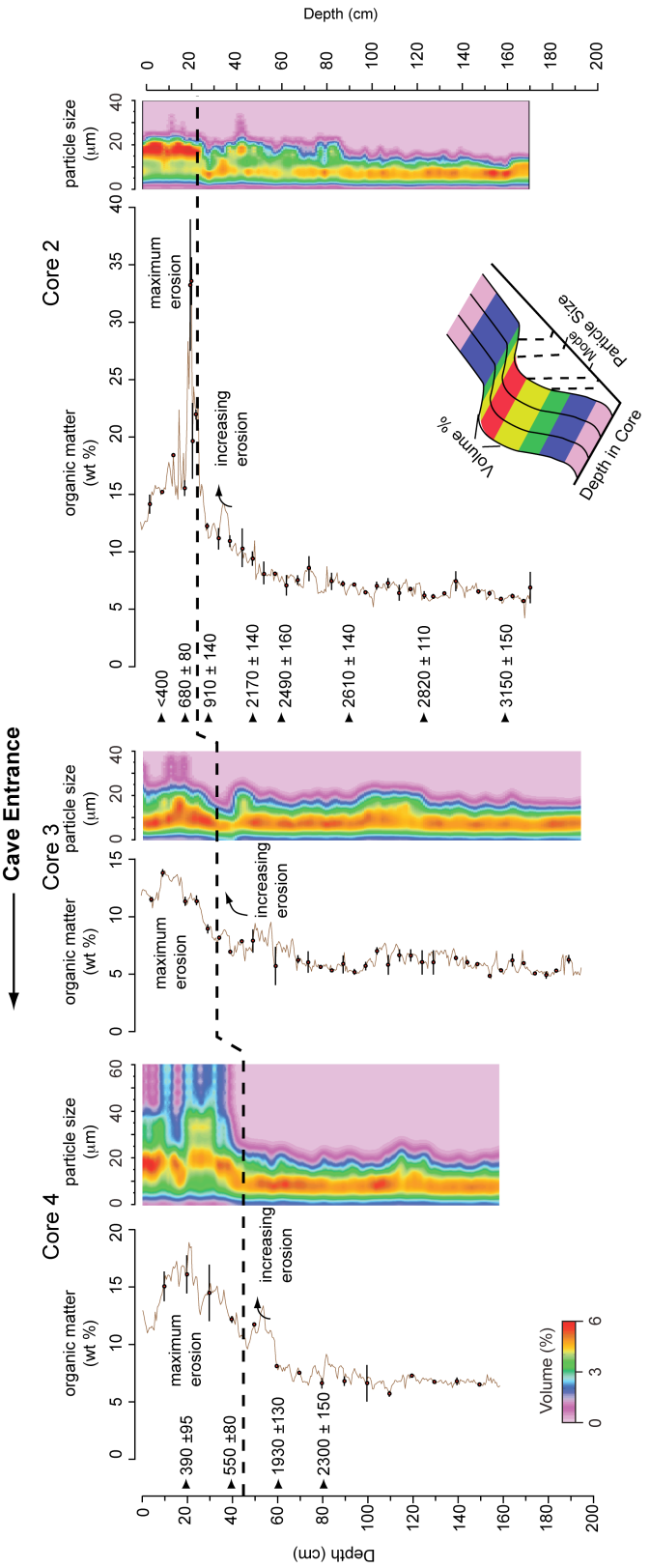

Figure 6.5: Interpolated particle size distributions and bulk organic matter content (2σ on replicates) in cave cores. Trianlges indicate the position of ^{14}C dates (calibrated yrs BP, 2σ). The line demarcates a widespread sedimentological change in the cave basin.

6.5.2 Oxygen Isotopes

The measured $\delta^{18}O_c$ values fluctuate between -0.61‰ and +0.25‰, and the time-averaged record oscillates between a minimum of -0.38‰ and maximum of +0.1‰ (Fig. 6.6). The most significant feature of the $\delta^{18}O_c$ record is strong departure from long-term $\delta^{18}O_c$ values in core 2 beginning at 0.9 ka. A $\delta^{18}O_c$ minimum occurs just prior to 0.9 ka with a measured value of -0.36‰, trending to a maximum at 0.65 ka of +0.12‰. Mean $\delta^{18}O_c$ values prior to this perturbation are -0.2‰, which re-adjust after the perturbation to a mean $\delta^{18}O_c$ value of -0.1‰. The increasing $\delta^{18}O_c$ trend at 0.9 ka coincides with increasing sedimentation rates in core 4, and 0.6 ka coincides with increasing sedimentation rates and maximum organic matter flux in the cave basin (i.e., terrestrial erosion). Although more subtle oscillations seemingly occur in the $\delta^{18}O_c$ record at decadal to multi-decadal level, we refrain from interpreting such isotopic variability in this pilot study because of uncertainties associated with using a miliolid proxy. Nevertheless, the $\delta^{18}O_c$ relationships from the cave can be correlated throughout the North Atlantic region and merit further attention (discussed further below).

A significant limitation of using $\delta^{18}O_c$ as a paleoclimate proxy is that it remains challenging to disentangle the effects of temperature and $\delta^{18}O_w$ (i.e., salinity; Katz et al., 2010). However, if salinity changes were responsible for the change in $\delta^{18}O_c$ at 0.9 ka, saltier conditions in both the SGW and seawater in the Bermuda region would be required from the inverse relationship between temperature and $\delta^{18}O_w$ effects on $\delta^{18}O_c$. However, sea surface salinity in Bermuda appears to have been less saline (fresher) during the Little Ice Age (0.6 to 0.15 ka, Goodkin et al., 2008a), which would act to decrease (deplete) $\delta^{18}O_c$ values. Instead, we observe enriched $\delta^{18}O_c$ values peaking at 0.65 ka ago that

suggest a strong cooling event, as observed throughout the North Atlantic Basin (discussed below). Therefore, we interpret the $\delta^{18}O_c$ (thermal) and sedimentological evidence in tandem from Walsingham Cave as preserving a useful paleoclimate signal.

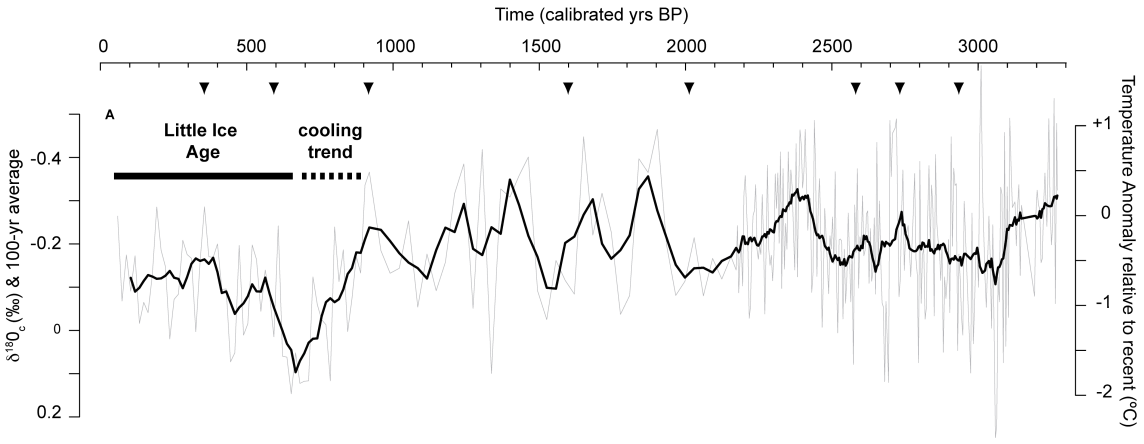

Figure 6.6: Walsingham Cave core 2 $\delta^{18}O_c$ (*Triloculina oblonga*) and temperature anomaly plotted time-wise using the age models from Fig 6.4.

6.6 Discussion

6.6.1 Little Ice Age Brings Maximum Cooling And Storminess At 0.65 ka

The significant positive $\delta^{18}O_c$ excursion at 0.65 ka suggests that the coolest saline groundwater was circulating in Walsingham Cave relative to the entire investigated time interval, followed by another cooling minima at 0.45 ka. The first minima at 0.65 ka ago is interpreted as initiation of the Little Ice Age in Bermuda, synchronous with strong cooling in the North Atlantic region, reduced northern hemispheric temperatures, global glacier advances, and Nordic population collapse in Iceland (Denton and Karlén, 1973; Keigwin, 1996; deMenocal et al., 2000; Mann et al., 2008; Patterson et al., 2010). Thereafter, the long-term mean $\delta^{18}O_c$ values from Walsingham Cave remain more

enriched than during the previous 3.2 ka, indicating persistent long-term cooling began in Bermuda.

Coldest Little Ice Age (LIA) temperatures in the North Atlantic are frequently observed as paired-cooling peaks beginning at ~0.6 ka (1400 AD). For example, deMenocal et al. (2000) documented synchronous ~3ºC paired-cooling events initiated in the northeastern Atlantic at 0.7 and 0.4 ka ago. Keigwin (1996) also documented ~1ºC paired-cooling events in the northwestern Atlantic, although the second was at 0.3 ka ago, centered at 0.6 and 0.3 ka ago. The variable timing of the paired-cooling between marine reconstructions may be from radiocarbon uncertainties and local accumulation rates, but a clear signal of two closely spaced cooling events is observed throughout the North Atlantic. In the recent northern hemispheric temperature reconstruction of Mann et al. (2008), two sharp cooling events (0.8 to 0.6ºC) occur centered at 0.65 and 0.55 ka ago, immediately before persistent long-term ~0.7ºC hemispheric cooling begins associated with the LIA. The general agreement between all North Atlantic marine proxies and the hemispheric thermal reconstruction of (a) paired cooling events, followed by (b) a long-term cooling trend indicates that Walsingham Cave has faithfully responded to regional climate change during the onset of the LIA.

The LIA interval (<0.65 ka) in Walsingham Cave is also associated with maximum terrestrial erosion from the recorded influx of organic matter and coarse particle sizes in all successions. The PSDs record a composite measurement of sedimentary particles, including organic matter fragments. Considering the cave is located on the pristine nature reserve, and the increase in grain size predates European colonization of Bermuda in 1609, deforestation cannot account for increased erosion observed at 0.65 ka. Furthermore, the only long-term record of Bermudian vegetation

suggests increased tree cover on the island at the onset of increased particle sizes entering Walsingham Cave (Rueger and von Wallmenich, 1996). Therefore, we argue that the sedimentary influx is related to the most intense and/or frequent storminess over the last 3.2 ka ago on Bermuda, which caused increased surficial erosion and deposition of coarser particles into Walsingham Cave.

Sediment-based reconstructions of storminess in the North Atlantic indicate that European coastlines in the northeast were stormiest from 0.43 to 0.1 ka (Clark and Rendell, 2009), this is observation is supported by increased sediment overwash events in northwestern lacustrine basins from 0.6 ka to present (Noren et al., 2002). Marine-sourced sea-salt sodium (ssNa) recovered from the Greenland Ice Sheet Project Two (GISP2) core is used as the longest resolved storminess proxy, where intensified atmospheric circulation in the North Atlantic causes increased ssNA deposition in Greenland ice sheets (O'Brien et al., 1995; Meeker and Mayewski, 2002). There is a long-term shift in ssNA at 0.6 ka, which has been attributed to the onset of persistently intense atmospheric circulation in the northern hemisphere related to change from positive to negative phase of the North Atlantic Oscillation (Meeker and Mayewski, 2002; Troulet et al., 2009; Fig. 6.7). The significant increase in ssNa at 0.6 ka coeval with (a) increased terrestrial erosion in Bermuda, (b) sediment overwash events in northeastern American lacustrine basins, and (c) storminess documented on European coastlines provides strong evidence for increased storminess in the North Atlantic basin during the LIA, related to a modal shift in the North Atlantic Oscillation (NAO). However, compounding effects from a shift to La Niña conditions at ~0.6 ka cannot be ruled out as a contributing factor (Donnelly and Woodruff, 2007).

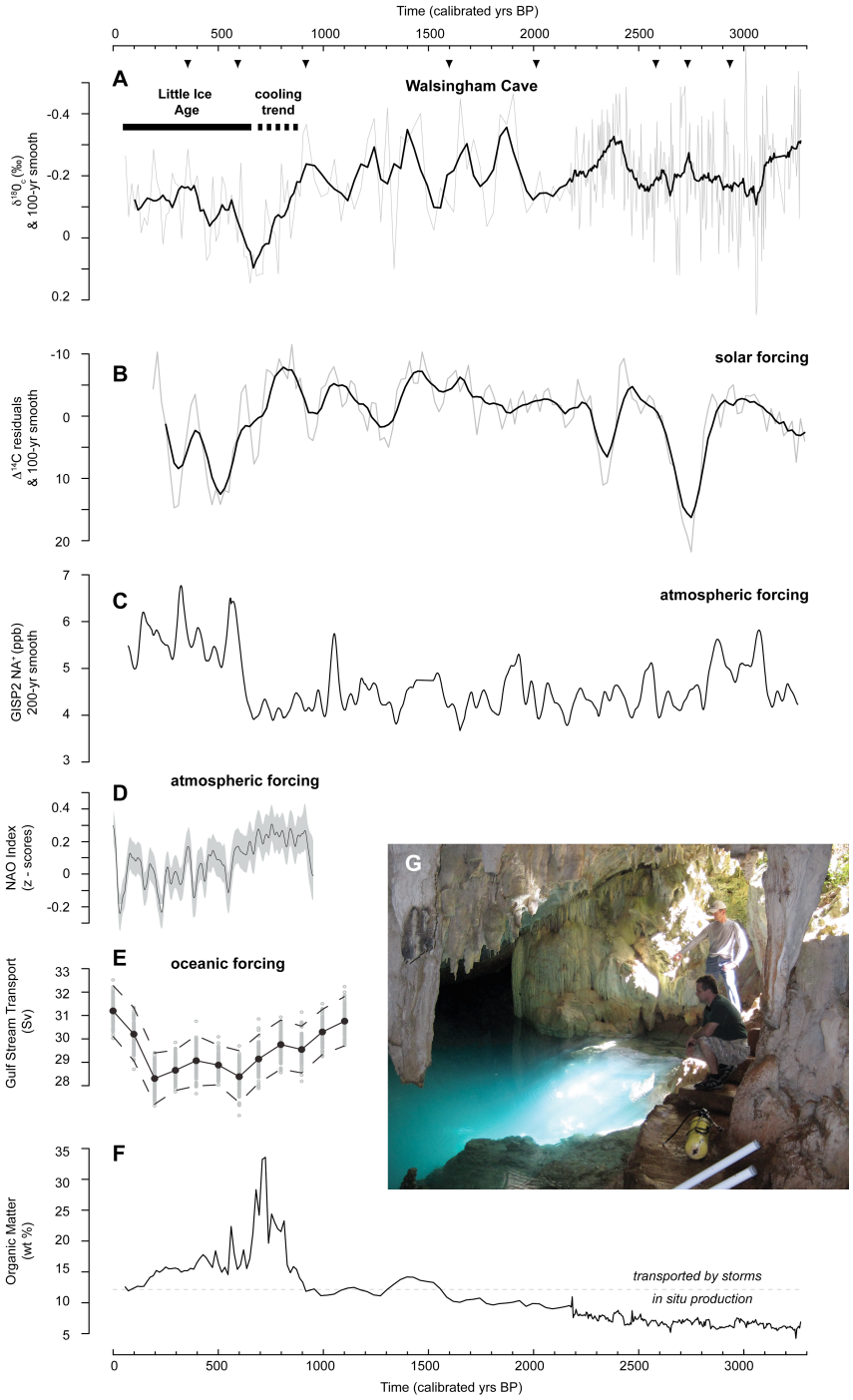

Figure 6.7: Climate forcing. (a) $\delta^{18}O_c$ from Walsingham Cave core 2 with 100-yr moving average (this work), (b) $\Delta^{14}C$ production as a proxy for solar flux (Stuvier and Braziunas, 1989), (c) ssNa from GISP2 core as a proxy for Northern hemispheric atmospheric circulation (O'Brien et al., 1995), (d) reconstructed NAO index (Troulet et al., 2009), (e) reconstructed Gulf Stream transport through the Florida Straits (Lund et al., 2006), (f) organic matter content from Walsingham Cave core 2 as a terrestrial erosion proxy that is not related to deforestation, (g) main entrance into Walsingham Cave and cave pool.

No other intervals of intense storminess are evidenced in Walsingham Cave, which is at odds with an apparent increase in storminess recorded at 2.6 ka in the lacustrine basins of Vermont and eastern New York (Northeastern USA: Noren et al., 2002). Based on geomorphology and speleothem deposits around the cave entrance, the collapse event that caused the cave to be subaerially open likely pre-dates the Holocene. The storminess documented at 2.6 ka by Noren et al. (2002) appears as a strong, short-term peak in comparison to their LIA signal that is a robust long-term increase in sediment overwash events. The GISP2 ssNa indicates only a very minor change at 2.6 ka, which does not approach the magnitude of the LIA signal (Fig. 6.7). The GISP2 ice core is arguably a more robust proxy for storminess and atmospheric circulation in comparison to particle size increases (i.e., overwash events) in lacustrine basins, which may be secondarily overprinted by non-storm related sediment flux. It may be that either storminess was not strong enough to cause significant terrestrial erosion in Bermuda at 2.6 ka, was too short-lived to archive a sedimentary signature, or was completely absent in Bermuda. The next storminess signal in the GISP2 ssNa that is analogous to the LIA signal is centered at ~5.7 ka, and lasted for >300 years. Based on the coherency of the storminess signals in GISP2 and in the cave during the LIA, longer cave successions may provide further insight into central North Atlantic storminess related to changing mode of the NAO (positive versus negative) during the mid-Holocene.

6.6.2 North Atlantic Cooling At ~0.9 ka Documented In Walsingham Cave

Earlier than the LIA, the multi-proxy cave results indicate that 0.9 ka ago was the onset of (a) a subtle increase in terrestrial erosion based on sedimentological proxies, and (b) a cooling trend (of ~1ºC) in the saline groundwater in the cave based on $\delta^{18}O_c$ (Fig.

6.8). $\delta^{18}O_c$ measurements on Bermudian corals do not predate 0.65 ka (e.g., Goodkin et al., 2008a; Draschba et al., 2000), but planktic foraminifera in the Sargasso Sea also indicate a robust decreasing $\delta^{18}O_c$ trend from ~0.9 to 0.65 ka (on *Globigerinoids ruber)*, corresponding to a cooling trend of ~1.5ºC. In the northwestern Atlantic, Cronin et al. (2003) documented a cooling trend of ~1.5ºC from 1 to 0.8 ka in the Chesapeake Bay estuary using ostracod Mg/Ca ratios (*Loxoconcha)*. This trend is similar to that of Cronin et al. (2010) in another location with higher sedimentation rates (~1 to 0.6 ka, ~5ºC cooling trend). In the northwestern Atlantic, deMenocal et al. (2000) documented a cooling of ~3-4ºC (±1.3 – 1.6ºC) at 0.95 ka using a planktic foraminiferal transfer function. The near synchronous detection of a North Atlantic cooling trend by multiple different proxies at 0.9 ka adds further evidence that Walsingham Cave faithfully responded to regional climate changes.

The classic definition for the LIA onset is ~0.6 (±0.05 ka), supported with global terrestrial and marine paleoclimate reconstructions. Using the 'wiggle room' of 2σ error on radiocarbon dating, many climatic cooling trends have been accommodated into a LIA onset at ~0.6 ka. However, the reconstruction of Mann et al. (2008) suggests that global cooling began at least by 0.9 ka (possibly earlier), with only maximum cooling (~1ºC) during the last millennium beginning at ~0.6 ka and coinciding with global glacier advance (Denton and Karlén, 1973). Mann et al. (2008) reduce the Medieval Warm Period to mainly a northern hemispheric climate feature from 0.9 to 1.1 ka, with temperatures analogous to present. The well-constrained $\delta^{18}O_c$ evidence from Walsingham Cave indicates that saline groundwater began a robust cooling trend at 0.9

ka, near synchronous to cooling trends observed in other North Atlantic climate reconstructions (Fig. 6.8).

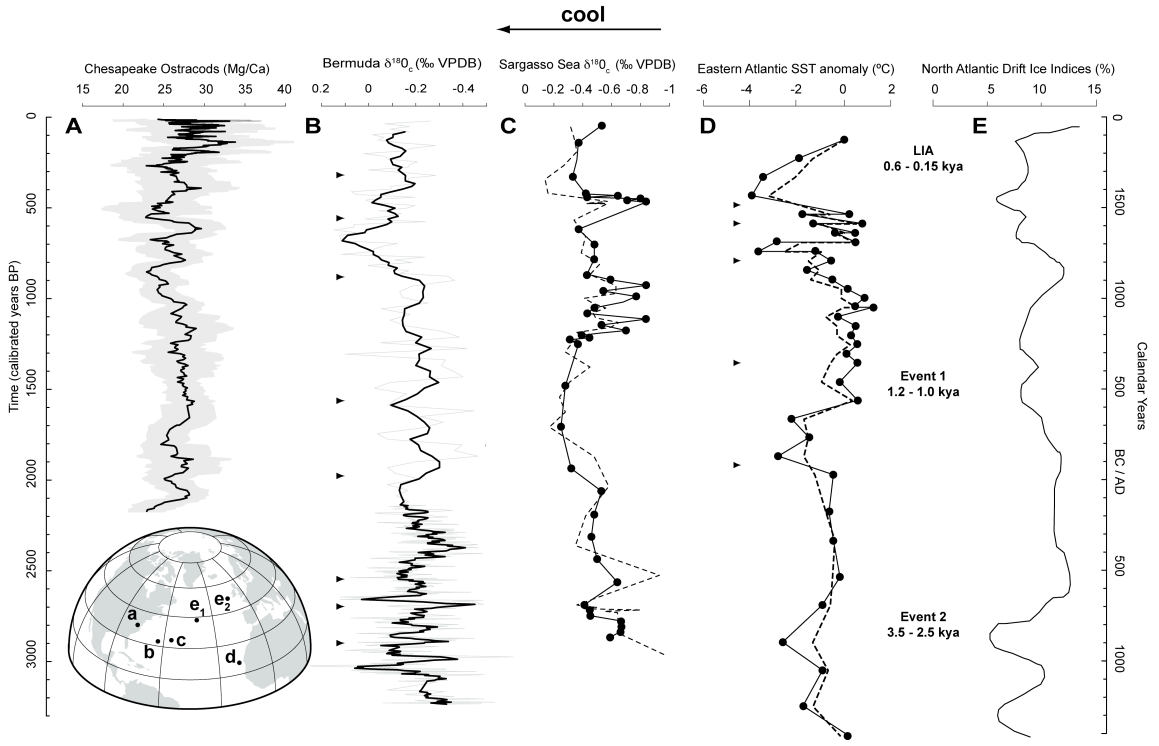

Figure 6.8: Thermal variability across the North Atlantic as documented in marine sediment records: (a) 9-point moving average with 95% confidence on ostracod (*Loxoconcha*) Mg/Ca ratios from Chesapeake Bay (Cronin et al., 2003), (b) Walsingham Cave $\delta^{18}O_c$ (*Triloculina*) with 100-yr moving average (this work), (c) Sargasso Sea $\delta^{18}O_c$ (*G. ruber*) from two cores (Keigwin, 1996), (d) summer (solid) and winter (dashed) Eastern tropical Atlantic SST anomaly (planktic foraminiferal transfer function with <1.6ºC error, deMenocal et al., 2000), (e), four-core multi-proxy stack of changing drift ice indicators (petrologic) in northeastern Atlantic (Bond et al., 2001). The North Atlantic-centered globe indicates the locations of the different marine records, and intervals of rapid climate change from Mayewski et al. (2004) are noted (LIA, Event 1, Event 2).

The increased terrestrial erosion observed at ~0.9 ka in Bermuda pre-dates the increase in North Atlantic storminess caused by atmospheric circulation changes at 0.6 ka (previously discussed, Fig. 6.7). Changes in hurricane frequency and/or intensity may also cause sedimentary influx into the cave (terrestrial erosion). A recent reconstruction of hurricane frequency over the last 1500 years by Mann et al. (2009) indicates that the

North Atlantic basin had the highest hurricane frequency period from 1.0-0.5 ka ago, which pre-dates the LIA. This interval coincides with a persistent positive phase of the North Atlantic Oscillation (NAO), which causes an increase in storms tracking along eastern North America (Troulet et al., 2009). The coeval organic matter increases observed (but not as high as during the LIA) in the cave successions may be related to this increased hurricane activity.

A significant peak in hurricane events is observed basin wide in the North Atlantic at 0.65 ka, which corresponds to the highest amount of organic matter transported into the distal cave (core 2). Unfortunately, the statistical model of Mann et al. (2009) was unable to model this peak in hurricane activity recorded by basin wide overwash events. The transport of significant quantities of organic matter into the distal part of Walsingham Cave is corroborative evidence for either: (a) high-frequency erosion-causing events, or (b) significant intensity of erosion-causing events in Bermuda at 0.65 ka. We envisage that abundant, coarse-grained organic matter fragments are blow by strong winds into the distal cave (core 2), whereas overwash from intense rain activity is likely washing a combination of sediments into the cave near the entrance (core 4, Fig. 6.5). Records of hurricane frequency in Bermuda are currently unavailable for comparison, but sedimentary influx into Bermudian caves appear sensitive to any local energy changes that would cause terrestrial erosion, including hurricane variability.

6.6.3 Forcing Of Observed Long-term Trends And Implications

Considering the sedimentation and thermal records in Walsingham Cave over the last millennium appear to be correlated to regional North Atlantic climate changes, questions are raised regarding external forcing of the observed signal over the complete

time interval (3.2 ka). The interval spans three periods of so-called rapid climate change in the Holocene; global cooling at 0.6, 1.4 and 2.8 ka ago (Mayewski et al., 2004). Solar forcing has been proposed as a critical driver of Holocene climate variability (Bond et al., 1997, 2001), but the nature, timing, and severity of Holocene cooling events are globally variable. A long-term paleoclimate record from Bermuda provides insight into climate change in a region significantly influenced by both oceanic circulation (heat from the Gulf Stream) and North Atlantic Oscillation (NAO). Therefore, any long-term thermal changes in Bermuda are likely to be caused by a combination of ocean-atmospheric forcing.

Attributing the climate signal in Walsingham Cave exclusively to solar forcing is unsatisfactory when considering the $\delta^{18}O_c$ variability over the last 3.2 ka. Indeed, the cooling trend observed in Walsingham Cave beginning at 0.9 ka ago does coincide with reduced solar radiation from the 70-year Oort solar minimum (0.99-0.92 ka) and the onset of reduced solar radiation throughout the LIA (Fig. 6.7b, Stuvier and Braziunas, 1989). Climate forcing analyses over the last millennium by Crowley (2000) and Hegerl et al. (2002) indicate that explosive volcanism is also responsible for compounding global cooling during the LIA. Both solar and volcanic forcing contributed to cooling in Bermuda over the last 225 years (Goodkin et al., 2008a), but these variables do not adequately explain why other periods of strong cooling observed elsewhere are not observed in Walsingham Cave. For example, there is a solar minimum at 2.8 ka ago (Fig. 6.7b; Stuvier and Braziunas, 1989), and explosive volcanism at 2.1 ka ago (Zielinski et al., 1996). These events likely contributed to global climate variability, but did not elicit a

strong coeval $\delta^{18}O_c$ increase (enrichment, cooling) in Walsingham Cave. Therefore, other mechanisms need to be invoked to understand the Walsingham Cave climate signal.

The North Atlantic Oscillation (NAO) is a critical driver of northern hemispheric climate variability (reviewed in Hurrell and Deser, 2009), including Bermuda. In general, positive NAO phases lead to warmer SST in the Bermuda region, whereas negative NAO phases lead to cooler SST. Over half the winter and fall SST variability in Bermuda (Sargasso Sea -"Hydrostation S") can be accounted for by the NAO index within the instrumental record, which is also reflected in proxy-records of SST from Bermudian corals ($r = -0.50$, Kuhnert et al., 2005). The shift to persistent cooler saline groundwater temperatures in Walsingham Cave at 0.65 ka ago is consistent with the interpretation of cooler SST in Bermuda related to atmospheric forcing. Furthermore, observed sedimentological changes also appear related to storminess and hurricanes caused by NAO variability during the last millennium. Although, the contribution of ocean forcing to proxy records of Bermudian climate has been discussed, the short coral record (0.75 ka maximum, Draschba et al., 2000) precludes long-term correlation of Bermudian climate with Gulf Stream transport changes (Lund et al., 2006). The fact remains that reduced Gulf Stream transport coincides with hemispheric and Caribbean-Atlantic region cooling at 0.9 ka that likely impacted Bermudian climate (Lund et al., 2006), which predates major atmospheric circulation changes at ~0.6 ka.

Heat transported to Bermuda by the Gulf Stream plays a critical role in local climate, allowing suitable habitat for the Atlantic's northernmost reef ecosystem. Lund et al. (2006) documented a ~3 Sv decrease in Gulf Stream volume from 1.1 to 0.6 ka, synchronous with the cooling trend observed in (a) the saline groundwater of Walsingham Cave and (b) the wider North Atlantic region, and predates atmospheric reorganization at

0.6 ka. Reduced Gulf Stream transport would have also slowed rates of deep saline groundwater circulation (Whitaker and Smart, 1990), providing constructive feedback for underwater cave cooling in addition to the effects of net reduced heat supply to Bermuda. Temperature fluctuations in the Sargasso Sea from 2.0 to 3.0 ka ago (Keigwin, 1996) dominantly fluctuate along with solar forcing (Bond et al., 2001), so it remains a challenge to disentangle the effects of changing Gulf Stream transport. In contrast, saline groundwater in Walsingham Cave is colder year-round than the open-ocean because it is protected from thermal extremes caused by seasonal solar radiation. This effect on longer time scales may have (a) attenuated the impact of late Holocene changing solar radiation variability, and (b) allowed the saline groundwater in Walsingham Cave to document long-term heat supplied to Bermuda by the Gulf Stream. Therefore, we argue that the cooling trend in the North Atlantic beginning at 0.9 ka is related to effects caused by reduced heat transport from the Gulf Stream, and archived in Walsingham Cave. If this hypothesis proves correct, then oceanic circulation played a pivotal role in global cooling before atmospheric changes during the LIA, as suggested by Keigwin and Boyle (2000). This raises further questions on the ocean's role within a perspective of the two preceding events of rapid climate change in the Holocene (0.6, 1.4, 2.8 ka: Mayewski et al., 2004), because no similar cooling events are observed in the Walsingham Cave thermal record related to either atmospheric or solar forcing.

If reduced heat transport by the Gulf Stream transport played a climatic role downstream in Bermuda, it would also have impacted upstream oceanographic regions. For example, Richey et al. (2007) documented cooling minima in the Pigmy Basin (Northwest Gulf of Mexico) centered at 0.85, 0.7, 0.45, and 0.25 ka using SST estimates derived from Mg/Ca ratio of planktic foraminifera (*G. ruber*). Richey et al (2007)

attributed the cooling at 0.85 ka to solar forcing, but the impact of a possibly reduced Caribbean current may also have been a contributing factor (Lund et al., 2006). These relationships emphasize that additional surface ocean transport reconstructions extending further back into the Holocene are required.

6.7 Conclusions

The temperature monitoring program in Walsingham Cave, Bermuda, provides strong evidence that saline groundwater on Bermuda is circulating with the ocean, as in underwater caves elsewhere (Yamamoto et al., 2009). The assumption that underwater caves on karst islands have remained hydrographically isolated from the ocean over the Cenozoic is no longer valid (e.g., Iliffe et al., 1983). Therefore, climate changes will impact underwater cave environments and ecosystems (e.g., Parravicini et al., 2010), and proxy-records of climate change can be archived in unbioturbated cave sediments. However, the need for annual records of groundwater temperature variability will remain for qualifying the degree of connectivity between underwater caves and the ocean (e.g., Novosel et al., 2007).

The paleoclimate record in Walsingham Cave (sediment and geochemical proxies) appears strongly related to ocean-atmospheric changes over the last 3.2 ka ago, which is consistent with coral-based paleoclimate records (e.g., Kuhnert et al., 2005; Goodkin et al., 2008b). The underwater cave sediments, however, span significantly longer time scales than corals. Maximum cooling and storminess in Bermuda was documented at 0.65 ka ago in cave sediments, thereafter followed by long-term persistent cooling that is coincident with hemispheric cooling patterns associated with the LIA (Mann et al., 2008). However, reduced Gulf Stream transport at 0.9 ka ago (Lund et al., 2006) is correlated

with cooling in Bermuda and the North Atlantic region, which precedes reorganization of atmospheric circulation at 0.6 ka ago. This suggests that conditions afforded by reduced oceanic circulation in the North Atlantic may have been pivotal for LIA cooling. At this stage, interpreting $\delta^{18}O_c$ trends with greater than centennial-scale resolution is hampered from the uncertainties associated with the $\delta^{18}O_c$ proxy. However, this pilot study clearly indicates that (a) climate trends are faithfully recorded in underwater cave sediments, (b) sub-decadal to multi-decadal sedimentation rates exist in underwater caves extending to at least 3.2 ka ago, and (c) the role of oceanic forcing can be observed in climate signals due to constructive feedbacks between saline groundwater circulation and regional oceanography. Therefore, underwater cave sediments on karst platforms represent an emerging source of long-term marine-based paleoclimate records in tropical and subtropical basins—areas that are often considered devoid of such records.

Chapter 7: Conclusions

The simple answer to the premise of this dissertation is that phreatic coastal cave environments unequivocally contain useful information about Quaternary sea level and climate. Many basic curiosities about coastal cave environments were presented in the introduction that framed this scientific exploration. Most important of these curiosities, however, was that sediments are abundant in phreatic coastal caves, yet they have received very little scientific study. In order to investigate this problem, this dissertation first systematically investigated the modern environmental processes occurring in the phreatic coastal caves of Bermuda. Once the modern environmental processes in the phreatic caves could be constrained, core records were then sought to investigate the climatic and sea-level history of Bermuda, with broader reference to the North Atlantic region and beyond.

7.1 Part I: Establishing Modern Marine Geological Processes In Phreatic Caves

The first part of this dissertation was primarily focused on constraining the modern environmental processes occurring in Green Bay Cave (GBC), Bermuda. Before starting this research, a major problem existed in coastal cave science: it was impossible to quantitatively separate anchialine versus submarine cave environments in passages completely saturated by saline groundwater. Furthermore, there were no sedimentologic or micropaleontologic proxies defined in phreatic coastal caves useful for reconstructing environmental change, and data on foraminiferal communities in underwater cave environments was non-existent. These problems precluded confident application of cave sediments to Quaternary sea-level or climate problems. As such, the following question

guided Part I of this research: *What are the general sedimentary characteristics and ecology of foraminifera in modern underwater caves?*

In short, diverse communities of benthic foraminifera were found living in GBC, which are organized into specific groups (or assemblages) colonizing the heterogeneous habitats throughout the cave (Chapter 2). Since their shells (tests) are preserved in the sediment record, foraminifera are obvious targets to develop into environmental proxies in underwater caves. Groundwater salinity, terrestrial influences (sediments, nutrients), and the supply and attenuation of nutrients into the cave were the primary factors influencing benthic foraminiferal ecology in GBC (Chapter 2). These conclusions were a successful result to the question that guided the research in Part I.

In addition to foraminifera, we also learned that sedimentological and organic geochemical proxies (particle size, C:N, $\delta^{13}C_{org}$) can easily distinguish anchialine versus submarine cave habitats. Green Bay Cave has perfect geomorphology for testing hypotheses relating to the difference between anchialine and submarine cave environments: an anchialine cave entrance is connected to a submarine cave entrance by over 250 m of phreatic cave passage. The most important difference between these two environments in GBC was the influx of terrestrial sediments entering the cave at Cliff Pool Sinkhole. Therefore, I emended the definition of anchialine habitats to require the nuance that terrestrial influences and processes *dominant* anchialine habitats (sedimentologic, hydrogeologic, or biochemical). In contrast, marine processes must *dominate* cave habitats for them to be classified as submarine cave environments (see Glossary). This subtle extension of the original classification system of phreatic coastal cave environments (Stock et al., 1986) allows for phreatic cave habitats to be quantitatively distinguished. This result solved an important research problem, as these

environments can now be quantitatively distinguished in the sediment record too. It will be interesting to learn if other phyla colonize the heterogeneous cave habitats similar to benthic foraminifera. Future research should continue to refine our understanding of the differences between coastal cave environments, and to test the principles we have established in Bermuda elsewhere (e.g., Mexico, Cuba, Bahamas, etc.).

As discussed, the influx of terrestrial nutrients into oligotrophic subterranean habitats has considerable impact on cave foraminifera (Chapter 2). This means that organic groundwater pollution should also be detectable by foraminiferal populations because pollution can alter the trophic state of an oligotrophic underwater cave. Benthic foraminifera are useful pollution monitoring proxies in other coastal environments (e.g., Yanko et al., 2003; Scott et al., 2005), which causes changes to foraminiferal assemblages and test (shell) morphologies. Therefore, foraminifera and other microfossil proxies may represent a future tool for detecting nutrient loading in coastal aquifers, which remains a primary concern along many urbanized karst coastlines.

Although this study has focused primarily on foraminifera, taxonomic based research has been completed on ostracods in Bermudian phreatic caves (e.g., Maddocks and Iliffe, 1986; Kornicker and Iliffe, 1989). Future work may target this group for paleoenvironmental research because their shells are also preserved in the sediment record, perhaps preserving useful information in the environment/cave history not recorded by the foraminifera. Anecdotal evidence suggests, however, that ostracods are responding to environmental variables in the phreatic cave similarly to foraminifera. The most important outcome of Part I was that the investigated proxies are responding to predictable environmental gradients in underwater caves. This outcome provided considerable confidence for moving forward with the project.

7.2 Part II: Sea-Level Signatures In Phreatic Coastal Caves

After developing proxies in Part I to reliably distinguish underwater cave environments, the next goal of this dissertation was to examine if sea-level histories are preserved in underwater cave sediments. Prior to this dissertation, glacioeustatic sea-level change had been hypothesized as forcing environmental development in underwater caves, but such a relationship had never been substantiated with convincing physical evidence. I expanded on this hypothesis by proposing that underwater caves to transition through vadose, littoral, anchialine, and submarine environmental conditions during sea-level rise. Therefore, the following research question guided Chapter 3: *Do successions in underwater cave systems track sea-level rise?*

After constraining 12 cores distributed in Green Bay Cave (GBC) with 20 radiocarbon dates, it became apparent that we recovered the first complete succession from an underwater cave spanning the Holocene. After a detailed sedimentological examination, all the different sedimentary units in the successions could be organized into four facies (vadose, littoral, anchialine, and submarine). These four facies were correlated to specific environmental conditions in GBC, and the timing of facies changes could be related to Holocene sea-level rise on the Bermudian platform. This result provides convincing support to the hypothesis that eustacy forces environmental change in underwater caves (Chapter 3). A corollary to this conclusion is that crevicular habitats and ecosystems will also have a concomitant response to sea-level change (rise or fall). As such, could decreased habitat availability during sea-level regressions have promoted allopatric speciation events due to habitat segregation in the subterranean realm? Such hypotheses that examine the linkages between sea-level change with biospeleological

evolution warrant further attention, especially considering that the present highstand conditions are not representative of dominant position of eustatic sea level throughout the Quaternary.

In the opinion of this author, the most important scientific advance from Chapter 3 is the conceptual model that links environmental change in all caves and sinkholes to eustacy (Fig. 3.10). More broadly, all caves and sinkholes (both vadose and phreatic) can be unified under the term speleogenetic karst basins, which describes any cave or sinkhole derived from speleogenetic processes in karst terrain that provides sea-level independent accommodation space for sediments and habitats. At the time of writing, any speleogenetic karst basin in the literature, or anecdotally, can be located within this model. Previous sedimentologic results from other speleogenetic karst basins have had very little means of comparison to other karst basins, with the exception of vadose cave environments (e.g., Woodward and Goldberg, 2001). This model now links all karst sedimentary facies within a framework of their environment of deposition, and can be used to describe the relationships between all speleogenetic karst basins. However, given that Fig. 3.10 is a model, future work in Caribbean, Mediterranean and Pacific karst basins needs to further test its utility. We anticipate that as our understanding of environments in karst basins becomes refined, the conceptual model in Figure 3.10 will also become refined.

An important caveat of the conceptual model it is most directly applied in the coastal zone at this point, where most of the present research has been focused. Conceptually, all inland caves can equally be unified under a vadose facies, which is envisaged at the present time. In such an inland vadose facies, previously described sedimentary units can be easily organized (Fluvial-based, lacustrine-based or pedogenic-

based lithofacies: Woodward and Goldberg, 2001; Bosch and White, 2007; White 2007). However, these ideas need further research, especially on inland telogenetic karst. Despite this caveat, this work is clearly a step towards developing a broader theory unifying sedimentation in caves within their environment of deposition, which has arguably been unsatisfactory until now when considering karst sedimentation throughout the vadose to phreatic continuum.

For Quaternary research, an important contribution from Part II is that sea-level index points can be derived from the littoral facies. Two specific case studies were presented, one from the Holocene and one from Marine Isotope Stage 11, which illustrate this point (Chapters 4 and 5). The problem for sea-level research in Bermuda is that basal brackish peat is scarce, or altogether unavailable, prior to 6.5 ka. Therefore, researchers have relied on relative sea-level index points (basal freshwater peat) for constructing a local Holocene sea-level curve. New sea-level index points can now be obtained from karst platforms by investigating and dating a littoral facies in karst basins (e.g., calcite rafts and mud, coastal sands; Mangrove peat in sinkholes: Gabriel et al., 2009).

An unaddressed problem in this dissertation is the Fe-oxide at the base of the strata in Green Bay Cave. This is not the only cave observed with Fe-oxide sediments in Bermuda: similar sediments are found at the modern sediment-water interface in Deep Blue Cavern! Furthermore, Fe-stained sediments occur in Mexican, Floridian, and Mallorcan underwater caves. Preliminary work on the Bermudian Fe-stained sediments suggests that anoxic, Fe-saturated groundwater is currently upwelling in Deep Blue Cavern, causing Fe-oxide to precipitate when the anoxic groundwater reaches the oxygenated cave (van Hengstum and Charette, unpublished data). However, this process is not currently occurring in GBC. This initial result only poses further questions. Why do

iron oxides precipitate in specific places? Does anoxic saline groundwater only upwell in specific places? Why does it change spatial location through time (e.g., currently in Deep Blue, not currently in GBC)? Do these sediments have any relation to the position of sea-level, similar to modern 'iron curtains' in clastic coastlines (e.g., Charette and Sholkovitz, 2002). Does upwelling dissolved iron in karst platforms impact coastal oceans? If upwelling saline groundwater is anoxic, what modern cave organisms live – or cant live – in Bermuda's anoxic crevicular habitats? This last question has especially important implications when considering the vertical migration of aquatic ecosystems during sea-level regressions. Further research is needed to examine Fe and Mn cycling in the Bermudian aquatic caves to fully appreciated these relationships.

A final implication of Chapter three is that factual paleohydrogeological data can now be obtained using microfossil proxies. For example, based on foraminiferal paleoecology, Green Bay Cave (GBC) was brackish for 4000 years from ~5.6 to 1.6 ka (Fig. 3.7). In short, the modern marine cave ecosystem in GBC has only been there for the last 1600 years! So, where were the fauna forming the modern submarine ecosystem prior to 1.6 ka? Considering the endemic cave ostracod *Paranesidea sterreri* and the oligotrophic foraminiferan *Spirophthalmidium emaciatum* were present in GBC prior to it becoming brackish, this indicates that cave fauna have remarkable rates of emigration and migration through the crevicular habitats in Bermuda. This is maybe not surprising, because although GBC may have been brackish until 1.6 ka, Walsingham cave was certainly marine, indicating salinity in subterranean cave habitats can be variable across a karst platform at the same time. However, this does not rule out the possibility that coastal circulation on the Bermudian platform (e.g., Morris et al., 1977) over short distances (<10 km) may be contributing to the migration of crevicular organisms between

suitable subterranean habitats. It is now apparent from the work in Part II that hydrogeology in karst basins and habitats is intimately related to the position of eustatic sea, relationships that will have inevitable feedbacks on the biology in crevicular habitats. Lastly, numerical modeling is often used to derive paleohydrogeological information on karst platforms. Coring studies of underwater cave sediments, where possible, now provide a method to ground truth paleohydrogeological data derived from numerical modeling.

7.3 Part III: Climate Signatures In Phreatic Coastal Caves

Considering Part II established how speleogenetic karst basins evolve in response to sea-level forcing, the last objective of this dissertation was to obtain a climate record from the underwater caves of Bermuda. Recent work in Japan indicates that climate records can be obtained from submarine cave environments once they are circulated with the ocean (e.g., Yamamoto et al., 2010), suggesting that similar paleoclimate records may also be present in Bermuda. The following research question guided the research in Chapter 6: *Does cave foraminiferal $\delta^{18}O_c$ and sedimentology document late Holocene Climate change on Bermuda?*

To answer this question, Walsingham Cave was chosen as the study site because it did not have a physical 'karst window' exiting at the ocean like Green Bay Cave. Sea cucumbers are found inside Green Bay Cave, especially in The Desert (see Fig. 2.2), which may be bioturbating any climate records there. Sea cucumbers are not found in Walsingham Cave. However, it remained a priority to demonstrate that Walsingham Cave actually experiences seasonal thermal variability. Iliffe et al. (1983) hypothesized that Bermudian caves were thermally isolated from the ocean, possibly throughout the

Pleistocene, so it was argued by other scientists that climate records would not be present in Bermuda's Caves. To test the hypothesis that Walsingham Cave ***is*** circulated with the ocean, a temperature monitoring program was launched in 2010. The results conclusively indicate that the temperature of saline groundwater in Walsingham Cave is seasonally variable, controlled by tidally forced saline groundwater circulation (Fig. 6.3). To our knowledge, this type of groundwater circulation has only been previously measured in the Yucatan (Beddows et al., 2005, 2007). Therefore, if Walsingham Cave is circulated with the ocean, then paleoclimate records could be preserved in the cave sediments.

The results of the paleoclimate investigation confirm the hypothesis that underwater cave sediments can preserve regional paleoceanographic records, which can be directly linked to paleoclimate changes (Chapter 6). Bermuda has two dominant sources of heat: solar radiation and heat transported by the Gulf Stream. Therefore, any changes to these factors can be expected to cause a concomitant change in Bermudian climate. Based on a centennial-scale reconstruction of Gulf Stream transport over the last 1000 years, Lund et al. (2006) documented a decrease in transport at 0.9 ka, that corresponds to a global cooling trend (Mann et al., 2008). A similar cooling trend was observed in Walsingham Cave, which peaked at the onset of the Little Ice Age at 0.6 ka. Therefore, if changes in surface ocean currents (i.e., Gulf Stream) can be preserved in the sediments of Walsingham Cave, can changes in the Caribbean current be preserved in the underwater caves of Cozumel (Mexico)? Future research should specifically investigate if high-resolution paleoceanographic records of surface ocean currents are routinely preserved in underwater caves, and the subsequent impact on Holocene paleoclimate changes. The paleoclimate results herein have enormous potential beyond Bermuda. Caves are ubiquitous throughout the Caribbean, which may provide a whole new class of

marine paleoclimate records that are currently untapped, and based on the results from Bermuda, possibly with decadal to sub-decadal resolution. A limitation is that the cave must be circulated with the ocean, as some underwater caves are more isolated than others (e.g., Novosel et al., 2007). However, this property can easily be tested with a saline groundwater thermal monitoring program (Novosel et al., 2007; Yamamoto et al., 2010; this study).

After completing the paleoclimate reconstruction, questions still surround the utility of miliolids for paleoclimate isotope work. At this stage, the isotopic results from miliolids can only be interpreted as systematically offset from isotopic equilibrium without better constraint on their modern stable isotope geochemistry. Therefore, either more work is needed to constrain miliolids as an isotopic proxy, or another biogenic carbonate microfossil (e.g., bivalves, ostracods) should be explored for paleothermometry in their stead. The most significant result of Part III, however, remains that continuous records of paleoclimate exist in Bermuda's phreatic caves, which warrant further research.

The conclusion that saline groundwater flooding Walsingham Cave experiences seasonal thermal variation similar to coastal waters and Sargasso Sea is also significant to regional cave biology (or biospeleology). Previously, it was hypothesized that Bermuda's phreatic caves do not experience annual thermal variation, but remain constant at ~20.5ºC all year round (Iliffe et al., 1983). Based on this hypothesis, it has been suggested that temperature in Bermudian underwater caves has remained constant, or only up to ~2ºC cooler, during the Pleistocene glacial periods (Iliffe et al., 1983; Manning et al., 1986), when eustatic sea level was ~120 m below present (Siddall et al., 2003) and tropical ocean temperatures may have been up to 8ºC cooler than present (e.g., deMenocal et al.,

2000). This is evidenced as critical support to the hypothesis that Bermuda's caves have been a refugia throughout Quaternary glacial and interglacial cycles, and that many organisms may be directly derived from ancient lineages, possibly of Mesozoic age (e.g., Manning et al., 1986).

We argue, based on the modern data temperature data collected from Walsingham Cave, that Bermuda's crevicular habitats in the eolianite have remained in direct communication with the ocean anytime they were flooded by eustatic sea-level rise (e.g., Marine Isotope Stages 5, 7, 11) This means that any changes in ocean temperature is directly translated into the crevicular habitats due to saline groundwater circulation (Whitaker and Smart, 1990; Moore et al., 1992; Beddows et al., 2007). It is certain that there will be some regional temperature variability in Bermuda between different caves because the degree of communication between the ocean and different lithologies may be variable (contrast: Green Bay Cave with Deep Blue Cavern). But it should not be assumed that any caves in Bermuda have remained isolated from the ocean during recent times, or throughout the Pleistocene. A primary implication of this result is that underwater cave habitats will not be immune to oceanic or climate changes due to anthropogenic forcing. Evidence from an Italian Phreatic cave has already documented ecosystem degradation in an underwater cave from sudden climate-forced changes to ocean temperature (Parravicini et al., 2010).

7.4 Final Remarks

Unfortunately, this dissertation has only contributed a small amount of science, which has generated more questions than answers. However, it does represent a good advance for sediment-based research in speleogenetic karst basins. There is still much to

be learned about the physical marine geological processes operating in underwater caves, but after the results presented here, it is apparent that this new avenue of cave and karst science will provide fruitful contributions to our understanding of global change in the Quaternary.

References

Abu-Zied, R. H., Rohling, E. J., Jorissen, F. J., Fontainer, C., Casford, J. S. L., and Cooke, S., 2008. Benthic foraminiferal response to changes in bottom-water oxygenation and organic carbon flux in the eastern Mediterranean during LGM to recent times: Marine Micropaleontology 67, 46-68.

Acosta, J. T., 1940. *Triloculina bermudezi*, un Nuevo foraminifero de las Islas Bahamas: Memorias de la Sociedad Cubana de Histora Natural 14 (1), 37-38.

Airoldi, L., and Cinelli, F., 1996. Variability of fluxes of particulate material in a submarine cave with chemolithoautotrophic inputs of organic carbon: Marine Ecology Progress Series 139, 205-217.

Alley, W. M., 2001. Groundwater and climate. Groundwater 39 (2), 161.

Alve, E., and Goldstein, S. T., 2010. Dispersal, survival, and delayed growth of benthic foraminferal propagules: Journal of Sea Research 63, 36-51.

Alverez Zarikian, C. A., Swart, P. K., Gifford, J. A., and Blackwelder, P. L., 2005. Holocene paleohydrology of Little Salt Spring, Florida, based on ostracod assemblages and stable isotopes: Palaeogeography, Palaeoclimatology, Palaeoecology 225, 134-156.

Anderson, D. L. T., and Corry, R. A., 1985. Seasonal transport variations in the Florida Straits: model study: Journal of Physical Oceanography 15, 773-786.

Anderson, H. V., 1953. Two new species of *Haplophragmoides* from the Louisiana Coast: Contributions from the Cushman Foundation for Foraminiferal Research 4 (1), 21-22.

Angell, R. A., 1980. Test morphogenesis (chamber formation) in the foraminifera *Spiroloculina hyaline* schulze: Journal of Foraminiferal Research 10 (2), 89-101.

Ashmore, S., and Leatherman, S. P., 1984. Holocene sedimentation in Port Royal Bay, Bermuda: Marine Geology 56, 289-298.

Bailey, J. W., 1851. Microscopical examination of soundings made by the United States Coast Survey off the Atlantic Coast of the United States: Smithsonian Contributions to Knowledge 2 (3), 1-15.

Baldini, J. U. L., 2010. The geochemistry of cave calcite deposits as a record of past climate: The Sedimentary Record 8 (2): 4-9.

Balkwill, F. P., and Wright, J., 1885. Report on some recent foraminifera found off the coast of Dublin and in the Irish Sea: Transactions of the Royal Irish Academic Society 28 (18), 317-368.

Bard, E., Hamelin, B., Arnold, M., Montaggioni, L., Cabioch, G., Faure, G., and Rougerie, F., 1996. Deglacial sea-level record from Tahiti corals and the timing of global meltwater discharge: Nature 382, 241-244.

Barker, R. W., 1960. Taxonomic notes on the species figured by H. B. Brady in his report on the foraminifera dredged by H. M. S. Challenger during the years 1873-1876: Society of Economical Petrology and Mineralogy, Special Publication No. 29, 238 p.

Beddows, P. A., Smart, P. L., Whitaker, F. F., and Smith, S. L., 2005. Density stratified groundwater circulation on the Caribbean coast of Yucatan Peninsula, Mexico. *In:* Martin, J. B., Wicks, C. M., Sasowsky, I. D., (eds.), Karst Waters Institute Special Publication 7: Hydrogeology and Biology of Post-Paleozoic Carbonate Aquifers, 129-134.

Beddows, P. A., Smart, P. L., Whitaker, F. F., and Smith, S., 2007. Decoupled fresh-saline groundwater circulation of a coastal carbonate aquifer: spatial patterns of temperature and specific conductivity: Journal of Hydrology 346, 18-32.

Behre, K. E., 2007. A new Holocene sea-level curve for the southern North Sea: Boreas 36, 82-102.

Beierle, B. D., Lamoureux S. F., Cockburn, J. M. H., and Spooner, I., 2002. A new method for visualizing sediment particle size distribution: Journal of Paleolimnology 27, 279-283.

Bemis, B. E., Spero, H. J., Bijima, J., and Lea, D. W., 1998. Reevaluation of the oxygen isotopic composition of planktonic foraminifera: experimental results and revised paleotemperature equation. Paleoceanography 13 (2), 150-160.

Bermúdez, P. J., 1935. Foraminíferos de la costa norte de Cuba: Memorias de la Sociedad Cubana de Historia Natural 9 (3), 129-224.

Bernhard, J. M., 1988. Postmortem vital staining in benthic foraminifera: duration and importance in population and distributional studies: Journal of Foraminiferal Research 18 (2), 143-146.

Bernhard, J. M., and Sen Gupta, B. K., 1997. Foraminifera of oxygen-depleted environments. *In:* Sen Gupta, B. K. (ed.) Modern Foraminifera: Kluwer Academic Press 201-216.

Bernhard, J. M., Sen Gupta, B. K., Borne, P. F., 1997. Benthic foraminiferal proxy to estimate dysoxic bottom-water oxygen concentrations: Santa Barbara Basin, U.S. Pacific continental margin: Journal of Foraminiferal Research 27 (4), 301-310.

Bernhard, J. M., Ostermann, D. R., Williams, D. S., and Blanks, J. K., 2006. Comparison of two methods to identify live benthic foraminifera: a test between rose Bengal and

Celltracker Green with implications for stable isotope paleoreconstructions: Paleoceanography 21 PA4210, doi: 10.1029/2006PA001290.

Bird, M. I., Austin, W. E. N., Wurster, C. M., Fifield, L. K., Mojtahid, M., and Sargent, C., 2010. Punctuated eustatic sea-level rise in the early mid-Holocene: Geology 38 (9), 803-806.

Bird, M. I., Fifield, L. K., Chang, C. H., Teh, T. S., and Lambeck, K., 2007. An inflection in the rate of early mid-Holocene sea-level rise: a new sea-level curve for Singapore: Eustarine, Coastal and Shelf Science 71, 253-536.

Birnstein, J. A., and Ljovuschkin, S. I., 1965. Fauna of the brackish underground waters of Central Asia: International Journal of Speleology 1 (3), 307-320.

Blanchon, P., and Shaw, J., 1995. Reef drowning during the last deglaciation: Evidence for catastrophic sea-level rise and ice-sheet collapse Geology 23 (1), 4-8.

Blanchon, P., Jones, B., and Ford, D., 2002. Discovery of a submerged relic reef and shoreline off Grand Cayman; further support for an early Holocene jump in sea level: Sedimentary Geology 147, 253-270.

Bock, W. D., Lynts, G. W., Smith, S., Wright, R., Hay, W. W., and Jones, J. I., 1971. A symposium of recent south Florida Foraminifera: Miami Geologic Society Memoir No. 1, 245 p.

Bond, G., Showers, W., Cheseby, M., Lotti, R., Almasi, P., deMenocal, P., Priore, P., Cullen, H., Hajdas, I., and Bonani, G., 1997. A pervasive Millennial-scale cylce in North Atlantic Holocene and Glacial Climates: Science 278, 1257-1266.

Bond, G., Kromer, B., Beer, J., Muscheler, R., Evans, M.N., Showers, W., Hoffmann, S., Lotti-Bond, R., Hajdas, I., and Bonani, I, 2001. Persistent solar influence on the North Atlantic climate during the Holocene: Science 294 (2130), 2130-2136.

Bornemann, J. G., 1855, Die mikroskopische fauna des septarienthones von Hermsdorf bei Berlin: Deutsche Geology Ges Zeitschrift 7 (2), 307-371.

Bosch, R. F., and White, W. B., 2007. Lithofacies and transport of clastic sediments in karstic aquifers. I*n:* Sasowsky, I. D., Mylroie, J. (eds.), Studies of Cave Sediments: Physical and Chemical Records of Paleoclimate, Springer 1-22.

Bradshaw, J. S., 1961. Laboratory experiments on the ecology of foraminifera: Contributions from the Cushman Foundation for Foraminiferal Research 12 (3), 87-106.

Brady, H. B., 1870. Foraminifera. *in:* Brady, G.S., Robertson D., Brady, H.B., (eds.) The Ostracoda and Foraminifera of Tidal Rivers: Annals and Magazine of Natural History-Series 4, 6, 273–306.

Brady, H. B., 1879a. Notes on some of the reticularian rhizopoda of the Challenger Expedition, Part 1, on new or little known arenaceous types: Quarterly Journal of the Micropaleontology Society 19, 20-63.

Brady, H. B., 1879b. Notes on some of the reticularian rhizopoda of the Challenger Expedition, Part 2, Additions to the knowledge of porcellaneous and hyaline types: Quarterly Journal of the Micropaleontology Society 19, 261-299.

Brady, H. B., 1881. Notes on some of the reticularian Rhizopoda of the "Challenger" Expedition, Part 3: Quaternary Journal of the Micropaleontological Society 21, 31-71.

Brady, H. B., 1884, Report on the foraminifera dredged by H.M.S. Challenger during the years 1873-1876. *in:* Reports on the Scientific Results of the Voyage of the H.M.S. Challenger during the years 1873-1876: Zoology, 9, 814 p.

Brady, H. B., Parker, W. K., and Jones, T. R., 1888. On some foraminifera from the Abroholos Bank: Transactions of the Zoological Society of London, 12 (part 7), no. 1, 211-239.

Bretsky, S. S., 1967. Environmental factors influencing the distribution of *Barbatia domingensis* (mollusca, bivalvia) on the Bermuda Platform: Postilla 108, 1-14.

Bretz, J. H., 1960. Bermuda: a partially downed, late mature, Pleistocene Karst: Geological Society of America Bulletin, 71, 1729-1754.

Buzas, M. A., 1968. On spatial distributions of foraminifera: Cushman foundation for Foraminiferal Research, 12, 87-106.

Buzas, M. A., Smith, R. K., and Beem, K. A., 1977. Ecology and Systematics of foraminifera in two *Thalassia* habitats, Jamaica, West Indies: Smithsonian Contributions to Paleobiology No. 31, 122 p.

Cairns, S.D., 2000. A revision of the shallow-water Azooxanthellate scleractinia of the western Atlantic: Studies on the Natural Historn of the Caribbean Region, 75, 1-208.

Caralp, M. H., 1989. Size and morphology of the benthic foraminifer *Melonis barleeanum*: relationships with marine organic matter: Journal of Foraminiferal Research 19 (3), 235-245.

Carlson, A. E., Clark, P. U., Raisbeck, G. M., and Brook, E. J., 2007. Rapid Holocene deglaciation of the Labrador sector of the Laurentide Ice Sheet: Journal of Climate 20, 5126-5133.

Carlson, A. E., Legrande, A. N., Oppo, D. W., Came, R. E., Schmidt, G. A., Anslow, F. S., Licciardi, J. M., and Obbink, E. A., 2008. Rapid early Holocene deglaciation of the Laurentide Ice Sheet: Nature Geosciences 1, 620-623.

Cate, J. R., 2009. Assessing the impact of groundwater pollution from marine caves on nearshore seagrass beds in Bermuda. MSc Thesis, Texas A&M University, 101 p.

Chapman, F., 1900. On some new and interesting foraminifera from the Funafuti Atoll, Ellice Islands: Journal of the Linnaean Society (Zoology) 28, 1-27.

Chapman, F., 1901. Foraminifera from the lagoon at Funafuti: Journal of the Linnaean Society (Zoology) 28, 161-210.

Chapman, F., Parr, W. F., and Collins, A. C., 1934. Tertiary foraminifera of Victoria, Australia – the Bacombian deposits of Port Philip: Part 3: Journal of the Linnaean Society (Zoology) 38 (262), p. 553-577.

Charette, M.A., and Sholkovitz, E.R. 2002. Oxidative precipitation of groundwater-derived ferrous iron in the subterranean estuary of a coastal bay: Geophysical Research Letters 29 (10), 144, doi:10/1029/2001GL014512.

Chaster, G. W., 1892. Report upon foraminifera of the Southport Society of Natural Science District: First Report Southport Society of Natural Science (1890-1891). Southport, England, 54-72.

Choi, D. R., and Ginsburg, R. N., 1983. Distribution of coelobites (cavity-dwellers) in coral rubble across the Florida reef Tract: Coral Reefs 2(3):165-172.

Cimerman, F., and Langer, M. R., 1991. Mediterranean Foraminifera: Slovenska Akademija Znanosti in Umetnosti, Ljubljana, 118 p.

Clarke, M. L., Rendell, H. M., 2009. The impact of North Atlantic storminess on western European coasts: a review. Quaternary International 195, 31-41.

Collins, A. C., 1958, Foraminifera. Great Barrier Reef expedition 1928-1929: Scientific Reports, British Museum of Natural History 6, 335-437.

Corliss, B. H., 1991, Morphology and microhabitat preferences of benthic foraminifera from the northwest Atlantic Ocean: Marine Micropaleontology17: 195-236.

Corriero, G., Liaci, L. S., Ruggiero, D., and Pansini, M. 2001. The sponge community of a semi-submerged Mediterranean Cave: Marine Ecology 21 (1), 85-96.

Cottey, T. L., and Hallock, P., 1988. Test surface degradation in *Archaias angulatus*: Journal of Foraminiferal Research 18 (3), 187-202.

Courty, M. A., and Vallverdu, J., 2001. The microstratigraphic record of abrupt climate changes in cave sediments of the Western Mediterreanean: Geoarchaeology 16(5), 467-499.

Craig, H., 1957. Isotopic standards for carbon and oxygen and correction factors for mass-spectrometric analysis of carbon dioxide. Geochimica et Cosmochimica Acta 12, 133–149.

Cronin, T. M., Dwyer, G. S., Kamiya, T., Schwede, S., Willard, D. A., 2003. Medieval Warm Period, Little Ice Age and the 20th century temperature variability from Chesapeake Bay. Global Planetary Change 36, 17-29.

Cronin, T. M., Hayo, K., Thunell, R. C., Dwyer, G. S., Saenger, C., Willard, D. A., 2010. The medieval climate anomaly and little ice age in the Chesapeake Bay and the North Atlantic Ocean: Palaeogeography, Palaeoclimatology, Palaeoecology 297, 299-310.

Cronin, T. M., Thunell, R., Dwyer, G. S., Saenger, C., Mann, M. E., Vann, C., Seal, R. R. II, 2005. Multiproxy evidence of Holocene climate variability from estuarine sediments, eastern North America. Paleoceanography vol. 20, PA4006, doi: 10.1029/2005PA001145.

Crowley, T. J., 2000. Causes of climate change over the last 1000 years. Science 289, 270-277.

Cushman, J. A., 1910. A monograph of the foraminifera of the North Pacific Ocean – Part I: *Astrorhizidae* and *Lituolidae*: United States National Museum Bulletin 71 (1), 1-108.

Cushman, J. A., 1919. Fossil foraminifera from the West Indies. *in:* Vaughan, T.W., 1919. Contributions to the geology and paleontology of the West Indies: Carnegie Institute of Washington Publications 291, 42 p.

Cushman, J. A., 1920. The Foraminifera of the Atlantic Ocean – Part 2: *Lituolidae*: United States National Museum Bulletin 104, 111 p.

Cushman, J. A., 1921a. Foraminifera from the north coast of Jamaica: Proceedings of the United States National Museum 59, 47-82.

Cushman, J. A., 1921b. Foraminifera of the Philippine and adjacent seas: United States National Museum Bulletin 100 (4), 608 p.

Cushman, J. A., 1922. Shallow-water foraminifera of the Tortugas region: Publications of the Carnegie Institution Washington, No. 311, Department of Marine Biology Papers 17, 85 p.

Cushman, J. A., 1923. The foraminifera of the Atlantic Ocean – Part 4: *Lagenidae*: United States National Museum Bulletin 104, 228 p.

Cushman, J. A., 1925. Recent foraminifera from British Columbia: Contributions from the Cushman Laboratory of Foraminiferal Research 1 (11), 38-47.

Cushman, J. A., 1926a. Recent foraminifera from Porto Rico: Publications of the Carnegie Institution of Washington 342, 73-84**.**

Cushman, J. A., 1926b. Foraminifera of the genera *Siphongenerina* and *Pavonina*: Proceedings of the United States National Museum 67 (25), 24 p.

Cushman, J. A., 1927. An outline of a re-classification of the foraminifera: Contributions from the Cushman Laboratory for Foraminiferal Research 3 (39), 77 p.

Cushman, J. A., 1928. Foraminifera their classification and economic use: Special Publications of the Cushman Laboratory for Foraminiferal Research No. 1, 401 p.

Cushman, J. A., 1929. The foraminifera of the Atlantic Ocean – Part 6: *Miliolidae*, *Opthalmidiidae*, and *Fischerinidae*: United States National Museum Bulletin 104, 101 p.

Cushman, J. A., 1930. The foraminifera of the Atlantic Ocean - Part 7: *Nonionidae*, *Camerinidae*, *Peneroplidae* and *Alveolinellidae*: United States National Museum Bulletin 104, 79 p.

Cushman, J. A., 1933a. Some new recent foraminifera from the tropical Pacific: Contributions from the Cushman Laboratory of Foraminiferal Research 9, 77-95.

Cushman, J. A., 1933b. New Arctic foraminifera collected by Captain R.A. Bartlett from Fox Basin and off the northeast coast of Greenland: Miscellaneous Collections from the Smithsonian Institution 89 (9), 1-8.

Cushman, J. A., 1933c. Some new foraminiferal genera: Contributions from the Cushman Laboratory of Foraminiferal Research 9, 77-95.

Cushman, J. A., 1935. Fourteen new species of foraminifera: Smithsonian Institution Miscellaneous Collections 91 (21), 1-9.

Cushman, J. A., 1944a. The genus *Articulina* and its species: Cushman Laboratory of Foraminiferal Research Special Publication 10, 24 p.

Cushman, J.A., 1944b. Foraminifera from the shallow water of the New England coast: Cushman Laboratory for Foraminiferal Research Special Publication 12, 37 p.

Cushman, J. A., 1947. New species and varieties of foraminifera from off the southeastern coast of the United States: Contributions from the Cushman Laboratory of Foraminiferal Research 23, 86-92.

Cushman, J. A., and Cahill, M. S., 1932. The Foraminifera of the upper, middle, and part of the lower Miocene of Florida: *In* Cushman, J. A., Ponton, G. M., (eds.) Florida State Geologic Survey Bulletin No. 9, 147 p.

Cushman, J. A., and Gray, H. B., 1946. A foraminiferal fauna fro the Pliocene of Timms Point, California: Cushman Laboratory for Foraminiferal Research Special Publication No. 9, 46 p.

Cushman, J. A., and Grant, U. S., 1927. Late Tertiary and Quaternary Elphidiums of the West Coast of North America: Transactions of the San Diego Society of Natural History 5, 69-82.

Cushman, J. A., and Wickenden, R.T.D., 1929. Recent foraminifera from off Juan Fernandez Islands: Proceedings of the United States National Museum 2780 (85), no. 75, 1-16.

Cushman, J. A., and McCulloch, I., 1939. Report on some arenaceous foraminifera. Allan Hancock Pacific Expeditions: The University of Southern California Press, Los Angeles, California 6 (1), 113 p.

Czjzek, J., 1848. Beitrag zur Kenntniss der fossilen foraminiferen des Wiener Beckens: Naturwissenschaftliche Abhandlungen 2 (1), 137-150.

Daniels, C. H. von, 1970. Quantitative ökologische analyse der zeitlichen und räumlichen verteilung rezenter foraminiferen im Limski Kanal bei Rovinj (nördl. Adria):

Göttinger Arbeiten zur Geologie und Pälaontologie 8, 1-109.

Debenay J. P., Eichler, B. B., Duleba, W., Bonetti, C., and Eichler-Coelho, P., 1998. Water stratification in coastal lagoons: its influence on foraminiferal assemblages in two Brazilian lagoons: Marine Micropaleontology 35, 67-89.

Debenay J. P., Tsakiridis, W., Soulard, R., and Grossel, H., 2001. Factors determining the distribution of foraminiferal assemblages in Port Joinville Harbor (Iled'Yeu, France): the influence of pollution: Marine Micropaleontology 43, 75-118.

Debenay J. P., and Guillou, J. J., 2002. Ecological transitions indicated by foraminiferal assemblages in paralic environment: Estuaries 25 (6A), 1107-1120.

De Goeij, J. M., and Van Duyl, F. C., 2007. Coral cavities are sinks of dissolved organic carbon: Limnology and Oceanography 52 (6), 2608-2617.

deMenocal, P., Ortiz, J., Guilderson, T., and Sarnthein, M., 2000, Coherent high- and low-latitude climate variability dring the Holocene Warm Period: Science 288, 2198-2202.

Denitto, F., Terlizzi, A., and Belmonte, G., 2007. Settlement and primary succession in a shallow submarine cave: spatial and temporal benthic assemblage distinctness: Marine Ecology 28 (S1), 35-46.

Denton, G. H., Karlén, W., 1973. Holocene climatic variations—their pattern and possible cause. Quaternary Research 3 (2), 155-174.

De Rijk, S., Jorissen, F. J., Rohling, E. J., and Troelstra S. R., 2000. Organic flux control on bathymetric zonation of Mediterranean benthic foraminifera: Marine Micropaleontology 40, 151-166.

De Waele, J., Brook, G. A., Oertel, A., 2009. Monk seal (*Monachus monachus*) bones in Bel Torrente Cave (Central-east Sardinia) and their paleogeographical significance. Journal of Cave and Karst Studies, v. 71, no. 1, p. 16-23.

DiNezio, P. N., Gramer, L. J., Johns, W. E., Meinen, C. S., and Baringer, M. O., 2009. Observed interannual variability of the Florida Current: wind forcing and the North Atlantic Oscillation: Journal of Physical Oceanography 39, 721-736.

Diz, P., and Francés, G., 2008. Distribution of live benthic foraminifera in the Ría de Vigo (NW Spain): Marine Micropaleontology 66, 165-191.

Donato, S. V., Reinhardt, E. G., Boyce, J. I., Pilarczyk, J. E., and Jupp, B. P., 2009. Particle-size distribution of inferred tsunami deposits in Sur Lagoon, Sultanate of Oman: Marine Geology 257 (1-4), 54-64.

Donato, S. V., Reinhardt, E. G., Boyce, J. I., Rothaus, R., and Vosmer, T., 2008. Identifying tsunami deposits using bivalve shell taphonomy: Geology 36 (3), 199-202.

Donnelly, J. P., and Woodruff, J. D., 2007. Intense hurrican activity over the past 5,000 years controlled by El Niño and the West African Monsoon: Nature 447, 465-468.

Dorale, J. A., Onac, B. P., Fornós, J. J., Ginés, J., Ginés, A., Tuccimei, P., and Peate, D. W., 2010. Sea-level highstand 81,000 years ago in Mallorca: Science 327, 860-863.

d'Orbigny, A., 1826. Tableau méthodique de la classes des Céphalopodes: Annales des Sciences Naturelles 7, 245-314.

d'Orbigny, A., 1839a. Foraminifères: *In* de la Sagra, R. (ed.) Histoire physique et naturelle de I'lle de Cuba. A. Bertrand, Paris 8, 1-224.

d'Orbigny, A., 1839b. Voyage dans l'Amérique Méridionale, Foraminifèrs: Strasbourg, France, Levrault 5 (5), 1-86.

d'Orbigny, A., 1840. Mollusques, échinodermes, foraminifèrs et polypiers, recueillis aux Îles Canaries: *in* Histoire Naturelle des Îles Canaries (eds.) Webb, P., Berthelot, S. Paris, France 152 p.

d'Orbigny, A., 1846. Foraminifères fossiles du basin tertiaire de Vienne (Autriche), Paris: Gide et Comp 298 p.

Draschba, S., Pätzold, J., and Wefer, G., 2000. North Atlantic climate variability since AD 1350 recorded in $\delta^{18}O$ and skeletal density of Bermuda corals: International Journal of Earth Sciences 88, 733-741.

Druffel, E. R. M., 1997. Pulses of rapid ventilation in the North Atlantic surface ocean during the past century: Science 275, 1454-1457.

Dutton, A., Bard, E., Antonioli, F., Esat, T. M., Lambeck, K., and McCulloch, M. T., 2009. Phasing and amplitude of sea-level and climate change during the penultimate interglacial: Nature Geoscience 2, 355-359.

Duplessy, J. C., Lalou, C., and Vinot, A. C., 1970. Differential isotopic fractionation in benthic foraminifera and paleotemperatures reassessed: Science 168 (3928), 250-251.

Earland, A., 1933. Foraminifera: Part II – South Georgia. Discovery Reports: Cambridge University Press, England 7, 27-138.

Earland, A., 1934. Foraminifera: Part III – The Falkland sector of the Antarctic (excluding south Georgia): Discovery Reports, Cambridge University Press, England 10, 1-208.

Egger, J. G., 1893. Foraminiferen aus Meeresgrundproben, gelothet von 1874 bis 1876 von S. M. Sc. Gazelle: Abhandlungen der Bayerischen Akademie der Wissenschaften, Müchen Math-Phys 18, 193-458.

Ehrenberg, C. G., 1843. Verbreitung und Einfluss des mikroskopischen Lebens in Sud- und Nord-Amerika: Physik Abhandlungen der Königlichen Akademie der Wissenschaften zu Berlin 1, 296-446.

Eichler, P. P. B., Eichler, B. B., De Miranda, L. B., Pereira, E. R. M., Kfouri, P. B. P., Pimenta, F. M., Bérgama, A. L., and Vilela, C. G., 2003. Benthif foraminiferal response to variations in temperature, salinity, dissolved oxygen, and organic carbon in the Guanabara Bay, Rio de Janeiro, Brazil: Anuário do Instituto de Geosciências 26, 36-51.

Einsiedl, F., Radke, M., and Maloszewski, P., 2010. Occurrence and transport of pharmaceuticals in a karst groundwater system affected by domestic wastewater treatment plants: Journal of Contaminant Hydrology 117 (1-4), 26-36.

Ellison, J. C., 1993. Mangrove retreat with rising sea level, Bermuda: Estuarine, Coastal, and Shelf Science 37, 75-87.

Ellison, J. C., 1996. Pollen evidence of late Holocene mangrove development in Bermuda: Global Ecology and Biogeography Letters 5, 315-326.

Emiliani, C., 1955. Pleistocene temperatures. Journal of Geology 63, 538-578.

Enos, P., and Sawatsky, L. H., 1981. Pore networks in Holocene carbonate sediments: Journal of Sedimentary Petrology 51, 961-985.

Epstein, S., Buchsbaum, R., Lowenstam, H. A., and Urey, H. C., 1953. Revised carbonate water isotopic temperature scale. Geological Society of America Bulletin 64, 1315-1325.

Erez, J., and Luz, B., 1983. Experimental paleotemperature equation for planktonic foraminifera. Geochimica Cosmochimica Acta 47, 1025-1031.

Eshel, G., Levy, G. J., Mingelgrin, U., and Singer, M. J., 2004. Critical evaluation of the use of laser diffraction for particle-size distributions analysis: Soil Science Society of America Journal 68, 736-743.

Fatela, F., and Taborda, R., 2002. Confidence limits of species proportions in microfossil assemblages: Marine Micropaleontology 45, 169-174.

Fichtel, L., and Moll, J. P. C., 1798 (1803 reprint). Testacea microscopia, aliaque minuta ex generibus *Argonauta* et *Nautilus*, ad naturum picta et descripta (Microscopische und andere klein Schalthiere aus den geschlechtern Argonaute und Schiffer: Camesina, Vienna 124 p.

Fillipsson, H. L., Bernhard, J. M., Lincoln, S. A., and McCorkle, D. C., 2010. A culture-based calibration of benthic foraminiferal paleotemperature proxies: $\delta^{18}O$ and Mg/Ca results. Biogeosciences 7, 1335-1347.

Fishbein, E., and Patterson, R.T., 1993. Error weighted maximum likelihood (EMWL): a new statistically based method to cluster quantitative micropaleontological data: Journal of Paleontology 67, 475-486.

Fichez, R., 1990. Decrease in allochthonous organic inputs in dark submarine caves, connection with lowering in benthic community richness: Hydrobiologia 207, 61-69.

Fichez, R., 1991. Suspended particulate organic matter in a Mediterranean submarine cave: marine Biology 108, 167-174.

Florea, L. J., Vacher, H. L., Donahue, B., and Naar, D., 2007. Quaternary cave levels in peninsular Florida: Quaternary Science Reviews 26, 1344-1361.

Fontanier, C., Mackensen, A., Jorissen, F. J., Anschutz, P., Licari, L., and Griveaud, C., 2006. Stable oxygen and carbon isotopes of live benthic foraminifera from the Bay

of Biscay: Microhabitat impact and seasonal variability: Marine Micropaleontology 58, 159-183.

Ford, D. C., and Ewers, R. O., 1978, The development of limestone cave systems in the dimensions of length and depth: Canadian Journal of Earth Sciences 15, 1783-1798.

Ford, D., and Williams, P., 1989. Karst Geomorphology and Hydrology: Unwin Hyman, London 601 p.

Fornasini, C., 1900. Intornoadalcuni esemplari di foraminiferi adriatici: Memorie della R. Accademia delle Scienze dell'Istituto di Bologna. Bologna, Italia 5 (8), 364 p.

Fornós, J. J., Ginés, J., and Gràcia, F., 2009. Present-day sedimentary facies in the coastal karst caves of Mallorca island (western Mediterranean): Journal of Cave and Karst Studies 71 (1), 86-99.

Forskål, P., 1775. Descriptiones animalium. Haunias, Carsten Nieubuhr: Copenhagen 164 p.

Gabriel, J. J., Reinhardt, E. G., Peros, M. C., Davidson, D. E., van Hengstum, P. J., and Beddows, P. A., 2009. Palaeoenvironmental evolution of Cenote Aktun Ha (Carwash) on the Yucatan Peninsula, Mexico and its response to Holocene sea-level rise: Journal of Paleolimnology 42 (2), 199-213.

Garrabou, J., and Flos, J., 1995. A simple diffusion-sedimentation model to explain planktonic gradients within a NW Mediterranean submarine cave: Marine Ecology Progress Series 123, 273-280.

Garrison, L. E., 1959. Miocene foraminifera from the Temblor Formation north of Coalinga, California: Journal of Paleontology 33(4), 662-669.

Gees R. A., and Medioli, F. S., 1970. A continuous seismic survey of the Bermuda Platform, Part 1: Castle Harbour: Maritime Sediments 6, 21-25.

Geroch, S., 1960. Microfaunal assemblages from the Cretaceous and Paleogene Silesian unit in the Beskid Slaski Mountains (Silesian Carpathians). Poland Instytut Geologiczny Biulytin No. 153, 7-138.

Gilbertson, D., Bird, M., Hunt, C., McLaren, S., Pyatt, B., Rose, J., and Stephens, M., 2005. Past human activity and geomorphological change in a guano-rich tropical cave mouth: the late Quaternary succession in the Great Cave Niah, Sarawak: Asian Perspectives 44 (1), 16-41.

Ginés, A., and Ginés, J., 2007. Eogenetic karst, glacioeustatic cave pools and anchialine environments on Mallorca Island: a discussion of coastal speleogenesis: International Journal of Speleology 36 (2), 57-67.

Gischler, E., 2003. Holocene lagoonal development in the isolated carbonate platforms off Belize: Sedimentary Geology 159 (1-2), 113-132.

Goldstein, S. T., 1997. Gametogenesis and the antiquity of reproductive pattern in the foraminiferida: Journal of Foraminiferal Research 27 (4), 319-328.

Goodkin, N. F., Hughen, K. A. Curry, W. B., and Doney, S. C., 2008a. Sea Surface temperature and salinity variability at Bermuda during the end of the Little Ice Age, Paleoceanography, v. 23, PA3203.

Goodkin, N. F., Hughen, K. A., Doney, S. C., and Curry, W. B., 2008b. Increased multidecadal variability of the North Atlantic Oscillation since 1781: Nature Geoscience 1, 844-848.

Gospodarič, R., 1988. Paleoclimatic record of cave sediments from Postojna karst: Annales de la Société géologique de Belgique 111, 91-95.

Gottstein, S., Ivković, M., Ternjej, I., Jalžić, B., and Mladen, K., 2007. Environmental features and crustacean community of anchihaline hypogean waters on the Kornati

islands, Croatia: Marine Ecology 28 (supplement 1), 24-30.

Grell, K. G., 1973. Protozoology: Berlin-Heidelberg-New York, Springer-Verlag 554 p.

Grell, K. G., 1979. Cytogenetic systems and evolution in foraminifera: Journal of Foraminiferal Research 9 (1), 1-13.

Grossman, E., L., 1984. Stable isotope fractionation in live benthic foraminifera from the Southern California Borderland: Paleogeography, Paleoclimatology, Paleoecology 47, 301-327.

Grossman, E. L., 1987. Stable isotopes in modern benthic foraminifera: a study of vital effect: Journal of Foraminiferal Research 17 (1), 48-61.

Grzybowski, J., 1898. Otwornice pokladów naftonosnych okolicy Krosna. Rozprawy Akadmia Umiejetnosci w Krakowie: Wydzial Matematyczno-Przyrodniczego series 2 (33), 257-305.

Guillem, J., 2007. Tafonomía, taxonomía y ecología de los foraminíferos de la albufera de Torreblanca. PhD Thesis, Universitat de València, 523 p., www.tdx.cbuc.es.

Haake, F.W., 1971. Ultrastructures of miliolids walls: Journal of Foraminiferal Research 1 (4), 187-189.

Haig, D. W., 1988. Miliolid foraminifera from the inner neritic sand and mud facies of the Papuan Lagoon, New Guinea: Journal of Foraminiferal Research 18(3), 203-236.

Hamilton, P., Larsen, J. C., Leaman, K. D., Lee, T. N., and Waddell, E., 2005. Transport through the Straits of Florida. Journal of Physical Oceanography, 35, 308-322.

Hammer, Ø., Harper, D. A. T., and Ryan, P. D., 2001. PAST: Paleontological statistics software package for education and data analysis: Palaeontologia Electronica 4 (1), 9 p.

Hansen, B. C. S., Grimm, E. C., and Watts, W. A., 2001. Palynology of the Peace Crek

site, Polk County, Florida: GSA Bulletin 113 (6), 682-692.

Harmon, R. S., Land, L. S., Mitterer, R. M., Garett, P., Schwarcz, H. P., and Larson, G. J., 1981. Bermuda sea level during the last interglacial: Nature 289, 481-483.

Harmon, R. S., Schwarcz, H. P., Gascoyne, M., Hess, J. W., and Ford, D. C., 2007. Paleoclimate information from speleothems: the present as a guide to the past: *In* Sasowsky, I. D., Mylroie, J., (eds.) Studies of Cave Sediments. Springer, pp. 199-226.

Hawkes, A. D., Bird, M., Cowie, S., Grundy-Warr, C., Horton, B. P., Hwai, A. T. S., Law, L., Macgregor, C., Nott, J., Ong, J. E., Rigg, J., Robinson, R., Tan-Mullins, M., Sa, T. T., Yasin, Z., and Aik, L.W., 2007. Sediments deposited by the 2004 Indian Ocean Tsunami along the Malaysia-Thailand Peninsula: Marine Geology 242, 169-190.

Haynes, J. R., 1973. Cardigan Bay rencent foraminifera: Bulletin of the British Museum (Natural History) Zoology, Supplement 4, 1-245.

Hayward, B W., and Hollis, C. J., 1994. Brackish Foraminifera in New Zealand: a taxonomic and ecologic review: Micropaleontology 40(3), 185-222.

Hayward, B W., Buzas, M. A., Buzas-Stephens, P., and Holzmann, M., 2003. The lost types of *Rotalia beccarii* var. *tepida* Cushman 1926: Journal of Foraminiferal Research 33 (4), 352-354.

Hearty, P. J., 2002. Revision of the late Pleistocene stratigraphy of Bermuda: Sedimentary Geology 153, 1-21.

Hearty, P.J., Kindler, P., Cheng, H., and Edwards, R.L., 1999. Evidence for a +20 m middle Pleistocene sea-level highstand (Bermuda and Bahamas) and partial collapse of Antarctic ice: Geology 27, 375-378.

Hearty, P.J., and Olson, S.L., 2008. Mega-highstand or mega-tsunami? Discussion of McMurtry, et al (Elevated marine deposits in Bermuda record a late Quaternary mega-tsunami - Sedimentary Geology 200, 2007:155-165): Sedimentary Geology 203 (3-4), 307-312.

Hearty, P. J., and Olson, S. L., 2010. Geochronology, biostratigraphy, and changing shell morphology in the land snail subgenus Poecilozonites during the Quaternary of Bermuda: Palaeogeography, Palaeoclimatology, Palaeoecology 293 (1-2), 9-29.

Hearty, P. J., Olson, S. L., Kaufman, D. S., Edwards, R. L., and Cheng, H., 2004. Stratigraphy and geochronology of pitfall accumulations in caves and fissures, Bermuda: Quaternary Science Reviews 23, 1151-1171.

Hegerl, G. C., Crowley, T. J., Baum, S. K., Kim, K.Y., and Hyde, W., 2002. Detection of volcanic, solar, and greenhouse gas signals in paleo-reconstructions of Northern Hemispheric temperature: Geophysical Research Letters 30 (5), 46.

Heiri, O., Lotter, A. F., and Lemcke, G., 2001. Loss on ignition as a method for estimating organic and carbonate content in sediments: reproducibility and comparability of results: Journal of Paleolimnology 25, 101-110.

Heron-Allen, R., and Earland, A., 1915. The foraminifera of the Kerimba Archipelago (Portuguese East Africa), part 2: Transactions of the Zoological Society of London 20, 543-794.

Heron-Allen, R., and Earland, A., 1922. Protozoa Part 2 – Foraminifera. Britain Antarctic ("Terra Nova") Expedition, 1910: Natural History Reports, Zoology 6 (2), 25-268.

Heron-Allen, R., and Earland, A., 1928. On the *Pegididae*, a new family of foraminifera: Journal of the Royal Micropaleontological Society of London Series 3 (48), 283-299.

Heron-Allen, R., and Earland, A., 1932. Foraminifera: Part I - The ice-free area of the Falkland Islands and adjacent seas: Discovery Report. University of Cambridge Press, England 4., 291-460.

Hickson, S. J., 1911. On *Polytrema* and some allied genera. A study of some sedentary foraminifera based mainly on a collection made by Prof. Stanley Gardiner in the Indian Ocean: Transactions of the Linnean Society of London, Zoology Series 2 14, 443-462.

Hodell, D.A., Charles, C.D., and Ninnemann, U.S., 2000. Comparison of interglacial stages in the South Atlantic sector of the southern ocean for the past 450 kyr: implications for Marine Isotope Stage (MIS) 11: Global and Planetary Change 24, 7-26.

Hofker, J., 1930. Foraminifera of the Sigboda Expedition, Part 2, Families Astrorhizidae, Rhizamminidae, Reophacidae, Anomalinidae, Peneroplidae in Sigboda-Expedite: Monographie Iva, Leiden, E.J., Brill, 79-170.

Höglund, H., 1947. Foraminifera in the Gullmar Fjord and the Skagerak: Zoologiska Bidrag Från Uppsala Band 26, 328 p.

Höglund, H., 1948. New names for four homonym species described in *Foraminifera in the Gullmar Fjord and the Skagerak:* Contributions from the Cushman Laboratory for foraminiferal Research 24, 45-46.

Horton, B.P., and Edwards, R.J., 2005. The application of local and regional transfer functions to the reconstruction of Holocene sea levels, north Norfolk, England: The

Holocene 15 (2), 216-288.

Horton, B P., and Edwards, R. J., 2006. Quantifying Holocene sea-level change using intertidal foraminifera: lessons from the British Isles: Cushman Foundation for Foraminiferal Research Special Publication 40, 97 p.

Hottinger, L., Halicz, E., and Reiss, Z., 1993. Recent foraminiferida from the Gulf of Aqaba, Red Sea. Slovenska akademija znanisti in umetnosti, Classis IV: Historia naturalis 179 p.

Hubbard, D. K., Gill, I. P., Burke, R. B., and Morelock, J., 1997. Holocene reef backstepping, southeastern Puerto Rico shelf. *in:* Lessios, H.A., Macintyre, I.G. (eds.) Proceedings 8th International Coral Reef Symposium, vol 2: Smithsonian tropical Research Institute, Panama 1779-1784.

Humphreys, W. F., 1999. Physico-chemical profile and energy fixation in Bundera Sinkhole, an anchialine remiped habitat in north-western Australia: Journal of the Royal Society of Western Australia 82, 89-98.

Hurrell, J. W., and Deser, C., 2009. North Atlantic climate variability: the role of the North Atlantic Oscillation: Journal of Marine Systems 78, 28-41.

Hyndman, R. D., Muecke, G. K., and Aumento, F., 1974. Deep Drill 1972, Heat flow and heat production in Bermuda: Canadian Journal of Earth Sciences 11, 809-818.

Iliffe, T. M., 1979. Bermuda's Caves: A non-renewable resource: Environmental Conservation 6 (3), 181-186.

Iliffe, T. M., 1987. Observations on the biology and geology of anchialine caves. *in:* Curan, H.A., (ed.) Proceedings of the Third Symposium on the Geology of the Bahamas: CCFL Bahamian Field Station 73-80.

Iliffe, T. M., Hart, C. W. Jr., and Manning, R. B., 1983. Biogeography and the caves of

Bermuda: Nature 302, 141-142.

Javaux, E., 1999. Benthic foraminifera from the modern sediments of Bermuda: implications for Holocene sea-level studies: PhD thesis, Dalhousie University, Canada, 625 p.

Javaux, E., and Scott, D. B., 2003. Illustration of modern benthic foraminifera from Bermuda and remarks on distributions in other subtropical/tropical areas: Paleontologica Electronica 6 (4), 29 p.

Jones, P. D., 2001. The evolution of climate over the last millennium: Science 292, 662-667.

Jones, R. W., 1994. The Challenger Foraminifera. Oxford University Press, 149 p.

Jones, T. R., and Parker, W. K., 1860. On the Rhizopodal fauna of the Mediterranean, compared with that of the Italian and some other Tertiary deposits: Quarterly Journal of the Geological Society 16, 292-307.

Jorissen, F. J., de Stigter, H. C., and Widmark, J. G. V., 1995. A conceptual model explaining benthic foraminiferal microhabitats: Marine Micropaleontology 26, 3-15.

Jorissen, F. J., and Wittling, I., 1999. Ecological evidence from live-dead comparisons of benthic foraminifera off Cape Blanc (Northwest Africa): Palaeogeography, Palaeoclimatology, Palaeoecology 149, 151-171.

Kaiho, K., 1994. Benthic foraminiferal dissolved-oxygen index and dissolved-oxygen levels in the modern ocean: Geology 22, 719-722.

Karner, D. B., Levine, J., Medeiros, B. P., and Muller, R. A., 2002. Constructing a stacked benthic $\delta^{18}O$ record: Paleoceanography 17(3), 2-17.

Katz, M. E., Cramer, B. S., Franzese, A., Hönisch, B., Miller, K. G., Rosenthal, Y., and Wright, J. D., 2010. Traditional and emerging geochemical proxies in foraminifera: Journal of Foraminiferal Research 40 (2), 165-192.

Kaufman, D.S., and Brigham-Grette, J., 1993. Aminostratigraphic correlations and paleotemperature implications, Pliocene-Pleistocene high sea level deposits, northwestern Alaska: Quaternary Science Reviews 12, 21–33.

Kawagata, S., Yamasaki, M., Genka, R., and Jordan, R. W., 2005. Shallow-water benthic foraminifers from the Mecherchar Jellyfish Lake (Ongerul Tketau Uet), Palau: Micronesica 37 (2), 215-233.

Keigwin, L. D., 1996. The little ice age and medieval warm period in the Sargasso Sea. Science 972 (5292), 1504-1508.

Keigwin, L. D., and Boyle, E. A., 2000. Detecting changes in thermohaline circulation. PNAS 97 (4), 1343-1346.

Kelley, J. T., Belknap, D. F., and Claesson, S., 2010. Drowned coastal deposits with associated archaeological remains from a sea-level “slowstand”: Northwestern Guf of Maine, USA: Geology 38, 695-698.

Kim, S. T., and O’Neil, J. R., 1997. Equilibrium and nonequilibrium oxygen isotope effects in synthetic carbonates: Geochimica et Cosmochimica Acta 61(16), 3461-3475.

Kitamura, A., Yamamoto, N., Kase, T., Ohashi, S., Hiramoto, M., Fukusawa, H., Watanabe, T., Irino, T., Kojitani, H., Shimamura, M., and Kawakami, I. 2007. Potential of submarine-cave sediments and oxygen isotope composition of cavernicolous micro-bivalve as a late Holocene paleoenvironmental record: Global Planetary Change 55 (4), 301-316.

Kobluk, D. R., and Lysenko, M. A., 1986. Reef-dwelling molluscs in open framework cavities Bonaire, N.A., and their potential for preservation in a fossil reef: Bulletin of Marine Science 39 (3), 656-672.

Kofoid, C. A., and Campbell, A. S., 1929. A conspectus of the marine and freshwater Ciliata belonging to the suborder Tintinnoinea with descriptions of new species, principally from the Agassiz Expedition to the Eastern Tropical Pacific (1904-1905): University of California Publications in Zoology 34, 1-403.

Kolesar, P. T., and Riggs, A. C., 2007. Influence of depositional environmental on Devil's Hole Calcite morphology and petrology. *In:* Sasowsky, I. D., Mylroie, J. (eds.), Studies of Cave Sediments: Physical and Chemical Records of Paleoclimate, Springer 227-241.

Kornicker, L. S., and Iliffe, T. M., 1989. Ostracoda (*Mycodoopina, Cladocopina, Halocypridina*) mainly from anchialine caves in Bermuda: Smithsonian Contributions to Zoology 475, 88 p.

Kuhnert, H., Crüger, T., and Pätzold, J., 2005. NAO signature in a Bermuda coral Sr/Ca record: Geochemistry Geophysics Geosystems 6, Q04004, doi:10.1029/2004GC000786.

Labourdette, R., Lascu, I., Mylroie, J., Roth, and M., 2007. Process-like modeling of flank-margin caves: from genesis to burial evolution: Journal of Sedimentary Research 77, 965-979.

Lacroix, E., 1931. Microtexture du test des Textularidae: Institut Océanographique (Monaco) Bulletin 582, 18 p.

Lacroix, E., 1932. Textularidae du plateau continental méditerranéen entre Sainte-Raphaël et Monaco: Institut Océanographique (Monaco) Bulletin 591, 28 p.

Lamarck, J. B., 1804. Suite des memoires sur les fossils des environs de Paris: Annales Muséum National d'Histoire Naturelle de Paris 5, 351 p.

Lamarck, J. B., 1816, Histoire naturelle des animaux sas vertèbres: Verdère, Paris 2, 568 p.

Lamb, A. L., Wilson, G. P., and Leng, M. J., 2006. A review of coastal paleoclimate and relative sea-level reconstructions using $\delta^{13}C$ and C/N ratios in organic material: Earth Science Reviews 75, 29-57.

Land, L. S., Mackenzie, F. T., and Gould, S. J., 1967. The Pleistocene history of Bermuda: Geological Society of America Bulletin 78, 993-1006.

Langer, M. R., 1993. Epipytic foraminifera: Marine Micropaleontology 20 (3-4), 235-265.

Langer, M. R., 1995. Oxygen and carbon isotopic composition of recent larger and smaller foraminifera from the Magang Lagoon (Papua New Guinea). Marine Micropaleonology 26, 215-221.

Lankford, R. R., and Phleger, F. B., 1973. Foraminifera from the nearshore turbulent zone, western North America: Journal of Foraminiferal Research 3 (3), 101-132.

Larcomb, P., Carter, R. M., Dye, J., Gagan, M. K., and Johnson, D. P., 1995. New evidence for episodic post-glacial sea-level rise, central Great Barrier Reef, Australia: Marine Geology 127, 1-44.

Lemke, W., 2004. Die kurze und wechselvolle Entwicklungsgeschichte der Ostee—Aktuelle meeresgeologissche Forschungen zum Verlauf der Litorina-Transgression: Bodendenkmalpflege in Mecklenburg-Vorpommern, Jahrbuch, p 43-54.

Lewis, R.D., and Tichenor, H.R., 2008. Recent foraminifera at the platform margin, Doolittle's Grotto and Double Caves dive sites, San Salvador Island, Bahamas: Geological Society of America, Abstract Program 40 (4), 21 p.

Linné, C., 1758. Systema naturae per regna tria naturae, secundum classes, ordines, genera, species, cum characteribus, differentiis, synonymis, locis: G. Engelmann (Lipsiae) 10 (1), 824 p.

Lipps, J. H., Langer, M. R., 1999. Benthic foraminifera from the Meromictic Mechechar Jellyfish Lake, Palau (Western Pacific): Micropaleontology 45 (3), 278-284.

Liu, M., Chase, C. G., 1989. Evolution of midplate hot spot swells: numerical solutions: Journal of Geophysical Research 94, 5571-5584.

Loeblich, A. R., and Tappan, H., 1953. Studies of Arctic Foraminifera. Smithsonian Miscellaneous Collections, 121: 1-150.

Loeblich, A. R. Jr., and Tappan, H., 1961. Suprageneric classification of the Rhizopodea: Journal of Paleontology 35 (2), 245-330.

Loeblich, A. R., and Tappan, H., 1964. Sarcodina chiefly "thecamoebians" and foraminifera. *In:* Moore R.C., (ed) Treatise on Invertebrate Paleontology Part C, Protista 2, Ed. Moore, R.C.: The University of Kansas Press 1-900.

Loeblich A. R., and Tappan, H., 1987. Foraminiferal Genera and Their Classification. Van Nostrand Reinhold Company, New York 970 p.

Loeblich A. R., and Tappan, H., 1994. Foraminifera of the Sahul Shelf and Timor Sea: Cushman Foundation for Foraminiferal Research Special Publication 31, 661 p.

Logan, A., Mathers, S. M., and Thomas, M. L. H., 1984. Sessile invertebrate coelobite communities from reefs of Bermuda: species composition and distribution: Coral Reefs 2, 205-213.

Longly, G. 1986. The biota of the Edwards Aquifer and the implications for paleozoogeography. *In:* Abbott, P.L., Woodruff, C.M. Jr., (eds.) The Balcones Escarpment: Geology, Hydrology, Ecology and Social Development in Central Texas 51-54.

Lund, D. C., Lynh-Stieglitz, J., and Curry, W. B., 2006. Gulf Stream density structure and transport during the past millennium: Nature 444 (30), 601-604.

Lundberg, J., and McFarlane, D., 2002. Isotope stage 11 sea level in the Netherlands Antilles: Geological Society of America, Abstract Program 9, 8 p.

Maddocks, R. F., and Iliffe, T. M., 1986, Podocopid ostracoda of Bermudian caves: Stygologia 2 (1/2), 26-76.

Mann, M. E., Zhang, Z., Hughes, M. K., Bradley, R. S., Miller, S. K., and Rutherford, S., and Ni, F., 2008. Proxy-based reconstructions of hemispheric and global surface temperature variations over the past two millennia: PNAS 105 (36), 13252-13257

Mann, M. E., Woodruff, J. D., Donelly, J. P., and Zhang, Z., 2009. Atlantic hurricanes and climate over the past 1,500 years: Nature 460, 880-885.

Manning, R. B., Hart, C. W., Jr., Iliffe, T. M., 1986. Mesozoic relicts in marine caves of Bermuda: Stygologia 2 (1/2), 156-166.

Marin, L. E., and Perry, E. C., 1994. The hydrogeology and contaminant potential of northwestern Yucatan, Mexico: Geofis International 33, 619-623.

Mayewski, P. A., Rohling, E. E., Stager, J. C., Karlén, W., Massch, K. A., Meeker, L. D., Meyerson, E. A., Gasse, F., van Kreveld, S., Holmgren, K., Lee-Thorp, J., Rosqvist, G., Rack, F., Staubwasser, M., Schneider, R. R., and Steig, E. J., 2004. Holocene climate variability: Quaternary Research 62, 243-255.

McCorkle, D. C., Corliss, B. H., and Farnham, C. A., 1997. Vertical distributions and stable isotopic compositions of live (stained) benthic foraminifera from the north Carolina and California continental margins: Deep Sea Research Part I 44, 983-1024.

McCulloch, I., 1977. Qualitative observations on recent foraminiferal tests with emphasis on the Eastern Pacific: Parts 1-3. Los Angeles: University of Southern California, 1079 p.

McMurtry, G. M., Tappin, D. R., Sedwick, P. N., Wilkinson, I., Fietzke, J., and Sellwood, B., 2007. Elevated marine deposits in Bermuda record a late Quaternary megatsunami: Sedimentary Geology 200, 155-165.

McMurtry, G. M., Tappin, D. R., Sedwick, P. N., Wilkinson, I., Fietzke, J., and Sellwood, B., 2008. Reply to "Mega-highstand or megatsunami? Discussion of McMurtry, et al (Elevated marine deposits in Bermuda record a late Quaternary megatsunami - Sedimentary Geology 200 (2007)155-165 by Paul J. Hearty and Stors L. Olson, Sedimentary Geology (2007) 155-165": Sedimentary Geology 203, 313-319.

Medina-Elizaalde, M., Burns, S. J., Lea, D. W., A, Y., von Gunten, L., Polyak, V., Vuille, M., Karmalkar, A., 2010. High resolution stalagmite climate record from the Yucatán Peninsula spanning the Maya terminal classic period: Earth and Planetary Science Letters 298 (1-2), 255-262.

Meeker, L. D., and Mayewski, P. A., 2002. A 1400-year high-resolution record of atmospheric circulation over the North Atlantic and Asia. The Holocene 12 (3), 257-266.

Meinen, C. S., Baringer, M. O., and Garcia, R. F., 2010. Florida Current transport variability: an analysis of annual and longer-period signals. Deep-Sea Research I 57, 835-846.

Melis, R., and Violanti, D., 2006. Foraminiferal biodiversity and Holocene evolution of the Phetchaburi coastal area (Thailand Gulf): Marine Micropaleontology 61, 94-115.

Meunier, A., 1919. Microplankton de la Mer Flamande Part 4 – Les tintinnides et caetera: Memoires de les Musee Royal d'Histoire naturelle de Beligique 8, 1-59.

Middleton, G., 1973. Johannes Walther's Law of the Correlation of Facies: Geological Society of America Bulletin 84, 979-988.

Mikhalevich, V.I., 1976. New data on the foraminifera of the groundwaters of Middle Asia: International Journal of Speleology 8, 167-175.

Millet, F. W., 1899. Report on the recent foraminifera of the Malay Archipelago, collected by Mr. A. Durrand - Part 4: Journal of the Royal Micropaleontological Society of London 694 p.

Mojitahid, M., Jorissen, F., Lansard, B., Fontanier, C., Bombled, B., and Rabouille, L., 2009. Spatial distribution of live benthic foraminifera in the Rhône prodelta: faunal response to a continental-marine organic matter gradient: Marine Micropaleontology 70, 177-200.

Montagu, G., 1803. Testacea Britannica, or natural history of British shells, marine, land, and fresh-water, including the most minute: Romsey, England, 521 p.

Montagu, G., 1808. Supplement to the Testacea Britannica: S. Wooler, Exeter, 183 p.

Montfort, D. P., 1808. Conchyliologie systématique et classification méthodique des coquilles: Paris, France, 123 p.

Moolenbeek, R. G., Faber, M. J., and Iliffe, T. M., 1988. Two new species of the genus *Caecum* (gastropoda) from marine caves on Bermuda: Studies in Honour of Dr. Pieter Wagenaar Hummelinck 123, 209-216.

Moore, Y. H., Sotessell, R. K., and Easley, D. H., 1992. Fresh-water/sea-water relationship within a ground-water flow system, northeastern coast of the Yucatan Penisula. Ground Water 30 (3), 343-350.

Morigi, C., Jorissen, F. J., Gevais, A., Guichard, S., and Borsetti, A. M., 2001. Benthic foraminiferal faunas in surface sediments off NW Africa: Relationship with organic flux to the ocean floor: Journal of Foraminiferal Research 31 (4), 350-368.

Morris, B., Barnes, J., Brown, F., and Markham, J., 1977. The Bermuda marine environment: a report of the Bermuda inshore waters investigations 1976-1977: Bermuda Biological Station Special Publication 17, St. Georges, Bermuda 120 p.

Munier-Chalmas, E., 1882. Sur les genres et Broeckina: Bulletin of the Geologic Society of France, Series 3 10 (6), 470-471.

Murray, J. W., 1965. Two species of British recent foraminiferida: Cushman Foundation Foraminiferal Research Contributions 16 (4), 148 p.

Murray, M. R., 2002. Is laser particle determination possible for carbonate-rich lake sediments? Journal of Paleolimnology 27, 173-183.

Murray, J., 2006. Ecology and Applications of Benthic Foraminifera. Cambride University Press, 426 p.

Mylroie, J.E., 2008. Late Quaternary sea-level position: evidence from Bahamian carbonate deposition and dissolution cycles: Quaternary International 183 (1), 61-75.

Mylroie, J. E., and Carew, J. L., 1988. Solution conduits as indicators of late Quaternary sea level position: Quaternary Science Reviews, 7 (1) 55-64.

Mylroie, J. E., and Carew, J. L., 1990. The flank margin model for dissolution cave development in carbonate platforms: Earth Surface Process Landforms 15 (5), 413-424.

Mylroie, J. E., Carew, J. L., and Vacher, H. L., 1995. Karst development in the Bahamas and Bermuda. *In:* Curran, H.A., White, B., (eds.). Terrestrial and Shallow Marine Geology of the Bahamas and Bermuda, Geological Society of America Special Paper 300, 251-267.

Mylroie, J. R., and Mylroie, J. E., 2007. Development of the carbonate island karst model. Journal of Cave and Karst Studies 69 (1), 59-75.

Mylroie, J.E., Mylroie, J.R., and Nelson, C.S., 2008. Flank margin cave development in telogenetic limestones of New Zealand: Acta Carsologica 37 (1), 15-40.

Mylroie, J.E., and Mylroie, J. R., 2009. Caves as sea level and uplift indicators, Kangaroo Island, South Australia: Journal of Cave and Karst Studies 71 (1), 32-47.

Natland, M. L., 1938. New species of foraminifera from off the west coast of North America and from the later Tertiary of the Los Angeles Basin: Technical Series Bulletin of Scripps Institution of Oceanography 4 (5), 137-152.

Natland, M. L., 1950. Report on the Pleistocene and Pliocene foraminifera. *in:* 1940 E.W. Scripps cruise to the Gulf of California: Geological Society of America Memoir 43 (4), 1-53.

Neumann, A. C., 1971. Quaternary sea-level data from Bermuda: Quaternaria, 14, 41-43.

Noren, A. J., Bierman, P. R., Steig, E. J., Lini, A., and Southon, J., 2002. Millennial-scale storminess variability in the northeastern United States during the Holocene epoch. Nature 419, 821-824.

Norman, A. M., 1878. On the genus *Haliphysema* with description of several forms apparently allied to it: Annual Magazine of Natural History 1 (5), 265-284.

Novosel, M., Bakran-Petricioli, T., Požar-Domac, A., Kužić, P., Radić, I., 2002. The benthos of the northern part of the Velebit Channel (Adriatic Sea, Croatia): Nature Croatia 2 (4), 387-409.

Novosel, Jalžić, B., Novosel, A., Pasarić, Požar-Domac, Radić, I., 2007. Ecology of an Anchialine cave in the Adriatic Sea with special reference to its thermal regime: Marine Ecology 28 (Supplement 1), 3-9.

O'Brien, S. R., Mayewski, P. A., Meeker, L. D., Meese, D. A., Twickler, M. S., and Whitlow, S. I., 1995. Complexity of Holocene climate as reconstructed from a Greenland Ice Core. Science 270 (5244), 1962-1964.

Ogrinc, N., Fontolan, G., Faganeli, J., and Covelli, S., 2005. Carbon and nitrogen isotope compositions of organic matter in coastal marine sediments (the Gulf of Trieste, N Adriatic Sea): indicators of sources and preservation: Marine Chemistry 95, 163-181.

Olson, S.L., and Hearty, P.J., 2009. A sustained +21 m sea-level highstand during MIS 11 (400 ka): direct fossil and sedimentary evidence from Bermuda: Quaternary Science Reviews 28, 271-285.

Omori, A., Kitamura, A., Fujita, K., Honda, K., and Yamamoto, N., 2010. Reconstruction of light conditions within a submarine cave during the past 7000 years based on the temporal and spatial distribution of algal symbiont-bearing large benthic

foraminifers: Palaeogeography, Palaeoclimatology, Palaeoecology 292, 443-452.

Osterman, L. E., 2003. Benthic foraminifers from the continental shelf and slope of the Gulf of Mexico: an indicator of shelf hypoxia: Estuarine, Coastal and Shelf Science 58 (1), 17-35.

Osterman, L. E., Poore, R. Z., and Swarzenski, P. W., 2008. The last 1000 years of natural and anthropogenic low-oxygen bottom-water on the Louisiana shelf, Gulf of Mexico: Marine Micropaleontology 66 (3-4), 291-303.

Palmer, A. N., Palmer, M. V., and Queen, J. M., 1977. Geology and origin of the caves of Bermuda: Proceedings of the Seventh International Congress of Speleology, Sheffield, UK 336-339.

Panno, S. V., Curry, B. B., Wang, H., Hackley, K. C., Liu, C., Lundstrom, C., and Zhou, J., 2004. Climate change in southern Illinois, USA, based on the age and $\delta^{13}C$ of organic matter in cave sediments: Quaternary Research 61, 301-313.

Parker, F. L., 1952. Foraminiferal distribution in the Long Island Sound – Buzzards Bay area: Museum of Comparative Zoology Harvard Bulletin 106 (10), 428-473.

Parker, F. L., 1954. Distribution of the foraminifera in the Northeastern Gulf of Mexico: Museum of Comparative Zoology, Harvard Bulletin 111 (10), 588 p.

Parker, F. L., 1962. *Quinqueloculina tenagos* new name for *Quinqueloculina rhodiensis* Parker, preoccupied: Contributions from the Cushman Foundation for Foraminiferal Research 13, p. 110.

Parker, F. L., Phleger, F. B., and Peirson, J. F., 1953. Ecology of foraminifera from San Antonio Bay and environs, southwest Texas: Cushman Foundation for Foraminiferal Research Special Publication 2, 75 p.

Parker, W. K., and Jones, T. R., 1859. On the nomenclature of the foraminifera, Part II: On the Species enumeratured by Walker and Montagu: Annals and Magazine of Natural History 3, 333-351.

Parr, W. J., 1932. Victorian and South Australian shallow-water foraminifera - Part 2: Proceedings of the Royal Society of Victoria, Melbourne, Australia 44, 1-14; 218-234.

Parravicini, V., Guidetti, P., Morri, C., Montefalcone, M., Donato, M., and Bianchi, C. N., 2010. Consequences of sea water temperature anomalies on a Mediterranean submarine cave ecosystem. Estuarine, Coastal and Shelf Science 86, 276-282.

Patterson, R. T., and Fishbein E., 1989. Re-examination of the statistical methods used to determine the number of point counts needed for micropaleontological quantitative research: Journal of Paleontology 63 (2), 245-248.

Patterson, R. T., Guilbault, J. P., and Thomson, R. E., 2000. Oxygen level control on foraminiferal distribution in Effingham Inlet, Vancouver Island, British Columbia, Canada: Journal of Foraminiferal Research 30 (4), 321-335.

Patterson, W. P., Dietrich, K. A., Holmden, C., and Andrews, J. T., 2010. Two millennia of North Atlantic Seasonality and implications for Norse colonies. PNAS (in press), doi: 10.1073/pnas.0902522107.

Pawlowski, J., 1991. Distribution and taxonomy of some benthc tiny foraminifers from the Bermuda Rise: Micropaleontology 37 (2), 163-172.

Pawlowski, J., and Lee, J. J., 1991. Taxonomic notes on some tiny, shallow water foraminifera from the northern Gulf of Elat (Red Sea): Micropaleontology 37 (2), 149-162.

Pearson, A. S., Ceaser, E. P., and Hall, F. G., 1936. The cenotes of Yucatan: a zoological

and hydrographical survey: Bulletin of the Carnegie Institution of Washington, Washington 304 p.

Perdue, E. M., and Koprivnjak, J. F., 2007. Using the C/N ratio to estimate terrigenous inputs of organic matter to aquatic environments: Estuarine, Coastal, and Shelf Science 73 (1-2), 65-72.

Phleger, F. B. and Parker, F. L., 1951. Ecology of foraminifera, northwest Gulf of Mexico - Part II - Foraminifera species: Geological Society of America Memoir 46, 64 p.

Phleger, F. B., Parker, F. L., and Pierson, J. F., 1953. Ecology of foraminifera from San Antonio Bay and environs, southwest Texas: Cushman Laboratory for Foraminfieral Research Special Publication No. 2, 75 p.

Phleger, F. B., and Walton, W. R., 1950. Ecology of marsh ad bay foraminifera, Barnstable, Mass.: American Journal of Science 248, 214-294.

Pohlman, J.W., Iliffe, T.M., and Cifuentes, L.A., 1997. A stable isotope study of organic cycling and the ecology of an anchialine cave ecosystem: Marine Ecology Progress Series 155, 17-27.

Polk, J. S., van Beynen, P. E., and Reeder, P. P., 2007. Late Holocene environmental reconstruction using cave sediments from Belize Quaternary Research 68, 53-63.

Proctor, C. J., and Smart, P. L., 1991. A dated cave sediment record of Pleistocene transgressions on Berry Head, Southwest England: Journal of Quaternary Science 6 (3), 233-244.

Rasmussen, K., Brett, C., 1985. Taphonomy of Holocene cryptic biota's from St. Croix, Virgin Islands: Information loss and preservational biases: Geology 13, 551-553.

Raynaud, D., Barnola, J.M., Souchez, R., Lorrain, R., Petit, J.R., Duval, P., and Lipenkov, V.Y., 2005. The record for marine isotope stage 11: Nature 436 (7047), 39-40.

Redfield, A. C., 1967. Postglacial change in sea level in the western North Atlantic Ocean: Science 157 (3787), 687-691.

Reimer, P. J., Baillie, M. G. L., Bard, E., Bayliss, A., Beck, J. W., Blackwell, P. G., Ramsey, C. B., Buck, C. E., Burr, G. S., Edwards, R. L., Freidrich, M., Groots, P. M., Guilderson, T. P., Hajdas, I., Heaton, T. J., Hogg, A. G., Hughen, K. A., Kaiser, K. F., Kromer, B., McCormac, F. G., Manning, S. W., Reimer, R. W., Richards, D. A., Southon, J. R., Talamo, S., Turney, C. S. M., van der Plicht, J., and Weyhenmeyer, C. E., 2009. IntCal09 and Marine09 radiocarbon age calibration curves, 0-50,000 years Cal BP: Radiocarbon 51 (4): 1111-1150.

Reinhardt, E. G., Goodman, B. N., Boyce, J. I., Lopez, G., van Hengstum, P., J. Rink, W. J., Mart, Y., and Raban, A., 2006. The tsunami of 13 December A.D. 115 and the destruction of Herod the Great's harbor at Casarea Maritima, Israel: Geology 34 (12), 1061-1064.

Reinhardt, E. G., Nairn, R. B., and Lopez, G., 2010. Recovery estimates for the Rio Cruces after the May 1960 Chilean earthquake: Marine Geology 269 (1-2), 18-33.

Reiswig, H. M., 1981. Particulate organic carbon of bottom boundary and submarine cavern waters of tropical coral reefs: Marine Ecology Progress Series 5, 129-133.

Reuss, A. E., 1850. Neues foraminiferen aus den Schichten des Österreichischen Tertiärbeckens: Denkschriften der Kaiserliche Akademie der Wissenschaften Mathematisch-Naturwissenschaftliche Classe 1, 365-390.

Rhumbler, L., 1904. Systematische Zusammenstellung der recenten Reticulosa: Archiv duer Protistenkunde 3, 181-294.

Rhumbler, L., 1906, Foraminiferen von Laysan und den Chatham-Inseln: Zoologischer Jahresbericht 24 (1), 21-80.

Rhumbler, L., 1911. Die foraminiferen (Thalamophoren) der Plankton-Expedition; Teil I. Die allgemeinen organisationsverhaltnisse der foraminiferen: Ergebnisse der Plankton-Expedition der Humboldt-Stiftung 3, 331 p.

Richards, D. A., Smart, P. L., and Edwards, R. L., 1994. Maximum sea levels for the last glacial period from U-series ages of submerged speleothems: Nature 367, 357-360.

Richey, J. N., Poore, R. Z., Flower, B. P., Quinn, T. M., 2007. A 1400 yr multiproxy record of climate variability from the northern Gulf of Mexico: Geology 35: 423-426.

Roberts, D.L., Jacobs, Z., Karkanas, P., and Marean, C.W., 2007. Onshore expression of multiple orbitally driven Late Quaternary marine incursions on the ultra-stable southern South African coast: Quaternary International 167–168 (Supplement 1), 3 - 486.

Roe, H. M., and Patterson, R.T., 2006. Distribution of thecamoebians (testate amoebae) in small lakes and ponds, Barbados, West Indies: Journal of Foraminiferal Research 36 (2), 116-134.

Rohling, E. J., Grant, K., Hemleben, C., Hoogakker, B. A. A., Bolshaw, M., and Kucera, M., 2008. High rates of sea-level rise during the last interglacial period: Nature Geoscience 1, 38–42

Rueger, B. F., von Wallmenich, T. N., 1996. Human impact on the forests of Bermuda: the decline of endemic cedar and palmetto since 1609, recorded in Holocene pollen record of Devonshire Marsh. Journal of Paleolimnology 16, 59-66.

Sánchez, S. O., Alcocer, J., Escobar, E., and Lugo, A., 2002. Phytoplankton of cenotes and anchialine caves along a distance gradient from the northeastern coast of Quintana Roo, Yucatan Peninsula: Hydrobiologia 467, 79-89.

Saunders, J. B., 1961. Helenina Saunders, new name for the foraminiferal genus Helenia Saunders, 1957, not Helenia Walcott, 1889: Contributions from the Cushman Foundation for Foraminiferal Research 12 (4), 128-148.

Schackleton, N., 1974. Attainment of isotopic eqilibrium between ocean water and the benthonic foraminifera genus *Uvigerina*: Isotopic changes in the ocean during the last glacial: Colloque Int. CNRS, 219, 203-209.

Schmitter-Soto, J. J., Comín, F. A., Escobar-Briones, E., Herrera-Silveira, J, Alcocer, J., Suárez-Morales, Elías-Gutiérrez, M., Día-Arce, V., Marín, L. E., and Steinich, B., 2002. Hydrogeochemical and biological characteristics of cenotes in the Yucatan Peninsula (SE Mexico): Hydrobiologia 467, 215-228.

Schneider, J. C., and Kruse, S., 2003. A comparison of controls on freshwater lens morphology of small carbonate and siliciclastic islands: examples from barrier islands in Florida, USA: Journal of Hydrology 284, 253-269.

Schnitker, D., 1971. Ecotypic variation in *Ammonia beccarii* (Linné): Journal of Foraminiferal Research 4 (4), 217-223.

Schwager, C., 1866. Fossile foraminiferen con Kar Nikobar, Riese der österreichischen Fregatte Novara um Erde in den Jahren Expedition 1857-1859 unter der en Befehlen des Commodore B. von Wüllerstorf-Urbair, Geologischer Theil 2 (1), Geologische Beobachtungen, Paleontologische Mittheilungen 187-268.

Scott, D. B., 1976. Brackish-water foraminifera from southern California and description of *Polysaccammina ipohalina* n. gen., n. sp.: Journal of Foraminiferal Research 6, 312-321.

Scott, D. B., and Medioli, F. S., 1980a. Quantitative studies of marsh foraminiferal distributions in Nova Scotia: implications for sea level studies: Cushman

Foundation for Foraminiferal Research 17, 57 p.

Scott, D. B., and Medioli, F. S., 1980b. Living vs. total foraminiferal populations: their relative usefulness in paleoecology: Journal of Paleontology 54, 814-831.

Scott, D. B., Williamson, M. A., and Duffet, T. M., 1981. Marsh foraminifera of Prince Edward Island: Their recent distribution and application for former sea level studies: Maritime Sediments and Atlantic Geology 17, 98-129.

Scott, D. B., Suter, J. R., and Kosters, E. C., 1991. Marsh foraminifera and Arcellaceans of the lower Mississippia Delta: controls on spatial distributions: Micropaleontology 37, 373-392.

Scott, D. B., and Hermelin, J. O. R., 1993. A device for precision splitting of micropaleontological samples in liquid suspension: Journal of Paleontology 67 (1), 151-154.

Scott, D. B., Schafer, C. T., and Younger, D. C., 1995. Temporal variations of benthic foraminiferal assemblages under or near aquaculture operations: documentation of impact history: Journal of Foraminiferal Research 25 (3), 224-235.

Scott, D. B., Medioli, F. S., and Schafer, C. T., 2001. Monitoring in Coastal Environments using Foraminifera and Thecamoebian Indicators: Cambridge University Press, New York, USA 192 p.

Scott, D. B., Tobin, R., Williamson, M., Medioli, S., Latimer, J. S., Boothman, W. A., Asioli, A., and Haury, V., 2005. Pollution monitoring in two North American estuaries: historical reconstructions using benthic foraminfera: Journal of Foraminiferal Research 35 (1), 65-82.

Scott, D. B., and Vilks, G., 1991. Benthonic foraminifera in the surface sediments of the deep-sea arctic ocean: Journal of Foraminiferal Research 21 (1), p. 20-38.

Seiglie, G. A., 1974. Foraminifers of Mayagúez and Añasco Bays and its surroundings: Caribbean Journal of Science 14 (1-2), 1-68.

Seiglie, G. A., and Bermúdez, P. J., 1965. Monografía de la familia de foraminíferos *Glabratellidae*: Geoscience 12, 15-65.

Shackleton, A., and Moore, R. C., 1954. Chiefly radiolarians and tintinnines. *In:* Moore R.C., (ed) Treatise on Invertebrate Paleontology Part D, Protista 3, Ed. Moore, R.C., The University of Kansas Press, 1-195.

Siddall, M., Rohling, E. J., Almogi-Labin, A., Hemleben, C., Meischner, D., Schmelzer, I., and Smeed, D. A., 2003. Sea-level fluctuations during the last glacial cycle: Nature 423, 853-858.

Silén, L., and Harmelin, 1976. *Haplopoma sciaphilum* sp.n., a cave-living bryozoan from the Skagerrak and the Mediterranean: Zoologica Scripta 5 (1-4), 61-66.

Sket, B., and Iliffe, T. M., 1980. Cave fauna of Bermuda: Internationale Revue der Gesmten Hydrobiologie 65, 871-882.

Sliter, W. V., 1965. Laboratory experiments on the life cycle and ecologic controls on *Rosalina globularis* d'Orbigny: Journal of Eukaryotic Microbiology 12 (2), 210-215.

Smart, P. L., Dawns, J. M., and Whitaker, F., 1988. Carbonate dissolution in a modern mixing zone: Nature 355, 811-813.

Smart, P. L., Beddows, P. A., Doerr, S., Smith, S. L., and Whitaker, F. F., 2006. Cave development on the Caribbean coast of the Yucatan Peninsula, Quintana Roo, Mexico. *In:* Harmon, R.S., Wicks, C., (eds.) Perspectives on karst geomorphology, hydrology, and geochemistry-a tribute volume to Derek C. Ford and William B. White, Geological Society of America Special Paper 404, 105-128.

Steadman, D. W., Franz, R., Morgan, G. S., Albury, N. A., Kakuk, B., Broad, K., Franz, S. E., Tinker, K., Pateman, M. P., Lott, T. A., Jarzen, D. M., and Dilcher, D. L., 2007. Exceptionally well preserved late Quaternary plant and vertebrate fossils from a blue hole on Abaco, The Bahamas: Proceedings of the National Academy of Sciences 104 (50), 19897-19902.

Sterrer, W., 1986. Marine fauna and flora of Bermuda: John Wiley and Sons 742 p.

Stock, J.A., Iliffe, T.M., and Williams, D., 1986. The concept "anchialine" reconsidered: Stygologia 2 (1/2), 90-92.

Stuvier, M., and Braziunas, T. F., 1989. Atmospheric ^{14}C and century-scale solar oscillations: Nature 338, 405-408.

Surić, M., Juračić, M., Horvatinčić, and Bronić, I. K., 2005. Late-Pleistocene-Holocene sea-level rise and the pattern of coastal karst inundataion: records from submerged speleothems alon the Eastern Adriatic Coast (Croatia). Marine Geology 214, 163-175.

Surić, M., Richards, D. A., Hoffmann, D. L., Tibljaš D., and M., Juračić, 2009. Sea-level change during MIS 5a based on submerged speleothems from the eastern Adriatic Sea (Croatia): Marine Geology 262 (1-4), 62-27.

Sweeney, E. N., McGillicuddy, D. J., Jr., and Buesseler, K. O., 2003. Biogeochemical impacts due to mesoscale eddy activity in the Sargass Sea as measured at the Bermuda Atlantic Time-series Study (BATS): Deep-Sea Research II 50, 3017-3039.

Taylor, M. P., Drysdale, R. N., and Carthew, K. D., 2004. The formation and environmental significance of calcite rafts in tropical tufa-depositing rivers in northern Australia: Sedimentology 51, 1089-1101.

Taylor, P. M., and Chafetz, H. S., 2004. Floating rafts of calcite crystals in cave pools,

central Texas, U.S.A.: crystal habit vs. saturation state: Journal of Sedimentary Research 74 (3), 328-341.

Teeter, J.W., 1975. Distribution of Holocene marine Ostracoda from Belize. *In:* Wantland, K.F., Pusey, W.C. (eds.) Carbonate Sediments, Clastic Sediments, and Ecology. American Association of Petroleum Geologists Studies in Geology 2, 400-499.

Teeuw, R., Rust, D., Solana, A., and Deweney, C., 2009. Large coastal landslides and tsunami hazard in the Caribbean: EOS 90 (10), 81-88.

Teodoro, A. C., Duleba, W., Gubitoso, S., Prada, S. M., Lamparelli, C. C., and Bevilacqua, J. E., 2010. Analysis of foraminifera assemblages and sediment geochemical properties to characterize the environment near Araçá and Saco de Capela domestic sewage submarine outfalls of São Sebastião Channel, São Paulo State, Brazil: Marine Pollution Bulletin 60, 536-553.

Terquem, O., 1876. Essai sur le classement des animaux qui vivent sur la plage et dans les environs de denkerque – Part 1: Memoire de la Société Dunkerquoise pour l'Encouragement des Sciences des Lettres et des Arts (1874-1875): 19, 405-457.

Thomas, M. L. H., Eakins, K. E., and Logan, A., 1991. Physical characteristics of the anchialine ponds of Bermuda: Bulletin of Marine Science 48 (1), 125-136.

Thomas, F. C., Medioli, F. S., and Scott, D. B., 1990. Holocene and latest Wisconsinan benthic foraminiferal assemblages and paleocirculation history, lower Scotian slope and rise: Journal of Foraminiferal Research 20 (3), 212-245.

Thornton, S. F., and McManus, J., 1994. Application of organic carbon and nitrogen stable isotopes and C/N ratios as source indicators of organic matter provenance in estuarine systems: evidence from the Tay Estuary, Scotland: Estuarine, Coastal and

Shelf Science 38 (3), 219-233.

Toscano, M. A., and Lundberg, J., 1998. Early Holocene sea-level record from submerged fossil reefs on the southeast Florida margin: Geology 26, 255-258.

Toscano, M. A., and McIntyre, I.G., 2003. Corrected western Atlantic sea-level curve for the last 11,000 years based on calibrated ^{14}C dates from Acropora palmata framework and intertidal mangrove peat: Coral Reefs 22, 257-270.

Troulet, V., Esper, J., Graham, N. E., Baker, A., Scourse, J. D., Frank, D. C., 2009. Persistent positive North Atlantic Oscillations mode dominated the medieval climate anomaly. Science 324, 78-80.

Usera, J., Blázquez, A. M., Guillem, J., and Alberola, C., 2002. Biochronological and paleoenvironmental interest of foraminifera in restricted environments: application to the study of the western Mediterranean Holocene: Quaternary International 93-94, 139-147.

Vacher, H. L., 1974. Groundwater hydrology of Bermuda. Bermuda Public Works Department, Hamilton, Bermuda 85 p.

Vacher, H. L., 1978. Hydrogeology of Bermuda – significance of an across-the-island variation in permeability: Journal of Hydrology 39, 207-226.

Vacher, H.L., 1988. Dupuit-Ghyben-Herzberg analysis of strip island lenses. Geological Society of America Bulletin 100 (4), 580-591.

Vacher, H. L., and Rowe, M. P., 1997. Geology and Hydrogeology of Bermuda. *In:* Vacher, H. L., and Quinn, T. M. (eds.) Geology and Hydrogeology of Carbonate Islands - Developments in Sedimentology 54: Elsevier 35-90.

Vacher, H. L., Rowe, M. P., and Garrett, P., 1989. The geological map of Bermuda: The Ministry of Works and Engineering, The Bermuda Government [map].

Vacher, H. L., Hearty, P. J., and Rowe, M. P., 1995. Stratigraphy of Bermuda: Nomenclature, concepts, and status of multiple systems of classification. *In:* Curran, H. A., and White, B. (eds.) Terrestrial and Shallow Marine Geology of the Bahamas and Bermuda: Geological Society of America Special Paper 300, 271-294.

van Hengstum, P. J., Reinhardt, E. G., Boyce, J. I., and Clark, C., 2007. Changing sedimentation patterns due to historical land-use change in Frenchman's Bay, Pickering, Canada: evidence from high-resolution textural analysis: Journal of Paleolimnology 37, 603-618.

van Hengstum, P. J., 2008. Paleoenvironmental analysis using thecamoebians and foraminifera in Mexican anchialine caves: a focus on Aktun Ha (Carwash) Mexico. MSc thesis, McMaster University.

van Hengstum, P. J., Reinhardt, E. G., Beddows, P. A., Huang, R. J., and Gabriel, J. J., 2008. Thecamoebians (testate amoebae) and foraminifera from three anchialine cenotes in Mexico: Low salinity (1.5 - 4.5 psu) faunal transitions: Journal of Foraminiferal Research 38 (4), 305-317.

van Hengstum, P. J., Reinhardt, E. G., Beddows, P. A., Schwarcz, H. P., and Garbriel, J. J., 2009a. Foraminifera and testate amoebae (thecamoebians) in an anchialine cave: surface distributions from Aktun Ha (Carwash) cave system, Mexico: Limnology and Oceanography 54 (1), 391-396.

van Hengstum, P. J., Scott, D. B., and Javaux, J. J., 2009b. Foraminifera in elevated Bermudian caves provide further evidence for +21 m eustatic sea level during Marine Isotope Stage 11: Quaternary Science Reviews 28, 1850-1860.

van Hengstum, P. J., Reinhardt, E. G., Beddows, P. A., and Gabriel, J. J., 2010. Investigating linkages between Holocene paleoclimate and paleohydrogeology preserved in Mexican underwater cave sediments: Quaternary Science Reviews 29, 2788-2798, doi:10.1016/j.quascirev.2010.06.034.

van Hengstum, P. J., and Scott, D.B., 2011. Ecology of foraminifera and habitat variability in an underwater cave: distinguishing anchialine versus submarine cave environments: Journal of Foraminiferal Research (in press).

Van Morkhoven, F. P. C. M., 1963. Post-palaeozoic ostracoda: their morphology, taxonomy, and economic use, volume 2: Elsevier, Amsterdam, 478 p.

Vesica, P. L., Tuccimei, P., Turi, B., Fornós, J. J., Ginés, A., and Ginés J., 2000. Late Pleistocene paleoclimates and sea-level change in the Mediterranean as inferred from stable isotope and U-series studies of overgrowths on speleothems, Mallorca, Spain: Quaternary Science Reviews 19, 865-879.

Voβ, M., and Struck, U., 1997. Stable nitrogen and carbon isotopes as indicator of eutrophication of the Oder river (Baltic sea): Marine Chemistry 59, 35-49.

Vogt, P. R., Jung, W. –Y., 2007. Origin of the Bermuda volcanoes and Bermuda Rise: history observations and puzzles: *In*: Foulger, G., Jurdy, D., (eds.) Plates, Plumes, and Planertary Processes. Geological Society of America Special Paper 430, p. 553-591.

Vollbrecht, R., 1996. Postglazialer Anstieg des Meeresspiegels, paläoklima und hydrographie, aufgezeichnet in sedimenten der Bermuda inshore waters. PhD Thesis, Universität Göttingen.

Walker, G., and Jacob, E. 1798. Testacea minuta rariora. *In:* Adams, E., (ed.) Essays on the Microscope. London. Second edition with considerable additions and improvements by F. Kanmacher: Dillon and Keating, London 712 p.

Walton, W. R., and Sloan, B. J., 1990. The genus *Ammonia* Brunnüich, 1772: Its geographic distribution and morphologic variability: Journal of Foraminiferal Research 20 (2), 128-156.

Ward, S. N., and Day, S., 2001. Cumbre Vieja Volcano—potential collapse and tsunami at La Palma, Canary Islands: Geophysical Research Letters 28, 3397-4000.

Warren, A. D., 1957. Foraminifera of the Buras-Scofield Bayou region, southeast Louisiana: Contributions from the Cushman Foundation for Foraminiferal Research 8, 29-40.

Weijers, J. W. H., Schouten, S., Schefub, E., Schnedier, R. R., and Damsté, J. A. S., 2009. Disentangling marine, soil, and plant organic carbon contributions to continental margin sediments: A multi-proxy approach in a 20,000 year sediment record from the Congo deep-sea fan: Geochimica et Cosmochimica Acta 73, 119-132.

Whitaker, F. F., and Smart, P. L., 1990. Active circulation of saline ground waters in carbonate platforms: evidence from the Great Bahama Bank: Geology 18, 200-203.

White, W. B., 2007. Cave sediments and paleoclimate: Journal of Cave and Karst Studies 69 (1), 76-93.

Wilkinson, I. P., 2006. Foraminifera from the putative tsunami deposits at Castle Harbour, Bermuda: British Geological Survey Internal Report: IR/06/001R, 14 p.

Williamson, W. C., 1848. On the recent British species of the genus Lagena: Annals and Magazine of Natural History, Series 2 1, 1-20.

Williamson, W.C., 1858. On the recent foraminifera of Great Britain. Royal Society of London, England 107 p.

Woodruff, F., Savin, S. M., and Douglas, R. G., 1980. Biological fractionation of oxygen and carbon isotopes by recent benthic foraminifera: Marine Micropaleontology 5, 3-11.

Woodward, J. C., and Goldberg, P., 2001. The sedimentary records in Mediterranean rockshelters and caves: archives of environmental change: Geoarchaeology 14 (4), 327-354.

Wurster, C. M., Patterson, W. P., McFarlane, D. A., Wassenaar, L. I., Hobson, K. A., Beavan-Athfield, N., and Bird, M. I., 2008. Stable carbon and hydrogen isotopes from bat guano in the Grand Canyon, USA, reveal Younger Dryas and 8.2 ka events: Geology 36, 683-686.

Yamamoto, N., Kitamura, A., Irino, T., Kase, T., and Ohashi, S., 2008. Reconstruction of paleotemperatures in the Northwest Pacific over the past 3000 years from $\delta^{18}O$ values of the micro-bivalvia Carditella iejimensis found in a submarine cave: Global and Planetary Change 62, 97-108.

Yamamoto, N., Kitamura, A., Irino, T., Kase, T., and Ohashi, S., 2010. Climatic and hydrologic variability in the East China Sea during the last 7000 years based on oxygen isotopic records of the submarine caverniculous micro-bivalve *Carditella iejimensis*: Global Planetary Change 72 (3), 131-140.

Yamamoto, N., Kitamura, A., Ohmori, A., Morishima, Y., Toyofuku, T., and Ohashi, S., 2009. Long-term changes in sediment type and cavernicolous bivalve assemblages in Daidokutsu submarine cave, Okinawa Islands: evidence from a new core extending over the past 7,000 years: Coral Reefs 28, 967-976.

Yanko, V., Arnold, A., Parker, W., 2003. Effects of marine pollution on benthic foraminifera: *In* Sen Gupta, B. K., (ed.) Modern Foraminifera. Kluwer Academic Publishers, pp. 217-235.

Yu, S., Berglund, B. E., Sandgren, P., and Lambeck, K., 2007. Evidence for a rapid sea-level rise 7600 yr ago: Geology 3 (10), 891-894.

Zheng, S., 1979. The recent foraminifera of the Xisha Islands, Guangdong Province China - Part II: Studia Marina Sinica 15 (8), 101-232.

Zheng, S., 1988. The agglutinated and porcelaneous foraminifera of the East China Sea, Part 2: The porcelaneous foraminifera of the East China Sea Beijing, 197 p.

Zielinski, G. A., Mayewski, P. A. Meeker, D. L., Whitlow, S., and Twickler, M. S., 1996. A 110,000-Yr record of explosive volcanism from the GISP2 (Greenland) ice core: Quaternary Research 45, 109-118.

Zinke, J., Reijmer, J. J. G., Taviani, M., Dullo W., and Thomassin, B., 2005. Facies and faunal assemblage changes to the Holocene transgression in the Lagoon of Mayotte (Comoro Archipelago, SW Indian Ocean): Facies 50, 391-408.

Appendix 1 – Bermuda Cave Radiocarbon Dates

Note for distinguishing cores (column 3): WH refers to a core from Walsingham Cave, whereas GB refers to a core from Green Bay Cave. For Example, GBC1 is core 1 from Green Bay Cave (see Chapter 3).

Index No.	Lab number	Core	Depth (cm)	Material	Conventional ^{14}C age	δ^{13}C (‰)	Calibrated age (2σ)
1	OS-80319	WHC2	7.5 ±1	foraminifera	270 ±40	0.03	< 400
2	OS-79182	WHC2	19 ±1	foraminifera	985 ±30	-0.12	600 ±80
3	OS-79183	WHC2	29 ±1	foraminifera	1330 ±35	-0.7	920 ±130
4	OS-74181	WHC2	33.25 ±0.25	bulk organics[§]	1200 ±50	-21.79	930 ±130
5	OS-80319	WHC2	49 ±1	foraminifera	2460 ±30	0.31	2170 ±140
6	OS-80296	WHC2	64 ±1	foraminifera	2700 ±30	0.28	2490 ±160
7	OS-78405	WHC2	78.25 ±0.25	woody debris	2300 ±30	-27.16	2270 ±90
8	OS-79184	WHC2	912?.25 ±0.25	marine gastropod	2830 ±30	1.44	2610 ±140
9	OS-79185	WHC2	124 ±1	foraminifera	3000 ±30	0.38	2830 ±110
10	OS-78404	WHC2	154.25 ±0.25	woody debris	2600 ±30	-25.6	2700 ±80
11	OS-80298	WHC2	159 ±1	foraminifera	3260 ±30	0.85	3150 ±160
12	OS-74182	WHC2	164.5±0.5	bulk organics[§]	3050 ±55	-18.97	2960 ±180
13	OS-81524	WHC4	21 ±1	foraminifera and ostracods	710 ±30	-0.19	390 ±95
14	OS-81446	WHC4	41 ±1	foraminifera	890 ±30	0	550 ±80
15	OS-81445	WHC4	61 ±1	foraminifera	2260 ±30	0.24	1930 ±130
16	OS-81450	WHC4	81 ±1	foraminifera and ostracods	2580 ±30	0.4	2300 ±150
17	OS-74175	GBC1	10 ±0.5	woody debris	2910 ±35	-27.27	3080 ±130
18	OS-74176	GBC1	21.5 ±0.5	woody debris	4190 ±45	-24.91	4710 ±130
19	OS-74177	GBC1	71.5 ±0.5	woody debris	5070 ±70	-25.89	5820 ±165
20	OS-79473	GBC5	14.5 ±0.5	bivalve - *Barbatia domingensis*	645 ±25	2.79	350 ±95
21	OS-78020	GBC5	27.5 ±0.5	bivalve - *Barbatia domingensis*	1610 ±25	0.39	1200 ±100
22	OS-78019	GBC5	31.25 ±0.25	bivalve - *Barbatia domingensis*	2040 ±25	-0.57	1670 ±130
23	OS-78451	GBC5	38.25 ±0.25	bulk organics	3590 ±30	-27.12	3900 ±70
24	OS-74180	GBC5	46.25 ±0.25	bulk organics	3800 ±40	-27.48	4200 ±190

25	OS-74179	GBC5	49.75 ±0.25	bulk organics	4930 ±45	-25.23	5670 ±80
26	OS-80321	GBC5	51.5 ±1	foraminifera and ostracods	6800 ±50	-0.14	7360 ±120
27	OS-79218	GBC5	61.25 ±0.75	foraminifera and ostracods	7160 ±65	-1.59	7690 ±150
28	OS-79474	GBC5	65.25 ±0.25	land gastropod - *Poecilozonites*	11100 ±65	-8.02	12,940 ±200
29	OS-74186	GBC6	27.5 ±0.5	Bivalve	1140 ±40	-0.18	760 ±110
30	OS-81363	GBC9	11.5 ±0.5	bivalve - *Barbatia domingensis*	595 ±25	2.9	280 ±140
31	OS-81364	GBC9	37.5 ±0.5	bivalve - *Barbatia domingensis*	2000 ±25	0.29	1630 ±130
32	OS-81373	GBC9	59.5 ±0.5	foraminifera and ostracods	6700 ±35	-0.72	7280 ±110
33	OS-81365	GBC11	37.25 ±0.25	bivalve - *Barbatia domingensis*	2020 ±25	0.88	1650 ±130
34	OD-81366	GBC11	41 ±0.75	foraminifera and ostracods	7030 ±30	0.42	7560 ±100
35	OS-81369	GBC11	46.75 ±0.75	foraminifera and ostracods	7210 ±40	-0.93	7720 ±120
36	OS-81367	GBC12	29.5 ±0.5	bivalve - *Barbatia domingensis*	1630 ±25	-0.1	1230 ±100

§ - bulk organics in underwater caves can be a mixture of terrestrial and marine organic matter. The marine fraction (F_m) was determined with a two-endmember mixing model where: -26.7‰ = δX_t; -16.8‰ = δX_t (van Hengstum and Scott, 2011); $1 = F_t + F_m$; $\delta X = F_m * \delta X_m + F_t * \delta X_t$; equations solved for F_m (e.g., Ogrinc et al., 2005), and age calibrated with Mixed Marine Northern Hemisphere curve (Reimer et al., 2009).

Marine carbonates (bivalves, foraminifera, ostracods) calibrated assuming a surface ocean reservoir age of 400 yrs, $\Delta R = -48 \pm 40$ (Druffel, 1997) and Marine09 dataset (Reimer et al., 2009); terrestrial material (woody fragments, *Poecilozonites*, etc.) calibrated with IntCAL09 data set (Reimer et al., 2009).

Note: All foraminifera are benthic.

Appendix 2 – Green Bay Cave Surface Sample Data

Data for the Green Bay Cave surface samples is to be permantantly archived as Electronic supplementary material at Dalhousie University. Appendix 2 includes:

(1) Measured sedimentological parameters for each surface sample

(2) Measured geochemical parameters for each surface sample

(3) Original census data for benthic foraminifera

(4) Relative abundance and standard error calculations (2s) for benthic foraminifera

(5) Foraminifera not included in the total assemblages due to taphonomic processes (see Chapter 2).

Appendix 3 – Green Bay Cave Sedimentologic Data for cores

Data for the Green Bay Cave surface samples is to be permantantly archived as Electronic supplementary material at Dalhousie University. Appendix 3 includes:

(1) Measured sedimentological parameters in each core

(2) Measured geochemical parameters in each core

Appendix 4 – Example of Isotopic Mixing

After measuring the $\delta^{13}C_{org}$ value in surface sediments throughout Green Bay Cave, Bermuda, the terrestrial end-member of organic matter was -26.7‰ and the marine end-member was -16.8‰. Therefore, the fraction of terrestrial organic matter (F_t) versus fraction of marine organic matter (F_m) contributing to a bulk $\delta^{13}C_{org}$ value (δX) downcore can be estimated using a simple 2-endmember mixing model.

Given: δX_t = -26.7‰, δX_m = -16.8‰ (van Hengstum and Scott, 2011, Chapter 2).

Equation 1: $1 = F_t + F_m$, where F_t is the unknown to be estimated.

Equation 2: $\delta X = F_m * \delta X_m + F_t * \delta X_t$, where δX is measured isotopic composition for the sample of interest (e.g., GBC5 3-4 cm).

Then: $\delta X = F_m * \delta X_m + F_t * \delta X_t$

$\delta X = (1- F_t) * (-16.8‰) + F_t * (-26.7‰)$

$\delta X = (-16.8‰) + (16.8‰ * F_t) – (26.7‰* F_t)$

$\delta X = (-16.8‰) – (9.9‰* F_t)$

$(\delta X + 16.8‰) / (-9.9‰) = F_t$

The fraction of marine organic matter (F_m) can then be easily be then calculated by substitution of F_t into Equation 1. Obviously, this calculation asumes that organic matter is *dominantly* derived from only two sources, which is a reasonable assumption for coastal environments.

Appendix 5 – All Bermuda Marsh Radiocarbon Dates

	Sample	Lab number	Depth (m bsl)	Material	Conventional ^{14}C age	$\delta^{13}C$ (‰)	Calibrated Age (±2s)	Citation
Devonshire marsh								
1	ACN #D7	ML 561	1.7	freshwater peat	770 ±80		735 ±175	Neumann (1971)
2	ACN #D12	ML 559	3.4	freshwater peat	3815 ±95		4220 ±290	Neumann (1971)
3	ACN #D9	ML 556	5.8	freshwater peat	4585 ±100		5270 ±310	Neumann (1971)
4	ACN #D11	ML 555	7.4	freshwater peat	5070 ±100		5840 ±250	Neumann (1971)
5	ACN #D1	ML 553	8.9	freshwater peat	6000 ±110		6870 ±300	Neumann (1971)
6	ACN #D5	Ml 552	10.7	freshwater peat	6510 ±110		7385 ±210	Neumann (1971)
7	ACN #D4	ML 550	12.5	freshwater peat	6970 ±120		7800 ±200	Neumann (1971)
Great Sound								
8	GS 01: 1.22-1.28	KI-1997	12.6	freshwater peat	7250 ±90	-27.2	8090 ±220	Vollbrecht (1996)
9	GS 02: 5.94-6.01	KI-1998	27.1	freshwater peat	9150 ±210	-27.9	10370 ±700	Vollbrecht (1996)
Harrington Sound								
10	ACN #HS	ML 69-2A	4.4	freshwater peat	4994 ±80		5750 ±150	Vollbrecht (1996)
11	ACN #HS	ML 69-3A	4.7	freshwater peat	4760 ±100		5510 ±210	Vollbrecht (1996)
12	HS-TB 02/2: 1.35-1.4	KI-2045.02	4.7	freshwater peat	3830 ±95	-26.4	4220 ±290	Vollbrecht (1996)
13	HS-TI: 1.8-1.85	KI-2117.02	5.5	freshwater peat	4990 ±65	-29	5750 ±143	Vollbrecht (1996)
14	ACN #HS	ML-69-13A	5.6	freshwater peat	4787 ±105		5522 ±220	Vollbrecht (1996)
15	HS-TB/1: 0.85-0.90	KI-2044	7	freshwater peat	5800 ±80	-27.7	6600 ±180	Vollbrecht (1996)
16	ACN #HS	ML 69-12A	7.6	freshwater peat	5829 ±110		6660 ±260	Vollbrecht (1996)
17	ACN #HS	ML 69-16A	9.4	freshwater peat	6785 ±120		7680 ±240	Vollbrecht (1996)

18	ACN #HS	ML 69-17B	11.2	freshwater peat	6800 ±120		7680 ±240	Vollbrecht (1996)
19	ACN #HS	ML 69-17A	11.4	freshwater peat	7221 ±110		8080 ±240	Vollbrecht (1996)
20	HS-PH/2: 3.45-3.5	KI-3408	12.3	freshwater peat	6850 ±100	-28.9	7720 ±210	Vollbrecht (1996)
21	ACN #HS	ML 69-18C	13	freshwater peat	7280 ±100		8130 ±200	Vollbrecht (1996)
22	ACN #HS	ML 69-18A	13.2	freshwater peat	7360 ±160		8150 ±300	Vollbrecht (1996)
23	8450ACN #HS	ML 69-19A	15.1	freshwater peat	7709 ±140		8590 ±380	Vollbrecht (1996)
24	ACN #HS	ML 69-20A	17.3	freshwater peat	7400 ±135		8190 ±240	Vollbrecht (1996)
25	ACN #HS	ML 69-15A	17.4	freshwater peat	7880 ±100		8730 ±270	Vollbrecht (1996)
26	ACN #HS	ML 69-22A	17.9	freshwater peat	8833 ±140		9880 ±330	Vollbrecht (1996)
27	ACN #HS	ML 69-27B	18.3	freshwater peat	8030 ±140		8940 ±400	Vollbrecht (1996)
28	ACN #HS	ML 69-27A	18.6	freshwater peat	8785 ±140		9870 ±320	Vollbrecht (1996)
29	ACN #HS	ML 69-24A	19.2	freshwater peat	8195 ±100		9130 ±340	Vollbrecht (1996)
30	HS-MR 05/2: 0.8-0.85	KI-2121	19.8	freshwater peat	8900 ±160	-27.9	9960 ±420	Vollbrecht (1996)
31	HS-MLB 02/2:2.2-2.26	KI-2120	19.9	freshwater peat	8760 ±125	-30.1	9850 ±310	Vollbrecht (1996)
32	HS-MR 08: 1.8-1.85	KI-2111.01	20.3	freshwater peat	8900 ±100	-28.3	9960 ±280	Vollbrecht (1996)
33	Unlabeled	ML-186	20.7	freshwater peat	9145 ±150		10275 ±450	Redfield (1967)
34	HS-CB 03: 2.59-2.64	KI-2119	21.6	freshwater peat	8800 ±100	-28.5	9860 ±300	Vollbrecht (1996)
35	HS-CD 02: 3.45-3.5	KI-2118	21.9	freshwater peat	9410 ±170	-28	10700 ±450	Vollbrecht (1996)
36	HS-CB 05/2: 3.75-3.80	KI-3932.38	22.2	freshwater peat	9370 ±95	-28.7	10670 ±400	Vollbrecht (1996)
37	HS-MR 07: 1.24-1.29	KI-2113	22.3	freshwater peat	9440 ±110	-28.2	10720 ±410	Vollbrecht (1996)

38	HS-SP 01: 392-3.98	KI-1800.03	23	freshwater peat	9940 ±170	-25.4	11440 ±640	Vollbrecht (1996)
39	HS-PT 02: 1.10 - 1.15	KI-2112	23.2	freshwater peat	9150 ±165	-28.2	10260 ±490	Vollbrecht (1996)
40	HS-PT 01: 1.71-1.76	KI-1733.01	23.2	freshwater peat	9640 ±95	-27.3	10970 ±250	Vollbrecht (1996)
41	ACN #HS 78ft	ML 526	23.8	freshwater peat	9180 ±140		10300 ±390	Vollbrecht (1996)
42	HS-GP (24.3): 2.39-2.43	KI-1732.01	23.9	freshwater peat	9020 ±115	-25.3	10120 ±370	Vollbrecht (1996)
43	HS-GP (01.4): 3.25-3.3	KI-1732.02	24.8	freshwater peat	9720 ±100	-26.3	11020 ±280	Vollbrecht (1996)
44	HS-CS/1: 2.85-2.90	KI-2114	24.8	freshwater peat	9450 ±170	-29.5	10733 ±450	Vollbrecht (1996)
45	HS-CD 01: 4.15-4.20	KI-2116	24.8	freshwater peat	10130 ±90	-29.4	11710 ±360	Vollbrecht (1996)
46	HS-SP 04: 5.72-5.75	Beta-88712	26.8	freshwater peat	9730 ±60	-29.3	11030 ±230	Vollbrecht (1996)
47	HS-SP 03: 5.78-5.82	KI-2172	27	freshwater peat	9750 ±120	-29.1	11160 ±440	Vollbrecht (1996)
48	HS-PB 01: 6.75-6.78	KI-2171	27.3	freshwater peat	10110 ±110	-29	11680 ±400	Vollbrecht (1996)
Mangrove Lake								
49	ACN #ML1	ML 557	5	freshwater peat	4120 ±100		4640 ±230	Vollbrecht (1996)
Pembroke Marsh								
50	ACN #P1	ML 547	14.5	freshwater peat	7630 ±120		8440 ±260	Vollbrecht (1996)
51	ACN #P2	ML 546	16.9	freshwater peat	8530 ±130		9520 ±380	Vollbrecht (1996)
Port Royal Bay								
52	PR o3/2: 5.46-5.49	KI-2000	20.8	freshwater peat	8890 ±70	-27.9	9970 ±230	Vollbrecht (1996)
53	Unlabeled	Unlabeled	25.2	freshwater peat	9552 ±89		10890 ±290	Ashmore and Leatherman (1984)
54	PR 01/1, 4.07-4.1	KI-1999	26.7	freshwater peat	9400 ±85	-28.8	10690 ±390	Vollbrecht (1996)

Shelly Bay, North Shore								
55	Unlabeled	I-1683	1.7	freshwater peat	1850 ±110		1780 ±260	Redfield (1967)
56	Unlabeled	I-1684	2.3	freshwater peat	1820 ±120		1730 ±310	Redfield (1967)
St. George's Harbour								
57	ACN #FR	ML 549	9.9	basal brackish peat	6070 ±110		6960 ±290	Vollbrecht (1996)
58	ACN #TC	ML 551	12.3	freshwater peat	7460 ±120		8260 ±250	Vollbrecht (1996)
59	SGH 02: 6.14-6.22	KI-2001	20.1	freshwater peat	8780 ±100	-29.1	9850 ±300	Vollbrecht (1996)
Somerset Long bay, South Shore								
60	Unlabeled	I-1685	0.5	freshwater peat	880 ±120		810 ±240	Redfield (1967)
61	Unlabeled	I-1969	0.6	freshwater peat	1210 ±95		1120 ±180	Redfield (1967)
62	Unlabeled	I-1764	1	freshwater peat	1510 ±110		1440 ±250	Redfield (1967)
63	Unlabeled	I-1971	1.3	freshwater peat	2440 ±110		2470 ±290	Redfield (1967)
64	Unlabeled	I-1973	1.7	freshwater peat	2530 ±100		2570 ±220	Redfield (1967)
65	Unlabeled	I-1975	2	freshwater peat	2690 ±90		2780 ±280	Redfield (1967)
66	Unlabeled	I-1686	2.3	freshwater peat	3900 ±120		4390 ±410	Redfield (1967)
67	Unlabeled	I-1762	3.1	freshwater peat	3600 ±120		3910 ±330	Redfield (1967)
68	Unlabeled	I-1763	3.2	freshwater peat	3930 ±120		4372 ±440	Redfield (1967)
North Lagoon								
69	NL 031/4: 4.73-4.81	KI-1991.02	26.1	freshwater peat	9700 ±90	-28.5	11000 ±240	Kuhn (1984)
70	NL 039: 1.5-1.6	KI-1992	19.6	freshwater peat	7870 ±95	-27.8	8730 ±270	Kuhn (1984)
71	NL 040: 4.78-4.81	KI-1993.04	23	freshwater peat	9230 ±150	-31.3	10500 ±270	Kuhn (1984)
72	NL 048: 2.31-2.35	KI-1994.02	17	freshwater peat	8710 ±80	-27.1	9830 ±300	Kuhn (1984)
73	NL049: 1.07-1.12	KI-1995	3.1	freshwater peat	3980 ±55	-24.3	4510 ±270	Kuhn (1984)
74	NL051: 2.83-2.87	KI-1996.04	14.6	freshwater peat	8010 ±95	-28.8	8860 ±270	Kuhn (1984)
75	NL 054:	KI-2585.0	19.1	freshwater peat	9010 ±125	-28.5	10100 ±390	Vollbrecht

	4.52-4.57	2						(1996)
76	NL055/2: 5.5-5.54	KI-2586.03	18.3	freshwater peat	8800 ±120	-28.1	9860 ±310	Vollbrecht (1996)
Mill Share								
77	MS-C6	GX-21542	2.71	mangrove peat	2940 ±60		3120 ±200	Javaux (1999)
78	DC06	GX-21545	2.9	basal brackish peat	2930 ±60		3100 ±220	Javaux (1999)
79	C05	GX-21543	2.32	basal brackish peat	1070 ±60		990 ±180	Javaux (1999)
80	C02	GX-21544	1.37	mangrove peat	510 ±55		565 ±85	Javaux (1999)
Mills Creek								
81	DC05	GX-21546	4.45	basal brackish peat	2940 ±60		3120 ±200	Javaux (1999)
Hungry Bay								
82	DC05	GX-21547	1.65	basal brackish peat	2010 ±50		1990 ±120	Javaux (1999)
83	HB1-9	not given (Beta)	5.55	basal brackish peat	4870 ±90	-27	5610 ±280	Ellison (1993)
84	HB2-1	not given (Beta)	5.45	basal brackish peat	4940 ±100	-27.6	5690 ±220	Ellison (1993)
85	HB5-2	not given (Beta)	2.25	basal brackish peat	3990 ±110	-27.4	4490 ±330	Ellison (1993)
86	HB1-1	not given (Beta)	0.65	mangrove peat	390 ±90	-25.1	310 ±310	Ellison (1993)
87	HB1-2	not given (Beta)	1.45	mangrove peat	1080 ±80	-26.4	990 ±190	Ellison (1993)
88	HB1-3	not given (Beta)	2.45	brackish peat	2090 ±90	-21	2100 ±220	Ellison (1993)
89	HB1-4	not given (Beta)	3.45	brackish peat	2740 ±110	-26.9	2860 ±350	Ellison (1993)
90	HB1-6	not given (Beta)	4.45	brackish peat	3880 ±100	-26.5	4280 ±290	Ellison (1993)
91	HB2-2	not given (Beta)	0.85	mangrove peat	720 ±80	-25.3	665 ±130	Ellison (1993)
92	HB4-1	not given	0.23	mangrove peat	750 ±60	-25.3	675 ±115	Ellison (1993)

		(Beta)						
93	HB5-1	not given (Beta)	0.35	mangrove peat	1460 ±60	-22.3	1400 ±120	Ellison (1993)
94	DC04	UGAMS-4589	2.57	basal brackish peat	2580 ± 20	-26.1	2690 ±65	This work
95	DC05	UGAMS-4590	1.19	basal brackish peat	810 ± 20	-23.3	725 ±40	This work
96	DC06	UGAMS-4591	0.85	basal brackish peat	230 ± 20	-24.7	150 ±150	This work
97	DC17	UGAMS-4592	0.7	basal brackish peat	530 ± 20	-24.2	570 ±55	This work
98	DC18	UGAMS-4593	0.6	basal brackish peat	490 ± 20	-24.2	520 ±15	This work
99	DC13	UGAMS-4594	1.96	basal brackish peat	3240 ± 25	-25.6	3730 ±100	This work
100	DC14	UGAMS-4595	1.82	basal brackish peat	2800 ± 25	-25.6	2890 ±80	This work
101	DC15	UGAMS-4596	2.02	basal brackish peat	3110 ± 30	-25.3	3320 ±70	This work
102	DC07	UGAMS-4597	3.44	basal brackish peat	3630 ± 25	-26.1	3970 ±100	This work
103	DCC8B	NOSA MS-72328	2.01	basal brackish peat	2490 ± 45	-26.4	2550 ±180	This work

Notes:

(1) Brackish peat verified by salt marsh foraminifera (Javaux, 1993 and this study) or botanical remains (Vollbrecht, 1996 and Ellison, 1993).

(2) Older ages without $\delta^{13}C$ values reported may be offset by an additional few hundred years because a $\delta^{13}C$-correction could not be preformed.

(3) A maximum vertical error estimate (most conservative) on basal mangrove depths is the maximum 1.2 m tidal range in Bermuda. No vertical error was applied to terrestrial peat dates, compaction likely introduces additional vertical error on non-basal mangrove peats, but are included here for a broader regional perspective.

(4) Sample Index points 80-83 were $\delta^{13}C$-corrected (Javaux, 1999, p. 283), although $\delta^{13}C$ values not reported.

(5) Table only includes samples collected from <30 m bsl.

References:

Ashmore, S., Leatherman, S.P., 1984, Holocene sedimentation in Port Royal Bay, Bermuda. Marine Geology, 56, 289-298.

Ellison, J.C., 1993, Mangrove retreat with rising sea-level, Bermuda. Estuarine, Coastal and Shelf Science 37, 75-87.

Javaux, E.J., 1999, Benthic foraminifera from the modern sediments of Bermuda: implications for Holocene sea-level studies. PhD Thesis, Dalhousie University, 614 p.

Kuhn, G., 1984, Sedimentations-geschichte der Bermuda North Lagoon im Holozän, PhD Thesis, Universität zu Göttingen, 272 p.

Neumann, A.C., 1971. Quaternary sea-level data from Bermuda. Quaternaria, 14, 41-43.

Redfield, A.C., 1967, Postglacial change in sea level in the western North Atlantic Ocean. Science, 157 (3787), 687-691.

Vollbrecht, R., 1996, Postglazialer ansteig des Meeresspiegels, Paläoklima und Hydrographie aufgezeichnet in Sedimenten der Bermuda inshore waters, PhD Thesis, Universität zu Göttingen, 383 p.

Appendix 6 – Green Bay Cave Cores Micropaleontologic Data

Micropaleontologic data for Green Bay cores 5 and 9 is to be permantantly archived as Electronic supplementary material at Dalhousie University. Appendix 6 includes:

(1) Original census counts in each core

(2) Relative abundance and standard error calculations (2σ) for benthic foraminifera

Appendix 7 – Walsingham Sedimentologic Data

Sedimentologic data for the Walsingham cores is to be permantantly archived as Electronic supplementary material at Dalhousie University. Appendix 7 includes:

(1) Measured sedimentological parameters in each core

(2) Measured geochemical ($\delta^{18}O_c$) parameters in each core

Appendix 8 – Copyright Permission Letters

ELSEVIER LICENSE TERMS AND CONDITIONS

Jun 28, 2010

This is a License Agreement between Peter J van Hengstum ("You") and Elsevier ("Elsevier") provided by Copyright Clearance Center ("CCC"). The license consists of your order details, the terms and conditions provided by Elsevier, and the payment terms and conditions.

All payments must be made in full to CCC. For payment instructions, please see information listed at the bottom of this form.

Supplier Elsevier Limited
The Boulevard,Langford Lane
Kidlington,Oxford,OX5 1GB,UK
Registered Company Number 1982084

Customer name	Peter J van Hengstum
Customer address	Dalhousie University, Halifax, NS B3H4J1
License number	***2457851096849***
License date	Jun 28, 2010
Licensed content publisher	Elsevier
Licensed content publication	Quaternary Science Reviews
Licensed content title	*Foraminifera in elevated Bermudian caves provide further evidence for +21 m eustatic sea level during Marine Isotope Stage 11*
Licensed content author	Peter J. van Hengstum, David B. Scott, Emmanuelle J. Javaux
Licensed content date	September 2009
Licensed content volume	number 28
Licensed content issue number	19-20
Number of pages	11
Type of Use	***reuse in a thesis/dissertation, including usage of the Library archives of Canada***
Requestor type	Not specified
Intended publisher of new work	n/a
Portion	full article
Format	electronic 28/06/10 7:02 PM
Rightslink Printable License	Yes
Order reference number	No
Title of your thesis/dissertation	Signatures of Quaternary Sea level and Climate in Phreatic Coastal Caves
Expected completion date	Dec 2010
Estimated size (number of pages)	500
Elsevier VAT number	GB 494 6272 12